



The
University
Of
Sheffield.



Ecto-secretions: A Comparative Study between Mucus, Venom and Silk

Edgar Barajas Ledesma

Supervisors

Dr Chris Holland

Prof. Gwen Reilly

A Thesis submitted to

The University of Sheffield

Department of Materials Science and Engineering

Natural Materials Group

For the Degree of

Doctor of Philosophy

Sheffield, September 2021

Thesis abstract

Edgar Barajas Ledesma

Natural Materials Group, Department of Materials Science and Engineering, 2021,
University of Sheffield

Animals have developed specific characteristics to facilitate a range of natural functions, from the chemical to the mechanical. One of these adaptations include producing ecto-secretions, materials secreted by specialised glands to be used outside the body. Three model ecto-secretions include gastropod locomotive mucus, used to facilitate animal's locomotion; snake venom, to facilitate the immobilization and digestion of prey; and silk, which has a range of functions, from protection to reproduction. However, even now, there are no studies analysing these three model ecto-secretions together.

To fill the gap in the study of ecto-secretions, the primary aim of this thesis was to investigate the structure-hydration-function relationship of gastropod locomotive mucus and snake venom for comparison to silk. To achieve this a set of experimental techniques was included, such as spectroscopy, electrophoresis, thermoanalytical techniques (differential scanning calorimetry and thermogravimetric analysis) and rheology.

This project was the first to directly correlate ecto-secretions' properties. Here, I have developed a novel scientific platform combining different experimental and analytical techniques. This approach has made it possible to compare and contrast the role of proteins in ecto-secretions and to use these materials as a novel grouping to explore the more general area of how proteins have been selected and optimised to perform outside the body.

The compositional and thermal characterisation of these materials revealed that proteins in gastropod locomotive mucus and snake venom exhibit a higher thermal stability than silk, due to glycosylation, hydration state and main function. Moreover, rheology offered a unique answer to a question regarding the flow properties of snake venom, proving it is a Newtonian fluid.

The developed Performance Map can be used as a guide to incorporate more and new ecto-secretions in the future. With my findings, I have a broader knowledge of these materials, which can be used during the industrial processing of materials inspired by ecto-secretions.

Dedication

In dedication to my mother, Rosa María Ledesma, who has been with me all the time, and who has taught me that life is an adventure that needs to be lived with passion and joy; for being an inspiration and an invaluable support in my life. This Ph. D. is also yours.

To my beloved husband and friend, Luis Alfredo Padilla, for his company, love, support, and for sharing with me beautiful moments. For making this stage a beautiful adventure in our lives.

To my brothers, Gaby and Rodrigo, for being an important part of my life, and for their motivation and support. Also to my nephews Abril, Vania and Jesus, because with their love they have always made me a happier person.

Edgar Barajas Ledesma

I, Edgar Barajas Ledesma, declare that this thesis titled **“Ecto-secretions: A comparative study between Mucus, Venom and Silk”** is my own work.

I confirm that:

- This work was done while in candidature for a research degree at this University of Sheffield.
- Where I have consulted the published work of others, this is always clearly cited and referenced.
- Where any sections of my thesis are based on work done by myself jointly with others, I have made clear exactly what was done by others and what was my contribution.

Edgar Barajas Ledesma

Signed:

Date:

Acknowledgements

This journey has been an important stage in my life and career and it has finished, but it will be the beginning of too many new opportunities and professional experiences. Enthusiasm, knowledge and passion for what we do are characteristics needed to successfully complete a Ph. D. However, this is not possible without the guidance, knowledge and support from our supervisors, collaborators and colleagues. This is why I would like to thank my supervisor, Dr Chris Holland, for giving me the opportunity to be a member of the Natural Materials Group, discussing and sharing with me this fascinating research project. I would also like to especially acknowledge Dr Holland for sharing with me time, knowledge and important concepts to understand Natural Materials, and for pushing my limits and letting me know that there is always a better version of ourselves. I liked my Ph. D. project since the beginning, but at this point I have surpassed my expectations.

Thank you to Prof. Gwen Reilly, my second supervisor, for facilitating my transition from Mexico to the UK, and for sharing with me valuable support, knowledge and time. Thank you for making me feel part of your research group and family, and for being so generous.

I would also like to thank all the members of the Natural Materials Group, but specially Dr Pete R. Laity, for showing me how to use the rheometer and the spectrometer. For providing me with infrared spectroscopy data on silk, which I used for my analysis, but also for the interesting discussions we had in the office and lab. To Dr Andreas Koeppel, for being an excellent colleague and friend and for all his support given during the first eighteen months of my Ph. D. And thank you to Lauren Eggleton, for the interesting conversations and discussions we had about gastropod mucus, and life in general.

I would also like to express my gratitude to Bev C. Lane, for helping me to get access to the Characterisation Laboratory, and for taking the time to train me on the DSC. In addition, I would like to acknowledge Dr Oday Hussein, for his support when I started my first DSC tests.

Finally, I would like to acknowledge my examiners, Prof. Sara Goodacre and Dr Joel Foreman, who kindly accepted to examine my thesis and for their valuable contributions.

For their vital financial support, I would like to acknowledge the Consejo Nacional de Ciencia y Tecnología (CONACYT).

Table of contents

Acknowledgements	5
Table of contents	7
List of abbreviations and symbols	11
Species (names in bold correspond to species tested)	11
Gastropods.....	11
Snakes	11
Silk.....	12
Others	12
Techniques	12
Ultraviolet-visible Spectroscopy (UV-vis).....	12
Fourier Transform Infrared Spectroscopy (FTIR)	13
Sodium Dodecyl Sulphate–Polyacrylamide Gel Electrophoresis (SDS-PAGE)	13
Differential Scanning Calorimetry (DSC)	13
Rheology	13
Fluid mechanics.....	14
CHAPTER 1: INTRODUCTION	15
1.1 WHAT IS AN ECTO-SECRETION AND WHAT ARE REPRESENTATIVE EXAMPLES OF THESE MATERIALS?	16
1.2 GASTROPOD MUCUS	19
1.2.1 DEFINITION, PROPERTIES AND PREVIOUS STUDIES	19
1.2.2 APPLICATIONS.....	27
1.3. SNAKE VENOM	31
1.3.1 DEFINITION, PROPERTIES AND PREVIOUS STUDIES	31
1.3.2 EFFECTS IN HUMANS AND POSSIBLE APPLICATIONS	38
1.4. CONCLUSION	43
1.5. THESIS AIM AND OBJECTIVES	44
1.5.1 AIM.....	44
1.5.2 OBJECTIVES	45
1.6. CHAPTER INTRODUCTION	45
CHAPTER 2: EXPERIMENTAL TECHNIQUES AND THEORY	48
2.1 SPECIES SELECTION	49
2.1.1 GASTROPODS	49
2.1.2 SNAKES.....	52
2.2 ECTO-SECRETIONS COLLECTION	54
2.2.1 GASTROPOD MUCUS.....	54
2.2.2 SNAKE VENOM	55
2.3 CHARACTERISATION TECHNIQUES	56
2.3.1 UV-VIS	59
2.3.2 FTIR	61
2.3.3 SDS-PAGE	63
2.3.4 TGA.....	66

2.3.5 DSC	68
2.3.6 RHEOLOGY	71
CHAPTER 3: ANALYSIS, CLASSIFICATION AND IDENTIFICATION OF GASTROPOD MUCUS BY FTIR	76
3.1 INTRODUCTION	78
3.2 MATERIALS AND METHODS.....	80
3.2.1 MATERIALS	80
3.2.2 METHODS.....	80
3.3 RESULTS AND DISCUSSION	83
3.3.1 GENERAL GASTROPOD MUCUS SPECTRAL FEATURES	83
3.3.2 BETWEEN-SPECIES COMPARISON OF THE CHEMICAL COMPOSITION OF GASTROPOD MUCUS	88
3.3.3 PROTEIN SECONDARY STRUCTURES: AMIDE I PEAK DECONVOLUTION.....	91
3.3.4 CLASSIFICATION OF GASTROPOD SPECIES	93
3.3.5 COMPARING FTIR AND PHYLOGENETIC TREES	95
3.4 CONCLUSIONS.....	100
CHAPTER 4: THE RHEOLOGICAL PROPERTIES OF GASTROPOD LOCOMOTIVE MUCUS: RELATING COMPOSITION TO FUNCTION	102
4.1 INTRODUCTION	104
4.2 MATERIALS AND METHODS.....	106
4.2.1 MATERIALS	106
4.2.2 METHODS.....	106
4.3 RESULTS AND DISCUSSION	109
4.3.1 COMPOSITIONAL PROPERTIES	109
4.3.2 FUNCTIONAL AND THERMAL PROPERTIES.....	114
4.4 CONCLUSIONS.....	119
CHAPTER 5: STRUCTURAL CHARACTERISATION, CLASSIFICATION AND IDENTIFICATION OF SNAKE VENOMS.....	120
5.1 INTRODUCTION	122
5.2 MATERIALS AND METHODS.....	124
5.2.1 MATERIALS	124
5.2.2. METHODS.....	124
5.3 RESULTS AND DISCUSSION	127
5.3.1 SNAKE VENOM REDUCED SDS-PAGE PROFILES.....	127
5.3.2 SNAKE VENOM SPECTRAL FEATURES.....	130
5.3.3 BETWEEN-SPECIES COMPARISON OF THE CHEMICAL COMPOSITION OF SNAKE VENOM	132
5.3.4 PROTEIN SECONDARY STRUCTURES: AMIDE I PEAK DECONVOLUTION.....	135
5.3.5 CLASSIFICATION OF SNAKE SPECIES.....	137
5.3.6 COMPARISON OF FTIR AND PHYLOGENETIC TREE	139
5.4 CONCLUSIONS.....	143
CHAPTER 6: CHARACTERISATION OF THE PHYSICAL PROPERTIES OF SNAKE VENOM	144
6.1 INTRODUCTION.....	147
6.2 MATERIALS AND METHODS.....	150
6.2.1 VENOM EXTRACTION	150
6.2.2 RHEOLOGICAL TESTS	151
6.2.3 CALCULATING FANG VENOM SHEAR RATE	151

6.2.4 CALCULATING THE PRESSURE NEEDED TO EJECT VENOM	152
6.2.5 PROTEIN CONCENTRATION	154
6.2.6 PH MEASUREMENTS	155
6.2.7 PHYLOGENETIC COMPARATIVE METHODS	155
6.3 RESULTS	157
6.3.1 PHYSICAL PROPERTIES OF THE VENOM	157
6.3.2 PHYLOGENETIC COMPARATIVE METHODS	159
6.4 DISCUSSION	160
CHAPTER 7: DIFFERENTIAL SCANNING CALORIMETRY OF ECTO-SECRETIONS	166
7.1 INTRODUCTION	168
7.2 MATERIALS AND METHODS.....	170
7.2.1 MATERIALS	170
7.2.2 Methods	171
7.3 RESULTS AND DISCUSSION	172
7.3.1 PROTEIN DENATURATION IN GASTROPOD MUCUS AND SILK	172
7.3.2 GLASS TRANSITION IN SNAKE VENOMS AND TREHALOSE	175
7.3.3 THERMAL TRANSITIONS	177
7.3.4 STABILITY OF ECTO-SECRETION' PROTEINS.....	179
7.4 CONCLUSIONS.....	182
CHAPTER 8: Summary and Future Outlook.....	183
8.1 THESIS SUMMARY	184
8.2 ECTO-SECRETIONS' STRUCTURE-HYDRATION-FUNCTION RELATIONSHIPS, AND PERFORMANCE MAP.....	186
8.3. MODEL SYSTEMS.....	189
8.4. THESIS IMPACT.....	191
8.4.1 PLATFORM TO TEST ECTO-SECRETIONS.....	191
8.4.2 ECTO-SECRETIONS' FTIR SPECTRA PROVIDE PHYLOGENETICAL INFORMATION	191
8.4.3 MUCINS IN GASTROPOD MUCUS SHOW AN ADAPTIVE RESPONSE TO THEIR NATURAL ENVIRONMENT	192
8.4.4 SNAKE VENOMS ARE NEWTONIAN FLUIDS.....	192
8.4.5 SNAKE FANG'S MORPHOLOGICAL ADAPTATIONS CONTROL THE SPITTING BEHAVIOUR	193
8.4.6 GLYCOSYLATION CONTRIBUTES TO THERMAL STABILITY OF PROTEINS	194
8.5. FUTURE OUTLOOK.....	194
REFERENCES	197
APPENDICES	A
APPENDIX A1. CHAPTER 4: UV-Vis.....	B
APPENDIX A2. CHAPTER 4: RHEOLOGY	D
APPENDIX A3. CHAPTER 5: SNAKES' DETAILS.....	E
APPENDIX A4. CHAPTER 5: SDS-PAGE.....	F
APPENDIX A5. CHAPTER 6: PROPERTIES OF VENOMS' SAMPLES	G
APPENDIX A6. CHAPTER 6: DELTA PRESSURE EQUATION	H
APPENDIX A7. CHAPTER 6: RHEOLOGY- EXPERIMENTAL WINDOW	K
APPENDIX A8: CHAPTER 7. DSC	L

APPENDIX A9: CHAPTER 8. THESIS SUMMARY..... V
APPENDIX A10: PUBLISHED PAPER..... W

List of abbreviations and symbols

Species (names in bold correspond to species tested)

Gastropods

A. fulica	Achatina fulica
A. marginata.....	Achatina marginata
P. boraceiensis.....	Phyllocaulis boraceiensis
C. aspersum	Cornu aspersum
C. nemoralis	Cepaea nemoralis
A. ater	Arion ater
A. hortensis	Arion hortensis
A. subfuscus.....	Arion subfuscus
A. columbianus.....	Ariolimax columbianus
L. flavus	Limax flavus
L. maximus	Limax maximus
L. marginata.....	Lehmannia marginata
D. reticulatum.....	Deroceras reticulatum
D. caruanae.....	Deroceras caruanae
G. maculosos.....	Geomalacus maculosos
T. pisana.....	Theba pisana
E. vermiculata.....	Eobania vermiculata
L. haroldi	Laevicaulis haroldi
V. sloanei	Venonicella sloanei
L. stagnalis	Lymnaea stagnalis
M. cornuaretis	Marisa cornuaretis
P. diffusa	Pomacea diffusa
L. limatula.....	Lottia limatula
P. vulgata.....	Patella vulgata
H. diversicolor.....	Haliotis diversicolor
D. maxima.....	Dendropoma maxima
L. irrorata.....	Littoraria irrorata
L. littorea.....	Littorina littorea
L. obtusata.....	Littorina obtusata
L. saxatilis.....	Littorina saxatilis
I. obsoleta.....	Ilyanassa obsoleta

Snakes

B. arietans	Bitis arietans
B. caudalis.....	Bitis caudalis
B. gabonica.....	Bitis gabonica

B. nasicornis..... *Bitis nasicornis*
C. durissus..... *Crotalus durissus*
H. haemachatus..... ***Hemachatus haemachatus***
N. pallida..... *Naja pallida*
N. nubiae..... *Naja nubiae*
N. mossambica..... *Naja mossambica*
N. nigricollis..... *Naja nigricollis*
N. subfulva..... *Naja subfulva*
N. nivea..... *Naja nivea*
N. haje..... *Naja haje*
N. annulifera..... *Naja annulifera*
N. naja..... *Naja naja*
N. siamensis..... *Naja siamensis*
N. philippinensis..... *Naja philippinensis*
N. atra..... *Naja atra*
N. kaouthia..... *Naja kaouthia*
O. hannah..... *Ophiophagus hannah*

Silk

B. mori.....***Bombix mori***
N. edulis.....***Nephila edulis***
A. pernyi.....***Antheraea pernyi***

Others

O. vulgaris..... *Octopus vulgaris*
H. suspectum..... *Heloderma suspectum*
E. goliath..... *Eptatretus goliath*
E. rowelli..... *Euperipatoides rowelli*

Techniques

Ultraviolet-visible Spectroscopy (UV-vis)

A..... Absorbance, a.u.
b..... Path length, cm
C..... Concentration, mol/L
 ϵ Molar absorptivity or molar extinction coefficient, L/mol.cm

Fourier Transform Infrared Spectroscopy (FTIR)

ATR.....	Attenuated Total Reflection
d_p	Depth of penetration, nm
λ	Wavelength of the light, nm
θ	Angle of incidence, °
n_1	Refractive index of the crystal
n_2	Refractive index of the sample
a.u.....	Arbitrary units

Sodium Dodecyl Sulphate–Polyacrylamide Gel Electrophoresis (SDS-PAGE)

R_f	Relative electrophoretic mobility
kDa.....	kilodalton
M.W.....	Molecular weight

Differential Scanning Calorimetry (DSC)

ΔH	Enthalpy of denaturation, J/mol
T_0	Initial temperature, °C
T_1	Final temperature, °C
ΔC_p	Heat capacity change, J/mol °C
ΔT	Temperature difference, °C
T_g	Glass transition temperature, °C
W.....	Watt

Rheology

$\dot{\gamma}$	Shear rate, s^{-1}
η	Viscosity, Pa.s
τ	Shear stress, Pa
Pa.....	Pascal
G'	Elastic modulus or storage modulus, Pa
G''	Viscous modulus or loss modulus, Pa
α	Cone angle, °
ω	Angular frequency, rad/sec

Fluid mechanics

Re.....	Reynolds number, dimensionless
ρ	Density, kg/m ³
D.....	Diameter, m
ΔP	Pressure differential, Pa
u_1	Velocity at the inlet point, m/s
u_2	Velocity at the outlet point, m/s
A_1	Cross section area at the inlet point, m ²
A_2	Cross section area at the outlet point, m ²
L.....	Length, m

CHAPTER 1: INTRODUCTION

“I have called this principle, by which each slight variation, if useful, is preserved, by the term of Natural Selection.”
Charles Darwin



This chapter introduces the concept of “ecto-secretion”, defining this term based on examples of materials produced by different species. Then, a comparison between ecto-secretions is provided, where two main groups of these materials are explored in detail: gastropod mucus and snake venom. This chapter also includes a bibliographic review of the information found related to gastropod mucus and venoms, comparing collection and storage methods, and characterisation techniques, in order to identify the gap in knowledge about these two fascinating ecto-secretions. The section “Gastropod Mucus” of this chapter, is based on my contribution to a review paper in preparation “Characterisation of Gastropod Mucus and its applications: A review”.

1.1 WHAT IS AN ECTO-SECRETION AND WHAT ARE REPRESENTATIVE EXAMPLES OF THESE MATERIALS?

Natural selection has led to the development of characteristics amongst species that allow them to adapt to their environment and deal with a range of challenging conditions or changes that may exist [1],[2]. The term ecto-secretion is formed by two words: ecto, derived from Greek *ektos*, meaning “outside”; and secretion, from a biological perspective defining the cellular process which involves the delivery of substances from the inside to the outside of the cell, transported by secretory vesicles [3], [4]. Therefore, an ecto-secretion is a compound used by species outside their body. Examples of ecto-secretions are some salivas produced by animals, such as predatory molluscs in the Gastropoda and Cephalopoda lineages [5]; silk produced by silkworms and spiders [6]–[8]; mucus produced by snails and slugs in the Gastropoda lineage [9]–[13]; and the venom produced by some animal species, such as cobras and vipers [14]–[16]. In this thesis we will focus on silk, gastropod locomotive mucus and snake venom.

The first example of ecto-secretions is saliva. This material has different functions such as oral digestion, lubrication, protection of soft and hard tissues, and antibacterial and antifungal activities [17]. One interesting example is found in predatory molluscs, such as octopuses in the class Cephalopoda, which produce ecto-secretions containing toxic substances [5]. This saliva consists of glycoproteins associated with mucus, and also contains hyaluronidase, an enzyme that decomposes hyaluronic acid into monosaccharides, to increase membrane

permeability by increasing molecular movement, and as a consequence facilitating the flow of the viscous mucus throughout the prey item [18]. Other proteins are also present, one of them named in the early 1960's as cephalotoxin [19]. In the species *O. vulgaris* (figure 1.1) two of these toxins were characterised by Cariello and Zanetti [20], where in prey such as crabs, these toxins can cause paralysis [19].

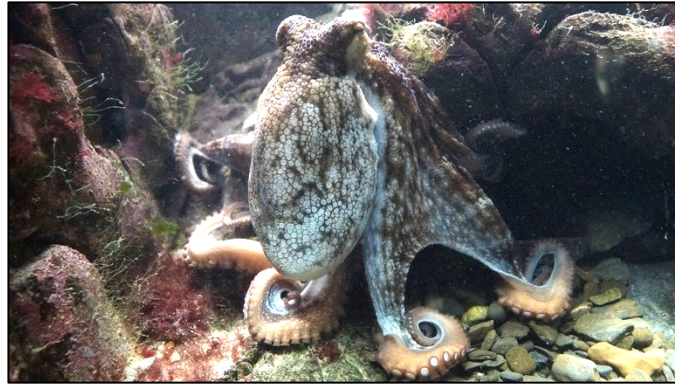


FIGURE 1.1 Common octopus, *O. vulgaris*. Credit: <https://pixabay.com/photos/octopus-kraken-octopus-vulgaris-428745/>

The second example is silk. Since ancient times, silk has been of strong interest to people for its high commercial value (the Silk Road), and for the luxury of the material itself. Today, this material continues to amaze us because of the great diversity of clothes that can be made with it and the wide range of fashion items that are designed every day. But silk, is more than a nice material to create clothing: it is a biomaterial with extraordinary mechanical properties [7], [21]–[27].

Silkworm silk is a natural protein fibre produced by insects in the order Lepidoptera such as *B. mori*, and it is used to protect the larva from external factors, such as the environment or predation, during metamorphosis [28]. Silk consists of two major protein components: fibroin, which makes the fibres (70 - 80 %); and sericin (20 - 30 %), which binds fibres together. [29], [30] Fibroin consists of heavy and light chain proteins, 390 and 26 kDa, respectively [31]. Sericin is a globular protein soluble in water, containing primary random coil and β -sheet structures [32]. Figure 1.2 shows the species *B. mori*: larvae, cocoon and moth.

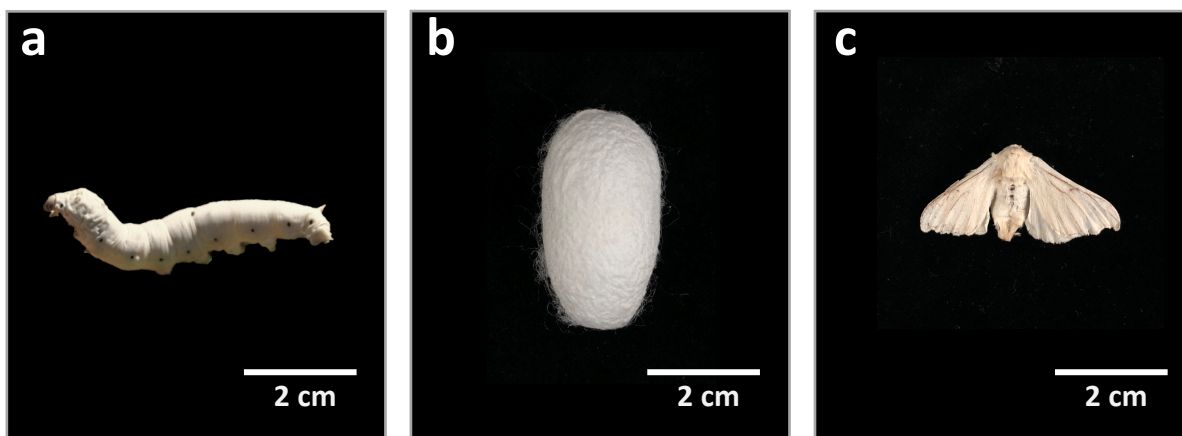


FIGURE 1. 2 *Species B. mori* in the order Lepidoptera: a) Silkworm, b) Cocoon, and c) Silk moth.

Another ecto-secretion is mucus produced by snails and slugs, which allow them to adhere to different surfaces, remaining in horizontal or vertical positions without falling yet still be able to move. From terrestrial to marine snails, they are all characterised by producing compounds that contain proteins and carbohydrates in their structure that give to mucus its particular properties [33]–[41]. This material is explained in detail in section 1.3.

The last example of ecto-secretions in this thesis are venoms produced by snakes, and these are powerful weapons for survival and defence against predators, or as mechanisms to facilitate digestion and obtain food, containing a mixture of toxins and proteins that vary depending on the species [14]–[16], [42]–[45]. Venoms are explained in detail in section 1.4.

These materials as we know them, have been changing over millions of years of evolution, modifying their structure, composition, protein hydration, and function, as a consequence of the survival needs of the animal producing them. Species need to develop adaptations to compete against each other if they want to survive, and different factors influence those changes. This includes the interactions and diversification between species, to deal with a wider range of other living organisms, gaining the ability to live in other environments. [46]. Despite the technological advances in different scientific fields, there are still many questions to be answered and properties to be discovered in the field of ecto-secretions. The correlation between properties will allow us to understand how each one of these materials has specific adaptations that make it suitable and stable for a chemical or mechanical function.

1.2 GASTROPOD MUCUS

1.2.1 DEFINITION, PROPERTIES AND PREVIOUS STUDIES

To understand why this ecto-secretion is unique, we need to start by defining what is a gastropod. Gastropods are snails and slugs in the class Gastropoda, the largest class of molluscs with more than 50,000 species described. These species started its diversification from a common ancestor 540-550 million years ago, by the early Cambrian, and interestingly, the shell of snails have appeared from a mucus coating. [47] The cladogram (Figure 1.3) shows the families within this class, detailing the Stylommatophora clade, where most of the terrestrial snails and slugs belong, including the species explored in this thesis [48]. Gastropods produce three types of non-Newtonian gels: defensive, adhesive and locomotive mucus, the last one which will be studied in detail in this thesis. Animals use this ecto-secretion to move (lubrication), for protection against pathogens, and to adhere to different surfaces. Mucus contains > 98% water and the rest consisting of mucins and other organic and inorganic materials [49]. The most important components in mucus are mucins, proteins highly glycosylated by large numbers of monosaccharides linked glycosidically, conferring mucus its viscoelastic properties [50], [51]. Mucins in gastropod mucus have a molecular weight between 50-200 kDa [52].

Since ancient cultures, gastropods have been observed and their behaviour used as indicator of some events, such as harvest time. However, the analysis of gastropod locomotion was not reported in more detail until the 1920s, where a study discussed wave deformations during slugs' locomotion [53]. Although in the 1980's more detailed studies described other characteristics of gastropods, such as their adhesive or locomotive mucus [54], until now there are no reports correlating the structure and function of this material. Two areas of study seem to be exclusive: adhesive and locomotive mucus.

To gain more knowledge in our understanding of gastropod mucus' function, its compositional, thermal and mechanical (rheological) properties need to be characterised. In the past, they have been analysed, and studies have been carried out in the three categories of gastropods: marine, freshwater and terrestrial, analysing their mucus from different perspectives and approaches. For the purposes of this thesis, a detailed analysis of the

literature up to 2021 was undertaken and it is shown in Table 1.1 To do this analysis only literature was included where gastropod mucus was collected from the animal's foot and where no animals were killed. Studies were classified depending on the type of mucus (adhesive or locomotive), as well as the characterised property (compositional, thermal, structural or functional). A distinction is also included in Table 1.1, corresponding to research group (life or physical sciences), this was classified based on author's affiliations; and species are related according to the cladogram in figure 1.3.

Certain families, and more specifically species, have been studied more, such as *A. columbianus* [55]–[58] or *A. subfuscus* [34], [59]–[65], and others are almost forgotten. This choice of gastropod to study can be attributed to the ease and availability of finding and maintaining certain species in the laboratory, or perhaps to build on previous studies showing great potential in the gastropod mucus in question.

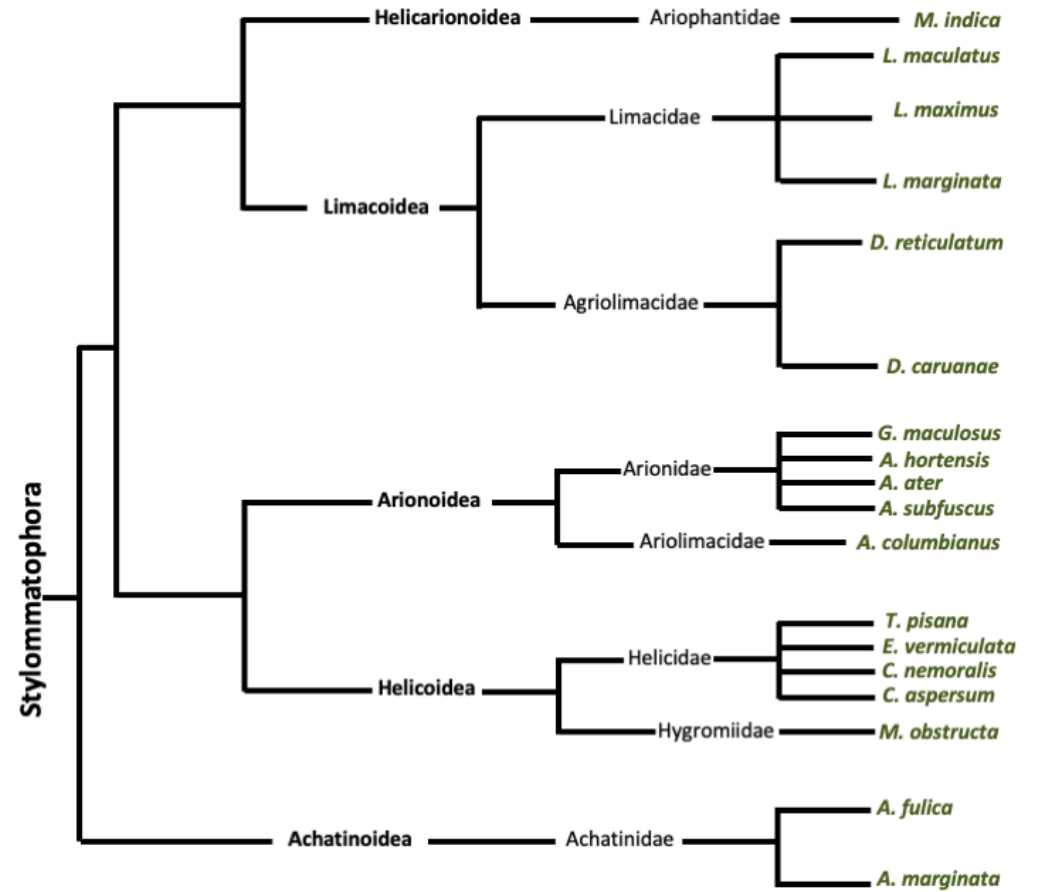
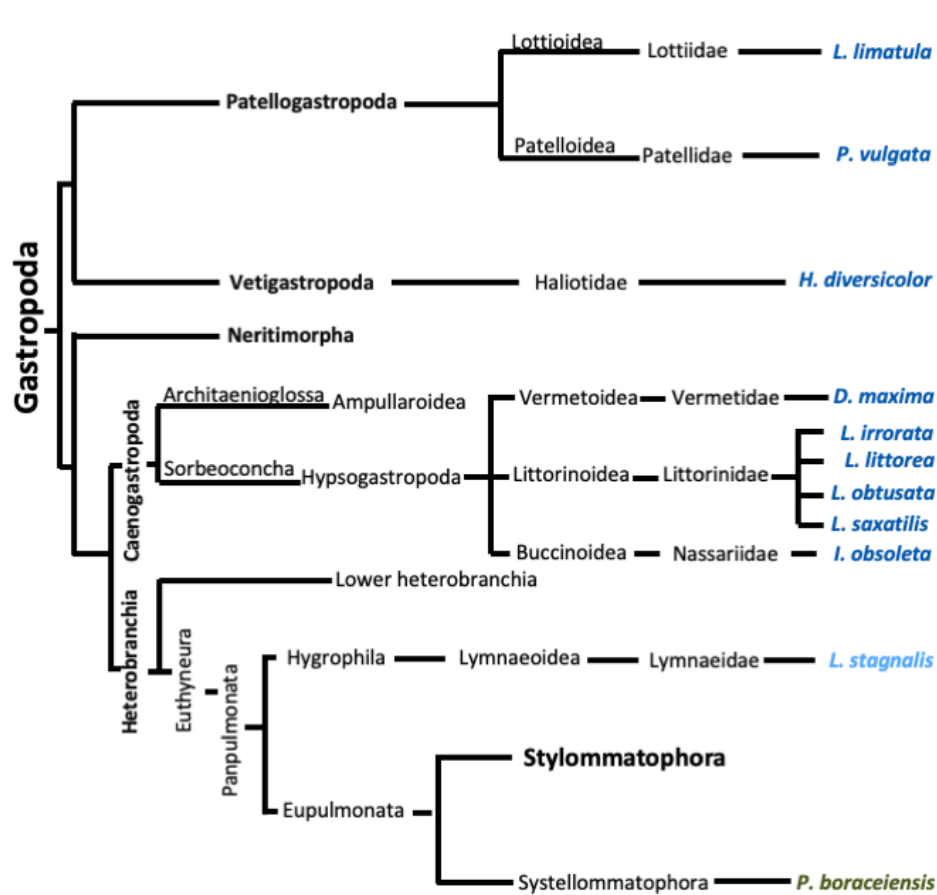


FIGURE 1.3 Cladogram of a) Class Gastropoda, b) Order Stylommatophora, based on [9], [13], [66]–[75].

TABLE 1. 1 List of species reported in literature, classified according to figure 3. Coloured cells represent the collection and storage method, and property and technique. Letters A and L represent Adhesive or Locomotive mucus, respectively. 1-31 represent the reference numbers. Pink numbers indicate **Life sciences**, in blue **Physical sciences**, and in black, **both** Life and Physical sciences groups.

SPECIES	Type of mucus	COLLECTION METHOD		STORAGE METHOD			PROPERTY AND TECHNIQUE							
		Sterile glass rod /Glass slide/direct stimulation of gastropod foot	Sterile razor blades/metal spatula/forceps/plastic straws	Room temperature	Cold (1-10 °C)	Frozen	Compositional			Thermal	Structural		Functional	
							FTIR	SDS-PAGE/DGGE	Chromatography/Mass and/or absorption spectrometry		TGA	Optical microscopy	Electron microscopy	Rheology
<i>L. limatula</i>	A, L	1	1			1		1				1		
<i>P. vulgata</i>	L	2	3	2,3	3				2	3		2		
<i>H. diversicolor</i>	A	4	4	4				4			4			
<i>D. maxima</i>	A		5	5					5					
<i>L. irrorata</i>	A	6	6	7		6		6,7	6					
	L		7	7				7						7
<i>L. littorea</i>	L	8		8		8						8		
<i>L. obtusata</i>	L	8		8		8						8		
<i>L. saxatilis</i>	L	8		8		8						8		
<i>I. obsoleta</i>	L		9	9							9			
<i>L. stagnalis</i>	L	10		10				10						
<i>M. indica</i>	A		11	11									11	11
<i>L. maculatus</i>	L	10		10				10						
<i>L. maximus</i>	A	12	13	12, 13								12	13	
	L	12	13,14	12-14								12	13, 14	
<i>L. marginata</i>	L		15			15						15		
<i>D. reticulatum</i>	L	10	15	10		15	10					15		
<i>D. caruanae</i>	L	10		10			10							
<i>G. maculosus</i>	L		15			15						15		
<i>A. hortensis</i>	L	10		10			10							
<i>A. ater</i>	A	12		12								12		
	L	10,12,16		10, 12	16		10	16	16			12		
<i>A. subfuscus</i>	A	17-19,20	20,21-23	17, 19		18, 20-23		17-19, 21	17,19, 20			17,2 2	22, 23	21, 23
	L	10		10			10							
<i>A. columbianus</i>	A	12		12								12		
	L	12,24-26		12, 24-26								12	24-26	
<i>T. pisana</i>	L	27				27		27						
<i>E. vermiculata</i>	L	27				27		27						
<i>C. nemoralis</i>	L	10		10			10							
<i>C. aspersum</i>	A	20	20			20	20	20						
	L	10, 20	13	10, 13			10	20	20				13	
<i>M. obstructa</i>	L	27				27		27						
<i>A. fulica</i>	L	28,29		29		28	28			28	28,2 9	29	28	28
<i>A. marginata</i>	L	30		30			30							
<i>P. boraceiensis</i>	L	31				31						31	31	

List of studies included in table 1: **1** [76], **2** [77] **3** [78], **4** [79] **5** [80], **6** [81], **7** [49], **8** [82], **9** [83], **10** [59], **11** [33], **12** [55], **13** [34], **14** [84], **15** [85], **16** [52], **17** [60], **18** [34], **19** [61], **20** [62], **21** [63], **22** [64], **23** [65], **24** [56], **25** [57], **26** [58], **27** [86], **28** [87], **29** [35], **30** [36], **31** [88]

The mucus collection process is as important as the selection of the species to be studied, since it has been reported that proteins undergo denaturation by mechanical processes [89]. Additionally, handling the animal during the collection process, could generate stress on the gastropod changing the mucus composition. For example, it has been reported that slugs can increase the production of minerals, such as calcium by external stimuli [85]. Of 29 species included in 32 studies, in 79.3 % the collection method consisted of razor blades to collect mucus from the foot of the animal.

There are three categories of storage described in table 1.1, in which mucus has been stored once collected: at room temperature, cold, or frozen. Samples of 23 species were stored at room temperature for later characterisation, and samples from two species were stored at temperatures between 1 to 10 °C. Although the procedures for collection and storage have been reported in these studies, there is no study that analyses the effect of collection or storage method on gastropod mucus' properties. It is likely that temperature will have an effect on the modification or stabilization of the proteins in mucins, the main components in gastropod mucus [90], [91].

Regarding the properties of gastropod mucus, in my literature review analysis I classified them into four categories:

1.- Compositional: including Fourier Transform Infrared Spectroscopy (FTIR), in order to determine the functional groups of organic compounds in mucus; Sodium Dodecyl Sulphate Polyacrylamide Gel Electrophoresis (SDS-PAGE), to separate the different groups of proteins in mucus; chromatography and mass spectrometry, to determine the organic and inorganic materials in mucus, as well as the molecular weights of proteins.

2.- Thermal: in this category only Thermogravimetric Analysis (TGA) is considered, where the quantity of dry mucus with respect to the fresh mucus was determined in the studies considered.

3.- Structural: including Optical Microscopy, to analyse mucus trails; and Scanning Electron Microscopy (SEM), to perform X-ray compositional analysis under SEM and to determine trails mucus morphologies.

4.- Functional: including Rheology, to determine the flow behaviour of mucus; and tensile testing, to determine the force required to break the adhesive mucus, i.e., its tensile strength.

Of the species examined, compositional properties were characterised in 19 of them; thermal properties in 2; structural properties in 16; and mechanical (functional) properties in 7. Thus, the broadest knowledge gained from the characterisation of gastropod mucus corresponds to compositional properties. Of the studies carried out on this topic, only one on *A. fulica* mucus [87], included the four groups of properties, where the correlation between mucus' composition with its function and thermal stability is described.

It is crucial to note that only one study covered nine different species [59], including terrestrial and freshwater gastropods, but only compositional properties of mucus by FTIR were characterised. In line with this, perhaps the characterisation method chosen by scientists to study the species described in Table 1.1, is also related to the fact that the topic has been approached fundamentally from two angles: life and physical sciences. Although the properties of gastropod mucus analysed in these studies have already been indicated, other important aspects are the groups of species (marine, freshwater or terrestrial), the two types of mucus studied (adhesive or locomotive), and the two research groups (life or physical sciences). Based on this, figure 1.4 shows the three groups of gastropods, with the studies that have been carried out in relation to adhesive or locomotive mucus, the percentages of each property analysed, and classified by research group.

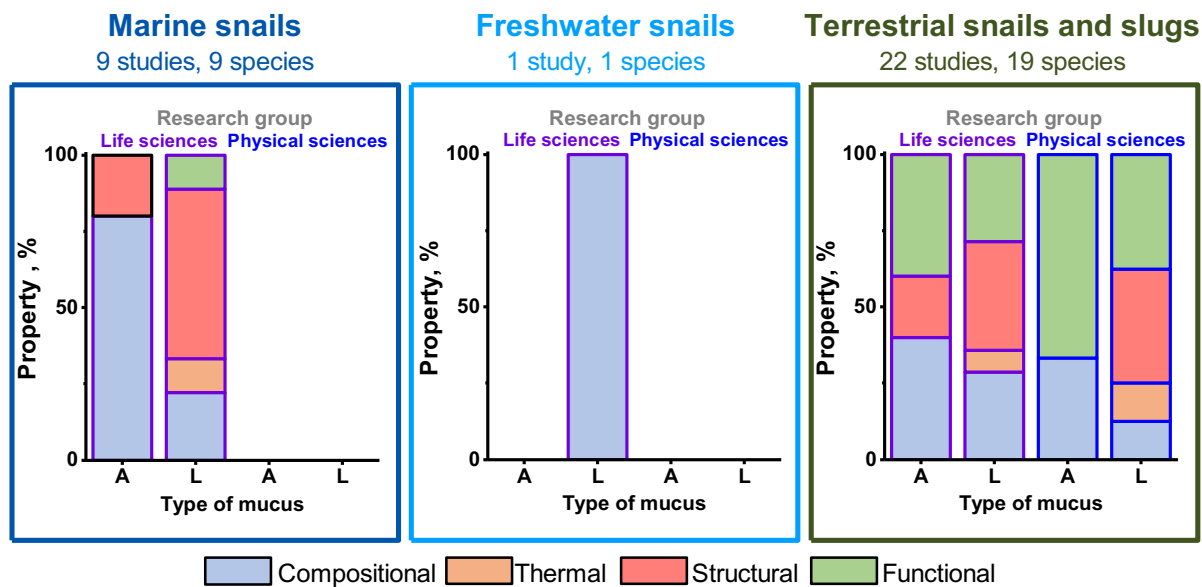


FIGURE 1.4 Classification of studies by research group, analysing adhesive or locomotive mucus according to four types of properties (compositional, thermal, structural and functional), based on table 1.1

From figure 1.4, marine snails correspond to 28.1% of the total studies, with 9 species analysed, and no studies have been reported by groups of physical scientists, only by life scientists. This fact can be attributed to the type of environment in which these species are found, the collection and storage methods in the laboratory, as well as the procedures for mucus collection. The two types of mucus have been analysed, and mainly compositional properties of adhesive mucus has been characterised. Structural aspects of locomotive mucus represent the most relevant in these studies, such as microanalysis by SEM and analysis of mucus trials. Freshwater snails correspond to 3.1% of the studies, which represents only one study and just one species, carried out by a research group of life sciences regarding to locomotive mucus, and characterising compositional properties, more specifically, by FTIR.

Finally, 68.7% of the total studies correspond to terrestrial gastropods, and 94.7% of them to the Stylommatophora clade, probably due to the ease of finding, collecting and maintaining species in the laboratory, in addition to the fact that this clade represents the majority of terrestrial gastropods [12]. In this group, both categories, life and physical sciences, have analysed species. From a life sciences perspective, the two main properties that have been studied in adhesive mucus are compositional and functional, while for locomotive mucus they include structural aspects. The groups of physical scientists have focused their attention on

mechanical (tensile strength) and compositional (molecular weight) properties of adhesive mucus; and structural properties of locomotive mucus, such as mucus trails and crystals formed when mucus is dry. A synergy between both groups, developing even more extensive studies in this field, is necessary, in order to share standardized or successfully tested methodologies, and the selection of representative “model systems” for each group of gastropods (marine, freshwater or terrestrial).

Despite the division of research groups and the exclusive characterisation of gastropod adhesive or locomotive mucus, each one of these studies have contributed to our knowledge on this type of ecto-secretion. The study of aquatic species, such as marine snails in the Littorinidae family, has demonstrated that trail following on deposited mucus reduces the energetic costs associated with mucus production. It has also demonstrated that mucus’ dehydration will reduce its aggregation (trail following) and its effectiveness for microbial growth [49], [76]–[82].

Regarding the study of terrestrial gastropods, four decades ago, pioneering studies were completed by Denny, the first person to study in detail the rheological properties of gastropod mucus, considering the environment and molecular weight as parameters affecting mucus’ viscosity. Denny contributed substantially to bring researchers’ attention to the study of this ecto-secretion, at a time when it was almost forgotten or not explored in detail. His research including the slug *A. columbianus*, answered some important questions regarding the relationship between structure-performance in gastropods, such as how locomotive mucus determines the limitations of gastropod size and speed [56],[57]. Another relevant study was carried out in the year 2000 by Skingsley *et al.*, [59], which included the characterisation of locomotive mucus from freshwater and terrestrial slugs to compare their composition, and to identify the main molecular components in mucus. This was the first detailed study including FTIR to analyse gastropod mucus.

These important contributions to this field opened the door to new studies. However, there are still unexplored areas and gaps that need to be filled. Some important questions remain unanswered, corresponding to each group of properties:

1.- Compositional: do marine, freshwater or terrestrial species have similar water content in their mucus? What is the composition of their mucus? Does mucus in all species show evidence of glycosylation?

2.- Thermal: What is the range of temperatures for mucus to be stable, maintaining its function as an adhesive or lubricant? How do protein secondary structures in mucus change as a response to an increase in temperature? How thermostable is gastropod mucus compared to other ecto-secretions?

3.- Structural: Do mucus trails show crystal growth during the drying process?

4.- Functional: How does molecular diversity affect mucus function?

These questions need to be answered, in order to contribute to our knowledge about gastropod mucus. All techniques detailed in table 1.1 can be transferred to different clades within the Gastropoda class, to learn more about these fascinating materials and their applications. For example, gastropod mucus shows antimicrobial activity [51]; it can be used as an bioindicator for heavy metals in the oceans or to show changes that marine ecosystems undergo as a result of pollution [92]; and to establish what are the locomotion mechanisms in freshwater snails [93]. This will allow us to elucidate more about the potential applications of gastropod mucus in different fields [51], [94]–[96].

1.2.2 APPLICATIONS

Gastropod mucus has been demonstrated to offer a wide range of applications, from soft robotics to super adhesives [49], [95], [97]–[99]. As explained in section 1.2.1, some clades have been studied in more detail than others. Figure 1.5 shows some examples of applications for adhesive and locomotive mucus, which includes super adhesives; skin regeneration products; the design of soft-crawling robots based on gastropods locomotion; and how snail mucus in freshwater and marine snails can be used as a substrate for microbial growth.

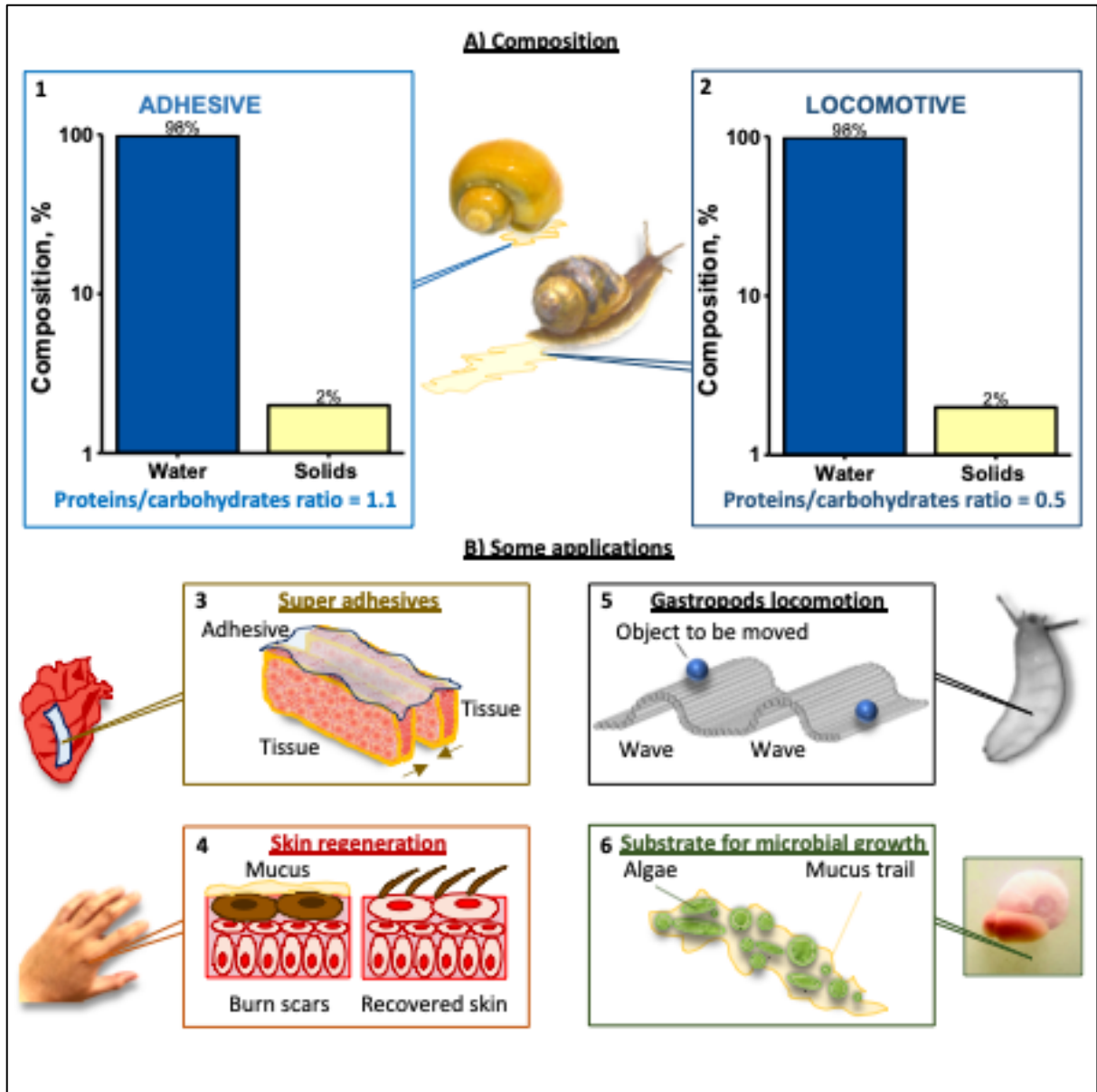


FIGURE 1.5 Gastropod mucus A) composition and B) applications. Numbers refer to data reported by 1 [49], 2 [49], 3 [95], 4 [97], 5 [98], and 6 [99].

1.2.2.1 ADHESIVE MUCUS

Super adhesives

Bio-inspired adhesives have been developed based on adhesive mucus produced by terrestrial snails [100]. However, slug's mucus has been studied in more detail because of its promising properties for medical applications and its toughness as a strong gel, more specifically, the slug *A. subfuscus* [63], [64]. This slug produces an adhesive mucus that forms a strong network between polysaccharides and proteins and its particular metal binding

proteins with a higher concentration than locomotive mucus (higher protein/carbohydrate ratio) [63]. In one study conducted by Li *et al.* [95], the design of bioinspired adhesives based on *A. subfuscus* adhesive mucus was proposed, because the existing adhesives designed for wet surfaces such as internal tissues can be cytotoxic affecting healthy cells, and they do not have strong adhesion to tissues. Contrary to this, the super glue produced by this slug has been demonstrated to have strong adhesion to diverse wet surfaces and due to electrostatic interactions, the glue can adhere to wet surfaces and act as a heart sealant [95].

Skin regeneration

It has been demonstrated that mucins in snail mucus can induce cell proliferation [88], but also *A. fulica* and *C. aspersum* mucus have antibacterial properties [101], and an antioxidant effect due to the glycosaminoglycans in mucus. As a result, snail mucus has been used in cosmetology and beauty care, for skin regeneration and also to treat dermatitis and burns [102], [103]. In one study conducted in 2009 by Tsoutsos *et al.* [97], they tested the efficacy of a repair cream containing 80 % of snail extract obtained from *C. aspersum* mucus, applied on deep partial thickness burns in adult humans. Results were visible on patient's skin between 12-14 days or until complete epithelialization, showing the healing effect of snail mucus on promoting cell proliferation and regeneration.

1.2.2.1 LOCOMOTIVE MUCUS

Soft-crawling robots based on gastropods locomotion

Soft-crawling robots, with designs based on gastropod's locomotion, have been developed during the past five years and are gaining more interest due to the high versatility and wide range of possible applications [98], [104], [105]. For example, a soft pneumatic actuator, consisting of a flexible material which can change its shape and size as a consequence of an external stimulus such as electricity or other type of energy, has been proposed for medical uses, especially for gastrointestinal endoscopy. This is because the current protocols and instruments used for this procedure have some disadvantages, such as the discomfort caused by a non-highly flexible apparatus [104]. Another design is a micro scale robot, based on

snail's locomotion and pedal waves, consisting of a 50 μm thick crystalline polymeric film with an area of 30 mm^2 , deformable by stimulation with light in order to generate the snail based pedal waves [105]. Another soft-robot consisting of flexible rubber tubes moved by pneumatics can recreate pedal waves, such as those produced when snails or slugs move, and this design can be used to move objects without damage and under irregular surfaces [98].

Substrate for microbial growth

In aquatic snails, locomotive mucus plays different roles apart from being a lubricant, it can help snails to obtain food that is attached to the mucus trail. It also facilitates microbial growth and has the ability to behave as a fertilizer for algae and other microscopic organisms, due to the presence of mineral ions and organic components, such as proteins and carbohydrates [99]. In addition, snails can be used to determine the concentrations of pollutants in their environment, i.e., they can be used as bioindicators if their trail mucus composition and microbial organisms deposited are analysed and tracked, to identify high concentrations of heavy metals or abnormal microbial growth or absence [106].

These applications based on gastropod locomotion and mucus have been explored more in recent years with a high potential in the medical field and micro and nano-engineering. This mucus has potential not only for its high versatility, but also for its biocompatible and biodegradable properties. The design of more complex soft structures is in process in many studies. This work will progress more successfully if gastropods are explored in more detail and if we know more about their peculiar characteristics, and of course, their distinctive ecto-secretions.

1.3. SNAKE VENOM

1.3.1 DEFINITION, PROPERTIES AND PREVIOUS STUDIES

Venom is another ecto-secretion produced by specialised glands in the body of the snake, it consists of a complex mixture of proteins and other organic compounds, which can be delivered using specific mechanisms [15], [16], [107], [108]. Phylogenetic analyses indicate that snake venom glands evolved 60-80 million years ago, and some venom toxins evolved from a single ribonuclease ancestor. [109] Snakes use venom for predation, protection and digestion [110]. This ecto-secretion has a different composition between species and is a clear example of how evolution has modified a material to become a potent weapon with properties and characteristics to be explored [111]. One study conducted in 2004 by Li *et al.* [112] identified 74 different components in snake venom, as a result they classified cobra venom as cytotoxic, and the one in vipers (venomous snakes in the Viperidae family) as haemotoxic. They compared the main biochemical differences in both groups of snakes, attributing the major variations to the presence of neurotoxins and absence of metalloproteinases in cobra venom, and the absence of neurotoxins and presence of metalloproteinases in viper venom.

Snake venom has a molecular weight ranging from 6 to 200 kDa, and the main group of components includes 3FTx (three- finger toxins), NUC (nucleases), CRISP (cysteine rich secretory proteins), LAAOs (L-amino acid oxidases), PDE (phosphodiesterases), PLA₂ (phospholipases A₂) and SVMP (snake venom metalloproteinases) [113]. Depending on the amount and presence of these components, venom will be more or less potent [108], [112], [114], [115].

Another interesting aspect about snake venom is related to delivery mechanisms. According to a recent study published in 2020 [111], snakes in the Colubroides clade are the most studied, more specifically their venom systems. In this clade, vipers and elapids are included. Figure 1.6 shows a cladogram of some common elapids and vipers, adapted from [116]. However, viperids separated from elapids about 61 Mya, as a consequence vipers *B. arietans*, *B. caudalis*, *B. gabonica*, *B. nasicornis* and *C. durissus* have not been included in the cladogram, only listed [117].

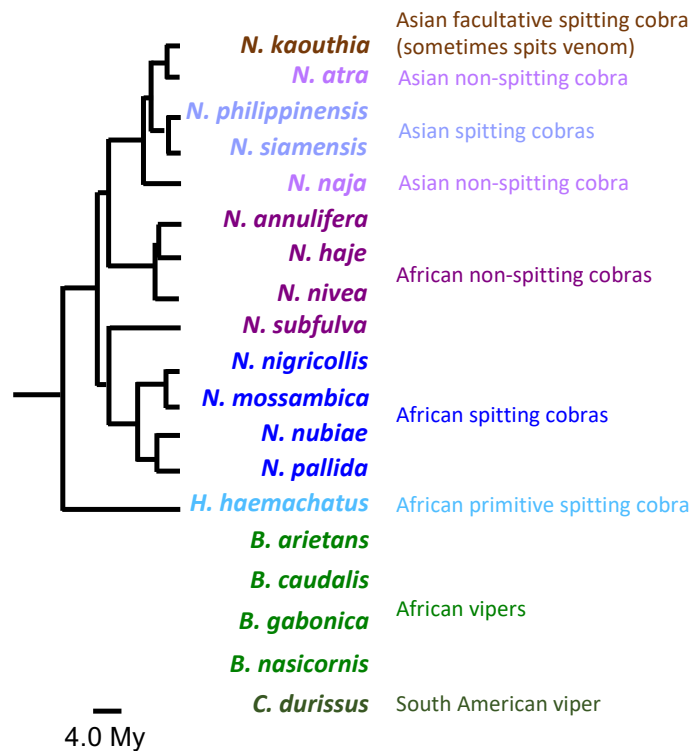


FIGURE 1.6 Cladogram showing the most common African and Asian Elapid species, which are studied in this thesis. Vipers are also listed. Adapted from [116]. The abbreviation “My” refers to million years.

The elapid species included in this cladogram correspond to the majority of Asian and African cobras, all of them will be studied in detail in this thesis. These elapids include *Naja* species, and some of them can spit this potent weapon as a defence mechanism, producing severe damage to the corneal tissue and extreme pain to the predator’s eyes [118], [119]. There are morphological differences in spitting and non-spitting cobras’ fangs. In spitting cobras, the orifice to discharge venom is rigid and as a consequence the process to spit the venom, occurring in milliseconds, requires high accuracy (if spat venom is not in contact with the eyes, then the effect in other external tissues is less severe) and fast movements of their heads [120]. This morphological variability has been investigated in previous studies as have the processes associated during venom spitting. There are two different mechanisms when venom is spat as a continuous horizontal stream, suggesting that fang muscle contraction and an increase in intraglandular pressure produce a pressurised flow [121], [122].

In line with this, another aspect which has been investigated in detail since 1980's is the adaptation of certain *Naja* species to spit venom, focusing on tracking the drops of spat venom using high speed video recording [123], [120], [124], [125]. Another group of researchers focused their attention on the understanding of morphological adaptations in snake fangs and venom channel, and few of them have characterised rheological properties of venom [126], [122], [127], [128], [129]. There is one study carried out in the year 2011 [128], where the effect of surface tension on the process of injecting venom into the prey was analysed. It was also studied in general, whether the venom corresponded to a Newtonian or non-Newtonian fluid, reporting that it is indeed a non-Newtonian fluid, because its viscosity was observed to change with the shear rate [128], [126].

In order to better identify the main areas of research reported before and including vipers and elapids in figure 1.6, table 1.2 shows a classification of techniques used to analyse snake venom from the African primitive spitter (*H. haemachatus*); the most common *Naja* species (African spitters: *N. pallida*, *N. nubiae*, *N. mossambica* and *N. nigricollis*; African non spitters: *N. subfulva*, *N. nivea*, *N. haje* and *N. annulifera*; Asian spitters: *N. philippinensis* and *N. siamensis*; Asian non-spitters: *N. naja* and *N. atra*; and Asian facultative spitter: *N. kaouthia*), African vipers (*B. arietans*, *B. caudalis*, *B. gabonica*, *B. nasicornis*), and the South American viper (*C. durissus*) from a literature review since 1980 to 2021, corresponding to studies where only venom was analysed and not any tissue or other part of the animal was considered. Species are classified according to figure 1.6.

TABLE 1.2 List of the most common *Naja* species and five vipers reported in literature. Coloured cells represent the collection and storage method, property and technique. Numbers 1- 46 represent the references.

SPECIES	COLLECTION METHOD		STORAGE METHOD		PROPERTY AND TECHNIQUE							
	Obtained from the snake, crude venom	Purchased from a company	Cold (1-10 °C)	Frozen	Compositional			Thermal	Structural		Functional	
					Bio-layer interferometry (BLI)	FTIR	SDS-PAGE/DGGE	Chromatography/Mass and/or absorption spectrometry	TGA/DSC	Optical microscopy	Electron microscopy	Rheology
<i>N. kaouthia</i>	1- 8	9- 15	2,9, 14	1,3 - 7, 10 - 15	2		1,3,4 , 6 - 10, 13	5- 15				
<i>N. atra</i>	2, 4, 16 - 21	10, 22, 23	2, 20	4,10, 16- 19, 21, 23	2		4,10, 18, 21, 22	10, 16- 19, 21- 23		20		
<i>N. philippinensis</i>	2		2		2							
<i>N. siamensis</i>	2, 4, 7, 24, 25	10	2, 24	4,7, 10, 25	2		4, 7, 10	7,10, 25				24
<i>N. naja</i>	2, 4	14, 26	2, 14	4, 26	2		4	14	26			
<i>N. annulifera</i>	2, 4		2	4	2		4					
<i>N. haje</i>	2, 4, 7	27	2	4, 7, 27	2		4, 7	7, 27				
<i>N. nivea</i>	2, 4	27, 28	2	4, 27, 28	2		4	27, 28				
<i>N. subfulva</i>	2, 4, 7	27, 28	2	4, 7, 27, 28	2		4, 7	7, 27, 28				
<i>N. nigricollis</i>	2, 7, 16, 24, 29- 32	13, 23, 27, 28, 33- 36	2, 13, 24, 29, 30, 34 - 36	7, 16, 23, 27, 28, 31- 33	2		7, 30, 31, 35	7, 16, 23, 27, 28, 30- 32, 34- 36		33	29, 33	24
<i>N. mossambica</i>	2, 4, 7, 37	23	2	4, 7, 23, 32, 37	2		4, 7, 37	7, 23, 32, 37				
<i>N. nubiae</i>	2	31	2	31	2		31	31				
<i>N. pallida</i>	4, 8, 24, 38	31	2, 24, 38	4, 8, 31	2		4, 8, 31,	31			38	24, 38
<i>H. haemachatus</i>	2	28, 39	2	28, 39	2		39	28, 39			39	
<i>B. arietans</i>	8, 40	41, 42		8, 40- 42			8, 41, 42	40, 41, 42				
<i>B. caudalis</i>		43		43			43	43				
<i>B. gabonica</i>	40, 43	41		40, 41, 43			41, 43	40, 41, 43				

<i>B. nasicornis</i>	40	41, 43		40, 41, 43			41, 43	40, 41, 43				
<i>C. durissus</i>	44, 45	41, 46		41, 44-46		45, 46	41, 44, 45	41, 44	46	45	46	

List of studies included in table 2: **1** [130], **2** [131], **3** [130], **4** [113], **5** [132], **6** [133], **7** [134], **8** [135], **9** [136], **10** [137], **11** [138], **12** [139], **13** [140], **14** [141], **15** [142], **16** [143], **17** [144], **18** [145], **19** [146], **20** [147], **21** [148], **22** [149], **23** [150], **24** [127], **25** [151], **26** [152], **27** [153], **28** [154], **29** [155], **30** [156], **31** [157], **32** [158], **33** [159], **34** [160], **35** [161], **36** [162], **37** [163], **38** [126], **39** [164], **40** [165], **41** [166], **42** [167], **43** [168], **44** [169], **45** [170], **46** [171].

From table 1.2, in terms of venom collection, the two ways for obtaining venom are: directly from the animal (milking) or purchased (from different companies). These collection methods depend on snake's availability, collaboration with research centres, trained technicians to milk snakes, and animal regulations for handling, keeping and working with vertebrates. An important procedure found in 90% of studies is the storage method, based on lyophilised venom once it was collected from the animal, to obtain a dry powder for further analyses. This means it is not possible to carry out functional properties of this ecto-secretion because a fresh wet sample is needed for viscosity tests.

As can be observed in table 1.2, the majority of studies have focused their attention on compositional properties, with two main groups of characterisation techniques: SDS-PAGE and chromatography, mass and/or absorption spectrometry. There are only two studies including FTIR, used to analyse crotoamine, a potent toxin which can penetrate cells causing and promoting necrosis, and this component is found in vipers. Those studies analysed the region between 1800-1600 cm^{-1} , more specifically amide I peaks at 1650 cm^{-1} [170], [171]. There are also two more studies referring to thermal characterisation of some thermostable toxins in the venom of non-spitter cobra *N. naja* and viper *C. durissus* [152], [171]. The rheological and thermal properties of cobra venom have not been analysed together in studies within this review. For example, the use of chromatography, mass spectrometry and SDS-PAGE, is considered in the majority of reports, possibly due to availability, venom complex composition, or perhaps because some analytical techniques are more on the materials and engineering side than in the life sciences field.

From information in table 1.2, a more specific analysis can be done, in order to quantify the percentage of studies focused on spitters, non-spitters and vipers. Figure 1.7 shows a

classification of snakes by behaviour and property percentages based on compositional, thermal, morphological and functional characteristics of snake venom.

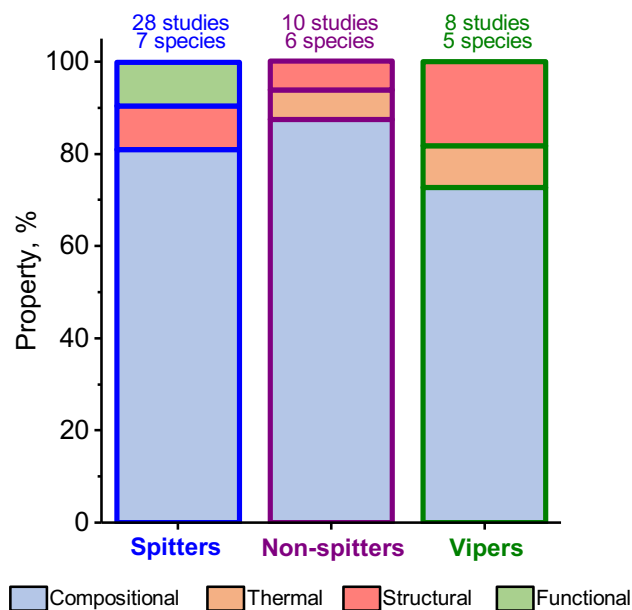


FIGURE 1.7 Classification of studies by snake behaviour (spitting and non-spitting cobras, including Asian and African species; and vipers, including African and the South American species), according to four types of properties: compositional, thermal, structural and functional, based on table 1.2.

According to figure 1.7 the highest number of studies corresponds to spitting cobras, while the lowest to vipers. However, all of them have a percentage from 72 to 87 % of compositional characterisation, which suggests, as previously mentioned, that researchers have focused on the identification and classification of venom’s toxins. This is possibly due to the promising medical applications of several of these components that require a better understanding of which species contains the highest number of specific enzymes such as PLA₂ or SVMP. These approaches have allowed researchers to continue with further studies to identify the post-translational modifications occurring in venom proteins, which cause venom variations and different toxicity.

However, there are areas underexplored and gaps that should be filled to obtain a wider understanding of snake venoms. For the four properties described in table 1.2, these unanswered areas can be grouped as follows:

1.- Compositional: despite the vast majority of snake venom studies includes proteomic characterisation, there are no studies including the analysis of snake venom describing how protein secondary structures vary between species and families, and if these variations can be attributed to the presence of the main components of venom. Another interesting aspect is that all studies reported include the use of very expensive and time-consuming techniques, where others such as a FTIR, could offer a new approach to this field.

2.- Thermal: to understand the thermostability of proteins and their performance at different temperatures. There are no reports studying a wide variety of snake venoms from a thermodynamic approach, where thermal transitions are described and linked to the external hydration state of this ecto-secretion and its composition.

3.- Structural: snake venom affects blood cells morphology, and this has been reported and indicated in table 1.2. However, to my knowledge, there are no studies indicating how this enzymatic activity of snake venom varies when pH is acidic or alkaline, and how this contributes to cells' shape variations.

4.- Functional: the mechanical properties of fresh snake venom remain widely unexplored, and there are no reports including the rheological characterisation of this ecto-secretion, including species from different families, geographical locations and behaviour (spitter or non-spitter).

Correlating these properties in a holistic way, will evidence the complexity of snake venom and the importance of studying this ecto-secretion using a wider range of techniques, to interpret the hydration-function relationships; glycosylation and its thermostability. This will add information about venom's properties to be considered for its applications.

1.3.2 EFFECTS IN HUMANS AND POSSIBLE APPLICATIONS

Due to the high number of components in snake venom, it can cause moderate to severe effects in animals when venom is injected or spat. Some components can have local damage close to the site of the bite, but other toxins have a systemic effect that can cause organ failure, and consequently death, within minutes. In humans, these effects can be severe and worldwide, every year snake bites cause thousands of deaths, reports estimate this at 138,000. The highest numbers of deaths occur in tropical countries and more specifically, rural areas where people are in close contact with snakes [111], [172].

In contrast, the same toxins found in snake venom can be used to treat specific diseases in humans. Some applications have been studied in the past years and many others are in their early stages with promising results. These components in the cocktail of biomolecules in snake venoms could be used to treat diseases such as Alzheimer, cancer or hypertension [15], [42], [43], [45], [173]–[190].

Figure 1.8 shows the five main groups of components identified in snake venom and studied previously as well as some examples of effects in humans when venom is injected or spat. In addition to this, some examples of possible medical applications are included.

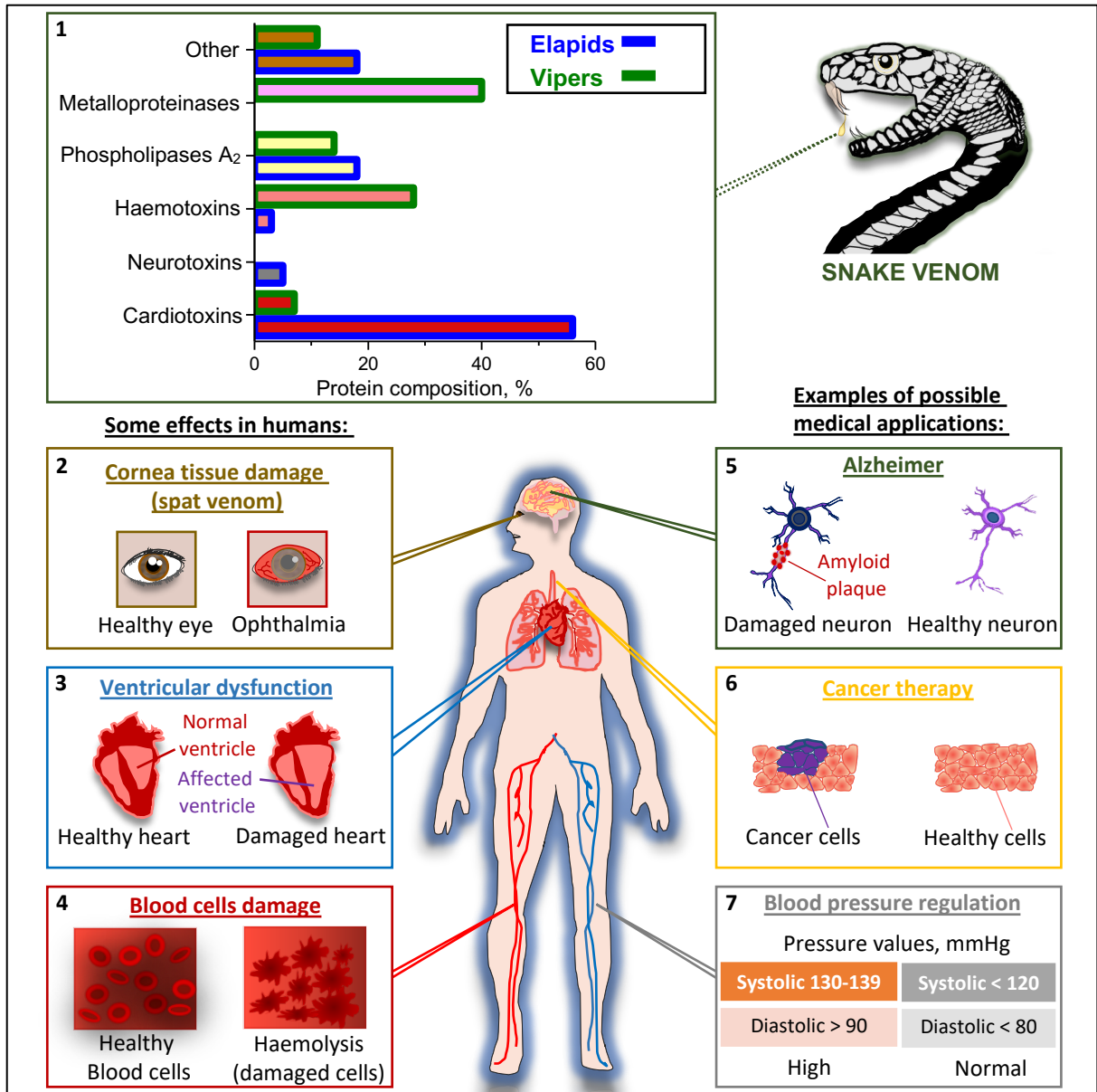


FIGURE 1.8 Snake venom composition, effects in humans and possible medical applications. Numbers refer to data reported by: **1** [112], **2** [191], **3** [192], **4** [181], **5** [193], **6** [194], **7** [195].

1.3.2.1 SNAKE VENOM EFFECTS

Some of the five groups of components in snake venom (Figure 1.8, section 1) are associated with different reactions when a human has been bit or spat at by a snake.

Cornea Tissue Damage (Ophthalmia)

Naja spitting cobras use their fang muscles and venom glands to increase the pressure of the fluid inside, then venom is ejected as a pressurised stream travelling more than 1 meter to finally touch the predator's eyes. This process can be repeated several times and a single spit can contain 0.01 to 0.5ml of venom occurring in approximately 50 milliseconds [120], [196]. The ocular surface of terrestrial animals is protected by a tear film containing several layers and tissues. The first layer consists of different molecules and proteins protecting the eyes against bacteria, as well as providing hydration. When venom is in contact with the eyes, mucins protecting the ocular tissue and cornea are damaged and the severity depends on the volume of spat venom and the time before any treatment is applied. As a result, conjunctivae are affected and the cornea can present patchy edema, and in some cases neovascularization [154], [191].

Ventricular dysfunction

There are reports of multiple organ failure in humans after one or several snake bites associated with the age of the human and with the amount of venom injected. The lungs, brain and heart can suffer several types of damage and as a consequence the death is imminent. The left ventricle of the heart can be strongly affected which leads to death, it can be caused by cardiogenic shock, and multiple infarcts derived from myocardial rupture and infarction. These problems are caused by the cardiotoxins, neurotoxins and haemotoxins in snake venom [192].

Blood cell damage

Haemolysis can be caused by the effect of haemotoxins in snake venom. This problem consists of the destruction of red blood cells (erythrocytes), i.e., modification and destruction of the erythrocyte membrane. Red blood cells are transformed into discocytes or echinocytelike (cells with abnormal membranes, with evenly-spaced spikes on their surfaces), because of morphological modifications of membranes [181]. This will also produce thrombocytopenia due to the reduction in the number of thrombocytes in the blood and consequently the development of thrombosis which can be lethal [192].

1.3.2.2 POSSIBLE MEDICAL APPLICATIONS

Snake venom offers a wide range of potential applications, due to the strong effect of toxins in other organic compounds. Researchers worldwide are studying in detail these components to be able to propose new and novel uses for snake venom in humans. Here, three examples of possible applications are described:

Alzheimer's disease (AD)

Alzheimer's disease (AD) starts with the formation of the amyloid plaque. Studies revealed that the amyloid peptide-42 (A β 42) is more abundant in brains with Alzheimer's, whereas in healthy brains the amyloid peptide-40 (A β 40) is found. In AD the breakdown of the amyloid precursor protein into fragments is one of its characteristics, and one of these fragments is the A β 42 which will form plaques. In AD the amyloid peptide has changed chemically and begins to pair with other protein strands to form a tangle. This causes the microtubules disintegration, collapsing the transport system of neurons, followed by poor communication between neurons and then the death of the cells [193], [197]. Inhibition of the process associated with the amyloid plaque and its destabilization could be useful for prevention and treatment of AD. In line with this, venom of the viper *D. russelli* contains some specific components, for example, phospholipases A₂, hyaluronidases, protease inhibitors, and one component identified as factor V activator (RVV-V). RVV-V is a glycoprotein forming small

peptides, which has been demonstrated in tests *in vitro* to affect A β 42, destabilizing the amyloid aggregate, offering a possible opportunity for the treatment of AD [193].

Cancer therapy

Cancer has been identified as the second most common cause of death in humans (the number one corresponds to cardiovascular diseases), with a 17 % of the total number of deaths worldwide [198]. This disease is characterised by the development of abnormal cells that divide uncontrollably and have the ability to infiltrate and destroy healthy tissue [199]. Different types of scientific approaches against cancer have been investigated and every year new treatments are tested in animals and on human cells. One group of studies is associated with snake venoms, because results revealed that cationic peptides in snake venom are characterised by hydrophobic residues, and using three mechanisms can contribute to tumour cell modification: 1) disruption of the membrane; 2) interfering with nucleic acid and protein synthesis; and 3) immune cell activation [194]. More specifically, crostamine a neurotoxic peptide isolated from the South American viper *C. durissus* has antitumoral properties which have been characterised using *in vitro* and *in vivo* tests. Results revealed that this peptide shows selective cytotoxicity against cancer cells when it is used at concentrations around 5 $\mu\text{g}/\text{ml}$, and in tests using a melanoma mouse model and *in vitro* human melanomas exhibit a significant inhibition of tumour size [200]. Derivates of this component have been designed and researchers are studying other snake species and components in their venoms to develop new possible applications to treat cancer.

Hypertension (blood pressure regulation)

Cardiovascular diseases, including hypertension, are the number one cause of deaths worldwide, according to data published in 2017 by the World Health Organization [201]. There are different factors considered as the main causes of hypertension: stress; high levels of sodium; low levels of potassium and calcium; other chronic diseases like diabetes mellitus; and modifications on adrenergic receptors' function [202]. To treat hypertension, the adrenergic receptors (AR) are crucial, because their guanine nucleotide regulatory protein (G protein)/adenylyl cyclase (AC) is related to the regulation of cardiac function. In the human

heart, there are two types of AR: α and β families [203]. Activation of β -AR increases heart rate, and toxins in venom from elapids and vipers have been studied in order to identify the effect on heart rate frequency and pressure regulation. More specifically, β -cardiotoxins, blocking the β -AR function, from the king cobra *O. Hannah*, have been shown to reduce heart rate in vivo in rats and ex vivo in isolated rat hearts [195].

Toxins in snake venoms attack the organ systems of the prey, in a similar way as doctors using prescription drugs treat patients against different diseases, like pressure regulation to control hypertension. Snake venom toxins have different effects from local to systemic as described before, and the individual effect of each toxin can be used for the development of new synthetic compounds to treat a wide range of top diseases in humans.

1.4. CONCLUSION

Since ancient times, humans have been interested in ecto-secretions. Traditional costumes made with pure silk decorated with vibrant colours were used in Chinese Dynasties, or even decorating metallic objects to enhance their beauty. Gastropods have been used to treat some skin problems in different small towns in Europe, where people believed and even now, that gastropod mucus regenerates damaged skin cells. In Mexico, Aztecs and Mayans made extensive use of snakes not only in religion, but also in food and traditional medicine. And in ancient Egypt, legends surround the death of Cleopatra by a snake bite.

Whatever the reason is, nowadays researchers are intrigued by the unique set of properties these ecto-secretions have, inspiring the creation of new robots; new medicines to treat diseases in humans; to understand more about evolutionary processes that modified animal's behaviours; or to identified and establish links between species in different families. Research groups in both fields, physical and life sciences, are starting to focus on particular properties (compositional, morphological, thermal or functional). However, still now there are no standardised protocols to handle, collect or store some of these ecto-secretions once they have been extracted from the animal, affecting its properties or not giving the opportunity to analyse them in their native state.

There are areas unexplored with gaps to be filled in order to incorporate more details that contribute to our knowledge about these materials. The main gaps identified are:

- If gastropod mucus contains mostly water and only 2% or less of solids (including proteins and carbohydrates), do mucus from different species share similar rheological properties, such as viscosity?
- Mucins in gastropod mucus and how they affect the rheological properties of this ecto-secretion.
- Rheological characterisation of snake venoms including spitting and non-spitting species from different families, and how this affects their behaviour (spitting).
- Thermodynamics of gastropod mucus and snake venom to identify the thermal events and what parameters contribute to their thermostability.
- The relationship between ecto-secretion's function and its compositional and thermal properties.

1.5. THESIS AIM AND OBJECTIVES

1.5.1 AIM

Given that proteins are responsible for ecto-secretions' function, they must have specific adaptations, unlike those used inside the body, to achieve this. However, the understanding of why ecto-secretions behave in those peculiar forms is still unknown. By studying a range of ecto-secretions that have been selected for different functions, such as chemical (venom) and mechanical (mucus and silk), it will be possible to identify some common components and optimisations that proteins require to be used outside of the body in their natural environments. This is most likely related to the precise control and maintenance of protein hydration.

1.5.2 OBJECTIVES

To fulfil this aim, the following objectives have been set:

- Characterise the compositional and mechanical properties of gastropod mucus and snake venom, in order to identify the main parameters contributing to each group of properties.
- Evaluate the effect of temperature on protein stability in gastropod mucus, snake venom and silk.
- Compare compositional and thermal properties of gastropod mucus, snake venom and silk with its function, in order to establish the structure-hydration-function relationship between them.

1.6. CHAPTER INTRODUCTION

This thesis consists of four sections: the introduction, methodology, results and discussion, and conclusions and future outlook, spanning eight chapters as follows:

Chapter 2: Experimental Techniques and Theory

In this chapter, the methods for gastropod mucus and snake venom collection are explained, as well as the principles and theory behind each technique used to analyse compositional, thermal and functional properties of ecto-secretions. Also, criteria for species selection are explained. This will facilitate the understanding of results and will give the reader an overview of how results were obtained.

Chapter 3: Analysis of Gastropod Mucus by Infrared Spectroscopy

This chapter is the first one of gastropod mucus analysis and it describes the characterisation, identification and classification of gastropod mucus by FTIR, including Caenogastropoda and Heterobranchia clades with a total of twelve species. Spectra were analysed from 1800 to 1000 cm^{-1} , including Gaussian fitting and contrasting my results with the only one study about FTIR reported in 2000 by Skingsley *et al.* [59], comparing the different spectral regions to establish the degree of glycosylation, protein ratios, and relationships between mucus by all the gastropods tested. Species were also classified based on their spectral similarities performing a Multivariate Analysis, representing a new methodology applied to gastropod's classification.

Chapter 4: Rheological and Compositional Properties of Gastropod Mucus

In this chapter, compositional and functional properties of six different mucus corresponding to terrestrial gastropods in the Stylommatophora clade are described in detail. Results show that mucins are the main component in mucus in all species tested. Mucins have been adapted to maintain mucus locomotive function and its stability as a lubricant depending on the natural environment.

Chapter 5: Rheological and Compositional Properties of Snake Venom

This chapter is the first one of two corresponding to snake venom. Viperidae and Elapidae families were included in this study in order to compare protein concentration, pH and viscosity of spitting and non-spitting cobras as well as one viper. These analyses determined if venom delivery mechanism and concentration (biting or spitting) affect venom's rheological properties. In order to establish the effect of viscosity on the delivery mechanisms, X-ray microtomography data reported by du Plessis *et al.* [129] were incorporated in flow calculations to obtain pressure requirements inside the venom channel. The main effect in venom delivery mechanism was attributed to morphological adaptations rather than rheological variations.

Chapter 6: Structural Characterisation, Classification and Identification of Snake Venoms

This chapter includes the compositional characterisation of snake venom in families Viperidae and Elapidae combining SDS-PAGE with FTIR, to determine the proteins present, but also to identify structural and compositional variations in snake venom, as a result of thermal stress. In addition, a multivariate analysis was performed to classify snakes based on the hierarchical clustering analysis of FTIR spectra. This approach is a novel strategy to provide new insights into venom's properties, as well as for the identification and classification of species.

Chapter 7: Differential Scanning Calorimetry of Ecto-secretions

This chapter presents a differential scanning calorimetry (DSC) study performed on gastropod locomotive mucus and snake venom. Data previously reported on silkworm silk was included in the analysis. The main thermal events occurring in all ecto-secretions were identified, to link them with the external hydration state. This contributed to elucidate the effect of protein type (globular or fibrous) and glycosylation, on the thermal stability of each ecto-secretion.

Chapter 8: Summary and Future Outlook

The last chapter of my thesis includes the answers to the main research questions, summarising the four groups of properties with their most important parameters, to obtain the Performance Map. It also includes "model" species as the most representative ones for each ecto-secretion. This chapter also incorporates recommendations for future work in other ecto-secretions, such as mucus produced by marine snails or Cephalopods, or the study of other venomous animals in addition to snakes, to expand the knowledge gained with this project to other species.

CHAPTER 2: EXPERIMENTAL TECHNIQUES AND THEORY

“If the experiments which I urge be defective, it cannot be difficult to show the defects, but if valid, then by proving the theory, they must render all objections invalid.” **Isaac Newton**



Experimental techniques and theory are described in this chapter, with the main purpose to help the reader to understand the criteria for species selection and collection methods, and the principle behind each characterisation technique. This information will be useful for the comprehension of the following chapters.

2.1 SPECIES SELECTION

Ecto-secretions included in this study (gastropod mucus and snake venom) were selected as two representative materials which main functions are when they are wet, but also because they have two opposite uses by the animal that can be compared. Gastropod locomotive mucus is used for mechanical roles (locomotion), while snake venom's function is chemical (digestion, defence and predation).

Gastropod and snake species were selected based on different criteria, and they are described as follows.

2.1.1 GASTROPODS

Gastropods can be found in different environments, from land to sea. As explained in Chapter 1, there are no more than a handful of studies including different gastropod mucus properties together (compositional, thermal, morphological and/or functional), and different species. With this in mind, the criteria for gastropod selection included in this study are:

- a) Availability: this is crucial considering that species are not found in cold environments or when the weather is dry and warm (above 20 °C). This limits the selection and collection months in the UK.
- b) Laboratory animal facilities: due to the wide range of gastropod species, some of them require special containers and equipment, which are not always available and require unique installation and permissions. Therefore, marine species were not included in this study. Only terrestrial and freshwater species were considered, in order to adapt their containers for them to live in healthy conditions. No species were damaged or killed during this research.

- c) Clades: gastropods are the most abundant molluscs with more than 50, 000 species included [48], and in order to compare different clades, Heterobranchia and Caenogastropoda clades were included, representing terrestrial gastropods and freshwater snails, respectively.
- d) Mucus production and facility to collect it: species such as the Japanese freshwater snail *C. chinensis*, or the Nerite snail *N. natalensis*, only move if they are in their containers and with no human intervention or disruption to collect the animal for different tests, so these species were discarded. Thus, freshwater snails studied are the only species available and fulfilling this criterion.
- e) Invasive species: Some gastropod species represent a major problem around the world, due to their ability to adapt to different environments. One of these examples is the African snail *A. fulica*, considered a polyphytophagous pest, i.e. can eat different plants, also this species has a high reproductive capacity [204], [205], [206]. These characteristics make this species suitable for study. Even when it represents a problem in different countries, there are interesting properties of its mucus, like antibacterial effects against some microorganisms. Therefore *A. fulica* snail was included in this study.

For gastropods tests, in total 7 species were collected (*C. aspersum*, *C. nemoralis*, *A. ater*, *A. hortensis*, *L. flavus*, *L. maximus* and *L. stagnalis*) and 5 were purchased (*A. fulica*, *L. haroldi*, *V. sloanei*, *M. cornuaretis* and *P. diffusa*), based on the 5 criteria mentioned above.

Figure 2.1 shows the geographical distribution of these species in their natural environments:

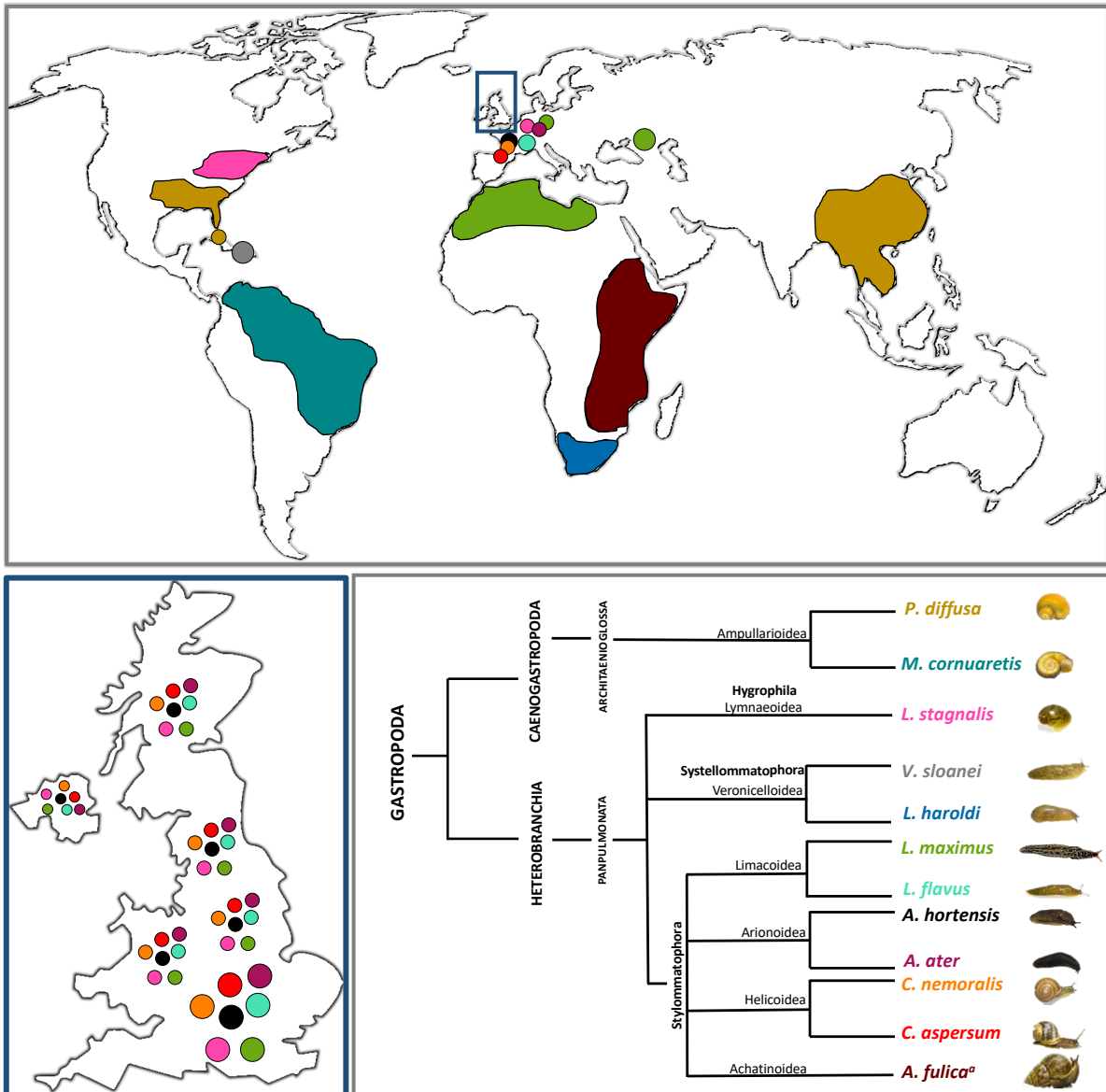


FIGURE 2. 1 Distribution of selected gastropod species. Colours indicate the geographical distribution of each species (highlighting the UK), not considering the non-native countries/continents where they are found, based on [207]. Cladogram extracted from figure 1.3, shows all species, including collected and purchased gastropods. ^a Refers to the African snail found in America, Africa, Asia and Europe as an invasive species.

Figure 2.1 shows the cladogram with selected species found in Africa, America, Asia and Europe, in order to compare properties and results between families, which will be discussed in Chapters 3 and 4. Selected species include tropical freshwater snails and gastropods native from the UK to identify the main variations in their mucus. The African snail is included in this study to compare mucus from a snail native from a different natural environment

(temperature, humidity, food, etc.) with gastropods native from Europe. This will offer insights into the impact of geographical location on locomotive mucus.

2.1.2 SNAKES

Species were selected based on the literature review discussed in Chapter 1, where it is clear the lack of studies including three or the four properties of snake venom (compositional, thermal, morphological or functional), and on the availability of *Naja* cobras and one outgroup (viper) for comparison purposes. This was done in collaboration with the Centre for Snakebite Research & Interventions, at the Liverpool School of Tropical Medicine (LSTM), UK, for several reasons: 1) the maintenance and husbandry of snakes requires special permissions approved by the UK Home Office and the LSTM Animal Welfare and Ethical Review Board; 2) specific health and safety procedures are required, especially when handling venomous and potentially lethal animals in case anyone who is in close contact with these species is bit or spat by the animal; and 3) the availability of antivenom in case there is an accident. At the LSTM, there are standardised protocols to address these issues, which are inspected and approved by the UK Home Office and the LSTM Animal Welfare and Ethical Review Board.

Figure 2.2 shows the geographical distribution of snakes and a cladogram including all species studied in this thesis.

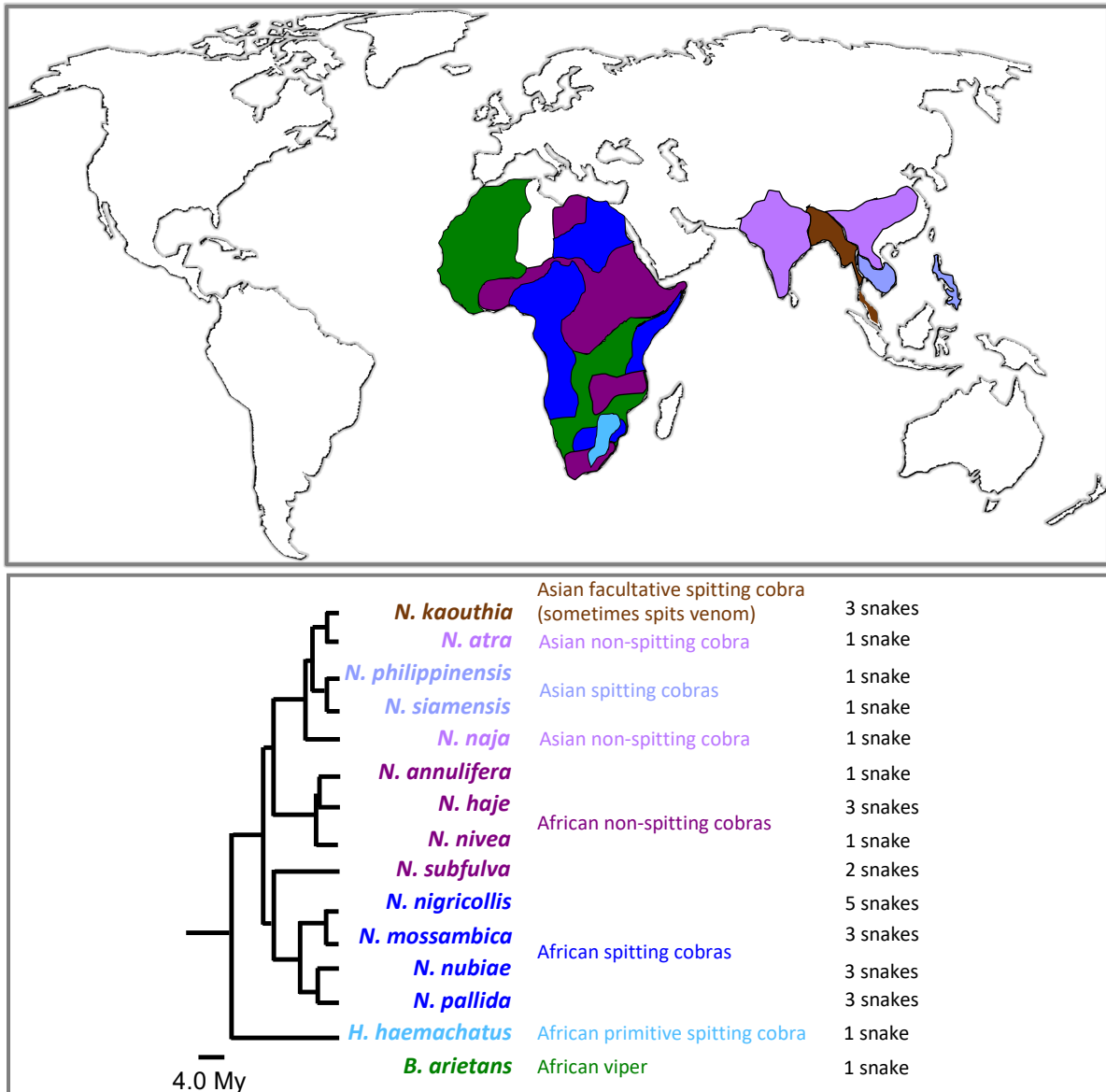


FIGURE 2.2 Geographical distribution of most common African and Asian *Naja* species, African primitive spitter *H. haemachatus*, and viper *B. arietans*. Colours indicate the geographical distribution of each species adapted from [113] and based on [208]. Cladogram extracted from figure 1.6, shows the list of species included in this study indicating the number of analysed snakes from each species and available at the LSTM.

From figure 2.2, most African territory occupied by *Naja* species is considered in this study, with the spitting, non-spitting cobras and viper. The Asian area where *Naja* cobras are found includes most of China, India, Thailand and the Philippines.

Once species have been collected, selected or purchased (gastropods), the next step is to collect the ecto-secretion, considering the available options and the different positive and negative effects they could have on the nature of this material.

2.2 ECTO-SECRETIONS COLLECTION

In all scientific areas, physical or life sciences, sample collection has a crucial effect on results, due to the effects each process can have on the sample, altering its nature, and as a consequence, modifying its compositional, thermal, morphological and/or functional properties. Another factor to consider is the knowledge on how to collect and store samples once extracted from the animal. Gastropod mucus and snake venom collection methods are explained in this section.

2.2.1 GASTROPOD MUCUS

As described in table 1.1 in Chapter 1, there are different methods used to collect terrestrial gastropod mucus reported in the literature from 1980 to 2021: 1) using a sterile glass rod on the foot of the gastropod; 2) direct stimulation of gastropod's foot by mechanical or electrical stimulation; 3) using sterile razor blades to collect the mucus behind the gastropod; and 4) using forceps or plastic straws (mostly for the adhesive mucus collection). All results presented in this thesis, related to gastropod mucus, correspond to locomotive mucus, and with this in mind, table 2.1 shows a comparison between the collection methods reported in other studies.

TABLE 2.1. A comparison between the different collection methods of gastropod locomotive mucus reported in the literature

Collection method	Effect on the animal	Effect on mucus
Sterile glass rod/Glass slide/direct mechanical or electrical stimulation of gastropod's foot	Stress and could cause the death of the animal due to the hyperproduction of mucus	Mucus collected from stressed animals can have different chemical composition, more specifically calcium concentration [85]
Sterile razor blades/metal spatula to collect mucus behind the gastropod	None, as mucus is collected behind the snail (trail of mucus), when animal is moving freely on a glass sheet	If mucus is not collected immediately, evaporation can occur, and dry mucus will be collected instead of fresh native one

Based on table 2.1, the best collection method for terrestrial gastropod mucus corresponds to the use of sterile razor blades, used while the snail is moving across a sheet of glass, to scrape up the fresh mucus from the smooth surface of the glass. Then mucus is transferred to a clean plastic Eppendorf centrifuge 1 ml tube to be used within 12 hours, i.e., immediately and the same day after being collected.

Freshwater snails are considered only for Fourier transform infrared spectroscopy (FTIR) characterisation, due to the difficulty to collect fresh mucus from an aqueous environment where mucus is dissolved. For these tests, freshwater snails were removed from their tanks, cleaned with type I water and then put in a clean Petri dish with 10 ml of water, to allow them to move and produce locomotive mucus for 10 minutes. After this period, snails were carefully removed from the plastic container and put close to the attenuated total reflectance crystal of the FTIR crystal to allow them to move for 1 minute, before returning animals to their tanks.

2.2.2 SNAKE VENOM

Snake venom can be obtained by a number of different procedures, but the most common and used these days is by massaging the venom glands, followed by the injection of venom into a sterile Petri dish or other container covered with parafilm, also known as the “milk” process [114]. This procedure is showed in figure 2.3.



FIGURE 2.3 Snake venom obtention manually by massaging venom glands.

Although the manual procedure to extract venom is used worldwide, there are some important considerations to keep in mind:

- Young snakes (< 3 years) could suffer glands traumatism and it could be potentially lethal for animals [114].
- According to procedures at the LSTM, snakes are milked once a month only if needed, in order to avoid infections, traumatism and irreversible gland damage to the animal.
- Sometimes due to the stress caused to the animal during venom extraction, snakes bite themselves producing some bleeding that can contaminate the venom. In these cases, samples are not considered.

All species showed in the cladogram in figure 2.2 were milked to extract their venom. Each native venom sample was transferred immediately into a sterile plastic Eppendorf 2 ml tube, and transported on ice from Liverpool to Sheffield, to carry on all the characterisation tests. As all species are available at the LSTM, there was no need to purchase any venom.

2.3 CHARACTERISATION TECHNIQUES

A wide range of techniques exists that can be used for materials characterisation, and depending on the type of material to be analysed, there are important aspects to be considered [209]:

- Sensitivity of the technique.
- Amount of sample required for the analysis.
- Time required for sample preparation and analysis.
- Previous knowledge of the technique, i.e., user expertise required.
- Availability
- Cost

These aspects can be included for different types of materials' characterisation (metals, polymers, ceramics and composites), and for natural and synthetic materials. Apart from these points, other details to think about are:

- What information can be obtained from each technique?
- Is the information obtained from that technique valuable for my research?
- Is the characterisation technique destructive or non-destructive?
- Is there another technique which can be used easily?

Considering all these points, for the characterisation of gastropod mucus and snake venom, there are six techniques that were chosen from a larger group available at the University of Sheffield and other institutions, and classified according to the property characterised:

- **Compositional:** UV-vis spectroscopy (UV-vis), Fourier transform infrared spectroscopy (FTIR), and sodium dodecyl sulphate-polyacrylamide gel electrophoresis (SDS-PAGE).
- **Thermal:** thermogravimetric analysis (TGA), differential scanning calorimetry (DSC) and rheology (ramp temperature tests).
- **Functional:** rheology.

Figure 2.4 shows the techniques indicating some examples of the information that can be obtained from each one.

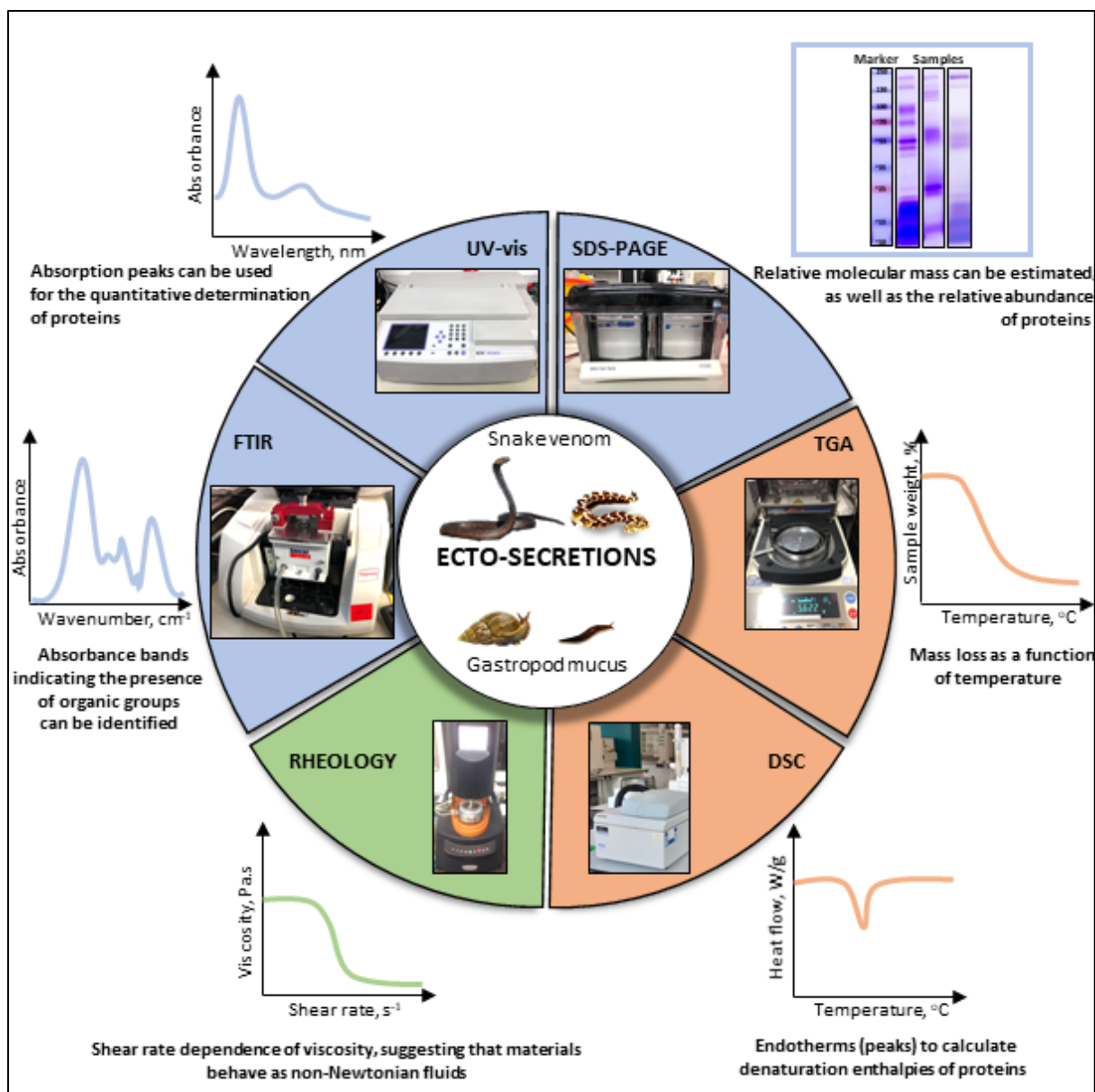


FIGURE 2.4 Characterisation techniques used to analyse ecto-secretions.

Protein concentration can be estimated from UV-Vis, based on absorption peaks and Lambert-Beer law [210]. FTIR provides absorbance bands which can be used to identify organic groups such as those associated with proteins and carbohydrates [211]; and SDS-PAGE is used to identify which group of proteins is more abundant in one sample based on their relative molecular weights [212]. TGA provides information about volatile compounds in one sample as well as the total solids present [213]; and DSC is a useful technique which gives us information about thermal stability of proteins, when the material is heated up [214].

Finally, rheology in general is used when flow behaviour and deformation of a material needs to be described, for example to study the viscoelastic behaviour of protein systems [215]. Each technique is explained in detail, including its principle and how the instrument works.

2.3.1 UV-VIS

UV-Vis spectroscopy consists of the absorption of ultraviolet-visible radiation (with a wavelength range between 200 and 800 nm) by a molecule. This process of absorbing radiation causes an electron to go from its ground state to an excited one. The electrons in molecules are those that are excited during this radiation absorption process and the absorption spectra and their maximum peaks are then associated with different types of bonds present in the analysed material. This is why UV-vis spectroscopy is widely used in the identification of functional groups in a molecule. A particular characteristic of this technique is the width of the bands that appear in a UV-Vis spectrum, and it is due to the superposition of vibrational and electronic transitions [210].

The mathematical relationship between sample concentration and absorbance, can be explained by the Beer-Lambert law [216]:

$$A = \log_{10} \frac{I_0}{I} = \epsilon \cdot b \cdot C$$

Where:

A = absorbance, a.u.

b = path length, cm

C = concentration, mol/L

ϵ = molar absorptivity or molar extinction coefficient, in L/mol·cm, and it is characteristic of each chemical species, representing how well the material absorbs light at a specific wavelength.

Figure 2.5 shows a schematic representation of the UV-vis spectrometer.

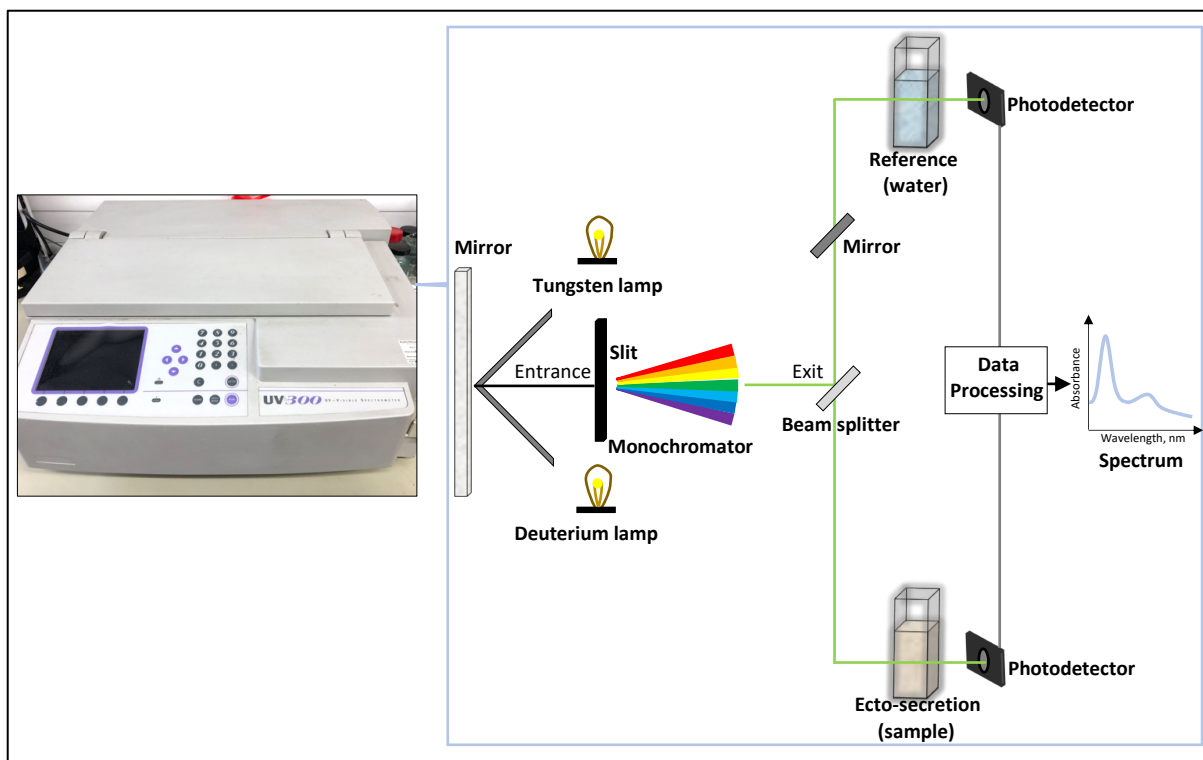


FIGURE 2.5 Diagram showing how a double beam UV-vis spectrometer operates. Schematic representation is based on [210].

According to figure 2.5, both lamps emit different types of light: the tungsten one corresponds to the visible light, while the deuterium lamp generates ultraviolet light. The emitted electromagnetic radiation is directed to the monochromator, which selects the corresponding wavelength to the sample. Then, the beam-splitter directs the light source through the cuvette with the sample to be analysed, for example an ecto-secretion (sometimes diluted in water if native sample consists of a non-translucid material, such as snake venom); the other cuvette contains the reference. If samples are diluted in distilled water, then the reference will contain the same type of water. And finally, the photodetector records the transmitted light and the signal is processed and the spectrum displayed on the monitor [210].

This technique can be used in the analysis of a wide range of materials, and its main applications include:

- Identification of metals in coordination compounds
- Colorimetric identifications
- Determination of the degradation process of organic dyes caused by photocatalysis

- Semiconductor analysis
- Determination of functional groups in organic compounds, such as proteins.
- By correlating the concentration of solutions and UV-vis spectra, the concentration of proteins in a sample can be quantitatively determined.

Some of the disadvantages of this method include the limitation that only liquid samples can be analysed and if cuvettes are handled incorrectly wrong measurements will be obtained.

2.3.2 FTIR

The principle for IR spectroscopy is that most molecules absorb light in the infrared range of the electromagnetic spectrum and this energy is converted into molecular vibrations. The spectrophotometer measures the absorption of infrared light through the analysed material, and it is measured as a function of the wavenumber between 4000 to 400 cm^{-1} . The absorption spectrum that is obtained is a "molecular fingerprint", since each material is different, and with this spectrum, organic compounds present in a material can be identified, such as functional groups in proteins or sugars [217].

The IR spectrophotometer consists of a continuous light source that produces light with a wide range of infrared wavelengths, which passes through the interferometer and directed to the sample. This process results in an interferogram, representing an unprocessed signal of light intensity as a function of mirror position. Then, this signal is Fourier transformed, producing the typical spectrum of absorbance vs wavenumber [218].

Initially, IR sample preparation requires prior procedures. For example, powder or fibres must be combined with potassium bromide (KBr), which is transparent to infrared rays, to obtain a sample that after being pressed, can be cut into thin layers for analysis. Liquid samples can be measured directly or by using a transparent solvent (such as water, or some organic compounds) under infrared rays. However, in most cases, sample preparation requires chemicals or additional instruments not always available in the laboratory. This is why the use of the Attenuated Total Reflectance (ATR) -FTIR is a good option, because it allows the study

of native liquids or solid samples without modifying or destroying them, such as fresh gastropod mucus, snake venom or silk [219].

ATR is based on the internal reflection and the light path of the sample, which depends on the depth of penetration (d_p) of infrared energy in the sample, so as long as the sample has a minimum thickness the depth of penetration (d_p) covers the entire material, resulting in the absorption spectrum, as described in Figure 2.6.

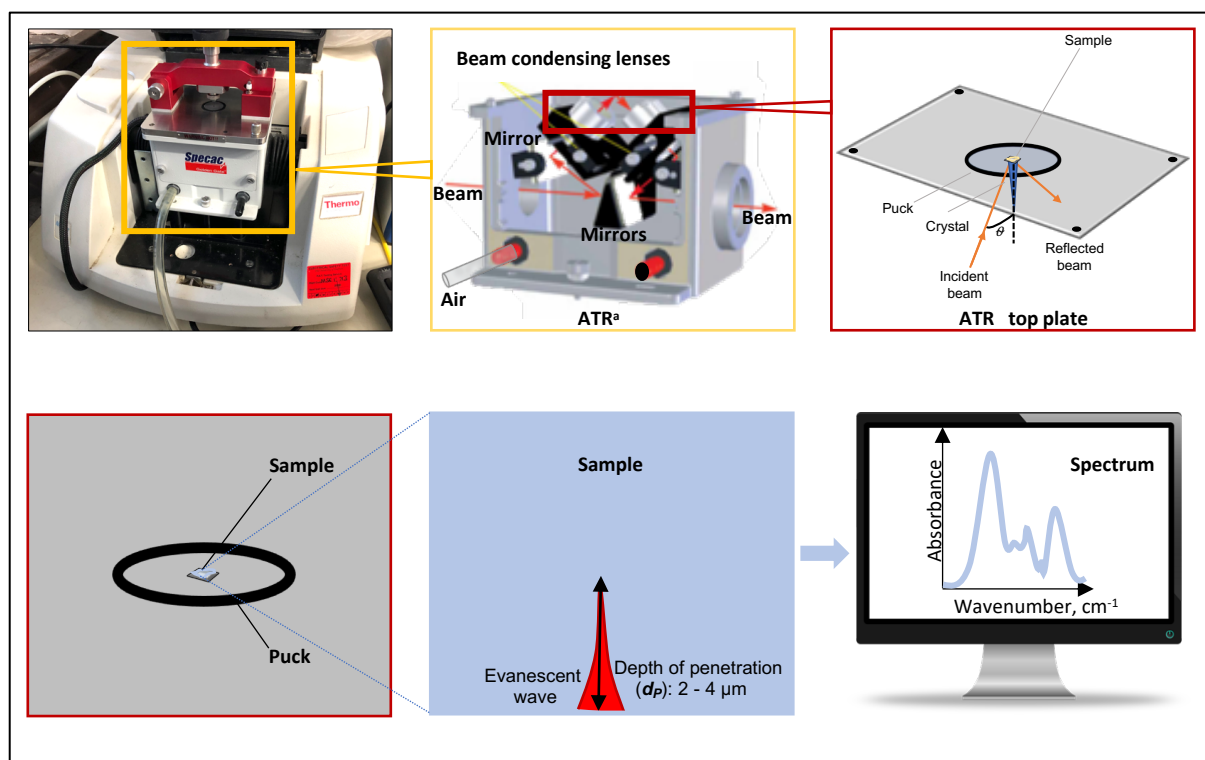


FIGURE 2.6 Diagram showing how the FTIR-ATR operates. ^a Schematic representation of the ATR has been adapted from [220].

First, in the ATR crystal (which can be diamond, Ge, ZnSe, etc.) IR light from the spectrophotometer is reflected by the mirrors, and at the crystal interface the interaction with the sample occurs (Figure 2.6). The effective light path of the ATR sensor is defined by the number of internal reflections multiplied by the depth of penetration of the evanescent wave. At each node, a wave of evanescent energy exits the surface as it decreases in intensity as a function of the distance from the sensor's surface [220].

The depth of penetration (d_p) also depends on the specific wavelength of the energy, and it is defined as [220]:

$$d_p = \frac{\lambda}{2\pi\sqrt{n_1^2 \sin^2\theta - n_2^2}}$$

Where:

d_p = depth of penetration, nm

λ = wavelength of the light, nm

θ = the angle of incidence

n_1 = the refractive index of the crystal

n_2 = the refractive index of the sample

The common value for d_p is between 2-4 μm . The evanescent wave produces partial penetration of the IR light and then an absorption spectrum will be recorded. That spectrum can be used to determine degree of glycosylation in ecto-secretions; to compare different samples and its structural variations; or to correlate similarities between species in the same family. The main disadvantage of FTIR-ATR is related to the small sampling area (fig 2.6).

2.3.3 SDS-PAGE

Polyacrylamide gel electrophoresis is one of the most widely used methods for the analysis and characterisation of proteins. Electrophoresis is relatively simple, fast and sensitive, which makes it a very useful technique. There are numerous variations of this technique depending on the equipment used, and physical-chemical properties in which the separation is to be carried out. For example, the capillary electrophoresis, electrophoresis on paper, and polyacrylamide gel electrophoresis. Protein electrophoresis in polyacrylamide gels can be carried out under native (ND-PAGE) or denaturing (SDS-PAGE) conditions. The differences between one type and another lie in the components of the gels and the buffer solutions used, as well as the treatment of the samples. SDS-PAGE is shown in figure 2.7, indicating how this technique works [212].

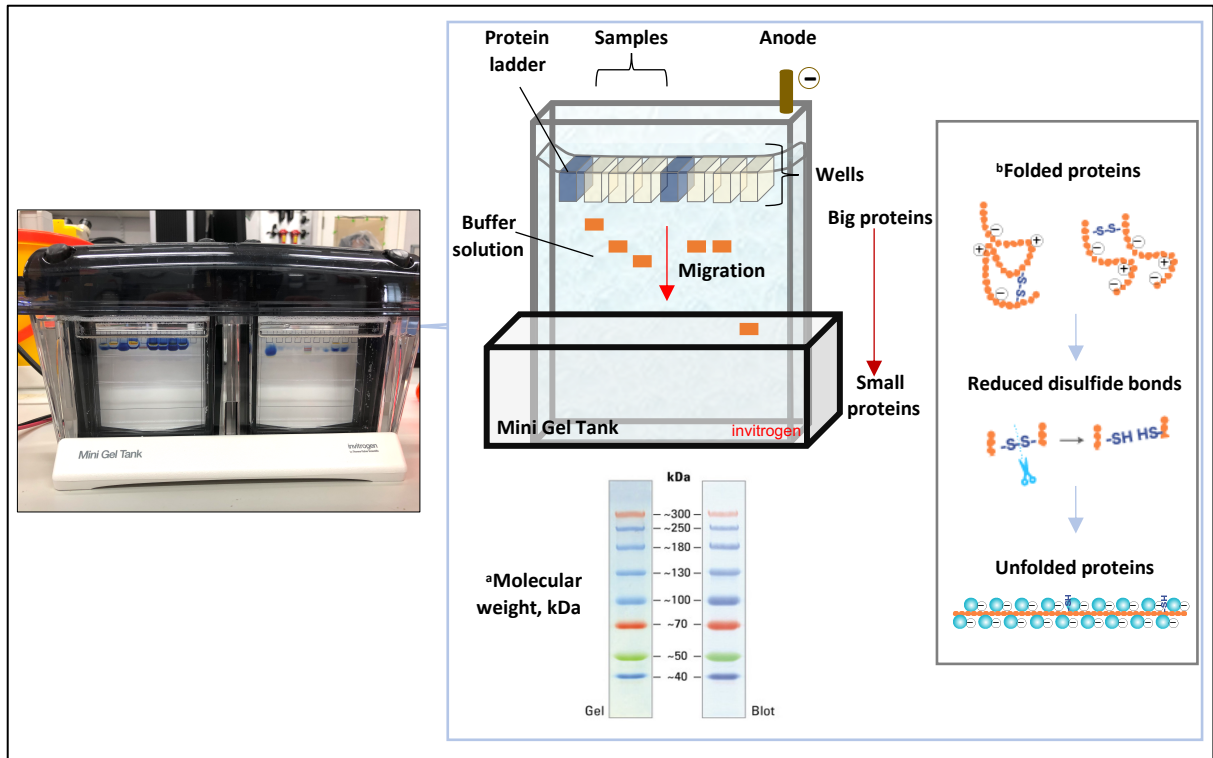


FIGURE 2.7 Diagram showing SDS-PAGE technique. ^a Refers to the picture taken from [221].

^b Schematic representation of proteins has been adapted from [222].

Denaturing, reducing agents and detergents are included in SDS-PAGE. Proteins are solubilized in the presence of the anionic detergent SDS, which binds to proteins, breaking down the hydrophobic interactions and denaturing them. Denatured proteins will adopt a linear structure with a series of negatively charged SDS molecules along the polypeptide chain. Because the amount of SDS that binds to proteins is proportional to their size, SDS-protein complexes have a constant charge-mass value, and as a consequence will separate according to their size, when they migrate from the cathode to the anode of the electrophoresis tank. In addition to SDS, other denaturing agents can be used, such as a 2-mercaptoethanol that reduces disulphide groups. To ensure the dissociation of proteins into their subunits and the loss of secondary structures, samples are usually heated up before being loaded on the gel, generally between 90-95 °C [212].

SDS-PAGE is frequently used to determine the molecular weight of unknown proteins by comparing their relative electrophoretic mobility (R_f) with that of the standard proteins of

known molecular weight (protein ladder) and to determine the number of subunits of a protein complex. R_f is defined as [223]:

$$\text{Relative migration distance} = R_f = \frac{\text{migration distance of the protein}}{\text{migration distance of the dye front}}$$

The Laemmli system consists of two types of gels: a gel, called a concentrator with a non-restrictive (large) pore size that is formed on a second gel called a separator. In this system, each one of the gels is prepared with buffers of different pH's, and the electrophoresis buffer is a third type of buffer. The mobility of a protein in the concentrator gel is intermediate between the mobility of the Cl^- ion in the gel, and the mobility of the Gly^- ion in the sample buffer. Thus, between the two gels, there is an area of low conductivity and a large voltage difference, so that the proteins are concentrated in a very small area between the two ions. Once in the separating gel, the basic pH promotes glycine ionization, and its ions migrate through the concentrated polypeptides, just behind the Cl^- ions. Proteins migrate through the separator gel in a zone of uniform voltage and pH and they are separated based on their size, as observed in figure 2.7 [212].

Once the protein separation is complete, the gel is carefully removed from the tank, and scanned to obtain a clear image and proceed with the molecular weight determinations of each band for all samples tested. In a double tank for SDS-PAGE as shown in figure 2.7, two gels can be run at the same time, with ten wells for each one.

Some limitations of this method include the time required for the preparation of gels and poor band resolution if protein concentration is too low or high (for ecto-secretions, gastropod mucus and snake venom, the minimum protein concentration to obtain clear bands is 5 mg/ml).

2.3.4 TGA

This technique is based on the thermogravimetric principle, in which the mass of a sample is measured while it is heated up under specific atmosphere, recording mass changes as a function of temperature. TGA measures also thermal processes where mass variations are not occurring, such as solid-solid transitions, melting point, etc. It is a useful technique for the determination of volatile compounds, moisture analysis and total solids [213].

Measurements are usually performed at heating rates between 0.5 and 50 °C/min, but more commonly at 20 °C/min. These tests can start at room temperature, but also at higher values (>50 °C), in order to detect possible drying of the sample. The final temperature depends on the type of sample and the property measured and it is usually relatively high, for example, 600 °C for organic substances or above 1000 °C for inorganic samples. Maximum temperatures are set based on the test, selected program and properties to be determined, because in some cases it is also important to know the decomposition of the sample. Under these conditions, a purge gas needs to be used during all measurements [213].

Based on the same principle, there are other variations of this technique, and more specifically, focused on the moisture analysis and total solids content, such as the TGA described in figure 2.8. This instrument is designed for the measurement of volatile compounds in the sample, as well as solids present, and it has been widely used in the food industry.

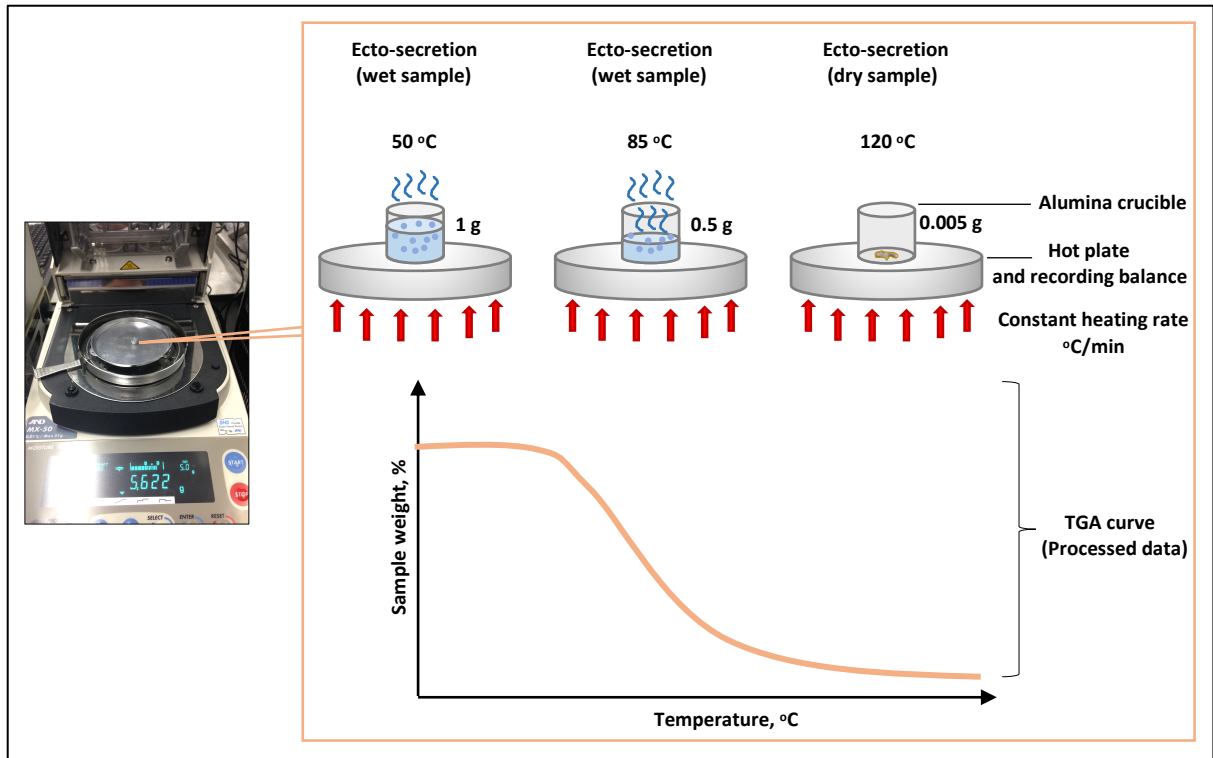


FIGURE 2.8 Diagram showing TGA, for the total solids content determination.

Figure 2.8 describes how the TGA-moisture analyser works. Different heating rates can be used, for example 1 °C/min with data intervals between 15 and 60 seconds. Tests can start at room temperature with a maximum value depending on the sample. Aluminium sample pans can be used or alumina crucibles. Mass variations in grams will be recorded, to monitor volatile compounds and the final mass, will correspond to total solids (dry sample). While volatile compounds are evaporated from the sample, a reduction in mass occurs, and the TGA curve shows this variation as a function of temperature. At the starting temperature, the initial mass remains unaffected, but once the heating program starts, sample mass will change, starting to decrease until the final mass is not changing. This indicates the total mass of volatile materials has been eliminated and the remaining mass will correspond to total solids in that specific sample. This instrument will stop automatically only if after five consecutive measurements sample mass remains constant, indicating moisture content is zero as well as volatile compounds. The atmosphere used during these tests was air [224].

The TGA curve can give us information about the water and volatile components, chemical reactions, etc. The interpretation of TGA curves plays an important role in the analysis,

because mass variations can be associated to chemical reactions (for example, reactions with gaseous substances in the purge gas such as oxygen, CO₂ or volatile compounds), or physical transitions (for example, adsorption of gaseous substances). Most TGA curves show weight losses, typically caused by decomposition or combustion; and physical transitions like evaporation, desorption, or drying [213].

TGA application areas include thermoplastics, metals, ceramics, polymers, composites (for example determination of the fibre content of composite materials), as well as a wide range of analyses in the chemical, food and pharmaceutical industries [213]. This technique can be used in natural materials characterisation, more specifically, ecto-secretions, to determine total solids concentration. The main limitation of this technique is related to mass loss, because it represents the volatiles.

2.3.5 DSC

Differential scanning calorimetry (DSC) is a technique used to thermally characterise a wide range of materials, such as synthetic polymers, nanomaterials, and in the food and pharmaceutical industries. The information obtained by DSC is used to identify amorphous and crystalline behaviour, polymorphic transitions, etc., for product design and fabrication. In terms of the study of proteins, this technique provides information about how stable a protein is in its native state [225]. This is performed using the heat capacity variation measurements, when the sample is heated up at a constant rate. With this information, processes associated with folding and unfolding of proteins can be described, because proteins form well-defined structures which change as a function of temperature. These structural rearrangements produce heat absorption due to the redistribution of covalent and non-covalent bonds [214]. Figure 2.9 shows a diagram of this technique, based on a two cell DSC chamber instrument, which was used to analyse gastropod mucus and snake venom.

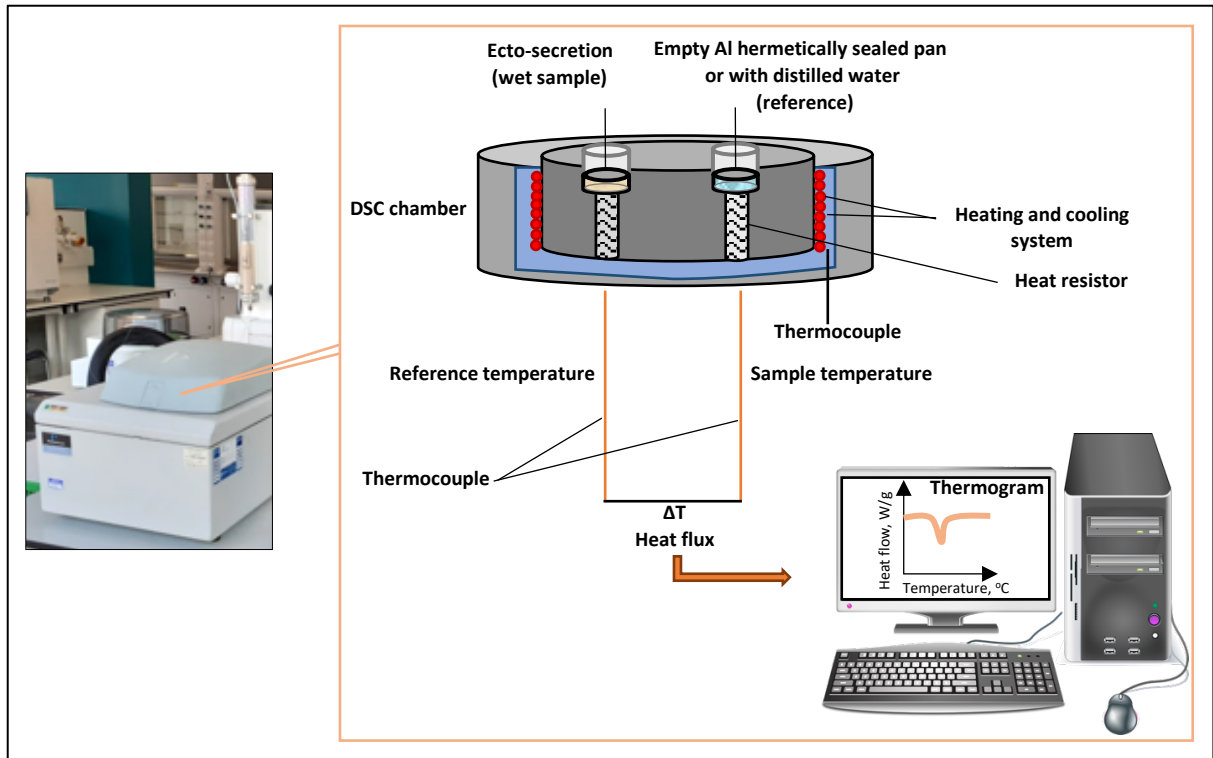


FIGURE 2.9 Diagram showing how a DSC works.

The DSC chamber with its heating and cooling system, consists of two cells, one for the reference and one for the sample. For liquid samples or gels with high percentages of water, such as gastropod mucus (98-99.5 % of water), the reference pan can consist of an Al hermetically sealed pan, containing water (approximately the same mass as the sample), in order to record only those changes associated with protein rather than water (solvent) events. For samples with less water content, for example, snake venom, the reference can consist only of an empty Al sealed pan.

The DSC device is designed to keep the two cells at the same temperature, regardless of the selected program (heat-cool-heat; heat only, or to stay at one specific temperature certain time) and heating rate. To carry out a measurement, both cells are heated with a constant scan increment. Depending on the type of sample, the heating rates are established to obtain good resolution and analysis of peaks or transitions. The absorption of heat that occurs when a protein unfolds causes a temperature difference (ΔT) measured by thermocouples between the two cells, resulting in a thermal gradient in the DSC chamber. The result will be a thermogram, showing all the events occurring during the test. For example, the enthalpy of

protein denaturation, which is the area under the DSC peak obtained based on the sample mass (initially the fresh sample mass is recorded, but later it is changed to the dry mass), expressed in J/mol or J/g [226]. DSC software can calculate peak areas, but also that area can be estimated manually, by using the following equation [227]:

$$\Delta H = \int_{T_0}^{T_1} \Delta c_p dT$$

Where:

ΔH = enthalpy for the process, in this case enthalpy of denaturation, J/mol

T_0 = initial temperature, °C (where the denaturation event starts, i.e., the starting point of the peak)

T_1 = final temperature, °C (where the denaturation event ends, i.e., the end point of the peak)

Δc_p = heat capacity change during unfolding, measured and registered by the instrument, J/mol·°C

Values obtained by DSC can be compared to determine if there is a thermal denaturation of proteins at specific temperatures, or if a glass transition is occurring, or both. By comparing samples, the thermal stability of materials is determined, and these parameters can be associated with other compositional or functional properties.

The disadvantages of this technique are the reduced sample size to be measured (in the order of mg); the effect of heating rate on resolution and identification of thermal events; and in the case of samples with high amount of water content, such as gastropod mucus, sample pan needs to be filled with water to measure changes in proteins only and not due to the solvent.

2.3.6 RHEOLOGY

2.3.6.1 DEFINITION AND CLASSIFICATION OF FLUIDS

In a general definition, rheology is the study of the deformation and flow of matter, and in any process involving fluids, rheology is present. Its applications include, for example: polymer solutions, particle suspensions, foods, coatings, biological fluids and tissues, and many others, such as ecto-secretions in their native state [228], [229].

Fluids can be classified as Newtonian and non-Newtonian. The first ones obey Newton's law of viscosity, which establishes a linear relationship between the shear stress, τ , and the shear rate, $\dot{\gamma}$; and viscosity, η , is independent of shear rate. In this group we can find some ecto-secretions. The second group of fluids (non-Newtonian) do not have a linear relationship between shear stress and shear rate [229] (figure 2.10).

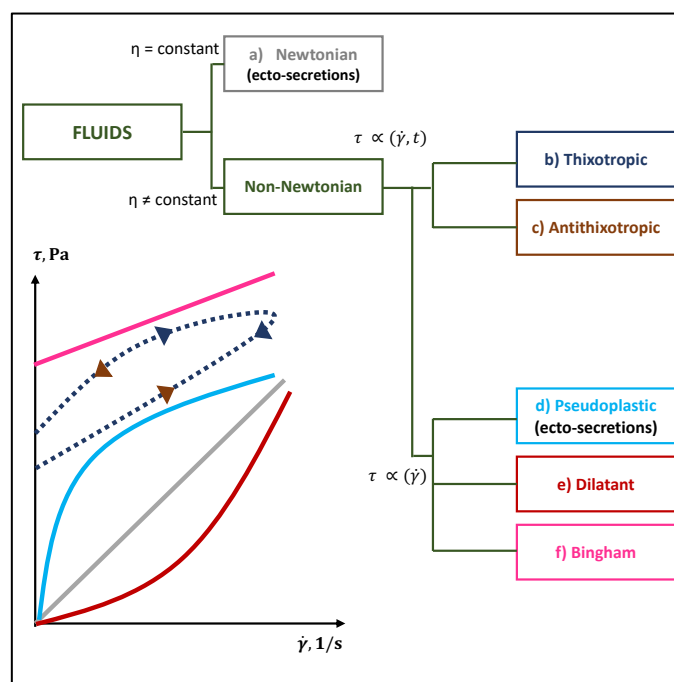


FIGURE 2.10 Rheological classification of fluids. Adapted from [230]

From figure 2.10, there are five groups of non-Newtonian fluids, two of them where shear stress is a function of shear rate and time, which are the thixotropic and antithixotropic. The other three, where shear stress is a function of shear rate, are the dilatant, Bingham and the pseudoplastic. This last group is also characterised for the shear-thinning behaviour, where

the fluid shows a reduction in viscosity when the shear rate increases, and some ecto-secretions such as silk are in this category.

2.3.6.2 TYPES OF RHEOMETERS

Depending on the sample to be tested, its characteristics and the type of information needed, rheometers can be used to determine the rheological properties of the material. New adaptations to rheometers are designed by experts to provide a more complete understanding of the functional properties of the material related to its compositional or thermal characteristics. For example, rheological measurements combined with microscopy attachments; or viscosity measurements as a function of temperature, to see how this property affects functionality. As previously discussed, each group of techniques can be combined with others to offer a complete characterisation of materials. In terms of rheometers, there are three main groups, where they are classified depending on the principle and operation [228], [229], [231]:

- Rotational rheometer: This instrument basically consists of two parts that are separated by the fluid to be studied. Those parts can be two cylinders, two parallel surfaces, or a surface and a cone of small angle, and it has a rotor inside a cylinder. The movement of one of these parts causes the appearance of a velocity gradient along the fluid. For example, to determine how the shear viscosity of a material is changing as a function of shear rate or temperature, or to test ecto-secretions in their native state (liquid/gel).
- Capillary rheometer: this instrument is designed to measure shear viscosity of a polymer, based on a fluid forced to flow through the capillary (narrow space) under certain specific conditions (T, P). For example, in the study of polymers, these instruments measure the viscosity of the polymer as a function of temperature and rate of deformation. A capillary rheometer is also capable of testing various composite materials with small sized particles or fibres.

- Extensional Rheometer: This instrument is designed to measure the flow and deformation of materials involving elongation or stretching. Extensional rheometers focus on pulling on a sample in an extensional way, which means there is no shear. The stress (F/A) is higher in the extensional deformation due to the extent of the deformation [231].

2.3.6.2.1 ROTATIONAL RHEOMETERS

As described in the previous section, the rotational rheometer is one type of instrument widely used for the analysis of polymer solutions. This instrument was used to analyse native ecto-secretions, such as gastropod mucus and snake venom. The analysis of samples in rotational rheometers reproduces the behaviour of the material subjected to a shear stress, which means that it is subjected to shear forces parallel to the deformation plane of the material. These forces are reproduced by two parallel plates, one mobile and the other fixed, and the sample is deposited in between, for example, cone-plate geometry, as it is shown in figure 2.11. On the sample, a shear is applied by rotation of the moving part on the fixed part [221].

With this type of rheometer, the flow curve of the material is obtained, in which sample viscosity variations with the shear rate are represented (viscosity vs shear rate), as shown in figure 2.11. This test consists of the complete rotation of the upper mobile part (cone or plate, in the example shown in Figure 2.11, it is a cone geometry) on the lower fixed part (plate). The sample is placed between both geometries, and depending on the type of geometry, the amount of sample varies. It is important to avoid placing too much or too little sample, since in both cases, incorrect results will be obtained. The amount of sample placed must be sufficient to cover the entire geometry, without being outside of the edges, and without leaving empty spaces between both geometries [221]. This is shown in figure 2.11. During the test, an environmental chamber is used to avoid evaporation. The Peltier controller, can increase the temperature or keep it constant if needed, depending on the test to be carried out.

Once the sample has been placed and the instrument adjusted to the “geometry gap” and any excess of sample has been removed, the mobile plate is rotated progressively. The stress values (Pa) for each shear rate ($1 / s$) are automatically recorded, and the viscosity variation is obtained. At low shear rates, viscosity provides information on the nature of the material at a structural level, as well as information on molecular weights (since molecular weight has a direct effect on the viscosity of the material), cross-linking, etc.

Other measurements that can be carried out in this type of rheometer are oscillatory tests, in which the viscoelastic response is monitored, and both the storage modulus (G') and loss modulus (G''), are obtained, while applying a frequency sweep for deformation. Differences in samples' response, can provide indications of molecular structure variations between them. In viscoelastic solids with $G' > G''$, it is due to chemical bonds or physical-chemical interactions in the material. However, viscoelastic liquids with $G'' > G'$ do not have strong bonds between the individual molecules in the material [221], [232].

Figure 2.11 shows a diagram of a rotational rheometer, with a cone-plate geometry used to test an ecto-secretion in its native state.

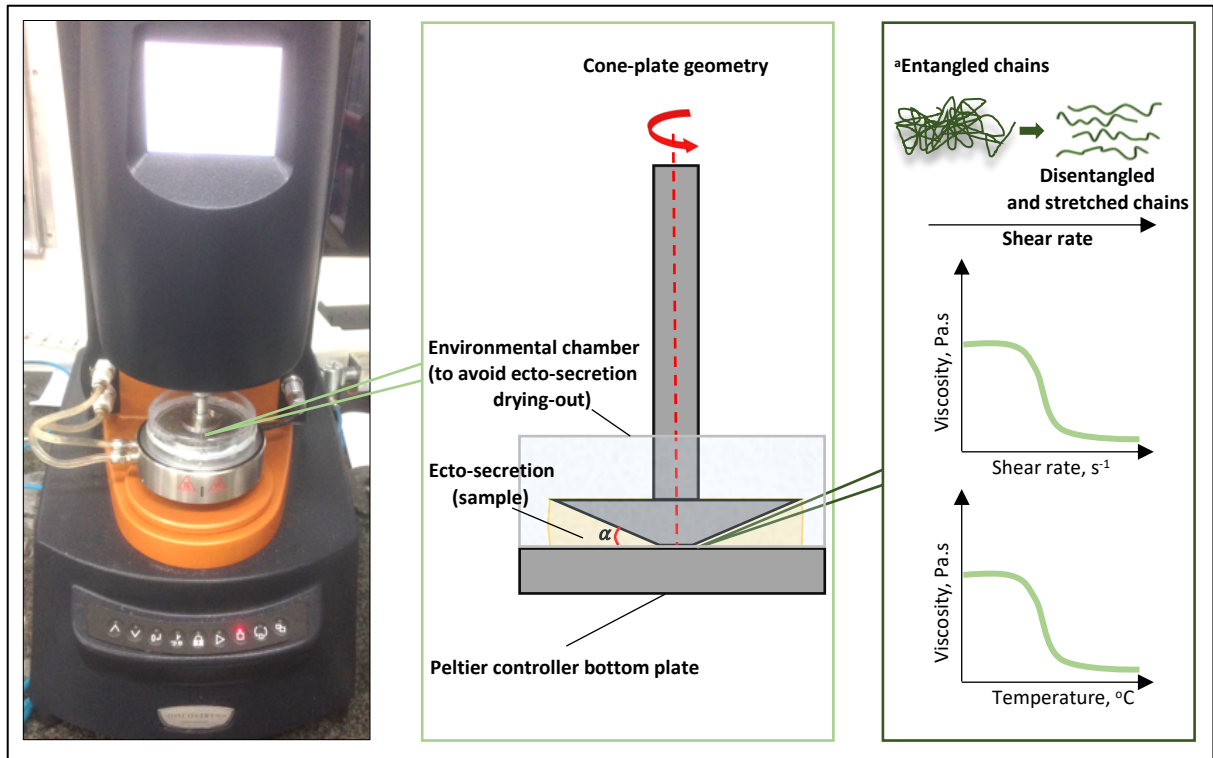


FIGURE 2.11 Diagram showing how a rotational rheometer works. ^a Refers to the explanation of protein changes, adapted from [228].

As the shear rate increases, this shear-thinning fluid will exhibit a reduction in viscosity due to effect of shear stress on the molecules, more specifically on the polymeric chains. This is because the long chains of the polymer are disturbed from their equilibrium conformation positions (entangled chains), causing elongation of chains in the direction of shear (stretched chains). A similar behaviour that occurs if viscosity is measured against temperature. As temperature increases, a clear reduction in shear viscosity is observed. This occurs because proteins are thermally affected or denatured [231].

Tests like this can be carried out in other ecto-secretions or materials to know more about their rheological properties and to determine the point at which the material fails to maintain its functionality under certain conditions. In chapters 3 to 7, all the techniques described in this chapter will be explored in detail, to characterise gastropod mucus, snake venom and silk.

CHAPTER 3: ANALYSIS, CLASSIFICATION AND IDENTIFICATION OF GASTROPOD MUCUS BY FTIR

“...**A** protein compound was chemically formed, ready to undergo still more complex changes, at the present such matter would be instantly devoured, or absorbed, which would not have been the case before living creatures were formed.” **Charles Darwin**



This chapter corresponds to the paper “Analysis, classification and identification of gastropod mucus by Fourier Transform Infrared Spectroscopy”, to be submitted for publication to the Journal of Molluscan Studies.

ABSTRACT

Gastropod mucus consists mostly of water (>98%) and less than 2% of other organic and inorganic components. Of these mucins are of particular interest, consisting of highly glycosylated proteins, which endow mucus with the ability to act as both an adhesive, lubricant and provide protection against pathogens. Mucins' performance relies on its molecular composition and structure however, to date, there are very few studies addressing this. In this chapter we use Fourier Transform Infrared Spectroscopy (FTIR) to analyse, identify and classify gastropod mucus. Specifically, the relative content of proteins, their secondary structures and degree of glycosylation were investigated for a range of gastropod mucus samples. Advancing the field beyond previously static spectroscopic studies performed, we probed mucus response to a temperature increase, in an effort to determine its propensity to remain hydrated (i.e., resist denaturation). Specifically, out of 648 total spectra, a multivariate analysis performed on 72 spectra from 12 gastropod species at 25 and 80 °C, revealed that it was possible to classify species based on their mucus composition. Hence our study shows that the classification of gastropods based on their mucus characterised by FTIR is an accurate and novel method, while providing information about the chemical composition of mucins. This was further compared to previously published phylogenetic data and taxonomies which demonstrated a resounding degree of correlation, implying that mucus FTIR may be also a powerful tool for biodiversity studies.

KEYWORDS: Gastropod mucus, FTIR, Multivariate analysis.

3.1 INTRODUCTION

The largest class of molluscs is Gastropoda, comprising of more than 50, 000 species, and within this, the Stylommatophora clade is the home to most of our terrestrial snails and slugs [48]. They are found across a vast diversity of habitats, from tropical to temperate regions with each requiring specific morphological and genetic adaptations to a particular environment [33]–[41].

One element of gastropod biology assumed to be under natural selection is their mucus, a material consisting of around 98 % water and 2 % organic and inorganic materials. Within that 2% are mucins, highly glycosylated proteins which represent the main functional component of mucus [50], [51]. Further evidence of selection is seen by the existence of multiple types of mucus, each with a specific function. The two main types of gastropod mucus are adhesive and locomotive, with adhesive containing twice the protein/carbohydrate ratio compared to locomotive [49].

To understand more about the diversity of mucus' compositional properties, several studies have been carried out on marine, freshwater and terrestrial species, analysing their mucus primarily using chromatography and mass spectrometry [49], [59], [76]–[81]. However, whilst informative, the time required for sample preparation and costs for characterisation in these experiments are high, and there are other alternatives to these techniques, such as Fourier Transform Infrared spectroscopy (FTIR).

To date there is only one study reported using FTIR to characterise gastropod mucus, conducted by Skingsley *et al.* 20 years ago [59]. They carried out FTIR characterisation of locomotive mucus from eight land snails and slugs and one freshwater snail. In their study, they were able to identify the groups associated with the sugar chains present in mucins and amide I and amide II groups associated with proteins. Although Skingsley *et al.*, were the first to successfully conduct a study, their results were limited to being able to suggest the formation of two groups of muco-polysaccharides present in locomotive and adhesive mucus and called for further work in this area [59].

However, whilst gastropod mucus has only seen a single study using this technique, FTIR as an alternative to characterise and classify species has been used before for everything from bacteria [233], to coffee beans [234] to hair [235], [236]. Taking silk as an example, Boulet-Audet, *et al.* collected over 1000 individual spectra from 41 different species, in order to group and classify silks [237]. With this information they produced an ultrametric tree generated from hierarchical clustering and found it bore a striking resemblance to a phylogenetic tree, suggesting FTIR may be able to classify species based on a material they secrete [237]. Beyond a holistic characterisation, FTIR spectra can also be used to obtain information to determine protein secondary structures [238], such as α -helix, β -sheets, β -turns, random coil or aggregated strands. Furthermore, information about sugar residues can be obtained too, which is related to the degree of glycosylation in mucins [239]. As mucins are highly glycosylated proteins, meaning their carbohydrate content is >80 %, and glycosylation is known to play an important role in mucins ability to hold onto water, and thus have higher denaturation temperatures and thermal stability [240], we propose that differences can be observed if we compare spectra at room temperature with others at higher temperatures, giving an indication of further specialisation.

In this work, we propose that the selection for performance across a range of habitats has driven molecular diversification and specialisation in mucus and that FTIR could be a rapid, non-destructive and appropriate tool to understand this. Probing the relative performance space of these materials further, we hypothesize that the degree of glycosylation in mucins plays an important role in thermal stability of gastropod mucus, an analogue to their hydrophilicity, and to address this, locomotive mucus of twelve gastropod species across the Heterobranchia and Caenogastropoda clades was analysed at 25 and 80°C. With this information and to complement this characterisation, the method described by Boulet-Audet *et al.*, for silk [237], is applied to classify gastropod species based on the mucus they produce. Hence this work represents the first reported gastropod mucus analysis and classification by FTIR including multivariate analysis, which considers both the compositional properties of mucus within the context of its evolution and biodiversity.

3.2 MATERIALS AND METHODS

3.2.1 MATERIALS

Three species of terrestrial snails (*A. fulica*, *C. aspersum* and *C. nemoralis*), six terrestrial slugs (*A. ater*, *A. hortensis*, *L. flavus*, *L. maximus*, *L. haroldi* and *V. sloanei*), and three freshwater snails (*L. stagnalis*, *M. cornuaretis* and *P. diffusa*) for a total of twelve species, were included in this study. *A. hortensis*, *A. ater*, *C. nemoralis*, *C. aspersum*, *L. flavus*, *L. maximus* and *L. stagnalis* were collected in Sheffield, UK, between May and September 2018. *A. fulica*, *M. cornuaretis* and *P. diffusa* snails, and *L. haroldi* and *V. sloanei* slugs were purchased as juveniles and reared in house. All terrestrial species were kept in plastic containers (39 cm x 48 cm x 20 cm) with ~ 6 cm of vermiculite layering the bottom of the box at $22 \text{ }^{\circ}\text{C} \pm 1 \text{ }^{\circ}\text{C}$ and high humidity. Freshwater snails *L. stagnalis* (native from the UK) were kept in a plastic container (39 x 25 x 29 cm) with 17 L of tap water at a temperature of $17 \pm 1 \text{ }^{\circ}\text{C}$. Freshwater snails *M. cornuaretis* and *P. diffusa* (tropical species) were kept in a plastic container (39 x 25 x 29 cm) with 17 L of tap water at a temperature of $21 \pm 1 \text{ }^{\circ}\text{C}$. Terrestrial species were fed *ad libitum* twice weekly with cucumber, lettuce and sweet potatoes. Freshwater snails were fed twice weekly with cucumber.

3.2.2 METHODS

3.2.2.1 SPECTRAL ACQUISITION AND TREATMENT

FTIR spectra were collected at room temperature ($22 \text{ }^{\circ}\text{C} \pm 1 \text{ }^{\circ}\text{C}$) using a Nicolet 380 spectrometer (Thermo Instruments, UK) purged with dry air and equipped with an Attenuated Total Reflection (ATR) accessory (Golden Gate, 45° single-bounce diamond sensor, Specac, UK). Clean animals were placed away from the diamond sensor on top of the ATR accessory and directly opposite a black box used to encourage terrestrial species to move in that direction over the sensor (see figure 3.1a). When the animal had passed completely over the sensor, the mucus trail was allowed to dry for 20 min, before collecting spectra at $25 \text{ }^{\circ}\text{C}$ (see figure 3.1b). Samples were then heated up to $80 \text{ }^{\circ}\text{C}$, at a heating rate of $3.23 \text{ }^{\circ}\text{C}/\text{min}$. In total, 648 individual spectra were collected, 3 at each temperature for each species. Data between 1000 cm^{-1} and 1800 cm^{-1} were obtained by collecting 64 scans at 4 cm^{-1} resolution.

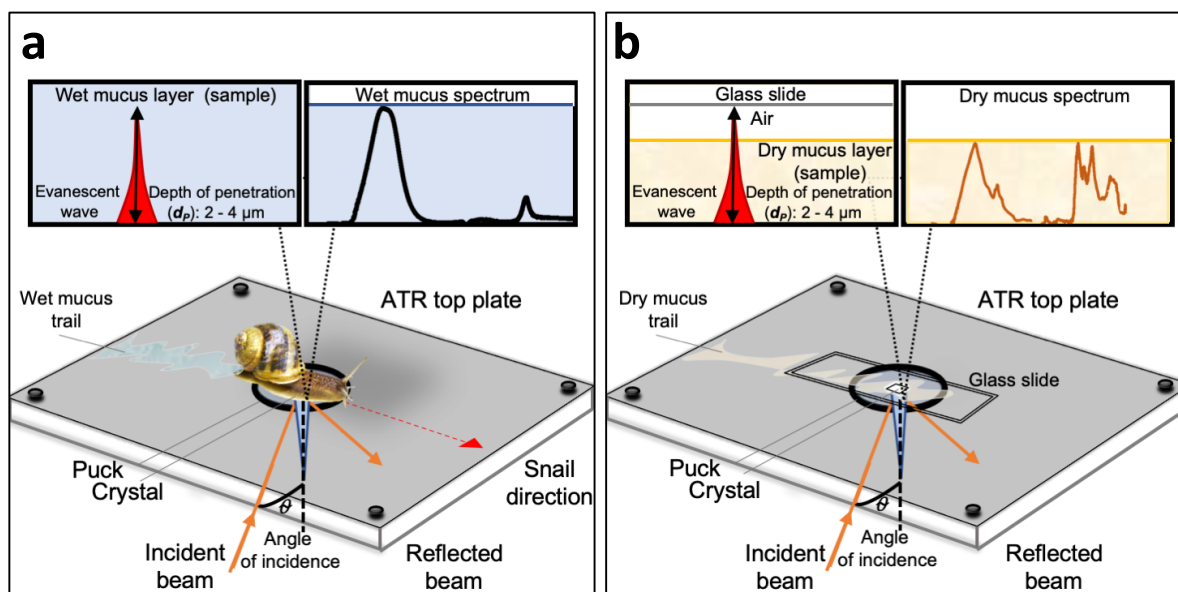


FIGURE 3.1 Procedure to collect gastropod mucus. a) Snail over the FTIR-ATR device following the red line direction, leaving wet mucus on the ATR crystal, as observed, wet mucus spectrum collected when the animal is over the crystal, is not showing all the main bands associated to proteins, the main band corresponds to H-O bonds. b) After 20 min covered with a glass slide, gastropod mucus is dry at room temperature to start spectra collection for FTIR analyses, from 25–80 °C. This procedure was used for all species. Diagram shows the operational principle behind the ATR and it was adapted from [241]. For freshwater snails, the procedure to collect spectra was the same, but species were removed from their containers and placed in a Petri dish with water to allow animals to move for five minutes before placing species on the FTIR-ATR. This reduces stress on the animals.

3.2.2.2 DATA PRE-PROCESSING

Spectral operations were performed using Origin software, v2020, USA. All spectra were normalised to the amide I peak (1645 cm^{-1}), to compensate for absolute signal variations due to different mucus film thickness deposited on the FTIR-ATR accessory. The five main spectral regions were identified in all species. The relative area of each peak for all samples was obtained by subtracting a linear baseline, selecting peaks according to each wavenumber values and range, and integrating peaks.

3.2.2.3 GAUSSIAN FITTING

Fourier self-deconvolution and curve fitting were performed on spectra between 1600 and 1700 cm^{-1} and an 8-point multipeak Gaussian fitting was done using Origin software, v2020,

USA, for all samples at 25 and 80 °C. Protein secondary structures were assigned according to previous studies [242]–[245].

Absorption bands and the corresponding groups are presented in table 3.1.

TABLE 3.1. Assignments of the main bands present in the twelve gastropod native mucus analysed, between 1800 and 1000 cm^{-1}

Position (cm^{-1})	Assignment	References
1646-1634	Amide I (C=O stretching)	[59], [246]
1534	Amide II (C-N stretching, N-H bending)	[219], [246]
1475-1350	CH ₃ bending	[211], [237]
1352	Tryptophan (Trp) residues	[211]
1250	Amide III (C-N stretching, N-H bending), random coil	[237], [246], [247]
1180-1024	O-Glycosidic bonding (sugar residues)	[41], [59], [248]

3.2.2.4 MULTIVARIATE ANALYSIS AND DENDROGRAM GENERATION

Absolute absorbances are not constant between measurements, depending on the mucus film thickness. To discriminate mucus, the first derivatives of 72 spectra were used for the multivariate analysis, i.e., 3 spectra at 25 and 80 °C per species, and then a Principal Component Analysis (PCA) was performed using Origin software, v2020, USA, to simplify the complexity of the dataset, while maintaining the main trends [249], [236]. Linear Discriminant Analysis (LDA) [250], [251] was performed on the principal component scores, in order to find a linear combination of features that characterises infrared spectra from mucus of different species. Then, LDA mean factor scores were used to calculate the Euclidean distance between species, for Hierarchical Cluster Analysis (HCA) [252], [253]. This method represents an algorithmic approach to identify groups with different degrees of similarity, which are constituted by a similarity matrix. Finally, the obtained dendrogram was compared with the cladogram built from reported data on different gastropod clades [9], [13], [66]–[75].

3.3 RESULTS AND DISCUSSION

3.3.1 GENERAL GASTROPOD MUCUS SPECTRAL FEATURES

As a basis for a more structured comparison of FTIR results, figure 3.2 shows a cladogram of the twelve species included in this study.

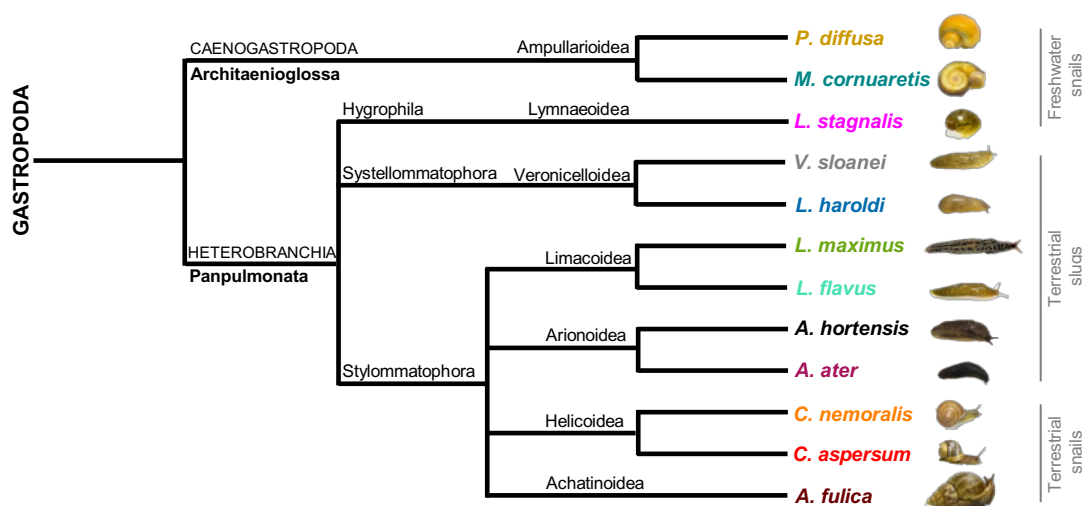


FIGURE 3.2 Cladogram of class Gastropoda, showing the twelve species included in this study. This cladogram was built with information from [9], [13], [66]–[75].

From the cladogram in figure 3.2, it is clear that seven different families represent the twelve species of gastropods: Achatinoidea, Helicoidea, Arionoidea, Limacoidea, Veronicelloidea, Lymnaeoidea and Ampullarioidea. Based on this cladogram, results in figure 3.3 are grouped, showing FTIR spectra at both 25 and 80 °C. Absorption bands are indicated and there are clear changes in chemical structure between species at both temperatures.

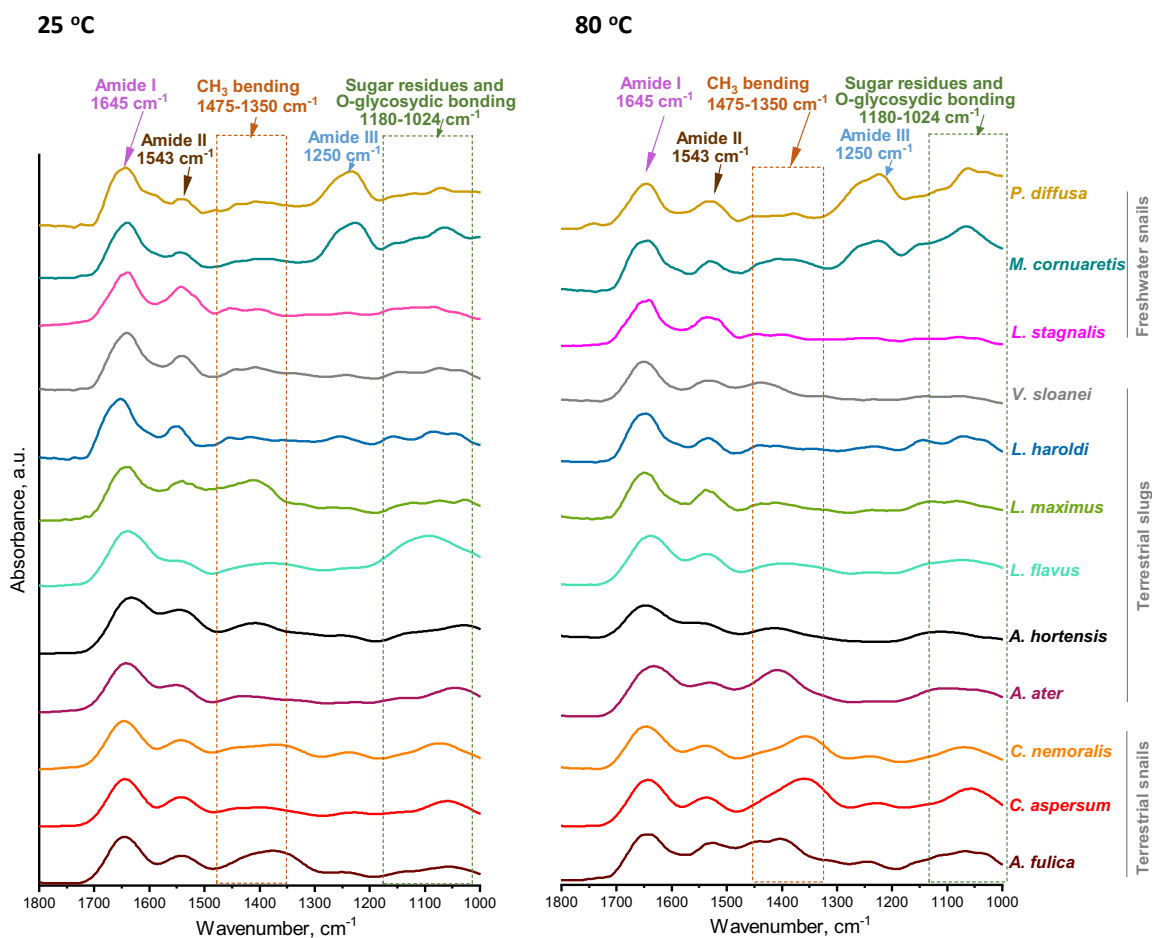


FIGURE 3.3 FTIR spectra of gastropod mucus from *A. fulica*, *C. aspersum*, *C. nemoralis*, *A. ater*, *A. hortensis*, *L. flavus*, *L. maximus*, *L. haroldi*, *V. sloanei*, *L. stagnalis*, *M. cornuaretis* and *P. diffusa* at 25 °C and 80 °C. The main regions are highlighted: amide I (1645 cm^{-1}); amide II (1543 cm^{-1}); CH_3 bending (1475-1350 cm^{-1}); amide III (1250 cm^{-1}); and sugar residues and glycosidic bonding (1180-1024 cm^{-1}).

In figure 3.3, at 25°C we can observe that all samples show major bands between 1634-1646 cm^{-1} , corresponding to amide I. With respect to the peak at 1543 cm^{-1} , associated to amide II, it is observed in all samples as well, but interestingly, *A. ater*, *A. hortensis* and *L. flavus* show a shoulder in this peak, that is not present in the other nine species. The region between 1475-1350 cm^{-1} is the most variable within the spectral range reported in this study, corresponding to CH_3 bending and aromatic residues like tryptophan (Trp). It shows a broad band and higher absorbance on *A. fulica*, *A. hortensis* and *L. maximus* spectra. The other nine species exhibit the same band but with lower absorbances. Peak at 1250 cm^{-1} , associated to amide III, has its maximum absorbance value corresponding to the freshwater snails *M. cornuaretis* and *P. diffusa*. Finally, in the region between 1180-1024 cm^{-1} , representing the

sugar residues, the slug *L. flavus* shows the highest absorbance, followed by the two snails *C. aspersum* and *C. nemoralis*.

At 80°C, the amide I peak is similar for all species. Amide II peak shows a similar pattern in all species, but a shoulder in *A. fulica* snail and *A. hortensis* slug is observed. The region corresponding to bending of methyl groups and Trp residues, is different in all species, showing in general, higher absorbance. Amide III region remains similar to 25°C in all species and sugar residues region, shows a reduction in absorbance for five species, including *A. ater*, *A. hortensis*, *L. flavus*, *V. sloanei* and *L. stagnalis*.

A detailed comparison between terrestrial gastropods and freshwater snails can be established, to identify differences between species, but also to compare our findings with those reported by Skingsley *et al* [20]. Starting with the terrestrial snails *A. fulica*, *C. aspersum* and *C. nemoralis*, we can observe that at 25 °C, amide I and II peaks are similar in position and intensity, indicating that protein secondary structures are almost the same, i.e., β -sheet, β -turns and random coils. The region corresponding to CH₃ bending is similar in position with *C. nemoralis* but different to *C. aspersum*, and this is caused by stretching vibrations of C-N in secondary amides, related to the percentage of water in the amino acids present [41], [59], [254], [255].

Skingsley *et al.* [20] reported the presence of a peak at 1380 cm⁻¹ in the snails *C. aspersum* but not in *C. nemoralis*, indicating a change in CH, OH bending or COO⁻ stretching. Our results contradict those findings reported previously, because that peak is present in both snails and the highest absorbance corresponds to *C. nemoralis*. We attribute these variations to the procedure used to collect mucus, because Skingsley *et al.*, collected mucus directly from the animal using a sterile glass rod to wipe the mucus from the foot of the gastropod, and then each sample was placed between calcium fluoride IR windows to be analysed. This could cause a disruption of the mucus granules, where our procedure described in Chapter 2, section 2.2.1, placing native mucus directly onto a chemically inert diamond window, reduces these effects on gastropod mucus.

Whilst not available to Skingsley at the time, our reflectance-based IR technique offers several improvements over their previous state of the art. Our procedure requires only very small samples, as it is only able to test $> 4 \mu\text{m}$ sample thickness, as a result variation in sample thickness are limited through our approach. Furthermore, the sample is collected *in situ* with no additional deformation or dehydration that could occur using a glass rod and then sandwiching between windows.

Moving to the region between $1180\text{-}1024 \text{ cm}^{-1}$, representing the OH and O-glycosidic bonding, it is less intense for *A. fulica* than in the other two land snails, suggesting a different degree of mucin glycosylation. This ties well with Skingsley *et al.* [239], where spectra reported for *C. aspersum* and *C. nemoralis* showed a strong band at 1080 cm^{-1} [20]. At $80 \text{ }^\circ\text{C}$, amide I and amide II peaks remain similar for the three species, but the CH_3 bending region shows a shoulder in the *A. fulica* spectrum, compared to the other two snails. Amide III region is lower in *A. fulica* than in *C. aspersum* and *C. nemoralis*, but *C. nemoralis* shows an absorption band higher than *C. aspersum*, indicating higher percentage of random coil and β -turns [247], [256]. All these three species exhibit an increase in the sugar residues region, which ties well with previous studies wherein bovine submaxillary mucins were studied at a range of temperatures from 5 to $85 \text{ }^\circ\text{C}$, and concluded that heavy glycosylation is the main factor influencing mucins structural stability [239].

Regarding to the six terrestrial slugs, at $25 \text{ }^\circ\text{C}$ we can observe that all species show similar amide I and II bands, but the region related to CH_3 bending and aromatic residues is higher in *A. hortensis* than in *A. ater*, and in *L. maximus* than in *L. flavus*. Skingsley *et al.* [20], reported the same differences in *A. hortensis* and *A. ater*, which are attributed to the carbon spin of the core proteins, i.e., CH_3 bending, and also to aromatic residues variations. The amide III peak is higher in *L. haroldi* mucus than in the other 11 species, and this is attributed to random coil variations. The main difference is in the region at $1180\text{-}1024 \text{ cm}^{-1}$ corresponding to glycosidic bondings and sugar residues, and it is observed in *L. flavus*, from the Limacidae family, showing the highest absorbance. Finally, *L. haroldi* shows higher absorption in the sugar residues region than *V. sloanei*, both from the Veronicelloidea family, most likely due to a higher state of glycosylation [59].

At 80 °C, the amide I and amide II peaks remains similar for the six species, but the CH₃ bending region is higher in *A. ater* than in the other five species, indicating skeletal vibrations of the proteins, and also related to the chain length, which suggests that this CH₃ bending increases proportionally with the number of times it occurs within the molecule [257]. The Amide III region is again more intense in *L. haroldi* than in the other species, maintaining its random coil structures when mucus is heated up, which dictates protein folding and stability in this particular case [256]. These observations also suggest differences in components of protein secondary structures: β-turns and random coil. There are bands related to sugar residues in all species, gastropods in the Arionoidea and Limacoidea families have similar pattern, while *L. haroldi* in the Veronicelloidea family shows a higher absorption band.

Finally, with regard to the last group of species, corresponding to freshwater snails *L. stagnalis*, *M. cornuaretis* and *P. diffusa*, at 25 °C it is clear that the three spectra show strong amide I and II bands, and this also ties well with observations made by Skingsley *et al.* [20] on the giant pond snail *L. stagnalis* and its amide I and amide II bands. However, one of the prominent features observed, corresponds to the region of CH₃ bending and aromatic residues which is higher in *M. cornuaretis* and *P. diffusa* than in *L. stagnalis*, i.e. the two tropical species exhibit different CH₃ bending events compared to the temperate species native to the UK [257]. Furthermore, the amide III peak is higher and similar in *M. cornuaretis* and *P. diffusa* and higher than in *L. stagnalis*, which we attribute to unordered structures such as random coil. In the region 1180-1024 cm⁻¹ corresponding to glycosidic bondings and sugar residues, both bands in *M. cornuaretis* and *P. diffusa* are similar, but different compared to *L. stagnalis*, which is due to a similar state of glycosylation in the tropical snails, and different from the pond snail. [59]. The same pattern is evident at 80 °C, where *M. cornuaretis* and *P. diffusa* are similar in the five regions, but different to *L. stagnalis*, suggesting not only different degree of glycosylation and thermal stability, but also different protein concentration, and protein chain length [58], [257]–[260].

Thus, in summary, it is possible to use the major bands observed in each spectrum to determine the type of protein structures and the degree of glycosylation in the measured gastropod mucus.

3.3.2 BETWEEN-SPECIES COMPARISON OF THE CHEMICAL COMPOSITION OF GASTROPOD MUCUS

To determine the relative content of each one of the main regions observed in spectra at 25 and 80 °C, peaks were integrated and results are shown in figure 3.4.

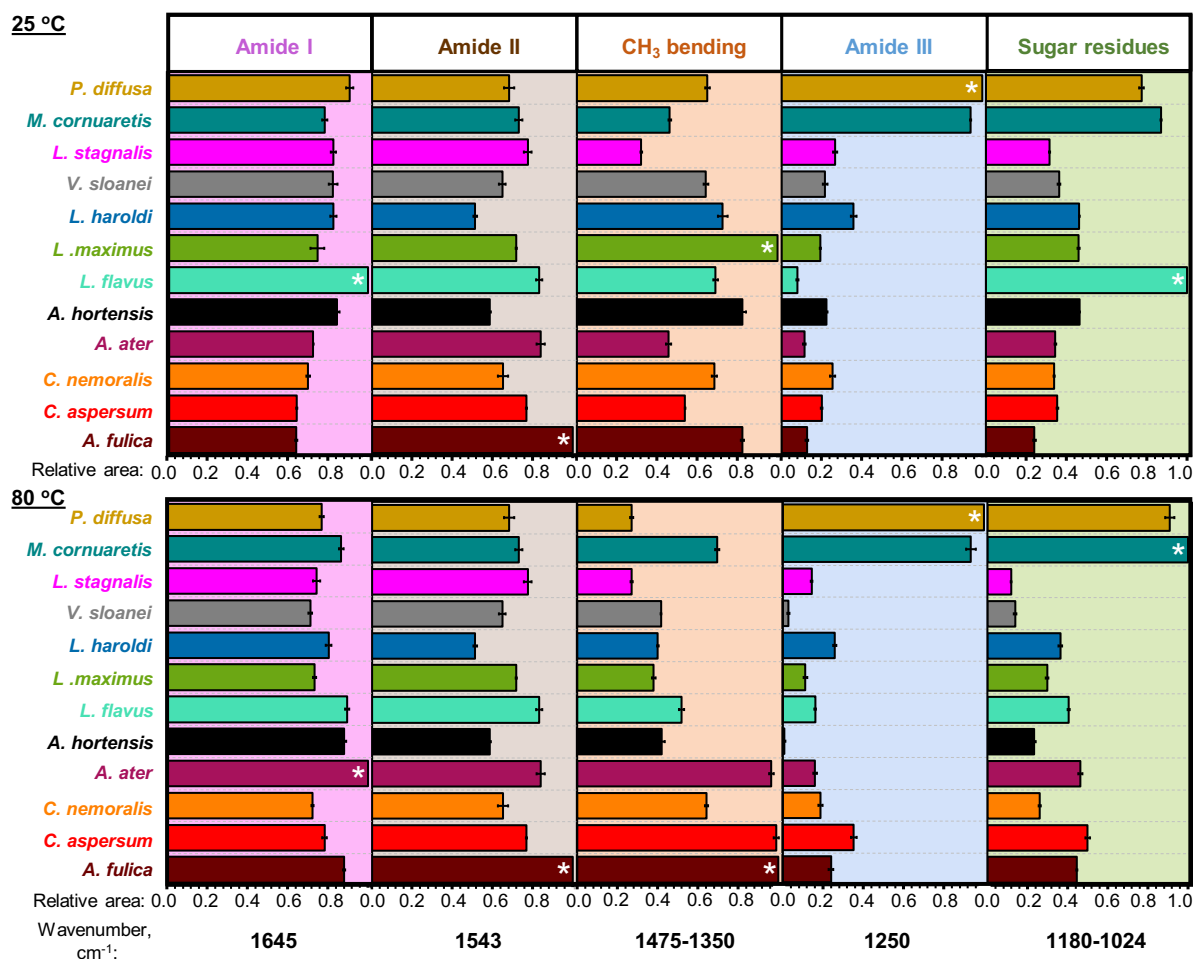


FIGURE 3.4 Composition of gastropod mucus from *A. fulica*, *C. aspersum*, *C. nemoralis*, *A. ater*, *A. hortensis*, *L. flavus*, *L. maximus*, *L. haroldi*, *V. sloanei*, *L. stagnalis*, *M. cornuaretis* and *P. diffusa* at 25 °C, and 80 °C, showing the relative areas of a band assigned to amide I (1645 cm⁻¹); amide II (1543 cm⁻¹); CH₃ bending (1475-1350 cm⁻¹); amide III (1250 cm⁻¹); and sugar residues and glycosidic bonding (1180-1024 cm⁻¹). White asterisks indicate the maximum values, and areas are relative within that category. The error bars represent the standard deviation of three different observations per species at each temperature. A value of 1 represents the highest area calculated and 0 represents the minimum measured.

Amide I

This region is attributed mainly to the C=O stretching vibrations of the peptide bonds present in the structure of protein, and secondary structural information can be obtained from this

band (α -helix, β -sheets, β -turns, random coil or aggregated strands) [211], [261]. For most species, the amide I region appears as a strong band at both temperatures, with the minimum value of 0.64 ± 0.01 for *A. fulica* and *C. aspersum*, and the maximum relative area of 1.00 for *L. flavus* at 25 °C; and 0.72 ± 0.01 for *C. nemoralis* and 1.00 for *A. ater* at 80 °C. This observation could be related to the relationships between taxonomic families, as discussed below.

Amide II

This region is due to the C-N stretching vibrations and N-H bending, due to tyrosine protonation state, and these aromatic interactions between the residues within a protein are essential for the correct function of the protein molecule. Amide II shows higher variations compared to amide I, with the minimum value of 0.26 ± 0.01 for *L. flavus*, and the maximum relative area of 1.00 for *A. hortensis* at 25 °C; and 0.51 ± 0.01 for *L. haroldi* and 1.00 for *A. fulica* at 80 °C. One interesting aspect of amide I and amide II, is that the ratio between these two bands indicates the relative degree of ionisation and hydration of the molecules, as can be seen from section 3.4, there are variations in those regions. As a result, amide I to amide II ratios for all of the gastropods included in this study show differences [20]. Table 3.2 indicates these ratios for each species at 25 and 80 °C.

TABLE 3.2. Amide I/Amide II ratios calculated for all species at 25 and 80 °C, with values from figure 3.4. Conditional formatting with colour scale red-yellow-green, represents the maximum, medium and minimum values, respectively.

Species	Amide I: Amide II ratio	
	25 °C	80 °C
<i>A. fulica</i>	1.09 \pm 0.04	0.85 \pm 0.06
<i>C. aspersum</i>	1.10 \pm 0.08	1.02 \pm 0.01
<i>C. nemoralis</i>	1.13 \pm 0.01	1.11 \pm 0.04
<i>A. ater</i>	1.46 \pm 0.09	1.19 \pm 0.03
<i>A. hortensis</i>	0.85 \pm 0.01	1.50 \pm 0.03
<i>L. flavus</i>	3.87 \pm 0.17	1.08 \pm 0.02
<i>L. maximus</i>	0.96 \pm 0.06	1.02 \pm 0.01
<i>L. haroldi</i>	1.75 \pm 0.08	1.61 \pm 0.08
<i>V. sloanei</i>	1.43 \pm 0.05	1.18 \pm 0.12
<i>L. stagnalis</i>	1.10 \pm 0.03	1.02 \pm 0.07
<i>M. cornuaretis</i>	2.06 \pm 0.07	1.19 \pm 0.02
<i>P. diffusa</i>	2.10 \pm 0.01	1.12 \pm 0.05

The maximum amide I/amide II ratio at 25 °C corresponds to *L. flavus* with 3.87 ± 0.17 and the lowest to *A. hortensis* with 0.85 ± 0.01 . At 80 °C the maximum value is for *L. haroldi* with 1.61 ± 0.08 , while the lowest is 0.85 ± 0.06 for *A. fulica*. These ratios suggest that in gastropod mucus the protein cores are different in some cases, with less variations in other families (Helicoidea and Ampullarioidea), but β -sheet and β -turns structural elements are present in all species. This aspect may be responsible for some characteristics of gastropod mucus, such as its rheological properties, because β -sheet move easily over the same structures, due to the compressed pleated sheet, compared to other protein secondary structures with different shapes or order [20], [262].

CH₃ bending

The other region between 1475 and 1350 cm⁻¹ corresponds to CH₃ bending and aromatic residues in proteins [211], [246], [263]. This region shows variations at both temperatures, with the minimum value of 0.32 for *L. stagnalis*, and the maximum relative area of 1.00 for *L. maximus* at 25 °C; and 0.27 ± 0.01 for *L. stagnalis* and *P. diffusa*, and 1.00 for *A. fulica* at 80 °C.

Amide III

Bands at 1250 cm⁻¹, corresponds to amide III region, and show major variations due to the C-N stretching, N-H bending in protein secondary structures, and also could indicate the presence of random coils [246], [247]. The amide III region has its minimum value of 0.08 for *L. flavus*, and the maximum relative area of 1.00 for *P. diffusa* at 25 °C; and 0.01 for *A. hortensis* and 1.00 for *P. diffusa* at 80 °C.

Sugar residues

At 1180 and 1024 cm⁻¹ the last region is identified, the presence of O-glycosidic bonding is clear, i.e., the covalent bond between a sugar molecule and a protein (mucins) [59]. Khajehpour *et al* [264] investigated glycosylation of proteins and, interestingly, the bovine submaxillary mucin sample showed the higher absorbance bands at around 1100 cm⁻¹, indicating a high degree of glycosylation, i.e., stabilisation of proteins by sugar molecules, when compared to non-glycosylated proteins. The sugar residues region shows clear variations at both temperatures, with the minimum value of 0.24 ± 0.01 for *A. fulica*, and the

maximum relative area of 1.00 for *L. flavus* at 25 °C; and 0.12 for *L. stagnalis* and 1.00 for *M. cornuaretis* at 80 °C. This observation could be related to the effect of sugar molecules on the stability of proteins and how mucins respond to dehydration and thermal stress [240], [265], but also related to the amount of glycosylation, because the absorbance in the sugar residues region is directly proportional to the amount of glycosylation in samples containing mucins, such as gastropod mucus [264].

However, in order to elucidate a more specific effect of protein secondary structures in locomotive mucus, a more detailed analysis of amide I region needs to be undertaken.

3.3.3 PROTEIN SECONDARY STRUCTURES: AMIDE I PEAK DECONVOLUTION

Gaussian fitting following the procedure described in section 3.2.2 was performed for samples at 25 and 80 °C, corresponding to the amide I region. Figure 3.5, shows the relative proportion of protein secondary structures, such as α -helices, characterised by a coil formed by amino-acid residues on the polypeptide chain [266]; β -sheet, extended polypeptide strands link together by hydrogen bonds [267]; β -turns, where a change occurs in the polypeptide chain [268]; random coil, or also classified as the unfolded structures [256]; and aggregated strands. A table indicating the presence or absence of each component is included.

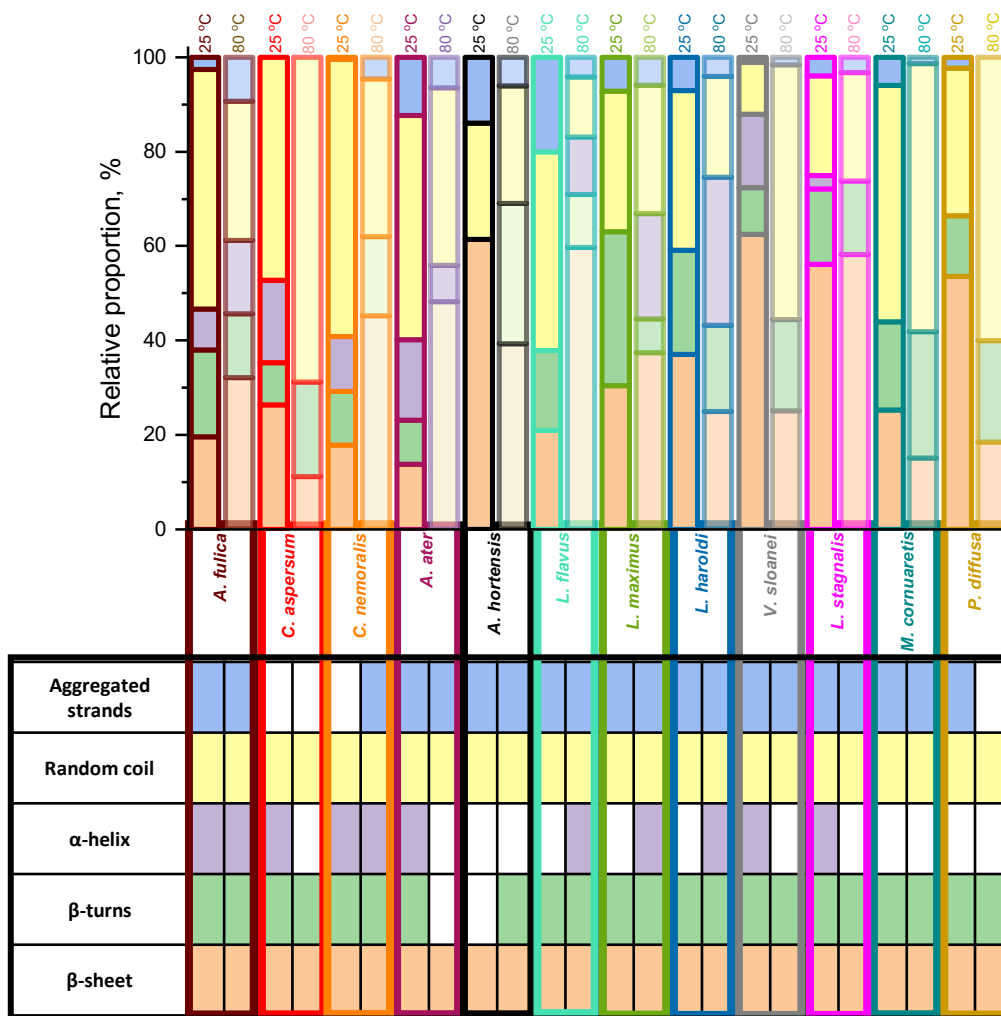


FIGURE 3.5 Distribution of elements present in protein secondary structure for each species, at 25 °C and 80 °C derived from FTIR measurements. A table showing the presence (coloured cell) or absence (white cell) of specific structures is included.

It is clear that the most stable material corresponds to *A. fulica* mucus because all structures are present at 80 °C, only the percentages change. For the other eleven species, one or two components are not present at both temperatures, indicating transitions between structures or new conformations. Another interesting observation corresponds to the lack of α -helices at 25, 80 °C or both temperatures, in ten of the twelve species, and the presence of β structures in all species. Our results match well with Denny [262], because he suggested that β structures are one of the main groups of protein secondary structures in gastropod locomotive mucus, contributing to mucus function as a lubricant. These structures can form

an infinite planar network facilitating the displacement of layers, and as a consequence, enhancing protein chain mobility.

These β structures of polypeptides can interact with each other by hydrogen bonds, giving place to β -sheet and β -turns, folded laminar structures present in proteins [267]. It has been reported that globular proteins consist of approximately 30 % or more of amino acid residues corresponding to β structures [246], this is in concordance with our results where these structures correspond to a range between 22-65 %. The predominant percentages of protein secondary structures in all species at 25 and 80 °C, correspond to a general transition from random coil to β -sheet. There is evidence that indicates disordered proteins can be adapted to different conditions due to their hydrophilicity and versatility, keeping their function when water deficit is clear, because they possess high flexibility [269], and the disordered regions in mucins could be the main factor influencing functionality of mucins [270].

In summary, our analysis of the amide I region of FTIR spectra has given clear information about the protein secondary structures in gastropod locomotive mucus and how these conformations may contribute to its function. However, with FTIR spectra a more holistic analysis can be performed, considering the full range from 1800 to 1000 cm^{-1} which can help classify species.

3.3.4 CLASSIFICATION OF GASTROPOD SPECIES

In the previous sections spectral analysis was performed to compare and determine the main groups associated to the compositional properties of gastropod locomotive mucus. However, Boulet-Audet, *et al.* studying silkworm silk [237], suggested that multivariable analysis is a useful tool for species classification and discriminating samples. Hence, we first performed a principal component analysis of spectra of twelve species at both 25 and 80 °C. Our initial multivariate analysis of gastropod locomotive mucus is summarized in Fig. 3.6, showing the values of the first and second factor scores calculated from the mucus spectra.

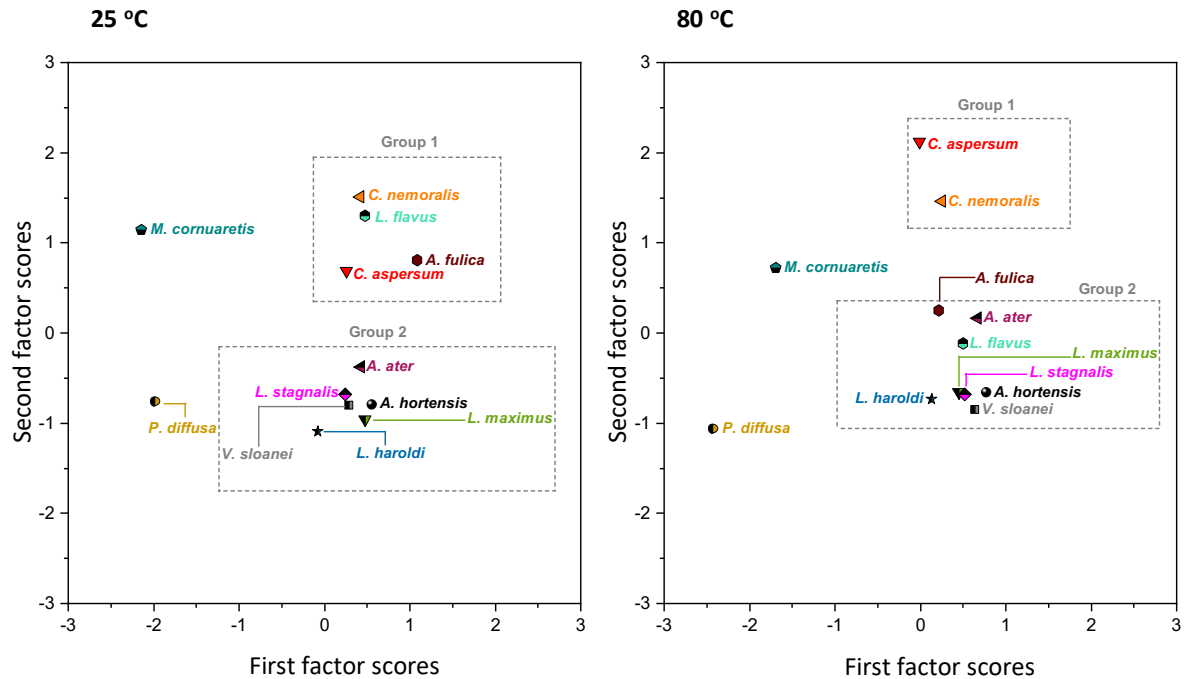


FIGURE 3.6 Factor scores of gastropod mucus at 25 and 80 °C. The first and second factor scores contribute to 65.6 % of species discrimination.

From figure 3.6, at 25 °C, we can observe different clusters, group 1 comprises terrestrial snails in Helicoidea (*C. aspersum* and *C. nemoralis*) and Achatinoidea families (*A. fulica*), as well as the terrestrial slug *L. flavus* in the Limacoidea family. Group 2, where most of the terrestrial slugs are grouped, corresponding to families Arionoidea (*A. ater* and *A. hortensis*), Limacoidea (*L. maximus*), Veronicelloidea (*L. haroldi* and *V. sloanei*), and the freshwater snail *L. stagnalis* in Lymnaeidae family. Finally, in the periphery of those two clusters we find *M. cornuaretis* and *P. diffusa* species, suggesting a greater dissimilarity with the average of the measured mucus. It is clear that these two species appear as outliers. Notably, our results imply that the tropical freshwater snails *M. cornuaretis* and *P. diffusa* produce similar mucus, most likely because both species are in the same family (Ampullarioidea).

At 80 °C, there are two clusters, group 1, including the two terrestrial snails *C. aspersum* and *C. nemoralis*, suggesting that mucus produced by these species has a similar response to temperature, which is not a surprise because both are from the same family, Helicoidea. There is another cluster, group 2, including all six terrestrial slugs in the families Arionoidea (*A. ater* and *A. hortensis*), Limacoidea (*L. flavus* and *L. maximus*), and Veronicelloidea (*L.*

haroldi and *V. sloanei*), the freshwater snail *L. stagnalis* in Lymnaeoidea family and the *A. fulica* snail in Achatinoidea family, indicating a lower dissimilarity with the average of the measured mucus. As observed in the protein secondary structures analysis, the only sample which shows all structures is the snail *A. fulica*. Interestingly, at 25 °C, the tropical freshwater snails *M. cornuaretis* and *P. diffusa* appear as outliers, indicating these two species produce mucus that responds in a similar way to heating.

In order to draw quantitative links between species, our HCA used the scores of the most important factors to group gastropod species according to their similarity.

3.3.5 COMPARING FTIR AND PHYLOGENETIC TREES

The ultrametric tree generated from the infrared spectra at 25 °C for native dry mucus (see Fig. 3.7b) was compared with a cladogram (see Fig. 3.7a). It was built from the sequencing of gastropod mucus in different clades and species, combining trees reported previously for the class Gastropoda, including the seven families of species selected for this study [9], [13], [66]–[75]. Importantly, the cladogram and ultrametric tree are similar, especially families. It is evident that terrestrial snails are close between each other and the tropical snails are together as well, remaining in the same position comparing figures 3.7a and b.

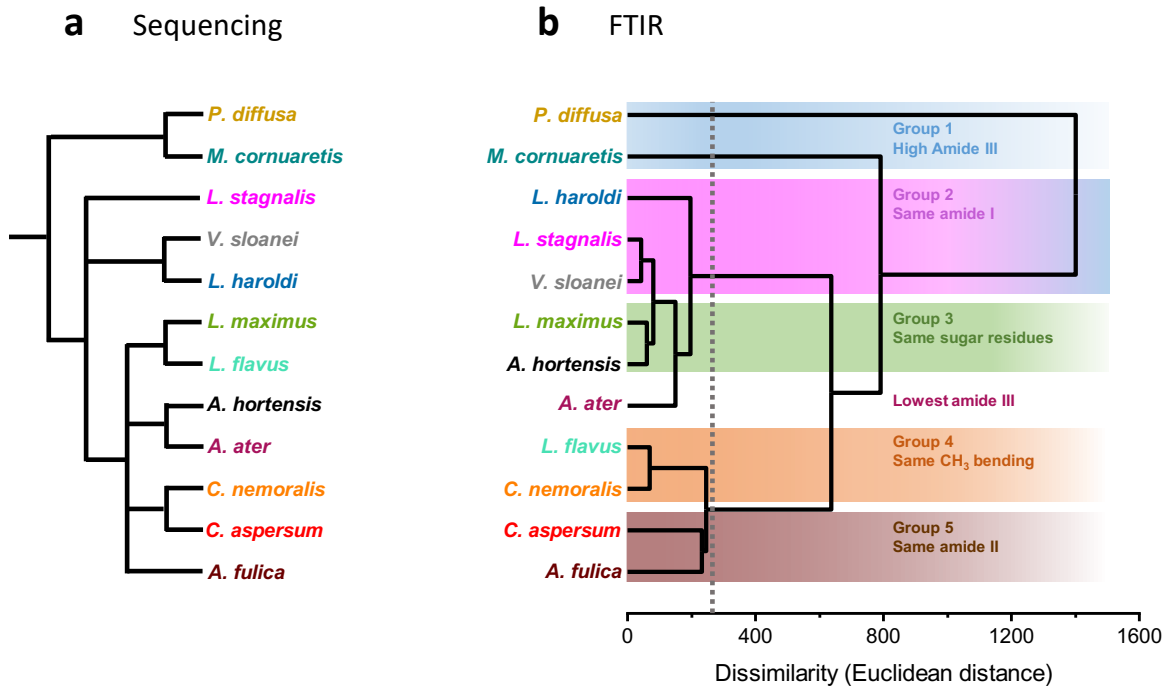


FIGURE 3.7 Classification of gastropod species. (a) Cladogram generated based on the phylogenetic analysis of [9], [13], [66]–[75]. (b) Ultrametric tree generated from the hierarchical clustering analysis of gastropod mucus infrared spectra LDA factor scores. Species with a Euclidean distance smaller than 250 were grouped together.

From the ultrametric tree generated from FTIR spectra (Fig. 7b), five main groups are identified. They were grouped together based on their similarities, more specifically, on their amide I, II, III, CH₃ bending and sugar residues values. This ties well with our findings about peak areas described in figure 3.4, at 25 °C.

Group 1: High amide III

This group encompasses the two tropical freshwater snails *M. cornuaretis* and *P. diffusa*, both in the Ampullarioidea family, displaying a larger Euclidean distance from the other four groups (> 250). The two species from this group have high absorbance at 1250 cm⁻¹ (Fig. 3.4), suggesting that these species were grouped together based on their high amide III absorbance, indicating a high random coil content. In this case, the presence of random coils suggests a high degree of internal rotation within the protein as limited side chain interactions take place [256]. This may help contribute to the viscoelastic properties of mucins, as a result of a higher entanglement density [271].

This finding could be related to the behaviour of these species of freshwater snails, which are primarily considered as shredders of plants and predators of other small animals [272]. Observations on the behaviour of these species, put them apart from other freshwater gastropods based on their unusual mode of feeding, consisting of small particles floating on the water surface (air-water interface) [273]. For example, snails in the Ampullarioidea family during the feeding process form a funnel-like shape with the anterior part of its foot. Then once the funnel is formed, it produces a current, drawing food particles in to combine with the mucus layer which is then ingested through the mouth. These observations indicate that species in the Ampullarioidea family use their locomotive mucus film not just as a lubricant, but also as a net that enables collection of particles [273]. These characteristics, suggesting a low protein concentration in gastropod mucus, contribute to form a viscous solution with a time-dependent properties attributed to a flexible random coil structure [274].

Group 2: Same amide I

This group includes the two terrestrial slugs *L. haroldi* and *V. sloanei*, both in the Veronicelloidea family, as well as the freshwater snail native from the UK, *L. stagnalis* in the Lymnaeoidea family. Species in this group have the same amide I absorbance, at 1645 cm^{-1} , as observed in figure 3.4, suggesting that these gastropods have similar protein concentration in their mucus. According to our Gaussian fitting (figure 3.5 at $25\text{ }^{\circ}\text{C}$), the main contribution to this band in these three species comes from the β -sheet presence. It has been reported before that in concavalin-A, a carbohydrate-binding protein, the percentage of β -sheet is around 58% [246], which is in agreement with our findings on these three gastropods. Species in the Veronicelloidea family are hermaphroditic and can perform self-fertilization and mucus of the slug *P. boraceiensis* in the same family, has been previously studied to determine its bactericidal and bacteriostatic effect on *E. coli* and *S. aureus*. Results demonstrate that the main components in mucus are lipids, proteins and glucose (mucins), where proteins identified have a molecular weight up to 300 kDa [275]. Mucus from the pond snail *L. stagnalis* has been characterised by gel chromatography, finding the major component in locomotive mucus, which is secreted into the water and remains as a biofilm on the substrate, being a high molecular glycoconjugate with a high molecular weight of 260 kDa [276], [277]. These studies including the three species in this group, indicate there is a clear similarity in molecular weight of proteins identified, and possibly in protein concentration in native mucus.

Group 3: Same sugar residues

In this group we find the terrestrial slugs *L. maximus* and *A. hortensis*, in Limacoidea and Arionoidea families, respectively. These species have the same absorption between 1180-1024 cm^{-1} , as observed in figure 3.4, indicating a similar glycosylation degree. To support our interpretation, a previous study, compared the degree of glycosylation from six proteins: cytochrome c, collagen type IV, soybean peroxidase, avidin, neutravidin, and bovine submaxillary mucin, showing that FTIR absorbances in the sugar residues region increases when the degree of protein glycosylation increases [264].

However, there are no studies which have focussed on gastropods mucus and glycosylation. One study based on the entire body of five different gastropod species provides some insight [278]. In this study, the species *L. maximus*, *C. hortensis*, *P. corneus*, *A. arbustorum* and *A. fulica* were characterised, to identify the N-glycans of gastropods. These components contribute to gastropod glycosylation abilities and offer information about the biosynthetic capacity for glycosylation. Their findings showed that these species are able to methylate terminal sugars [278]. These studies provide a glimpse into glycosylation in gastropods, and our results demonstrate that this modification is also present in locomotive mucus from all species of terrestrial and freshwater gastropods.

Group 4: Same C-H bending

This group encompasses the slug *L. flavus* and the snail *C. nemoralis*, in Limacoidea and Helicoidea families, respectively. Species in this group show the same absorption bands between 1475-1350 cm^{-1} , as described in figure 3.4. This band represents the carbon spins of the core backbones of the glycosaminoglycans and proteoglycans, for example, CH_3 bending [59], [58], [279]. The same CH_3 bending in all species in this group, suggests that glycosaminoglycans (GAGs), described as isolated proteoglycans linked to a protein, are similar, with the same disaccharide building block consisting of N-acetylated or N-sulphated glucosamine or N-acetylgalactosamine in mucus. These characteristics, as well as the structure of the protein cores and conformation of protein structures, establish the biological role associated with glycosaminoglycans and proteoglycans [280], [281].

Group 5: Same amide II

Finally, in this group we find the terrestrial snails *C. aspersum* and *A. fulica*, in the Helicoidea and Achatinoidea families, respectively. This group is characterised by the same amide II absorption at 1543 cm^{-1} , as observed in figure 3.4. The amide II region is characterised by the hydrogen bonding by the NH bending and CN stretching vibration, affected by side chain vibrations [282]. Interestingly, these species not only have the same amide II, but also similar amide I and III peak areas, which suggests there are also similarities in protein structures.

In one study of different polypeptides and proteins, poly (L-glutamic acid) and poly (L-lysine) in various conformational forms characterised by Vibrational Circular Dichroism (VCD), Gupta and Keiderking found interesting results when comparing groups based on their amide II bands [282]. The FTIR absorption of amide II spectra of concanavalin-A, a carbohydrate binding protein, gives its major contribution to the amide II band due to the high β -sheet content, and this is attributed mainly due to the mixed structure of the globular protein. The deconvoluted FTIR spectra show evidence of multiple components, possibly some of the main three groups of protein secondary structures (random coil, α -helix, and β -sheet), but these peaks are poorly resolved. The distinction is better when considering amide I peak, as we showed above, it provides a clearer identification of peaks and protein secondary structures [282].

Thus, translating these observations to proteins in gastropod mucus, we can assume that the structures of these proteins in *C. aspersum* and *A. fulica* are highly correlated, i.e., they have similar higher amount of β -sheet than α -helix. This finding can be corroborated with our analysis on amide I peaks.

In summary, the five groups indicated in the ultrametric tree (Figure 3.7b) can be correlated based on their similar absorption bands. However, there is one species which represents an outlier, *A. ater* in Arionoidea family which has the lowest amide III content. Although this species is excluded of these five main groups, it is close to *A. hortensis*, the other one species in the same family, as it is shown in Figure 3.7a. According to molecular phylogeny of gastropods, the divergent species in Arionoidea family is monophyletic and the closest clade

corresponds to the Limacoidea family [283]. This observation ties well with our ultrametric tree (Figure 7b), where *A. ater* is close to *L. flavus*.

Despite similarities between species and groups, some species were classified differently using FTIR spectra and these variations could be the result of proteins and sugar molecules (mucins) in gastropod mucus. Although, species such as *A. ater* is not together with the other Arion species, they are close in the ultrametric tree, and most important, species corresponding to tropical freshwater snails were classified together based on their similarities. Hence selection may be driving the composition of locomotive mucus towards convergent functional properties as opposed to the diversification seen in other aspects of animal's morphology and genetics, which typically are used to create a tree.

In summary, even with these differences comparing the cladogram based on phylogeny with the ultrametric tree, FTIR with multivariate analysis offers a powerful tool to classify gastropod species based on their absorbances, while reducing the effect of external factors, such as temperature or humidity which could affect results, when temperature is controlled, and dry samples are analysed.

3.4 CONCLUSIONS

FTIR spectroscopy provides a relatively simple, non-destructive and real-time methodology for gastropod mucus characterisation, collecting native mucus directly from the foot of the animal, reducing the effects of sample's modification due to collection or storage processes. This technique allowed us to analyse samples from terrestrial and freshwater gastropods, to identify the main groups of components responsible for mucus compositional properties, as well as the determination of protein secondary structures in proteins, which are important for the understanding of how folding and unfolding mechanisms affect mucus stability.

Although small changes in amide I bands were observed with an increase in temperature, the transition from a native folded state to an unfolded state of the proteins (secondary structures variations), seem to be the major changes in the FTIR spectra of proteins. With the correlation between amide I and sugar residues regions, it was possible to identify the main

glycosylation variations in the twelve species included in this study, proving our hypothesis that mucins, play an important role in mucus stability.

The classification of species based on mucus' structural information suggests there are relationships between families, possibly related to adaptations to a terrestrial or aquatic environment. Spectral changes detected by FTIR will contribute to the hierarchical classification performed here. Variations observed by FTIR indicating different protein structures, could be further validated by other techniques, such as ultraviolet-visible spectroscopy (UV-Vis), to determine protein concentration in locomotive mucus; sodium dodecyl sulphate polyacrylamide gel electrophoresis (SDS-PAGE), to know the molecular weight of proteins in mucus. Additionally, as any structural and compositional change affects thermal stability of mucus and its functionality as a lubricant, thermal and rheological tests can be performed to correlate all properties of gastropod mucus.

This chapter provides the first study reported on gastropod mucus using FTIR to analyse, identify and classify gastropod mucus based on their structural characteristics. This procedure could be used to expand our interpretation of this group of molluscs to other clades, such as marine species.

CHAPTER 4: THE RHEOLOGICAL PROPERTIES OF GASTROPOD LOCOMOTIVE MUCUS: RELATING COMPOSITION TO FUNCTION

“...**W**e don't often see a snail that way,
and that's because we've only recently had the tiny lenses
and electronic cameras that we need
to explore this miniature world...” **David Attenborough**



This chapter corresponds to the paper “The rheological properties of gastropod locomotive mucus: relating composition to function”, to be submitted for publication to the Journal of Molluscan Studies.

ABSTRACT

The main component in gastropod locomotive mucus are mucins, conferring mucus its viscoelastic properties. However, there are no studies reported contrasting compositional, thermal and rheological properties of mucus from different gastropods. To fill this gap, in this study, we analysed native locomotive mucus from *Achatina fulica* (*A. fulica*), *Cornu aspersum* (*C. aspersum*), *Cepaea nemoralis* (*C. nemoralis*), *Arion ater* (*A. ater*), *Arion hortensis* (*A. hortensis*) and *Limax flavus* (*L. flavus*). Mucus samples were characterised using Sodium dodecyl sulphate-polyacrylamide gel electrophoresis, SDS-PAGE; Ultraviolet-visible spectroscopy, UV-vis; Thermogravimetric analysis, TGA; and rheology, in order to correlate and compare characteristics between species, to elucidate how mucins influence mucus behaviour. Here we show that mucins are the main factor influencing mucus' function under different mechanical or thermal stresses. We found that all mucus tested comprised of glycosylated proteins (41-377 kDa) acting as weak gels (1.58-36.33 Pa.s at 1 rad/sec). The lowest ratio of protein to total solids was found in *A. fulica* (0.007), and the highest (0.042) in *A. hortensis*. Our results demonstrate that members from the same family exhibit similar characteristics, suggesting there is a common response to specific environments. We expect our study to be a terminus a quo in the comprehension of how a correlation between properties is crucial for the understanding of the stability and functionality of snail mucus.

KEYWORDS:

Ecto-secretion, gastropod, mucins, function.

4.1 INTRODUCTION

Most natural materials remain inside or close-to the body, allowing for repair and reconfiguration. However, some species have evolved the ability to produce and use materials outside of their bodies. Termed ecto-secretions, these are a remarkably overlooked, yet important class of materials, selected to perform in extreme environments and facilitate a range of functions, from structural (silks) to chemical (venoms) [108], [284]. Gastropod mucus is a prime example of such an ecto-secretion, which when excreted as a thin layer (between 10-20 μm) aids locomotion, adhesion and defence as well as preventing desiccation and infection [40], [49], [285]–[292], and in some cases even serves as a substrate for microbial “farming” [293]. Yet despite its natural ubiquity and utility, there are only a limited number of studies focused on gastropod mucus per se [33]–[36], [49], [52], [55]–[61], [63]–[65], [76]–[88]. This apparent dearth of knowledge surrounding the composition and structure of gastropod mucus is compounded when considering its material/mechanical properties.

Although the interest in learning more about gastropods, their behaviour and characteristics has existed for centuries, it was not until the 1980's that Denny [58], [258] systematized the study of gastropod mucus with a broader vision, and through a combination of experimental and theoretical studies related a range of mucus' physical properties to the animal's biology and habitat [58]. Denny was the first to study the mechanical (rheological) properties of gastropod locomotive mucus, demonstrating that in the slug *A. columbianus* its shear stiffness is indirectly proportional to its water content (degree of hydration) [58]. Twenty years later, Ewoldt *et al.* [34], extended this line of research and compared the non-linear rheological properties of locomotive mucus from a snail (*H. aspersa*) and a slug (*L. maximus*). Their findings suggested that the timescale by which a mucus is deformed determines whether it behaves as an adhesive or a lubricant. They categorized mucus as having viscoelastic properties and behaving as a non-Newtonian gel [34]. More recently in 2019, Smith *et al.* [65], attributed the complex rheological properties of the adhesive mucus from the slug *A. subfuscus*, to sacrificial bonds between components in the mucus, which can readily reform if broken. They tested mechanical properties of adhesive mucus in order to determine the effect of those sacrificial bonds. Stress relaxation tests demonstrated that slug's glue behaves like a viscoelastic material, showing elastic and viscous characteristics when it experiences

deformation; tensile tests showed that adhesive mucus samples stretched six times their initial length before yielding. This is supported by other studies that demonstrated that metal ions are essential to maintain the stiffness of the slug's gel (adhesive mucus), more specifically, calcium, magnesium, zinc, manganese, iron and copper. It is precisely the role of calcium which is crucial in the stabilisation of the polymer network, due to the cross-links, because calcium is the most common cation bound to the glue (40 mmol l^{-1}) [61], [64].

Facilitating these mechanical properties are mucus' proteins, mucins, which are heavily glycosylated [294]. As a result, most compositional studies have used SDS-PAGE to identify molecular mass of the main group of proteins in gastropod mucus, characterising the marine snails *L. limatula*, *H. diversicolor*; terrestrial slugs *A. subfuscus*, *A. ater*, and the garden snail *H. aspersa* [34], [49], [52], [60], [61], [63], [76], [79], [81]. Also, mass spectroscopy and chromatography have been used, characterising the marine snails *P. vulgate* and *D. maxima*; terrestrial slug *A. subfuscus*; and terrestrial snails *H. aspersa*, *E. vermiculata*, *T. pisana* and *M. obstructa* [60], [61], [77], [80], [81], [86]. However, the use of UV-vis to correlate structural variations between samples has not been widely included in gastropod mucus' studies, and this technique could complement the compositional characterisation of mucus using one of the well-used techniques, such as SDS-PAGE.

As such a cohesive understanding, within an appropriate evolutionary context, between mucus' molecular components and behaviour across a range of species is required. To address this, we propose that proteins in mucins are the most likely component to influence phenotype and in line with our wider classification of these materials as ecto-secretions, proteins will be key in delivering functionality for the required timescale of use. Hence this work presents a combination of thermal (TGA and Rheological ramp temperature tests), compositional (UV-Vis and SDS-PAGE) and functional (Rheology) techniques to characterise locomotive mucus across six different terrestrial gastropod species: *A. fulica*, *C. aspersum*, *C. nemoralis*, *A. ater*, *A. hortensis* and *L. flavus*.

4.2 MATERIALS AND METHODS

4.2.1 MATERIALS

Three species of terrestrial snails (*A. fulica*, *C. aspersum* and *C. nemoralis*), and three terrestrial slugs (*A. ater*, *A. hortensis* and *L. flavus*), were included in this study. Apart from the snail *A. fulica*, which is native to Africa, all other species are found in Europe. *A. hortensis*, *A. ater*, *C. nemoralis*, *C. aspersum* and *L. flavus* were collected in Hillsborough Park, Hillsborough, Sheffield (53.4080° N, 1.5015° W). *A. fulica* snails were purchased as juveniles and reared in house. All species were kept in plastic containers (39 cm x 48 cm x 20 cm) with ~ 6 cm of vermiculite layering the bottom of the box at 22 °C ± 1 °C and high humidity. Animals were fed *ad libitum* twice weekly with cucumber, lettuce and sweet potatoes.

For each species three specimens were removed from the containment area and cleaned using type II water and placed into an empty and clean plastic container. Animals were then allowed to move freely across a clean sheet of glass for five minutes, to avoid collecting adhesive mucus. After that, locomotive mucus was collected from the glass surface using two razor blades (cleaned using ethanol and then type II water) and kept in a 2.0 ml polypropylene graduated centrifuge tube with cap, stored at room temperature and subjected to analysis on the day of collection.

4.2.2 METHODS

4.2.2.1 THERMOGRAVIMETRIC ANALYSIS

TGA tests were carried out using a MX-50 (A&D Instruments UK) moisture content analyser. An alumina crucible (9.5 mm diameter and 14 mm high, Almath Crucibles Ltd, UK) with 1 ml of fresh native mucus was used for all experiments. The heating rate was 1 °C/min from 25 to 120 °C with a data interval of 15 seconds. All experiments were repeated three times for each species, with separate samples collected for each test, from the same group of individuals.

4.2.2.2 UV-VIS SPECTROSCOPY

With concentrations obtained from TGA analysis, dilutions were prepared for all species and samples were set to the same concentration 1 mg/ml approximately. Type II water was used as a solvent and native mucus collected as described in section 2.2.1. Then, using a UV300 Spectronic Unicam spectrometer (Thermo, UK), all samples were analysed at room temperature ($22\text{ }^{\circ}\text{C} \pm 1\text{ }^{\circ}\text{C}$), in 1 cm path-length polystyrene cuvettes. Type II water was used as a blank and mucus samples were manipulated using a 1000 μl micro-pipette. Scans were performed from 200 - 500 nm, at a scan speed of 240 nm/min and 300 steps in total.

Using maximum absorbance at 215, 225-230 and 260nm, concentrations can be estimated for each samples using the following equations [45]:

$$\text{Concentration (mg/ml)} = (0.183 \times A_{230\text{nm}}) - (0.075 \times A_{260\text{nm}}) \quad \text{Equation 1}$$

$$\text{Concentration } (\mu\text{g/ml}) = 144 \times (A_{215\text{nm}} - A_{225\text{nm}}) \quad \text{Equation 2}$$

The use of equations 1 or 2 depends on the presence of peaks at 215 with absorbance values < 2.0 [45]. To corroborate the use of equation 1 or 2 for each species based on maximum absorption peaks, deconvolution of UV-vis spectra and curve fitting were performed between 200 and 350 nm, and a 10-point multipeak Gaussian fitting (every 10 nm) was performed using Origin software, v2020 (See Appendix A1). Equation 1 was used for *C. aspersum*, *C. nemoralis*, *A. ater*, *A. hortensis* and *L. flavus* (snails and slugs native from the UK), while equation 2, for *A. fulica*.

4.2.2.3 SDS-PAGE

Mucus from each one of the six species was collected as described in section 2.1. Samples were weighed, placed in a 2 ml polypropylene graduated centrifuge tubes and diluted with type I water to 5.92 mg/ml, based on the lowest dry weight measured previously by TGA. Aliquots of 20 μl were taken and mixed with an equal volume of a solution containing sodium dodecyl sulphate and β -mercaptoethanol, according to the method of Laemmli [296]. Aliquots of 20 μl of the resulting solutions were resolved on 4-20 % tris-glycine gel under reducing conditions, using a mini gel tank Invitrogen (Thermo Fisher Scientific, USA), power

supply PS 250 (Hybaid Ltd, UK), over 100 minutes at 120 V. Protein bands were visualised by staining with 0.25% Coomassie Brilliant Blue R-250 (VWR Chemicals, USA) and imaged using a Scanjet G2710 scanner (HP Inc., USA). A Hi-Mark Pre-Stained protein standard (Thermo Fisher Scientific, USA) was used as a ladder.

4.2.2.4. RHEOLOGY

Rheological measurements (frequency sweep and temperature ramp tests) were performed using an AR-2000 (TA Instruments, Delaware, USA) rheometer, with cone-plate geometry (cone angle 40 mm 2° and 55µm truncation) and a Peltier temperature controlled bottom plate. Native mucus, sufficient to completely fill the geometry gap, was placed onto the bottom plate and the geometry was lowered to the truncation gap at a slow speed to avoid any undue shearing of the sample. To avoid the native mucus drying out, the area outside and on top of the cone was filled with type II water and enclosed using an environmental chamber. Frequency sweep tests were performed from 0.6 to 62.8 rad·s⁻¹ (0.1 to 10 Hz) at 10% strain at 25 °C (chosen to be within the materials linear viscoelastic region). Single frequency oscillatory tests were then carried out at 0.63 rad·s⁻¹ 10% strain between 15 °C to 80 °C using a ramp temperature of 5 °C/min.

4.2.2.5 STATISTICAL ANALYSIS

Statistical analysis was performed using a Student's *t* test and *P* < 0.05 significance level (Origin software, v2020, USA).

4.3 RESULTS AND DISCUSSION

We present results from a comparative study of gastropod locomotive mucus, relating compositional, thermal and functional properties.

4.3.1 COMPOSITIONAL PROPERTIES

To determine the compositional properties of gastropod locomotive mucus, TGA, UV-vis, and SDS-PAGE were performed. In order to gain an initial, broad appreciation of composition, total solids concentration and protein concentration was determined using TGA and UV-Vis respectively (Figure 4.1).

Species	a Total solids concentration, mg/ml	b Protein concentration, mg/ml
<i>L. flavus</i>	10.93 ± 1.254	0.29 ± 0.006
<i>A. hortensis</i>	25.15 ± 0.180	1.07 ± 0.070
<i>A. ater</i>	15.95 ± 0.396	0.67 ± 0.021
<i>C. nemoralis</i>	12.10 ± 0.250	0.43 ± 0.008
<i>C. aspersum</i>	13.78 ± 0.464	0.47 ± 0.108
<i>A. fulica</i>	5.97 ± 0.057	0.04 ± 0.004

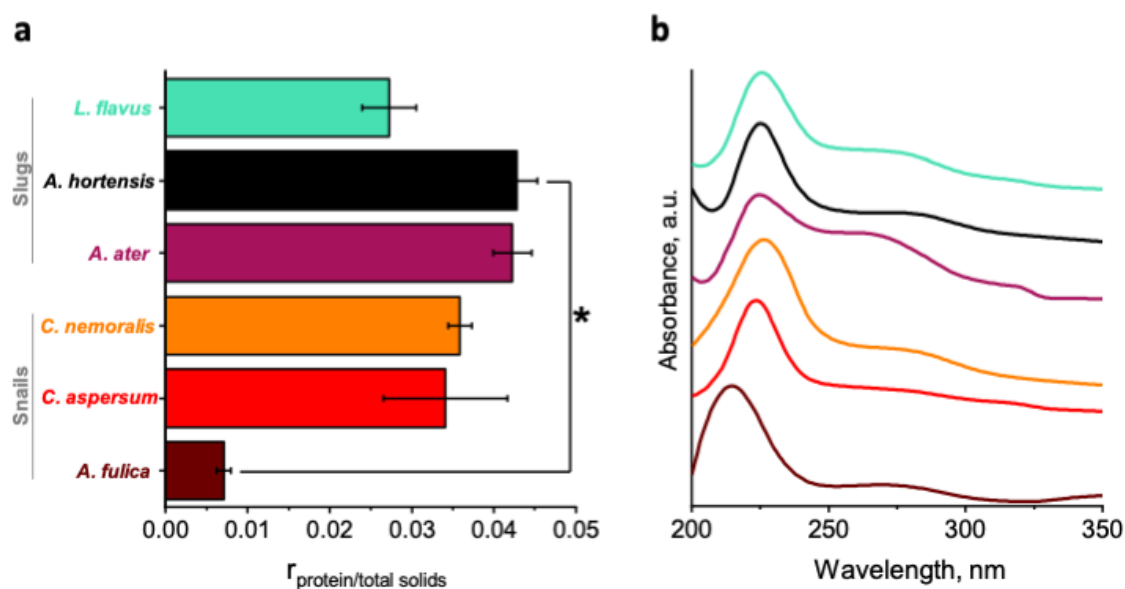


FIGURE 4.1 a) Protein to total solids concentration ratio, and b) UV-vis spectra of native locomotive mucus from *A. fulica*, *C. aspersum*, *C. nemoralis*, *A. ater*, *A. hortensis* and *L. flavus*. Significant differences between *A. fulica* and *A. hortensis* ($P < 0.05$) are indicated with black asterisk brackets. Standard deviation error bars correspond to a series of three experiments per species. A table with a) total solids and b) protein concentration in mg/ml, used to calculate $r_{\text{protein/total solids}}$, is included.

Water composition in gastropod mucus is 97.4 ± 0.07 in the slug *A. hortensis* and $99.4 \% \pm 0.004$ in the snail *A. fulica*. Between these values we found the other four species. *C. aspersum* and *C. nemoralis* have similar percentage of water, 98.7 ± 0.10 and $98.6 \% \pm 0.08$, respectively, they are from the same family Helicidae. The slugs *A. ater* and *L. flavus*, from two different families, have values of 98.3 ± 0.02 and $98.9 \% \pm 0.006$, respectively. Again, the two snails in the Helicidae family show similar water content. Our findings agree with previous studies where pedal mucus in terrestrial snails and slugs has been shown to consist of around 91-98 % water, and the rest corresponds to inorganic material and high molecular weight organic compounds, such as proteins [58], [258], [259], [260].

According to figure 4.1, table a, the lowest total solids concentration corresponds to the African snail (*A. fulica*) with 5.97, while the highest value is for the slug *A. hortensis*, 25.15 mg/ml. That difference could be associated with the presence of minerals such as calcium, because it has been demonstrated that terrestrial slug mucus contains substantial quantities of metals, contributing to total solids concentration, such as zinc, iron, copper and manganese. Ireland [297], analysed *A. ater* dry mucus and found that calcium concentration is 60 % higher than the total concentration of magnesium, phosphate, manganese, zinc and copper. These metals reduce the solidification speed of mucus and also they are necessary for the correct function of proteins, giving mucins the ability to absorb water, creating a protection against harmful pathogens, as well as facilitating gel formation [36], [51], [60], [298]–[300].

From figure 4.1b, proteins to total solids ratio, if we look at the three slugs, we immediately identify a lower value in the slug *L. flavus* from Limacidae family, compared to the other two slugs, *A. ater* and *A. hortensis*, respectively, both from the Arionidae family. In terms of the three snails, a similar pattern is observed which suggests members in the same family show similar ratio. The species *A. fulica*, in the Achatinidae family has the lowest ratio in comparison with the other two snails, *C. aspersum* and *C. nemoralis*, both in the Helicidae family. With a value of 0.007, the African snail *A. fulica* has the lowest ratio, while the highest one is for the slug *A. hortensis*, with 0.042. There is a significant difference between *A. fulica* and *A. hortensis* ($P = 0.0030$) and this could be attributed to the variation in other organic compounds like carbohydrates.

In this figure, 4.1b, UV-vis spectra are included, corresponding to the six gastropod species, with the main band observed at 225-230 nm, and a shift in this band in the snail *A. fulica* is observed at 215 nm, attributed to tryptophan (Trp) [301]. UV-vis spectra show the maximum absorption band between 215-230 nm, due to aromatic amino acids present in proteins being the major chromophores, due to $\pi \rightarrow \pi^*$ transition by absorption of a photon with particular energy leading it from a low energy level to a higher one (excited state) [302]–[304]. This could also be attributed to the presence of different components in protein secondary structures, because ionization of dissociable groups effects can change protein absorbance, even if there are no structural transitions associated with denaturation [305].

In mucus, there are globular proteins and mucins, consisting of glycoconjugates [306]. Previous studies related to other globular proteins suggest that tryptophan (Trp) and tyrosine (Tyr), two of the main aromatic amino acids in proteins, affect absorption maxima when the nature of the environment changes, i.e., a polar solvent. In native proteins residues will have contribution in the absorption coefficient, and as a consequence, in the absorbance. Butnarusu *et al.* [307] reported that the main peak observed in mucin from pig gastric mucus was due to the presence of the amino acid phenylalanine (Phe) [305]. In another study, egg albumin was analysed and they concluded that changes in absorbance were due to the lack of ionization of Tyr residues in the native protein, due to steric constraints in protein secondary or tertiary structures [308]. These different amino acid structures could be the main factor for the peak shift in spectra comparing European gastropods with the African snail.

In order to compare these results and to determine the molecular weight of proteins in locomotive gastropod mucus, we analysed our samples by SDS-PAGE. Also, this test is important to establish if protein length influences the rheological properties of gastropod mucus. Figure 4.2 shows the electrophoregram corresponding to SDS PAGE of native mucus from the six gastropod species.

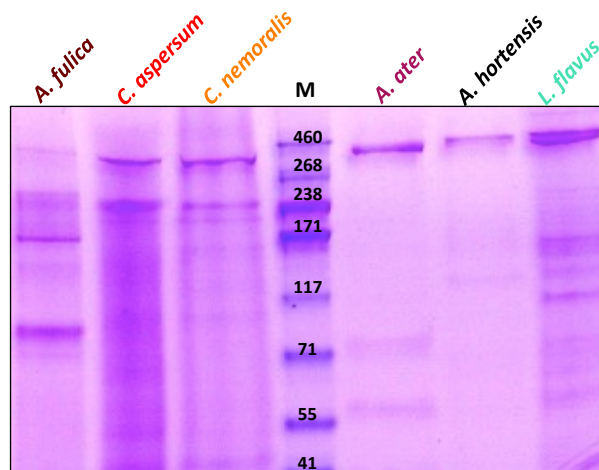


FIGURE 4.2 Electrophoregram of gastropod locomotive mucus. Lines correspond to *A. fulica*, *C. aspersum*, *C. nemoralis*, *A. hortensis*, *A. ater* and *L. flavus* mucus. Molecular weights corresponding to ladder bands are indicated.

Proteins were separated into 2-9 main bands, with molecular weight ranging from 41-377 kDa (See Table 4.1). Table 4.1 indicates that mucus from the three snails does not have the 377 kDa band compared to slugs, and this result could be attributed to post-translational modifications of proteins due to glycosylation, i.e., different degrees of glycosylation, suggesting variations in protein/carbohydrate ratio [292].

TABLE 4.1. Identities of specimens in each lane and main bands observed. Coloured cells indicate the presence of that protein group. GP1-GP19 are protein groups of bands identified in gastropod mucus.

kDa	Protein group	<i>A. fulica</i>	<i>C. aspersum</i>	<i>C. nemoralis</i>	<i>A. ater</i>	<i>A. hortensis</i>	<i>L. flavus</i>
41	GP1						
51	GP2						
66	GP3						
78	GP4						
96	Achacin						
100	GP6						
104	GP7						
113	GP8						
128	GP9						
145	GP10						
151	GP11						
165	GP12						
179	GP13						
194	GP14						
229	GP15						
249	GP16						
260	GP17						
271	GP18						
333	GP19						
347	Lectins						
377							

When comparing our results to those reported in previous studies, it must be pointed out that *A. fulica* mucus is the only one showing the achacin band at 96 kDa, which is the glycoprotein associated to antimicrobial activity of the African snail mucus [51], [309]. Bands between 41 -100 kDa, and 333-377 kDa are present in all species analysed in this study. Our results tie well with those reported previously, with main bands identified between 45 and 97 kDa, corresponding to mucus from *A. fulica*, *C. bistrialis*, *P.globosa*, *P.virens*, *B. Dissimilis*, *B.(Digoniostoma) pulchella* and *M. tuberculata* [310]; and 350 kDa corresponding to high molecular weight lectins observed in the African snail *A. fulica*, where it has been studied that lectins have a saccharides specificity which is crucial for its function, as well as their roles in host defence mechanism [311].

4.3.2 FUNCTIONAL AND THERMAL PROPERTIES

Locomotive gastropod mucus is necessary to facilitate gastropod locomotion, reducing friction between the animal and the surfaces. In order to analyse the effect of protein composition on gastropod mucus, rheological tests at different temperatures were performed, and results are shown as follows.

Figure 4.3 shows the average complex viscosity vs angular frequency. Gastropod mucus clearly exhibits non-Newtonian fluid properties [292], which means viscosity will change with the rate of deformation. Complex viscosity in all samples tested at low frequencies increased gradually while for higher frequencies it is considerably reduced. This clearly indicates that proteins and sugar molecules in mucus provide a melt-viscosity-lowering effect due to the hydrogen bonds in the corresponding polymeric structure [312]. *A. fulica* shows the lowest values (brown hexagon) for viscosity while *A. hortensis* (black sphere) presents the highest ones.

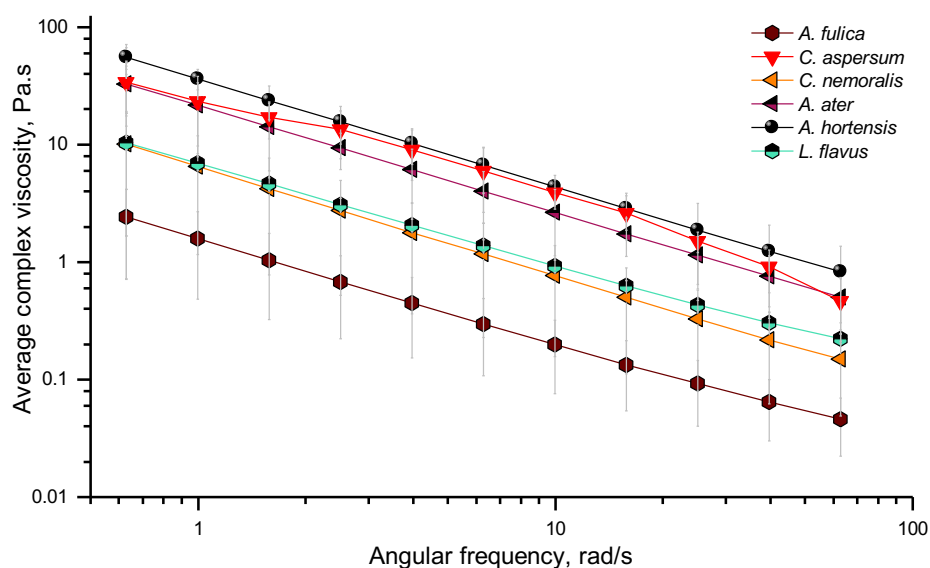


FIGURE 4.3 Average complex viscosity vs angular frequency of *A. fulica* (brown hexagon), *C. aspersum* (red down triangle), *C. nemoralis* (orange left triangle), *A. ater* (magenta half up left triangle), *A. hortensis* (black sphere) and *L. maximus* (cyan half up hexagon). Standard deviation error bars correspond to a series of three experiments per species.

In order to establish clear relationships between protein content in gastropod mucus and viscosity, figure 4.4 shows the average complex viscosity at two different angular frequencies vs protein concentration for all species. As the protein concentration increases, the viscosity shows the same trend, indicating proteins in mucins have a major effect on the rheological properties of mucus, which means that the amount of protein in the total solids' concentration determines viscosity variations between species.

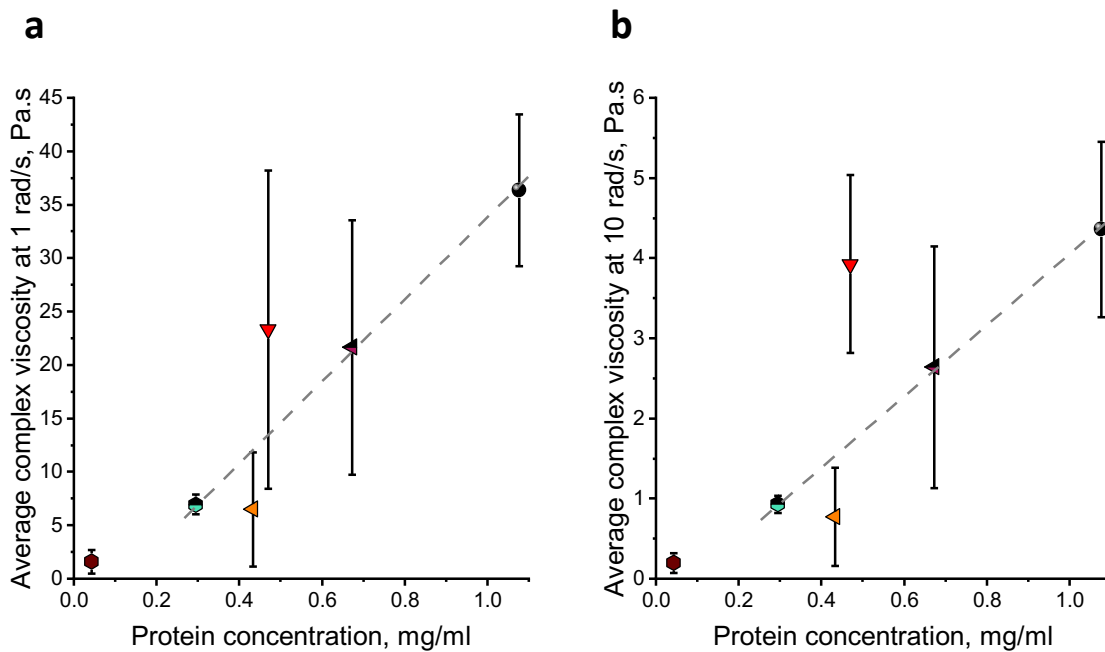


FIGURE 4.4 a) Average complex viscosity at 1 rad/sec vs protein concentration, b) Average complex viscosity at 10 rad/sec vs protein concentration of *A. fulica* (brown hexagon), *C. aspersum* (red down triangle), *C. nemoralis* (orange left triangle), *A. ater* (magenta half up left triangle), *A. hortensis* (black sphere) and *L. maximus* (cyan half up hexagon). Standard deviation error bars correspond to a series of three experiments per species.

A linear relationship between slugs is observed in figure 4.4, and in the case of snails, similar pattern is evident, because the African snail shows the lowest viscosity compared to the other two snails and the protein concentration is the lowest too. The slug *A. hortensis* has the highest viscosity and protein concentration.

Additionally, as described before by Lai *et. al.* [50], studying the micro and macro rheology of mucus in different biological systems, to describe the rheology of this ecto-secretion, two parameters are important: the loss modulus (G''), describing the extent to which this material resists the tendency to flow; and the elasticity or storage modulus (G'), measuring the

tendency of mucus to recover its original shape. Thus, for each species, linear viscoelastic moduli were measured (storage modulus G' , and loss modulus G''), as observed in figure 4.5 (detailed information is included in Appendix A2). It is clear that the viscoelastic properties are dominated by rearrangements of molecular segments in mucins for all samples, which are sufficiently short to not depend so much on cross-links with other chains, as the molecular weight of chains [312].

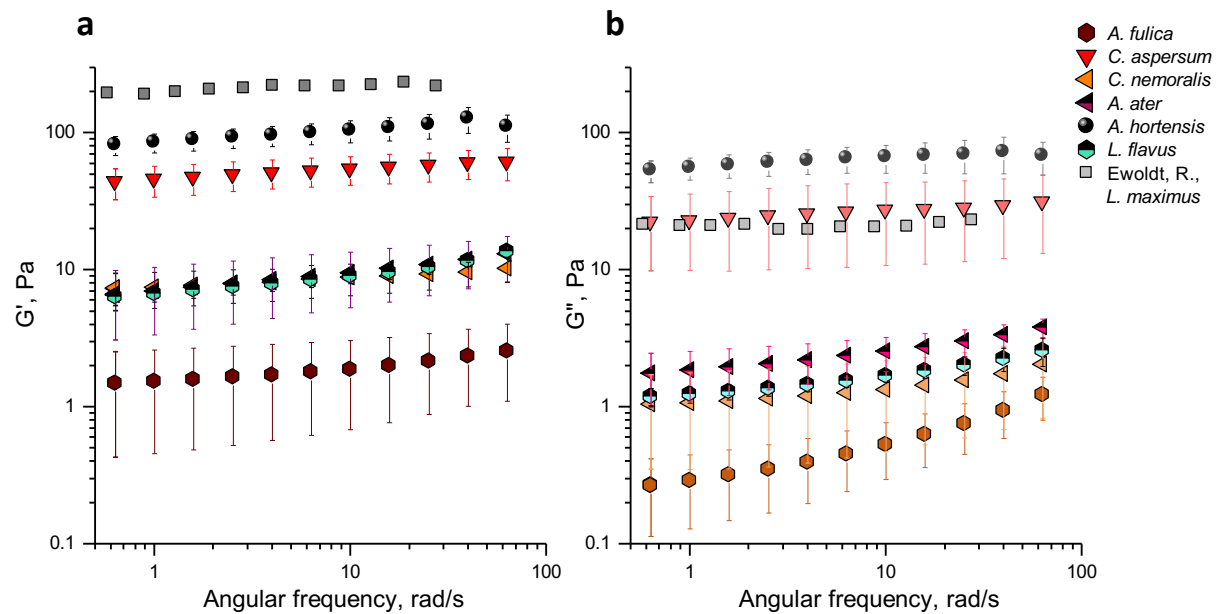


FIGURE 4.5 Average linear viscoelastic moduli, a) G' , and b) G'' , of locomotive mucus from *A. fulica* (brown hexagon), *C. aspersum* (red down triangle), *C. nemoralis* (orange left triangle), *A. ater* (magenta half up left triangle), *A. hortensis* (black sphere) and *L. flavus* (cyan half up hexagon), including digitized data reported before by Ewoldt et al. [34], corresponding to *L. maximus* (grey square), for comparison purposes. Standard deviation error bars correspond to a series of three experiments per species.

From figure 4.5, our analysis of the viscoelasticity of locomotive mucus indicates that in all samples over the range of angular frequencies $G' > G''$, which means that mucus has an elastic-solid behaviour [313], in agreement with previous studies on other types, such as human respiratory and intestinal mucus, and porcine respiratory mucus [314]–[317]. The differences on G' and G'' can be attributed to mucus' composition and hydration level (water content) [313]. Interestingly, locomotive mucus tested in one previous study analysing mucus from the slug *L. maximus* and included in figure 4.5 [34], showed that G' and G'' at around 1 rad/s are 198.7 and 20.8 Pa, respectively. Values corresponding to G' are slightly higher than those from our measurements, but G'' is in the same range of our results. In one pioneering study by

Denny [56], locomotive mucus from the slug *A. columbianus* showed that G' and G'' were 1.75 and 0.75 Pa, respectively, again in the range of our results. These studies on gastropod mucus where rheological properties were analysed in detail, have contributed to the understanding of the rheology of gastropod mucus. However, they did not include several species to compare their behaviour.

In order to further compare our findings with other mucus' analyses, there is one interesting report published in 2021, on human laryngeal mucus [313]. Their results indicate that the average G' and G'' moduli are 12.28 and 4.19 Pa, respectively, which ties well with our findings on gastropod mucus. This comparison supports our hypothesis that mucins are the main parameter controlling the rheological properties of mucus, because different types of secreted mucus exhibit a similar gel character and moduli in the same range of values, tested at the same angular frequencies.

If previous assumptions and observations on different kinds of mucus are valid, and mucins and their proteins are the main factors governing the rheological behaviour of mucus [318], [319], then an examination of viscosity as a function of temperature could add valuable information to this hypothesis. Figure 4.6 shows the average complex viscosity vs temperature.

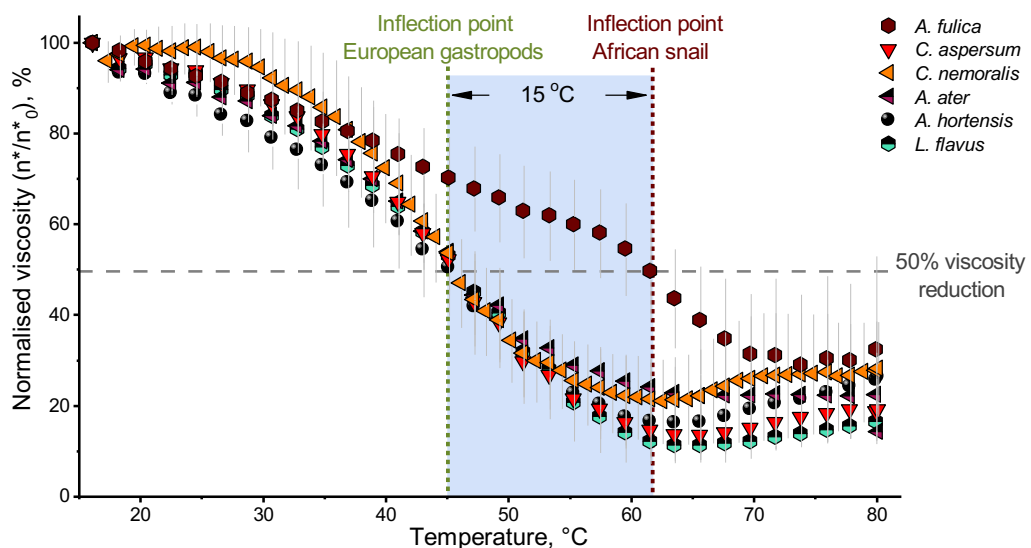


FIGURE 4.6 Normalised complex viscosity vs temperature of native locomotive mucus from *A. fulica* (brown hexagon), *C. aspersum* (red down triangle), *C. nemoralis* (orange left triangle), *A. ater* (magenta half up left triangle), *A. hortensis* (black sphere) and *L. maximus* (cyan half up hexagon). Standard deviation error bars correspond to a series of three experiments (each one normalised to its first value of complex viscosity taken at $0.63 \text{ rad}\cdot\text{s}^{-1}$, η^*_0) for all the species.

From figure 4.6, between 45°C and 48°C, a reduction in viscosity is clear for *A. hortensis*, *A. ater*, *C. aspersum* and *L. maximus* mucus (inflection point of European gastropods' mucus), where the 50% of initial viscosity has reduced, indicating a change in terms of the stability of mucins. An atypical behaviour is observed for *A. fulica* mucus compared to the other five species native from Europe, which means that at normal conditions and with the characteristic natural environment, mucus will maintain its function. The other five gastropod mucus show a similar response with the increase of temperature. Between 15 °C and 35 °C, all the species exhibit the same trend except the snail *C. nemoralis*, with higher amplitude. At this stage the variations in terms of viscosity are minimal and the materials seem to be decreasing in viscosity while the temperature is increasing. At around 35 °C, *A. fulica* native mucus immediately shows a different trend with a more constant viscosity, testing the hypothesis that mucins and their proteins are the main factors affecting compositional and functional properties of gastropod mucus, and glycosylation influences the stability of mucins under thermal, mechanical stress or both. This also suggests that *A. fulica* mucus has a higher heat capacity and so takes longer to warm up compared to the others.

There is a clear difference between *A. fulica* and the other five species. Mucus from this snail exhibits a higher stability in viscosity when the temperature is increased and it changes 15 °C after the other samples reduce their viscosity drastically. This variation could be due to *A. fulica* having the highest water content of all the mucus tested. A higher water content would mean the proteins are more stable in the African snail, resisting denaturation when temperature is higher [320]. Also, this mucus shows the lowest viscosity, indicating this property is not entirely dependent on proteins, but also on molecular interactions with sugar chains (glycosylation) in mucins [303].

Terrestrial snails and slugs come from the same ancestor and during millions of years of evolution, Stylommatophora clade increased its diversity, adapting animals' behaviour, functions and secretions [321]. Chemical relationships among species from the same super families are an indication that gastropods share some phylogenetic characteristics to live in specific environments [321]. *A. fulica* snail shows the more stable material under thermal or mechanical stress, which means, mucins keep their function in a wider range of temperatures, assuming this species requires a higher desiccation mechanism to protect the snail because it

is native from a region with higher average temperature compared to the other five species included in this study.

4.4 CONCLUSIONS

The different compositional and rheological tests confirmed my hypothesis that mucins in gastropod mucus have been adapted to specific environments to preserve mucus natural function as a lubricant, reducing dehydration and ensuring its stability. This is clear in my results, which indicate a different composition, stability and behaviour of mucus from the African snail *A. fulica*, compared to the European snails and slugs.

This is the first report analysing six different species and correlating protein concentration and composition to function. My study also demonstrates that the shell or external components of gastropods are not the only feature with which we can compare species and their evolutionary, chemical and physical relationships. These relationships can also be explored by characterising gastropod mucus, an ecto-secretion used as a survival adaptation to live and continue expanding their populations to new and changing environments.

Although my study demonstrates a clear relationship between compositional, thermal and mechanical properties of locomotive mucus in terrestrial snails and slugs from the order Stylommatophora, the incorporation of a complete thermal characterisation including Differential Scanning Calorimetry (DSC), could add information about protein denaturation.

CHAPTER 5: STRUCTURAL CHARACTERISATION, CLASSIFICATION AND IDENTIFICATION OF SNAKE VENOMS

“It is not the strongest of the species that survives,
not the most intelligent that survives.
It is the one that is the most adaptable
to change.” **Charles Darwin**



This chapter corresponds to the paper “Structural characterisation, classification and identification of snake venoms”, to be submitted for publication to the Journal of Experimental Biology.

ABSTRACT

Species in Elapidae, Viperidae and Colubridae families produce a toxic liquid, an ecto-secretion containing proteins, and other organic and inorganic compounds. Particular toxins have demonstrated temperature-dependent enzyme activity, with potential uses in pharmacological applications or in antivenoms production. The proteomic analysis of snake venoms has included different techniques, such as mass spectrometry, providing valuable information to the knowledge and understanding of snake venoms, and new approaches in this field are combined with the aim of achieving a broader knowledge on the compositional, structural and thermal properties of this ecto-secretion. However, the use of non-destructive and less time-consuming techniques, such as Fourier transform infrared spectroscopy (FTIR), has only been included in few studies. To fill this gap on the understanding of how temperature affects snake venom’ compositional and structural properties, here we present the first study combining SDS-PAGE with FTIR, to analyse venom from one viper in the *Bitis* genus, one primitive spitting cobra in the genus *Haemachatus*, and thirteen species in the genus *Naja*. This combination of methods allowed us to determine the proteins present, and also to identify structural and compositional variations in snake venom as a function of temperature. In addition, a multivariate analysis was performed to classify snakes based on the hierarchical clustering analysis of FTIR spectra. Our approach represents a novel route to provide new insights into venom’s properties, as well as for the identification and classification of species.

KEYWORDS: Snake venom, SDS-PAGE, FTIR, carbohydrate-binding protein, Multivariate Analysis.

5.1 INTRODUCTION

For millennia humans have been fascinated by snakes, finding their way into several ancient mythological and religious texts, and are often seen as a symbol of fertility, life, rebirth and power. Today, whilst feared by some, they continue to offer positive inspiration in many aspects surrounding their biology (biodiversity), behaviour (soft-robotics) and materials (venoms) [322]–[325]. Of the total number of extant snakes species around 20% of them secrete a toxic substance, venom, from specialised glands located in both sides of the head on the upper jaw [111], [129], [326]. Found primarily in the Elapidae, Viperidae and Colubridae families [14], [115], [327] venom has evolved to disable and kill prey, facilitate digestion, and for some cobras in the *Naja* genus act in defence, via spitting [113], [118], [120], [125], [127], [154], [172], [191], [192], [328]–[330]. The biodiversity of venom has helped taxonomic classification, and through a biochemical understanding of its toxicity, even helped identify compounds for medicinal use [127], [193], [195], [200], [331], [332].

Proteomic characterisation of snake venoms has primarily been achieved through sodium dodecyl sulphate-polyacrylamide gel electrophoresis (SDS-PAGE), high-performance liquid chromatography (HPLC), and mass spectrometry [113], [130], [132], [133], [137]–[140], [142], [143], [146], [148]–[150], [153], [154], [156]–[158], [160]–[169]. Whilst typically used in isolation, recently the combination of these techniques is helping to build a better and more holistic overview of venom composition [333]. Several studies have identified proteins such as phospholipases A₂ (PLA₂), snake venom metalloproteinases (SVMP), snake venom serine proteases (SVSP), and three-finger toxins (3FTx) as underpinning venoms diverse range of functions [14], [113], [116], [131], [132], [165]–[171], [332], [334]. Yet despite the major contributions made with these techniques, there are others, outside of the typical molecular biologists' toolkit, that can be introduced and combined to add new perspectives and insights into this field.

One example is Fourier Transform Infrared spectroscopy (FTIR), which measures a sample's infrared absorption and provides a "molecular fingerprint", giving insight into its organic compounds, such as proteins and carbohydrates [217], [219]. In contrast to the techniques

above, there is no sample preparation required, it is non-destructive and a measurement takes less than 5 minutes [237], [242]–[245].

Adopting alternative techniques such as this may help address some peculiarities seen in venom proteins, namely that they appear remarkably thermally and electrophoretically stable when compared to other enzymes [335]–[338]. This has led some to the conclusion that SDS-PAGE may not be sensitive to changes between the nated and a denatured state of venom proteins [335]. However, FTIR has the ability to measure a structural response over a range of temperatures, providing insights into adaptations to maintain biological activity of a protein solution when outside the body and environmentally challenged [237], [242]–[245]. When applied to venom, this may be useful for basic research and medicinal applications, helping the development of antivenoms, or the design of pharmacologically active and stable drugs for therapeutic applications [339], [340].

These benefits have led to FTIR being employed to identify the composition of everything from blueberries [341], cyanobacterial strains [233], human hairs [235], Indonesian coffee bean varieties [234], wines [236], to silkworm silk [237]. A more advanced analysis of the data can even generate ultrametric trees for species classification [237]. Hence it is surprising that, to the authors knowledge, only two studies have tried to analyse snake venom composition using FTIR, let alone combining it with traditional proteomic characterisation [170], [171].

Here I present the largest dataset of venom SDS-PAGE profiles and FTIR spectra to date. Our results include native venom from one viper, *B. arietans*; one primitive spitting cobra: *H. haemachatus*; and thirteen species in the *Naja* genus, including spitting and non-spitting cobras from Africa and Asia. I demonstrate that FTIR can successfully identify significant structural and compositional changes in venom's response to temperature at 25 and 80 °C. Beyond basic identification of the protein secondary structures present, I build a classification of species based on their spectral similarities. I believe the combinatorial approach described here, represents a step towards a more integrated and cohesive route for the identification, classification and potential applications of venoms from species in the Viperidae and Elapidae families.

5.2 MATERIALS AND METHODS

5.2.1 MATERIALS

In this study, venom samples from thirty individual snakes were collected, corresponding to 15 different species: 1 viper, *B. arietans*; 1 primitive spitting cobra, *H. haemachatus*; and 13 *Naja* species, *N. pallida*, *N. nubiae*, *N. mossambica*, *N. nigricollis*, *N. subfulva*, *N. nivea*, *N. haje*, *N. annulifera*, *N. naja*, *N. siamensis*, *N. philippinensis*, *N. atra* and *N. kaouthia*. The viper as the outgroup, was included to compare results with the primitive spitter and the *Naja* spitting and non-spitting species (see table A3 in Appendix A3, where a detailed information is included). All snakes listed in table A3 were maintained in individual containers within controlled environmental conditions (temperature, humidity and light) at the Centre for Snakebite Research and Interventions, Liverpool School of Tropical Medicine (LSTM), UK. All protocols referring to the expert husbandry of the snakes are regularly inspected and approved by the UK Home Office and the LSTM Animal Welfare and Ethical Review Board. Venom was extracted by milking each snake and fresh venoms were transferred into 2 ml low-protein binding cryotubes (Simport Scientific, Beloeil, Canada) using a pipette. All samples were kept on ice, and all FTIR and SDS-PAGE tests were carried out at the Department of Materials Science and Engineering at the University of Sheffield.

5.2.2. METHODS

5.2.2.1. SDS-PAGE

Native snake venom corresponding to each snake was collected as described in section 5.2.1. For each sample, 0.5 μ l of fresh venom was placed in a 2 ml polypropylene graduated centrifuge tubes and diluted with 800 μ l of distilled water. Aliquots of 20 μ l were taken from each sample and then mixed with 20 μ l of sodium dodecyl sulphate and β -mercaptoethanol solution, based on Laemmli's method. [296] From the resulting solution, aliquots of 20 μ l were resolved on 4-20 % tris-glycine gel under reducing conditions, using a mini gel tank Invitrogen (Thermo Fisher Scientific, USA), power supply PS 250 (Hybaid Ltd, UK), at a voltage of 120 V for 100 minutes. In order to visualise protein bands, a staining solution with 0.25% Coomassie Brilliant Blue R-250 (VWR Chemicals, USA) was used, and gels were imaged using a Scanjet G2710 scanner (HP Inc., USA). The ladder used was a pre-stained protein standard (Thermo Fisher Scientific, USA), of broad molecular weight (10-250 kDa).

5.2.2.2. FTIR

5.2.2.2.1. SPECTRAL ACQUISITION AND TREATMENT

A volume of 4 μl of native venom from each snake was placed on the Attenuated Total Reflection (ATR) crystal and the starting temperature was set to 25 $^{\circ}\text{C}$, using a Nicolet 380 spectrometer (Thermo Instruments, UK) purged with dry air and equipped with an ATR accessory (Golden Gate, 45 $^{\circ}$ single-bounce diamond sensor, Specac, UK). Samples were then covered with a glass slide to avoid evaporation, and were then heated up to 80 $^{\circ}\text{C}$, at a heating rate of 3.23 $^{\circ}\text{C}/\text{min}$. In total, 1620 individual spectra were collected, 3 at each temperature for each specimen. Data between 1000 cm^{-1} and 1800 cm^{-1} were obtained by collecting 64 scans at 4 cm^{-1} resolution.

5.2.2.2.2. DATA PRE-PROCESSING

Spectral analyses were performed using Origin software, v2020, USA. Spectra were normalised to the amide I peak (1645 cm^{-1}), to compensate for absolute signal variations due to different venom film thickness deposited on the FTIR-ATR accessory. For the venom composition analysis divided into five groups, the average relative areas per species were obtained by subtracting a linear baseline, selecting peaks according to each wavenumber values and range, and peaks were integrated.

5.2.2.2.3. GAUSSIAN FITTING

Fourier self-deconvolution and curve fitting were performed on spectra between 1600 and 1700 cm^{-1} (amide I) and an 8-point multipeak Gaussian fitting was done using Origin software, v2020, USA, for all samples at both temperatures, 25 and 80 $^{\circ}\text{C}$. Finally, based on previous studies, protein secondary structures were assigned [242]–[245].

The corresponding groups and absorption bands are indicated in table 5.1.

TABLE 5.1. Main bands present in all species, between 1800 and 1000 cm⁻¹.

Position (cm ⁻¹)	Assignment	References
1646-1634	Amide I, due to C=O stretching	[59], [246]
1534	Amide II, due to C-N stretching and N-H bending	[219], [246]
1475-1350	Methyl group bending (CH ₃ bending)	[211], [237]
1352	Aromatic residues, mainly Tryptophan (Trp)	[211]
1250	Amide III, due to C-N stretching and N-H bending. It also indicates random coil	[237], [246], [247]
1180-1024	Sugar residues region, due to O-Glycosidic bonding	[41], [59], [248]

5.2.2.2.4. MULTIVARIATE ANALYSIS AND DENDROGRAM GENERATION

To discriminate snake venom while reducing the complexity of dataset and keeping the main trends [249], [236], a Principal Component Analysis (PCA) was performed using Origin software, v2020, USA. To do this, the first derivative of 180 spectra was used for the multivariate analysis, corresponding to 3 spectra at each temperature, 25 and 80 °C, per snake. Subsequently, a Linear Discriminant Analysis (LDA) was performed on the principal component scores to find a linear combination of features that guarantee maximal separability of data [250], [251], [342]. The obtained LDA, mean factor scores were then used for Hierarchical Cluster Analysis (HCA), to estimate Euclidean distances between species [252], [253]. HCA represents an algorithmic method to dissimilarity identification between groups, which are constituted by a similarity matrix. Finally, a comparison between the ultrametric and phylogenetic trees was done.

5.3 RESULTS AND DISCUSSION

5.3.1 SNAKE VENOM REDUCED SDS-PAGE PROFILES

Overall, our findings both agree with, and extend, previous molecular studies on venoms [113], [130], [132], [133], [137]–[140], [142], [143], [146], [148]–[150], [153], [154], [156]–[158], [160]–[169]. Figure 5.1 summarises the SDS-PAGE profiles for each species, with bands highlighted that appear to correspond to sizes of proteins where the protein family has been identified based from previous studies on venom [113], [116], [343], [344]. Note unadulterated gels can be seen for all snakes in Appendix A4.

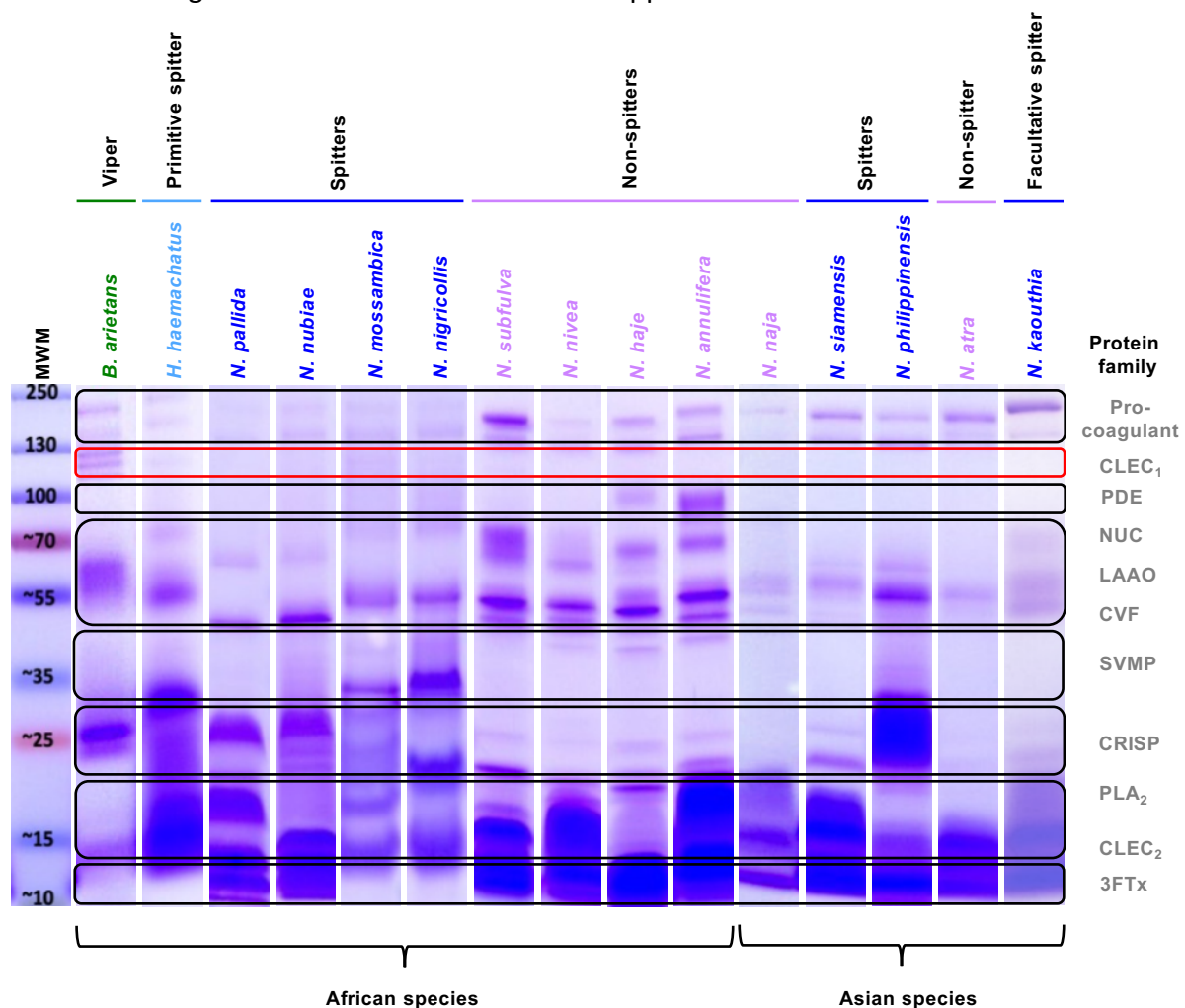


FIGURE 5.1 Selected electrophoregrams of snake venom from *B. arietans*, *H. haemachatus*, *N. pallida*, *N. nubiae*, *N. mossambica*, *N. nigricollis*, *N. subfulva*, *N. nivea*, *N. haje*, *N. annulifera*, *N. naja*, *N. siamensis*, *N. philippinensis*, *N. atra* and *N. kaouthia*, to show a comparison between species.

Molecular weights corresponding to ladder bands are indicated. Protein families refer to: Procoagulant (Factor X and V); C-type lectins (CLEC₁ and CLEC₂ refer to high and low molecular weight, respectively); phosphodiesterase (PDE); nuclease (NUC); L-amino acid oxidase (LAAO); cobra venom factor (CVF); snake venom metalloproteinase (SVMP); cysteine rich secretory protein (CRISP); phospholipases A₂ (PLA₂); and three- finger toxin (3FTx).

From figure 5.1, between 7 and 14 protein bands are observed for all species [345]. The main protein families identified, based on previous proteomic and SDS-PAGE studies on snake venoms, correspond to: pro-coagulant (Factor X and V); C-type lectins (CLEC); phosphodiesterase (PDE); nuclease (NUC); L-amino acid oxidase (LAAO); cobra venom factor (CVF); snake venom metalloproteinase (SVMP); cysteine rich secretory protein (CRISP); phospholipases A₂ (PLA₂); and three- finger toxin (3FTx) [113], [116], [343], [344].

A previous study on *Naja cobras* and *O. hannah* species, identified between 9 and 17 protein bands, with the highest number corresponding to non-spitting cobras, and the lowest to the spitting species [113]. Our results match these findings reasonably, with the Asian non-spitting cobras *N. naja* and *N. atra* showing the lowest number of bands. The African non-spitting cobras show the highest number of bands with 14, in line with this previous report [113]. In terms of the outgroup viper, *B. arietans*, it shows three distinct bands between 100-130 KDa not present in any of the other 14 species, which may correspond to high molecular weight C-type lectins (CLEC₁) as have been reported in another viper, *B. gabonica* [343].

Based on the main bands identified, procoagulant proteins are present in all snakes (Factor X and V) and in many viperid species [346], [347]. The second group of proteins are the CLEC, characterised by their proteins containing a carbohydrate domain and most stabilised by Ca²⁺ ions [343]. Previous studies show that snake venoms are a rich source of CLEC and this ties well with our results where bands assigned to CLEC₂ are present in all samples. This protein family could be indicative of the existence of interactions with sugar molecules in snake venoms [343]. The third group of proteins in our samples corresponds to PDE, which served to reduce arterial pressure in prey [348]. The strongest bands attributed to PDE, correspond to *N. haje* and *N. annulifera*, which supports previous findings [113]. The next group is NUC, proteins which act upon nucleic acids and, depending on their activity, are classified as endonucleases and exonucleases, or more recently as a multitoxin [348], [349], [110]. Here, bands are present in all African non-spitting cobras (*N. subfulva*, *N. nivea*, *N. haje* and *N. annulifera*) in line with previous observations [348], [349], [110], in two African spitting species (*N. mossambica* and *N. nigricollis*), in the primitive spitting cobra *H. haemachatus*, and in the Asian spitting cobra *N. kaouthia*. Such a variation in the presence of NUC components could be attributed to the origin of each snake (see table A3, in Appendix A3).

The next protein family identified in our profiles, corresponds to LAAOs, which are present in 13 of 15 species, except from *N. pallida* and *N. nubiae*, which ties well with previous studies, where the absence of this band is clear on *N. pallida* venom [113]. LAAOs are abundant glycoproteins found across a range of species [350] [351] and the carbohydrates in LAAOs facilitate interaction with cell surfaces, producing a high concentration of H₂O₂, causing cytotoxicity [352] apoptosis, haemorrhage and possess antimicrobial activity [36].

Another component found in our samples, is CVF, found in all species except from *B. arietans* and *H. haemachatus*. This result is not a surprise because these bands are present in venom from all the *Naja* genus cobras. CVF is an activating protein in cobra venom [353], and comparing our results to one previous study [113], this component is present in all *Naja* species, as expected. In terms of the SVMP, these are clearer in the African and Asian spitting species than in the other snakes. This fact could be attributed to the ability to spit venom, as well as evolution of cytotoxicity in snake venom, because SVMP in snake venoms inhibit platelet aggregation and blood coagulation, which is one of the more common effects when venom envenomation occurs [113].

The group corresponding to CRISP is present in all species, and this ties well with previous reports in snake venoms, where they confirmed the existence of these bands in SDS-PAGE reduced profiles [113]. CRISP's are abundant in snake venoms but have not been characterised in detail. However, it has been demonstrated that they inhibit ion channels and contribute to angiogenesis, and promote inflammatory responses [354], [355]. The family corresponding to PLA₂ are clear in all species except the viper *B. arietans*. This result is corroborated with previous studies, where all *Naja* species showed this band [113]. Finally, the presence of 3FTx is evident in all *Naja* species except in the viper *B. arietans*, showing slightly stained bands, indicating the high abundance of proteins of lower molecular mass below 15 KDa, supported by previous reports with similar findings [113], [116]. These 3FTXs are one of the major components found in elapid snakes, including *Naja* species, and they are responsible for neurotoxic effects when venom is injected [116], [334].

Overall, our findings both agree with, and extend, previous molecular studies on venoms. It is clear that there are differences in the presence of protein families identified in our profiles,

with variations also between spitting and non-spitting cobras, attributed to the concentration of specific proteins in venoms [113]. In order to identify if the presence of carbohydrates binding proteins is different in viper, spitters and non-spitters, and how this affects venom stability, further analysis was done, surrounding FTIR characterisation, identification and classification.

5.3.2 SNAKE VENOM SPECTRAL FEATURES

In order to compare our results more easily, FTIR spectra are grouped by taxonomic families and results are shown in figure 5.2.

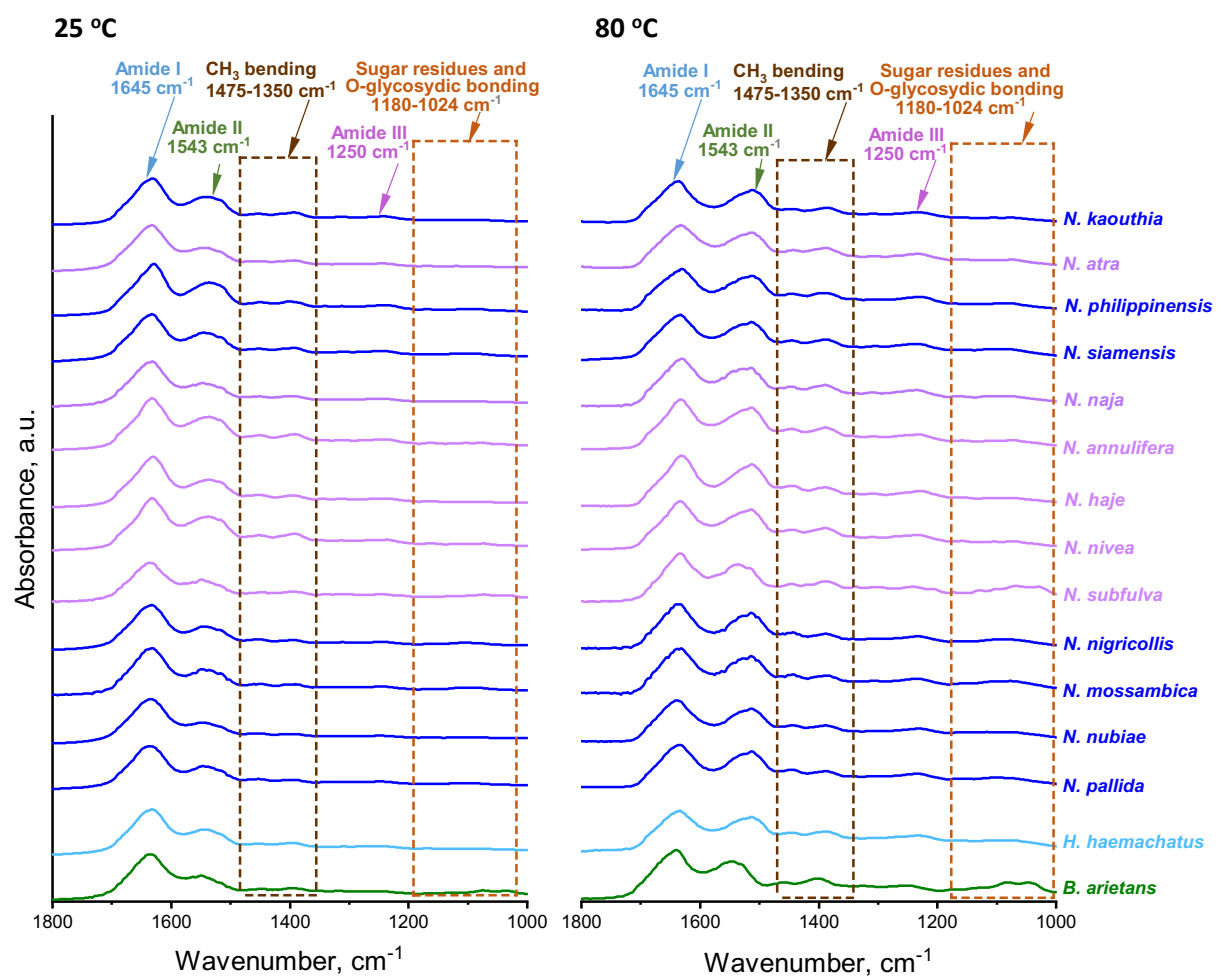


FIGURE 5.2 FTIR spectra of venom from *B. arietans*, *H. haemachatus*, *N. pallida*, *N. nubiae*, *N. mossambica*, *N. nigricollis*, *N. subfulva*, *N. nivea*, *N. haje*, *N. annulifera*, *N. naja*, *N. siamensis*, *N. philippinensis*, *N. atra* and *N. kaouthia*, at 25 °C and 80 °C. The main regions are highlighted: amide I (1645 cm^{-1}); amide II (1543 cm^{-1}); CH_3 bending (1475-1350 cm^{-1}); amide III (1250 cm^{-1}); and sugar residues and glycosidic bonding (1180-1024 cm^{-1}). Species in green represent the viper; light blue, primitive spitter; dark blue, spitters; and light purple, non-spitters.

Figure 5.2 shows the five major bands observed at 25 and 80 °C, corresponding to amide I, at 1645 cm^{-1} ; amide II at 1543 cm^{-1} ; CH_3 bending at 1475-1350 cm^{-1} ; amide III at 1250 cm^{-1} ; and finally, in the region between 1180-1024 cm^{-1} , the sugar residues. It is interesting to note that the amide I peak shows a similar intensity between species at both temperatures, indicating that protein concentration in snake venom does not vary significantly [356]. Amide I and II were also observed in two studies on *C. durissus* venom, where the amide I and II bands were observed in samples at 25°C, obtained from lyophilised venom [170], [171].

Comparing our results at 25 and 80°C, some spectral variations are clear, indicating that snake venom structures change upon heating. The amide II peak in the *B. arietans* sample, shows a shoulder and a shift compared to the other 14 samples corresponding to the *Naja* genus, which indicates a different degree of protein hydration or ionisation [238]. The sugar residues region shows an increase in absorbance in all species compared to spectra at 25 °C, with the highest value associated to the viper, *B. arietans*. This increase in the sugar residues is also related to the glycoproteins or carbohydrate binding proteins, as observed in our snake venom SDS-PAGE reduced profiles, the presence of more bands associated to CLEC_{1, 2} has been attributed to the viper. This observation confirms our findings on the corresponding absorption bands and also confirms that *B. arietans* venom has a higher degree of glycosylation compared to the *Naja* species [59].

In this section, I demonstrated that all species show the same main bands in both spectra at 25 and 80 °C, with clear variations. However, in order to quantitatively and qualitatively compare these absorbances, a more detailed analysis needs to be performed.

5.3.3 BETWEEN-SPECIES COMPARISON OF THE CHEMICAL COMPOSITION OF SNAKE VENOM

To establish a more detailed comparison between spitting, non-spitting cobras and the viper, the five main regions observed in all spectra in figure 5.2 were integrated and results are included in Figure 5.3. With this analysis, it is clear that venom structure changes when temperature is increased to 80 °C.

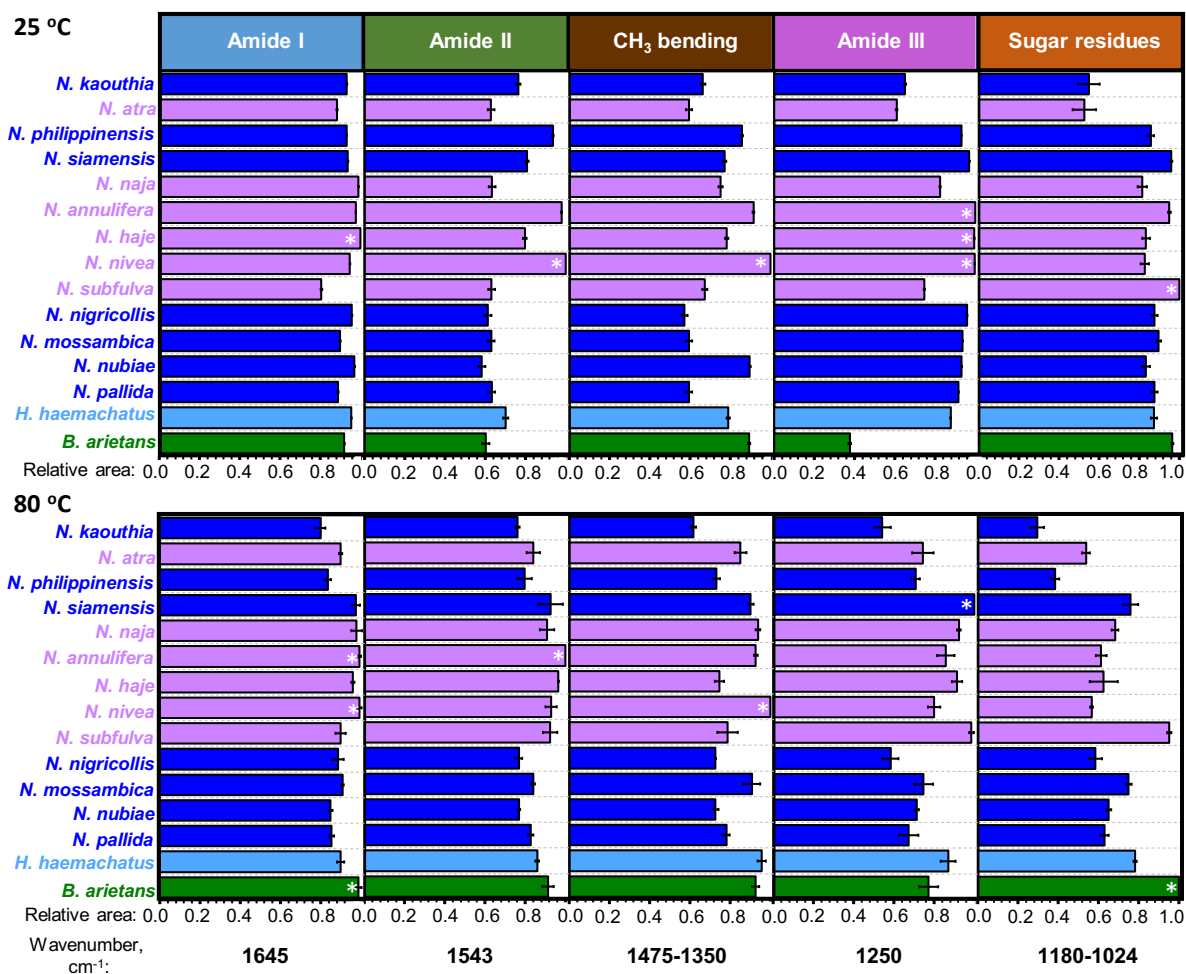


FIGURE 5.3 Composition of venom from *B. arietans*, *H. haemachatus*, *N. pallida*, *N. nubiae*, *N. mossambica*, *N. nigricollis*, *N. subfulva*, *N. nivea*, *N. haje*, *N. annulifera*, *N. naja*, *N. siamensis*, *N. philippinensis*, *N. atra* and *N. kaouthia*, at 25 °C and 80 °C. Relative areas of bands assigned to amide I (1645 cm⁻¹); amide II (1543 cm⁻¹); CH₃ bending (1475-1350 cm⁻¹); amide III (1250 cm⁻¹); and sugar residues and glycosidic bonding (1180-1024 cm⁻¹). White asterisks indicate the maximum values, and areas are relative within that category. The error bars represent the standard deviation of at least three different observations per species at each temperature. A value of 1 represents the highest area calculated and 0 represents the minimum measured.

Amide I

This region has been widely used to determine protein secondary structures, such as α -helix, β -sheets, β -turns, random coil or aggregated strands [211], [261]. It is attributed mainly to the C=O stretching vibrations of the peptide bonds. It is clear that in all species, in figure 5.3, the amide I region is the strongest band at both temperatures. This information can be associated with the protein concentration in native snake venom, suggesting that concentrations are similar between species, even when comparing viper, spitting and non-spitting cobras. If that is the case, then the main differences are in the group of protein families present in snake venom, rather than the overall protein concentration, as it was observed in our electrophoregrams [157]. These peak areas are also linked to the classification of species based on spectral features.

Amide II

Peaks in this region are attributed to the C-N stretching vibrations and N-H bending, due to aromatic protonation states, more specifically linked to tyrosine, and interactions between the aromatic residues within a protein and are necessary for the correct function of proteins. Figure 5.3 shows the amide II relative peak areas, where there is a clear variation between species.

CH₃ bending

The third region between 1475 and 1350 cm^{-1} corresponds to CH₃ bending and aromatic residues in proteins [211], [246], [263], showing variations between species at both temperatures. The maximum and minimum areas at 25 °C correspond to *N. nigricollis* and *N. nivea*, respectively. At 80 °C, the minimum area corresponds to *N. kaouthia*, while the highest is found in the sample corresponding to *N. nivea*.

Amide III

The fourth region observed in figure 5.3 corresponds to amide III, at 1250 cm^{-1} , and even when it is the result of the C-N stretching and N-H bending in proteins, it is also an indicative of the unordered secondary structures present and attributed to random coil [246], [247]. From figure 5.3, the minimum area at 25 °C correspond to the viper *B. arietans*, while the maximum area is observed in *N. nivea* and *N. annulifera*, both African non-spitting cobras. At

80 °C, the minimum value is found in the sample corresponding to *N. kaouthia* and the maximum relative area is clear in *N. siamensis*.

Sugar residues

This final region indicated in figure 5.3, between 1180 and 1024 cm^{-1} , represents the sugar residues [59]. Our SDS-PAGE profiles demonstrated that all samples showed strong bands attributed to CLEC₂, and 13 of 15 species show the presence of LAAOs, both protein families indicating the existence of carbohydrate-binding proteins. There are various types of lectins in snake venom identified before, some related to the sugar-binding and others non-sugar-binding [357]. However, with the FTIR characterisation and analysis, as well as the identification of the relative major areas observed in all spectra, I can elucidate that the type observed in all species correspond to the sugar-binding one. In figure 5.3, the minimum and maximum areas at 25 °C correspond to *N. atra* and *N. subfulva*, respectively. While at 80 °C, the minimum and maximum relative areas correspond to *N. philippinensis*, and *B. arietans*. It is not a surprise to see that *B. arietans* has the second highest value at 25 °C and the maximum at 80 °C, because previously, on the SDS-PAGE profiles three main bands were identified only in this species, attributed to CLEC₁, which suggests that the presence of sugar-binding proteins is higher than in the other 14 species. In all species, the high relative amount of sugar residues, can be correlated with the presence of glycoproteins in CLEC and in LAAOs, where it has been reported before that the content of carbohydrates can represent up to 12 % of the overall mass of the glycoprotein [352].

The existence of these components can also be linked to the high thermal stability of snake venom reported before [358], because during thermal stress proteins can exhibit a modification and change of order structures into unordered ones, or increasing/decreasing the relative amounts of these structures, to maintain its stability [359]. To further identify and analyse how protein secondary structures vary between species and on heating, the amide I region can be explored in more detail.

5.3.4 PROTEIN SECONDARY STRUCTURES: AMIDE I PEAK DECONVOLUTION

The amide I region was also studied in more detail by performing Gaussian fitting as described in section 5.2.2.3. With this procedure, information about the percentages of protein secondary structures can be obtained, as presented in figure 5.4: α -helices, rod-like structures formed by amino-acid residues on the polypeptide chain [266]; β -sheet, where hydrogen bonds maintain polypeptide strands together [267]; β -turns, formed by a tight loop, where a direction in change occurs in the polypeptide backbone [268]; random coil, with the monomers oriented randomly [256]; and aggregated strands or intermolecular β -sheets [360].

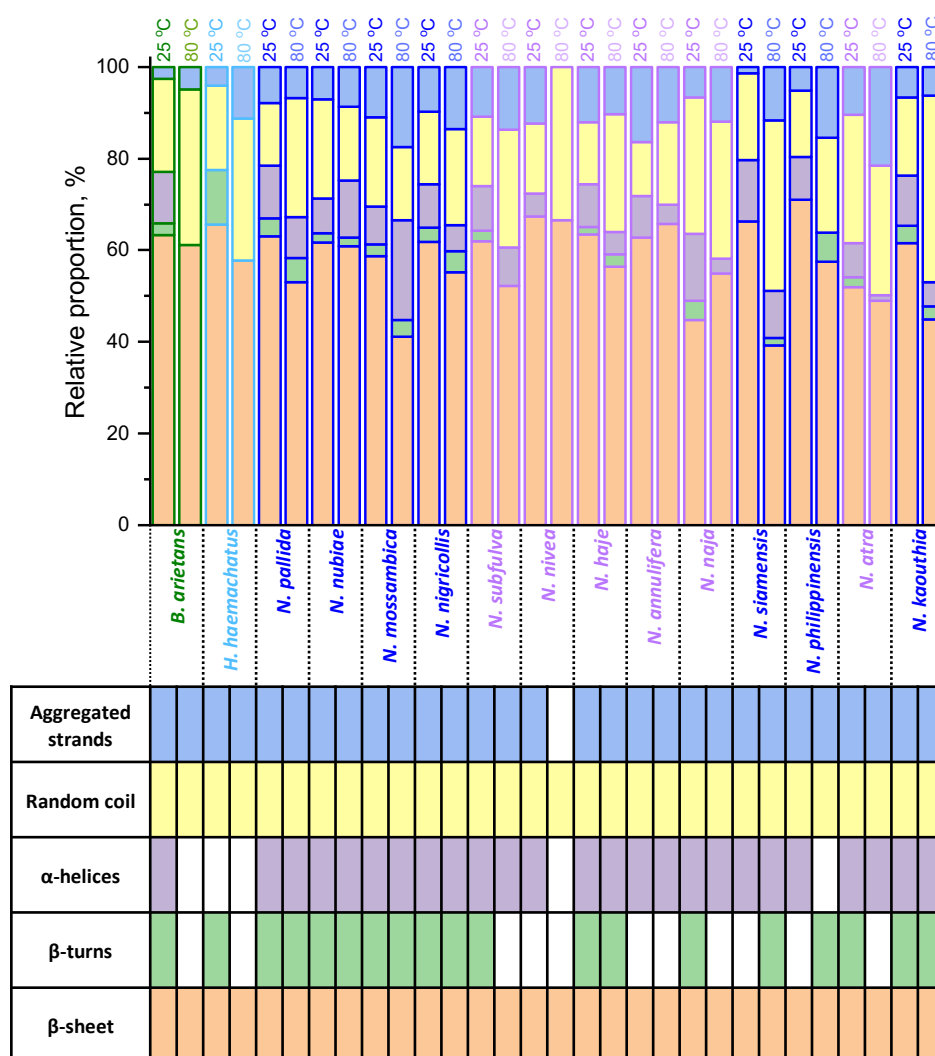


FIGURE 5.4 Distribution of elements present in protein secondary structure for all species, at 25 °C and 80 °C, derived from FTIR measurements, and table showing the presence (coloured cell) or absence (white cell) of specific structures.

From figure 5.4, it is clear that at both temperatures the four protein secondary structures are present in 12 of the 15 species. Interestingly, the viper *B. arietans*, shows a different pattern compared to the other 14 species, with the lack of α -helices and β -turns at 80 °C, which indicates a protein composition variation, corroborated with the SDS-PAGE profiles. It can be extracted from figure 5.4, that at both temperatures, the predominant structures in snake venom in all species are β -sheet and random coil, which are in agreement with previous studies related to proteins [267]. Most toxins in snake venom, such as CLEC, LAAOs, SVMP and 3FTx, have α -helices, β -strands and random coil, as the major protein secondary structures [361], [362]. The presence of β -sheet and random coils in all species, with no major variations, indicates the thermal stability of these structures even when samples are subjected to a thermal stress, suggesting the presence of thermostable components in snake venom, as previously described [340]. These β structures of polypeptides are capable of interaction due to hydrogen bonds, conforming the β -sheet and β -turns, which represent the ordered and folded laminar structures in proteins [267]. More specifically, in globular proteins, It has been estimated that at least 30 % of amino acid residues corresponds to β structures [246]. Our results tie well with this observation, with the overall β structures accounting for between 45-75 % of the protein secondary structure composition.

In terms of the unordered structures or random coil, they mostly serve to connect β structures [170], and there is evidence that indicates disordered protein structures have high flexibility and adaptability to different conditions, like hydration variations, contributing to protein stability [269]. Therefore, there is a clear relationship between these two major structures observed in snake venom from species in the Elapidae and Viperidae families. This suggests that snake venom stability is maintained by the laminar structures, which can be linked to the mechanical properties of this material, including the spitting and biting behaviours. This fact is also related to the evolvability of protein systems in snake venom, to preserve its specific functions and toxicity unaltered [363].

The Gaussian fitting analysis described in this section, allowed us to correlate protein secondary structures with venom composition, as well as thermal stability. Although this information contributes to the understanding of snake venom from a spectroscopic

perspective, the classification of snakes based on venom's spectral properties is another analysis that can be performed, which has not been reported before.

5.3.5 CLASSIFICATION OF SNAKE SPECIES

The compositional characterisation can be highly complemented with the classification of species based on spectral features in snake venom. This method of classifying species based on FTIR spectra has not been reported extensively and there is only one complete study by Boulet-Audet *et al.* where a multivariate analysis was used to classify silkworm species based on their cocoon silk [237]. Therefore, in this section, I present the classification of snake species by following the procedure described by Boulet-Audet *et al.*, where I first performed a PCA for all spectra at 25 and 80 °C. Our initial multivariate analysis of snake venom is summarized in Fig. 5.5, showing the values of the first and second factor scores calculated from the venom spectra.

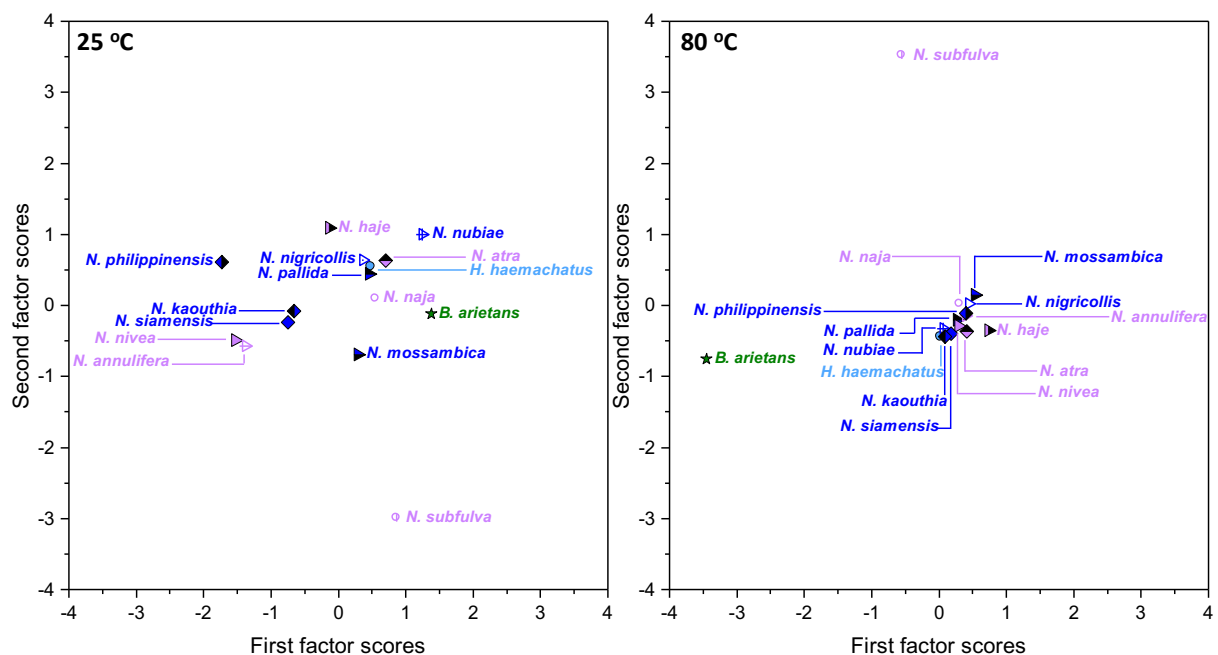


FIGURE 5.5 Factor scores of snake venoms at 25 and 80 °C. The first and second factor scores contribute to 61.8 % of species discrimination.

With information from figure 5.5, it is clear that the structure and composition in snake venom changes when the temperature is higher, indicating a modification in protein

secondary structures, such as β strands or α -helices, to an unfolded state; which could affect venom's enzymatic activity [335]. From figure 5.5, I can identify some groups and outlier species at both temperatures. First, at 25 °C, there are some visible clusters, one comprises the primitive spitter *H. haemachatus* and the two African spitters *N. pallida* and *N. nigricollis*. There is another cluster, including two of the Asian spitting cobras *N. siamensis* and *N. kaouthia*, and on the same positive axes of the second factor scores, I find *N. philippinensis*, the other Asian spitter. The two African non-spitting cobras *N. nivea* and *N. annulifera* are together, and the rest of the species are on the positive axes of the first factor scores, indicating a possible relationship which will be identified with the HCA. Finally, and more evident in the periphery of all species and clusters, I find the African non-spitting cobra *N. subfulva*, appearing as an outlier and indicating a major dissimilarity with the average of the analysed venoms. In one study published recently [116], results revealed substantial variations in the Principal Coordinate Analysis of proteomic characterisation of venom toxins between spitting and non-spitting species, but more specifically, in the African species. This finding is partially in agreement with our results, because I can see that the Asian spitting species show little variation between different lineages of spitting and non-spitting, compared to the African species.

It is not a surprise that at 80 °C from 14 of the Elapidae species, 13 appear in one cluster indicating a similar behaviour at higher temperature, the only exception is the African non-spitting cobra *N. subfulva*. This outlier shows different spectral features from the rest of the *Naja* species. Another outlier corresponds to the viper *B. arietans*, which also was showing compositional differences compared to the *Naja* species, as well as the corresponding family and behaviour (biting). Although, the fact that one of the cobras appears as an outlier and not just the viper as expected, this result is atypical, because our SDS-PAGE profiles and Gaussian fitting of the amide I peak, did not show any differences comparing the snake *N. subfulva* with the other *Naja* species. However, the peak area analysis offers an insight into this dissimilarity, because from the 13 *Naja* cobras, *N. subfulva* is the one with the lowest amide I, II and III relative areas and the one with the highest sugar residues value, which may dictate these outlier trend.

The information from the first and second factor scores offers insights into the spectral features in snake venoms. However, and in order to draw quantitative links between species, HCA needs to be performed on group species based on their similarity.

5.3.6 COMPARISON OF FTIR AND PHYLOGENETIC TREE

To draw quantitative relationships between species, I generated an ultrametric tree from the infrared spectra at 25 °C for native venom (see Fig. 5.6b) and it was compared to a phylogenetic tree (see Fig. 5.6a) from [116]. The phylogenetic and ultrametric trees show similarities, especially between viper and the other species, i.e., Viperidae and Elapidae families. It is clear that some of the African spitting and non-spitting cobras are close to each other, as well as the Asian spitting cobras, *N. siamensis*, *N. kaouthia* and *N. philippinensis*. As we mentioned in figure 5.5, the African non-spitting cobra *N. subfulva* appears as an outlier.

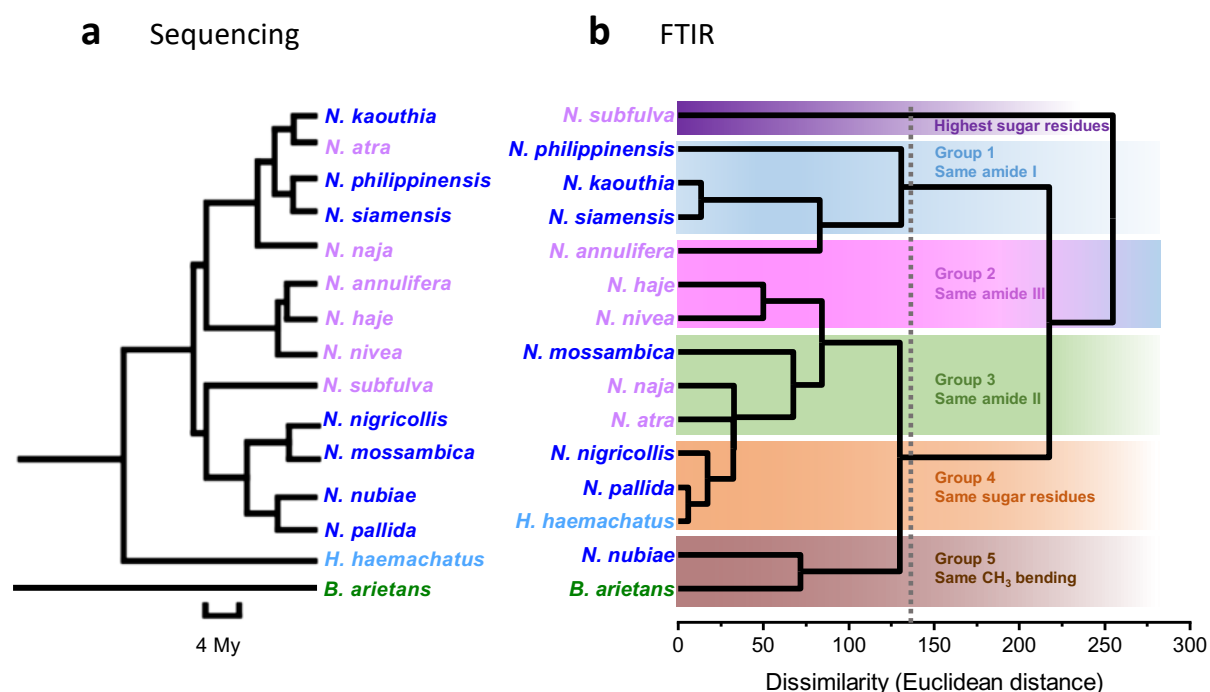


FIGURE 5.6 Classification of species in the Viperidae and Elapidae families. (a) Phylogenetic tree adapted from [116]. (b) Ultrametric tree generated from the hierarchical clustering analysis of snake venom infrared spectra, using LDA factor scores. Species with a Euclidean distance smaller than 130 were grouped together.

From figure 5.6b, five main groups are identified as well as one outlier, and they are grouped together based on their similarities, related to amide I, II, III, CH₃ bending and sugar residues absorbances. I can compare this ultrametric tree with figure 5.3 and this ties well with our estimated peak areas at 25 °C.

Group 1: Same amide I

The three Asian spitting cobras *N. philippinensis*, *N. kaouthia* and *N. siamensis* are included in this group. Species were grouped together because they display the same amide I absorbance, at 1645 cm⁻¹, as observed in figure 5.3, indicating these species could have similar protein concentration. From information showed in figure 5.4, at 25 °C it is clear that the maximum relative proportion of protein secondary structures in these three species, as well as in the other snakes, comes from the β-sheet presence, with a range between 62-68 %. It has been reported before that venom composition of spitting cobras is also characterised by their ability to cause ocular irritation and damage to the corneal tissues of potential predators if venom is in contact with their eyes, where cardiotoxins are the responsible components for this damage [154]. Interestingly, β-sheets are present in cardiotoxins, playing an important role in maintaining proteins active [364], [365]. Also, these three species are native from the same continent [208], sharing similar ancestors, which may also be the reason for spectral affinities.

Group 2: Same amide III

This group encompasses three African non-spitting cobras *N. annulifera*, *N. haje* and *N. nivea*, all of them showing high absorbance at 1250 cm⁻¹ (Fig. 5.3). They have the same amide III values, as described before, this region also indicates a high random coil content in protein secondary structures. This specific structure, random coil, is dependent on the molecular aspects of the polypeptide chain, showing no side chain interactions [256]. This group of African non-spitting cobras has been studied before in order to identify morphological, compositional and geographical similarities. Mitochondrial preliminary DNA sequences on southern African non-spitting cobras, showed that *N. nivea* was close to *N. haje* complex, and on the phylogram of cytochrome b sequences, *N. annulifera* appears next to *N. haje* [366]. This observation ties well with our findings on FTIR classification.

Group 3: Same amide II

In this group I find the African spitting cobra *N. mossambica* and the two Asian non-spitting cobras *N. naja* and *N. atra*. These species are characterised by the same amide II absorption at 1543 cm^{-1} , as confirmed in figure 5.3. This spectral region is characterised by N-H bending, as well as the presence of CN stretching vibrations [282]. Although these three species do not share the same behaviour, i.e., two are non-spitting and one is spitting; and two are from Asia and one from Africa, they share common ancestors. This spectral similarity can be explained based on the hydrogen bonds (H-bonds), because they play a major role in protein stability. It has been reported before that H-bonds stabilize the protein secondary structures, such as α -helices and β -sheets. It is precisely the interaction between the backbone with α -helices and β -structures the most frequently observed H-bonds. This assumption is confirmed on our Gaussian fitting on another spectral region, where the presence of α -helices and β -structures is clear at both temperatures. These observations indicate that N-H bending and H-bonds have further implications on the thermal and functional stability of proteins, by keeping its protein structures stable [367].

Group 4: Same sugar residues

This group includes two African spitting cobras *N. nigricollis* and *N. pallida*, as well as the primitive spitting cobra *H. haemachatus*. These three species have the same absorption between $1180\text{-}1024\text{ cm}^{-1}$, as corroborated in figure 5.3, suggesting they have similar glycosylation degrees, which was also confirmed by the presence of CLEC₂ in our SDS-PAGE profiles. In previous studies involving globular proteins, it was demonstrated that absorbances in the sugar residues region are directly proportional to the degree of glycosylation [264]. This spectral coincidence observed in these three species is also attributed to similar geographical distribution, as well as their behaviour, i.e., they have the ability to spit their venoms [208]. Additionally, in one recent study of the different proteins families in spitting and non-spitting species, it was found that despite their divergence, *H. haemachatus* was grouped close to the African spitting cobras, indicating a relationship and possibly, molecular convergence [116].

Group 5: Same CH₃ bending

Finally, the last group encompasses the African spitting cobra *N. nubiae* and the viper, *B. arietans*. These two species exhibit the same spectral absorption between 1475-1350 cm⁻¹, as confirmed in figure 5.3, which represents a similar CH₃ bending, providing us with information about the basic structure of proteins, related to protein chain, as well as the degree of regularity in the linear backbone structure [59], [58], [279]. Another aspect in common between these two species, is the fact that their venoms have cytotoxic activity [368], as the majority of spitting cobras in the *Naja* genus produce venom predominantly cytotoxic, which can cause necrosis, but the venom of the species *N. nubiae* is different, as it has both cytotoxic and neurotoxic properties [369]. Another similarity between these two species is found in our SDS-PAGE profiles, showing that the most intense bands associated to CRISP in the African spitting cobras, correspond to *N. nubiae*, and these protein families are present also in the viper *B. arietans*. This group of components in snake venom has not been studied in detail, but there are reports suggesting it could have more important roles in venom toxicity apart from blocking Ca²⁺ channels and blocking smooth muscle contraction. This component has been also used in phylogenetic hypothesis testing, and interestingly, the genus *Ophiophagus* was grouped together with vipers, but more studies need to be done in order to confirm these results [370].

These five groups observed in the ultrametric tree (Figure 5.6b) are correlated based on their spectral similarities. However, there is one species which is an outlier and it corresponds to the African non-spitting cobra *N. subfulva*, with the highest sugar residues, and the highest amide I/amide II ratio compared to the other African non-spitters. This result is atypical as it was supposed to be grouped close to the other African species. However, there is one study about *Naja* species, which indicates this species shows considerable geographical variation and it suggests a phylogeographic structure [371]. This previous finding has a significant impact on the current results, because it has been demonstrated that the habitat and diet in snakes, plays an important role in venom composition [322]. I attribute this result in our multivariate analyses to specific variations in snake venom composition in this particular species. Our ultrametric tree and the corresponding Euclidean distances obtained from analysed spectra reveal major differences between the different species of spitting and non-spitting cobras, as well as the viper, more specifically between African species, which agrees

with one previous study. In this study, researchers found substantial differences among the African species, based on their Euclidean distance matrix from venom proteomics [116]. These variations are attributed to the evolution of venom spitting and the defence mechanism as the major factor affecting venom composition.

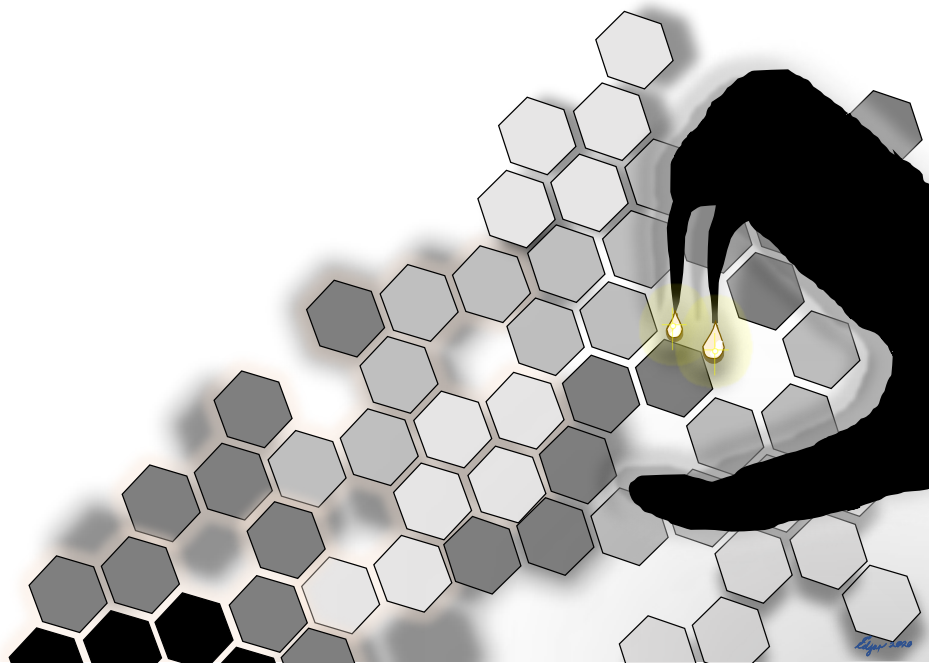
In this section, despite the observed differences comparing the phylogenetic tree with the ultrametric one, it is clear that the multivariate analysis performed on FTIR spectra, can be considered as a reliable approach on snake's classification and it can be extrapolated to other taxonomic families or clades.

5.4 CONCLUSIONS

I demonstrated here that the FTIR can be used as a valuable complementary technique to be combined with one of the most common used alternatives in venom proteomics, such as SDS-PAGE, to offer a better understanding of the compositional and structural properties of snake venom. It is possible to identify and classify species based on their spectral properties, while obtaining information in real time, at a relatively simple and non-destructive way, which can be replicated in other species. With the combination of techniques described here, it is evident that proteins in snake venom and their interaction with carbohydrates, play an important role in venom's thermal stability, maintaining protein structures under thermal stress. I also identified one interesting outlier species, *N. subfulva*, with its venom showing a different chemical composition, providing an indication of its origin and evolution. This new and different approach on snake's classification could have greater potential for use in the understanding of venoms, and how the spitting ability is related to venom composition and structure.

CHAPTER 6: CHARACTERISATION OF THE PHYSICAL PROPERTIES OF SNAKE VENOM

“Everything flows (πάντα ῥεῖ).” **Heraclitus**



This chapter corresponds to the published paper “Unexpected lack of specialisation in the flow properties of spitting cobra venom”, 2021, Journal of Experimental Biology. See Appendix A10, for the published paper. This paper was completed with contributions from all authors, and the first authorship is shared between Ignazio Avella and Edgar Barajas Ledesma. However, I performed all the characterisation, analysis (including the pressure differential calculation) and figures which are described in this chapter. The section corresponding to Phylogenetic Analyses is included to contribute to the understanding of this chapter. These analyses were performed by Ignazio Avella. The specific contributions to each author are as follows:

Methodology: Ignazio Avella, Edgar Barajas Ledesma, Wolfgang Wüster, Chris Holland and Arie van der Meijden; Validation: Edgar Barajas Ledesma, Chris Holland and Arie van der Meijden; Formal analysis: Ignazio Avella, Edgar Barajas Ledesma, Wolfgang Wüster, Chris Holland and Arie van der Meijden; Investigation: Ignazio Avella, Edgar Barajas Ledesma and Chris Holland; Resources: Edgar Barajas Ledesma, Nicholas R. Casewell, Robert A. Harrison, Paul D. Rowley, Edouard Crittenden, Wolfgang Wüster, Chris Holland and Arie van der Meijden; Data curation: Ignazio Avella, Edgar Barajas Ledesma, Paul D. Rowley and Edouard Crittenden; Writing-original draft: Ignazio Avella, Edgar Barajas Ledesma, Nicholas R. Casewell, Robert A. Harrison, Wolfgang Wüster, Riccardo Castiglia, Chris Holland and Arie van der Meijden; Writing-review and editing: Ignazio Avella, Edgar Barajas Ledesma, Nicholas R. Casewell, Robert A. Harrison, Paul D. Rowley, Edouard Crittenden, Wolfgang Wüster, Riccardo Castiglia, Chris Holland and Arie van der Meijden; Visualization: Ignazio Avella, Edgar Barajas Ledesma, Nicholas R. Casewell, Robert A. Harrison, Riccardo Castiglia, Chris Holland and Arie van der Meijden.

ABSTRACT

Venom-spitting is a defence mechanism based on airborne venom delivery used by a number of different African and Asian elapid snake species ('spitting cobras'; genus *Naja* and *Hemachatus*). Adaptations underpinning venom spitting have been studied extensively at both behavioural and morphological level in cobras, but the role of the physical properties of venom itself in its effective projection remains largely unstudied. Here, the first comparative study of the physical properties of venom in spitting and non-spitting cobras is provided. Viscosity, protein concentration and pH were measured, corresponding to venom of 13 cobra species of the genus *Naja* from Africa and Asia, alongside the spitting elapid *Hemachatus haemachatus* and the viper *Bitis arietans*. Using available microCT scans, the pressure required to eject venom through the fangs of a spitting and a non-spitting cobra was calculated. Despite noticeable differences in the modes of venom delivery between the variety of snake species studied here, no significant differences in the rheological and physical properties of the studied venoms between these functional groups were found. A species (spitting and non-spitting) showed a Newtonian behaviour, suggesting possible selection for conservation. Although results imply that the evolution of venom spitting did not significantly affect venom viscosity, the model of fang pressure described here, suggests that the pressure requirements to eject venom are lower in spitting than in non-spitting cobras.

KEYWORDS: Cobra, Venom, Rheology, Viscosity, Concentration, pH

6.1 INTRODUCTION

A plethora of defensive behaviours can be found across the animal kingdom. Such variety can be explained by natural selection acting more strongly on defence mechanisms than on offense/predation mechanisms, as suggested by the “life-dinner principle” [372]. According to this principle, evolutionary selective pressure on the prey is much stronger than on the predator, because in a predator-prey encounter, the prey may lose its life, while the predator may only lose a meal. Defensive behaviours can be summarised in three main categories: freezing, fleeing, and fighting/defensive attack [373]. As part of the latter category, some organisms employ venom, defined as an injectable harmful chemical secretion, to mount a more effective defensive attack, e.g., hymenoptera, arachnids, and venomous snakes. The noxious effects of venom increase the dissuading effect of the defence, enabling even small animals to ward off larger attackers [374]. Snake venom consists of a complex mixture of peptides and proteins, small organic molecules and salts in an aqueous medium [375]. The high peptide and protein content makes it more viscous than water [128], and it has been previously identified as a non-Newtonian shear-thinning fluid [128], [196].

Venomous snakes (superfamily Colubroidea) inject venom into the body of their prey, or defensively into the body of their attackers, through specialised fangs or grooved teeth [376], [377]. Members of the families Viperidae, Elapidae and Atractaspididae use an advanced front-fanged venom delivery system [378]. In these snakes, the venom originates from the primary venom gland, and is expelled by the pressure of a skeletal muscle (referred to as *m. compressor glandulae* in viperids or *m. adductor mandibulae externus superficialis* in elapids); through the primary duct, the secondary (accessory) gland and into the fang, which acts like a hypodermic needle [379]–[382]. Once injected, venom toxins become systemic via dispersal by the bloodstream and lymphatic system, interacting with the prey/attacker’s physiological proteins and receptors, ultimately disrupting the nervous system, the blood coagulation cascade, the cardiovascular and neuromuscular system, and/or homeostasis in general [378]. The Elapidae family of snakes includes taipans, mambas, coral snakes, kraits and cobras. Snakes of this family inject their venom through short, fixed fangs located in the frontal part of the upper jaw, as opposed to the movable front fangs of the Viperidae and Atractaspididae [383], [384]. Cobra species of the genus *Naja* Laurenti, 1768, possess venoms with neurotoxic

and/or cytotoxic properties, which they use to rapidly immobilize their prey for consumption, or to dissuade predators [157], [384]. Members of this genus are present in both Africa and Asia [384], [385], [386], and cobras from these two continents separated about 16 Mya [386].

Several *Naja* species are well known for their peculiar ability to spit venom as a defence mechanism, expelling it as pressurised jets or sprays at their attackers [125], [383], [387]–[390]. These spits are generally aimed at the face and eyes of an aggressor [391], and once in contact with the eyes, can cause severe pain and inflammatory pathology [191], [391]. The ability to spit venom likely evolved from non-spitting ancestors on three independent occasions, once in African cobras and once in Asian cobras, in addition to a third occasion in the closely related *Naja*-relative, the rinkhals, *Hemachatus haemachatus* [388], [392], [393].

The venom delivery system of spitting cobras possesses several subtle morphological adaptations that enable them to eject their venom over long distances, and which distinguish them from non-spitting cobras. The discharge orifice, for example, has a more circular shape [383], [390], and is directed more anteriorly, creating a 90° bend in the venom channel inside the fang [127], [196]. This channel has internal ridges unique to spitting cobras [124] that reduce the pressure loss by about 30% compared to an identical channel without ridges, thus helping to achieve a longer reach of the jet [196]. Furthermore, spitting cobras actively displace the fang sheath (thus removing a physical barrier to venom expulsion), unlike other venomous snakes, where displacement of the fang sheath is passive [121]. Additional behavioural adaptations found in African spitting *Naja* species include adjusting head movements to distance from target to optimise the spread of venom [387], and tracking and anticipating target movements to improve accuracy [120]. Spitting cobras also show a certain degree of variation in their spitting modes: as demonstrated by previous studies [125], [389]; some specialised spitters eject their venom in streams (e.g., *Naja pallida*) while others produce a fine mist (e.g., *Naja nigricollis*). The combination of morphological and behavioural adaptations allows most spitting cobras to eject venom up to at least 1 m, with some species (e.g., *Naja mossambica*) able to spit up to about 3 m [125].

To date, considerable research effort has been focused on the anatomical features of the specialised venom delivery apparatus of spitting cobras [121], [124], [196], [383], [390], and on their associated peculiar defensive behaviour [387], [389], [120]. In contrast, the possibility of changes in the composition of the venom itself, as an adaptation for its new role as a venom applied outside of the body, or toxungen [394], has remained largely neglected. Nevertheless, a recent study [388] suggested that, in African cobras at least, the venom of spitting species appears to have a higher cytotoxicity than the venom of the non-spitters, which may increase its effectiveness when applied externally.

However, in addition to new selective pressures relating to its function as a toxungen, venom spitting may also have changed the mechanical demands of the venom, but so far this has not been studied. Since the venom has to pass through the narrow ducts of the venom apparatus, it is expected that a lower venom viscosity (i.e., resistance to flow) would serve to reduce pressure loss during venom expulsion, thereby reducing the energetic requirements of ejection. Furthermore, for a given ejection force, venom projection distance would also be aided by more rapid expulsion, obtainable with a less viscous venom. On the other hand, in spitting cobras, a higher viscosity would aid jet cohesion after venom ejection, keeping the jet of venom from breaking up into droplets for longer, thus improving spitting distance and accuracy. These two seemingly conflicting demands could be met if venom in spitting cobras exhibits a shear-thinning non-Newtonian behaviour, which would benefit ejection and cohesion.

Here the rheological properties of the venoms of twelve spitting and non-spitting cobra species of the genus *Naja* from both Africa and Asia were measured and compared, the only known “non-*Naja*” species of spitting elapid *Hemachatus haemachatus*, and the African viperid *Bitis arietans* (used as outgroup). Also protein concentration and pH were compared, two properties, known to play an important role in the stability of some snake venom components [395] and are often directly correlated to the severity of the envenomation [396]–[398]. Given the morphological differences between the fangs of spitting and non-spitting cobras [121], [124], [196], [383], [390], the hypothesis in this study is that the two venom delivery mechanisms (spitting and biting) might be associated with different pressure requirements for venom ejection, and that venom of non-spitting species behaves as a

Newtonian fluid, and in spitting cobras, as a non-Newtonian material. To test this, the pressure needed for venom to flow through the fang channel of one spitting and one non-spitting cobra species was calculated and compared (*Naja nigricollis* and *Naja nivea*, respectively), using previously available microCT scanning data [129] and rheological data obtained in this study.

6.2 MATERIALS AND METHODS

6.2.1 VENOM EXTRACTION

In total, venom samples of thirty snakes were used in this study. Venom was extracted from 28 cobras belonging to 13 different species of the genus *Naja*, namely: *Naja annulifera*, *Naja atra*, *Naja haje*, *Naja kaouthia*, *Naja mossambica*, *Naja naja*, *Naja nigricollis*, *Naja nivea*, *Naja nubiae*, *Naja pallida*, *Naja philippinensis*, *Naja siamensis* and *Naja subfulva*. Venom was also extracted from one rinkhals, *Hemachatus haemachatus* and one puff adder, *Bitis arietans*, used for comparative analyses, respectively as a “non-*Naja*” venom spitter and non-spitter. Twelve of the specimens were captive bred (CB), while the remaining eighteen were collected in the wild (see Appendix A5, table A5, for details). All snakes were maintained in individual cages within the temperature, humidity and light-controlled environment of the herpetarium at the Centre for Snakebite Research & Interventions, Liverpool School of Tropical Medicine, UK. This facility and its protocols for the expert husbandry of the snakes are inspected and approved by the UK Home Office and the LSTM Animal Welfare and Ethical Review Board. After milking, the snakes were immediately put back into their enclosures and the venom transferred into 2 ml low-protein binding cryotubes (Simport Scientific, Beloeil, Canada) using a pipette. Appendix A5, table A5, shows the total solids concentration for each species. The tubes were then transferred on ice to the laboratory of the Department of Materials Science and Engineering of the University of Sheffield for rheological, pH and concentration measurements on the same day. Unless otherwise stated all samples were tested at room temperature $22 \pm 1^\circ \text{C}$.

6.2.2 RHEOLOGICAL TESTS

Shear viscosity measurements were performed at the Department of Materials Science and Engineering, University of Sheffield, using a DHR-2 rheometer (TA Instruments, USA), equipped with a cone-plate geometry (20 mm diameter, 1° angle cone, 27 μm truncation gap, 36 μl to fill), and subjecting samples to a shear rate ramp from 1.0 s⁻¹ to the maximum shear rate possible in this instrument [10,000 s⁻¹], (41 steps, 15 s per step) at 25° C. 25° C was chosen from direct comparison to other protein rheology work conducted in the group and as it approximates previous field reports ranging between 26-31 °C capturing spat volumes spitting cobras *N. nigricollis*, *N. pallida*, *N. mossambica* and *H. haemachatus*. Only species where sufficient venom was obtained to perform at least two replicates are shown (up to three repeats for 70% of species included in this study were achieved). Venom samples that were not sufficient included *H. haemachatus* (African “non-*Naja*” spitter), *N. subfulva* (African non-spitter) and *N. naja* (Asian non-spitter). In order not to overlook the potential presence of intraspecific variation in the considered rheological properties, all measurements were carried out on the venom of individual specimens.

6.2.3 CALCULATING FANG VENOM SHEAR RATE

To support the range of shear rates tested and their biological relevance, it is necessary to calculate the natural range of shear rates encountered by venom. If venom is considered to be flowing down a channel, assuming all four species (one reported by Triep *et al.* [196], and three by du Plessis *et al.* [129]) could spit over the same timescale and volume, the maximum shear strain rate at the fang wall is given by:

$$\dot{\gamma}_w = \frac{4Q}{\pi R^3} \quad (\text{equation 6.1})$$

Where Q is the volumetric flow in m³ s⁻¹ and R is the radius of the venom channel in m, and $\dot{\gamma}_w$ is the shear rate in s⁻¹. According to data from [196], and from [129], the values considered during the venom spitting process are:

Volume of a single spitting event, $V_{\text{single spit}} = 1.0 \times 10^{-8} \text{ m}^3$

Time for a single spitting event, $t_{\text{single spit}} = 40\text{ms} = 4 \times 10^{-2} \text{ s}$

$R = 3.8 \times 10^{-4} \text{ m}$, *B. arietans* [129]

$R = 2.2 \times 10^{-4} \text{ m}$, *N. nigricollis* [129]

$R = 2.0 \times 10^{-4} \text{ m}$, *N. nivea* [129]

$$\therefore Q = \frac{1.0 \times 10^{-8} \text{ m}^3}{4 \times 10^{-2} \text{ s}} = 2.5 \times 10^{-7} \text{ m}^3 \text{ s}^{-1}$$

And finally, using Eqn 6.1, from [129],

$$B. \text{ arietans: } \dot{\gamma}_w = \frac{4 * 2.5 \times 10^{-7} \text{ m}^3 \text{ s}^{-1}}{\pi * (3.8 \times 10^{-4} \text{ m})^3} = 5,801 \text{ s}^{-1}$$

$$N. \text{ nigricollis: } \dot{\gamma}_w = \frac{4 * 2.5 \times 10^{-7} \text{ m}^3 \text{ s}^{-1}}{\pi * (2.2 \times 10^{-4} \text{ m})^3} = 29,894 \text{ s}^{-1}$$

$$N. \text{ nivea: } \dot{\gamma}_w = \frac{4 * 2.5 \times 10^{-7} \text{ m}^3 \text{ s}^{-1}}{\pi * (2.0 \times 10^{-4} \text{ m})^3} = 38,051 \text{ s}^{-1}$$

6.2.4 CALCULATING THE PRESSURE NEEDED TO EJECT VENOM

If the venom is considered to be flowing down a venom channel of converging radius from R_1 to R_2 , the pressure drop will be the result of the radius reduction from the fang base to the end of the fang where the exit orifice of the venom channel is located, plus the losses due to the viscous material or venom flowing in the venom channel [399]. In order to corroborate if the flow is laminar or turbulent for the appropriate use of equations, the Reynolds number for the three species considered needs to be determined. The maximum Reynolds number defined for a Newtonian fluid can be calculated with the following equation:

$$Re_{\text{max}} = \frac{\rho * u_1 * D_1}{\mu_{\text{min}}} \quad (\text{equation 6.2})$$

Where:

Re_{max} is the maximum Reynolds' number

ρ is the density of the venom, $\text{kg} * \text{m}^{-3} = 1084 \text{ kg} * \text{m}^{-3}$ [196]

u_1 is the venom velocity at the channel inlet, $\text{m} * \text{s}^{-1}$, $1.33 \text{ m} * \text{s}^{-1}$ (calculated with information from [196]).

D_1 is the diameter at the channel inlet: 7.6×10^{-4} m, *B. arietans* [129]; 4.4×10^{-4} m, *N. nigricollis* [129]; and 4.0×10^{-4} m, *N. nivea* [129].

μ_{\min} is the dynamic viscosity of venom, Pa*s, from our own data at $10,000 \text{ s}^{-1}$: $0.026 \text{ Pa}\cdot\text{s} \pm 8.5 \times 10^{-4}$, *B. arietans*; $0.031 \text{ Pa}\cdot\text{s} \pm 8.6 \times 10^{-3}$, *N. nigricollis*; and $0.170 \text{ Pa}\cdot\text{s} \pm 0.079$, *N. nivea*.

Assuming that all species have the same velocity at the channel inlet and density, Reynolds numbers are:

$$B. arietans: Re_{\max} = \frac{1084 \text{ kg}\cdot\text{m}^{-3} \cdot 1.33 \text{ m}\cdot\text{s}^{-1} \cdot 5 \times 10^{-4} \text{ m}}{0.026 \text{ Pa}\cdot\text{s}} = 27.72$$

$$N. nigricollis: Re_{\max} = \frac{1084 \text{ kg}\cdot\text{m}^{-3} \cdot 1.33 \text{ m}\cdot\text{s}^{-1} \cdot 5 \times 10^{-4} \text{ m}}{0.031 \text{ Pa}\cdot\text{s}} = 23.25$$

$$N. nivea: Re_{\max} = \frac{1084 \text{ kg}\cdot\text{m}^{-3} \cdot 1.33 \text{ m}\cdot\text{s}^{-1} \cdot 5 \times 10^{-4} \text{ m}}{0.170 \text{ Pa}\cdot\text{s}} = 4.24$$

Reynolds numbers are < 100 , and in line with [196] predictions, corresponding to a laminar flow, which is below the critical Reynolds number of 2300, where turbulent flow is observed.

As the flow is in the laminar region, then the following equation will be used to calculate the total pressure differential in the venom channel (see Appendix A6 for the detailed deduction of this equation), which corresponds to an Extended Bernoulli Equation:

$$\Delta P = P_1 - P_2 = \frac{\rho}{2} \cdot u_1^2 \left(\left(\frac{A_1}{A_2} \right)^2 - 1 \right) + \frac{64}{Re} \cdot \frac{l}{D} \cdot \frac{\bar{u}^2}{2} \cdot \rho \quad (\text{equation 6.3})$$

Where:

ΔP is the pressure differential in the venom channel, in Pa.

P_1 and P_2 are the pressures at the inlet (1) and outlet (2) points, in Pa.

u_1 and u_2 are the velocities at the inlet (1) and outlet (2) points, in $\text{m}\cdot\text{s}^{-1}$.

ρ is the density of venom, in $\text{kg}\cdot\text{m}^{-3}$.

A_1 and A_2 are the cross-section areas at the inlet and outlet points, in m^2 .

Re is the Reynolds number, dimensionless.

l is the length of the venom channel, in m.

D is the average diameter of the venom channel, in m.

\bar{u} is the average velocity of the venom in the venom channel, in m.

To directly relate these calculations to the natural system and measured rheological data, microCT scans from [129], and available at the GigaScience Database (<http://dx.doi.org/10.5524/100389>), were used to calculate venom channel length and radius. Fang morphology data was available for three species included in this study: *Bitis arietans* (viper), *Naja nigricollis* (African cobra, spitter) and *Naja nivea* (African cobra, non-spitter). MicroCT image stacks were imported into Amira (Thermo Scientific, version 2019.4) and 10 evenly spaced measurements were taken along the length of the venom channel (l) from the end of the entry orifice into the channel at the base of the fang to the opening point of the exit orifice at the tip of the fang. Of the ten measurements per species, the average diameter was obtained (D) for input into Eqn 6.3.

Table 6.1 summarises the values used for each variable as well as the pressure differential results for *B. arietans*, *N. nigricollis* and *N. nivea*.

TABLE 6.1. Parameters used for ΔP calculations.

Species	D_1 , m	D_2 , m	D , m	Length, m	u_1 , m.s ⁻¹	ΔP , Pa
<i>B. arietans</i>	1.4×10^{-3}	4.4×10^{-4}	7.6×10^{-4}	0.00915	1.33	0.104×10^6
<i>N. nigricollis</i>	8.0×10^{-4}	2.3×10^{-4}	4.4×10^{-4}	0.00333	1.33	0.172×10^6
<i>N. nivea</i>	7.7×10^{-4}	1.0×10^{-4}	4.0×10^{-4}	0.00352	1.33	2.829×10^6

6.2.5 PROTEIN CONCENTRATION

Protein concentration was measured for each venom sample using a UV300 Thermo Spectronic spectrometer (Unicam/Thermo, UK). All samples (dilutions consisting of 1.5 μ l of fresh venom + 1 ml of water) were analysed at room temperature in 1 cm path-length polystyrene cuvettes from 200 to 500 nm wavelength. Double distilled water was used as a blank and for all dilutions. Protein concentration was estimated as follows, using absorbance at 260 and 230 nm [400]:

$$\text{Concentration (mg ml}^{-1}\text{)} = (0.183 \times A_{230\text{nm}}) - (0.075 \times A_{260\text{nm}}) \quad (\text{equation 6.4})$$

Where $A_{260\text{nm}}$ and $A_{230\text{nm}}$ correspond to absorbance at 260 and 230 nm, respectively.

6.2.6 PH MEASUREMENTS

A Sentron pH meter (Netherlands) equipped with a cupFET pH probe was used to make pH measurements at room temperature. Two 3 μl droplets from each undiluted venom sample were measured individually and averaged to generate a pH measurement.

6.2.7 PHYLOGENETIC COMPARATIVE METHODS

The aim of the analyses reported here was to test for patterns in the measured parameters between spitting and non-spitting cobra venoms across the sampled species. All the analyses were performed using R 3.6.1 implemented using RStudio 1.2.1335, always taking the species phylogeny into account. Species tree reported in [401] were used. This tree contained 46 elapid species belonging to 11 different genera and was generated using a multispecies coalescent model based on DNA sequence alignments of both mitochondrial (partial *cytb* and *ND4* gene sequences) and nuclear genes (*CMOS*, *NT3*, *PRLR*, *UBN1* and *RAG1*). For the analyses in the current study, the original tree was pruned, and the species used in the venom rheology tests were retained (i.e., *Hemachatus haemachatus* and the various *Naja* species). The viper *B. arietans* was added manually to the tree as an outgroup, considering previous research suggesting that viperids separated from elapids about 61 Mya [117].

Within spitting cobras, a further division can be made in the different ways venom is ejected, which likely require different rheological properties of the venom. Following previous studies [125],[389], the modes of venom ejection were divided into three categories: i) “streams”: venom is ejected in the form of more or less continuous jets; ii) “mist”: venom is ejected in the form of a fine spray; iii) “mixed”: venom is ejected in a form in between the other two categories (see Appendix A5, table A5). Information about the venom spitting modes of seven species of spitting elapids considered in this study (*N. atra*, *N. kaouthia*, *N. mossambica*, *N. nigricollis*, *N. pallida*, *N. siamensis* and *H. haemachatus*) was gathered from the literature [125], [389], [402], [403]. The spitting mode category for *N. nubiae* and *N. philippinensis* was

assigned based on the authors' personal observations. The category "non-spitter" was assigned to the non-spitting cobras *N. annulifera*, *N. haje*, *N. naja*, *N. nivea* and *N. subfulva*.

To first test evaluates if there was a difference between spitting and non-spitting cobras and/or between Asian and African cobras across all the measured physical properties, a MANOVA using spitting behaviour was performed (defined in the analysis as "spit") as a binary factor (spitter or non-spitter), and the data about protein concentration and viscosity at 10,000 s⁻¹ as multivariate dependent variables. Spitting behaviour as a binary trait was considered only in this analysis. After this preliminary MANOVA, the same test was performed considering the three different spitting mode categories, to look for possible correlation between differences in spitting modes and the measured physical properties of the venoms.

To test if there was a difference in venom viscosity due to spitting behaviour, protein concentration or pH, an ANCOVA test was performed using viscosity at 10,000 s⁻¹ ("visc10000") as dependent variable and "spit", protein concentration ("ProtConc") and pH ("pH") as independent variables.

To test if there was a difference in protein concentration due to spitting behaviour, an ANCOVA was performed, using protein concentration as dependent variable and 'spit' as independent variable. To look for possible presence of phylogenetic signal for pH, protein concentration and viscosity at 10,000 s⁻¹, both Blomberg's K [404] and Pagel's λ [405] were calculated, using the R packages *caper* (<https://cran.r-project.org/web/packages/caper/>), *geomorph* (<https://cran.r-project.org/web/packages/geomorph/>) and *phytools* (<https://cran.r-project.org/web/packages/phytools/>). Finally, Blomberg's K was calculated for protein concentration and viscosity at 10,000 s⁻¹ at the same time.

6.3 RESULTS

6.3.1 PHYSICAL PROPERTIES OF THE VENOM

For all *Naja* venoms tested, the protein concentrations had an average of 132.6 mg ml⁻¹, ranging from 51.11 mg ml⁻¹ (*N. nivea*) to 159.1 mg ml⁻¹ (*N. annulifera*). The venoms of *B. arietans* and *H. haemachatus* had similar protein concentrations (132.4 and 132.5 mg ml⁻¹, respectively). No differences were found between species or groups. The same was also true following quantification of venom pH, where the average pH of the *Naja* venoms was 5.77, ranging from 5.49 (*N. kaouthia*) to 6.02 (*N. pallida*). The pH of *H. haemachatus* venom was 5.76, and finally the pH of *B. arietans* venom was the lowest at 5.43 (Fig. 6.1).

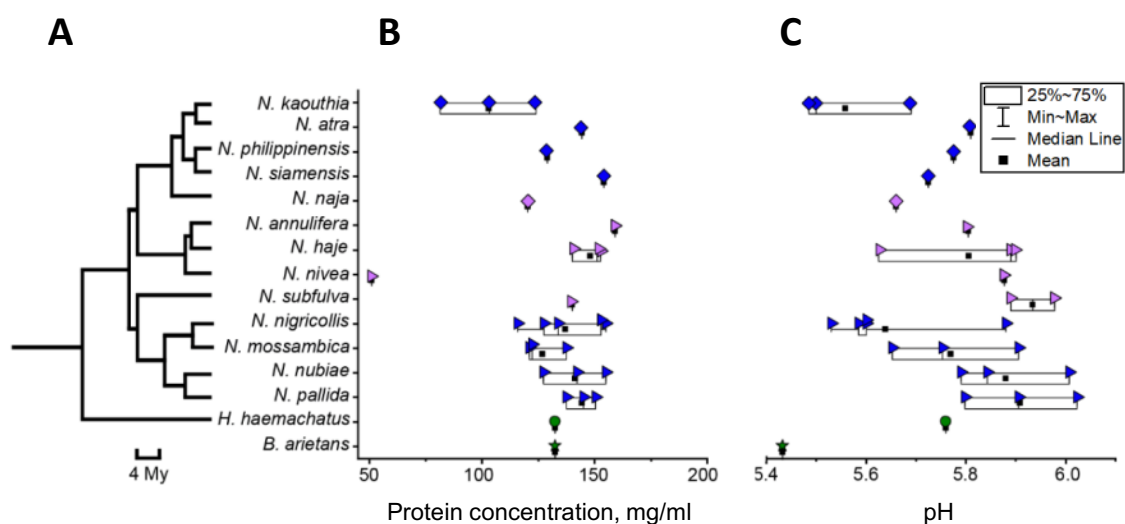


FIGURE 6.1 Physical properties of the venoms. A) Cladogram of the elapid species analysed, extrapolated from the phylogenetic analyses performed (following [117], viperids separated from elapids about 61 Mya, therefore *B. arietans* has not been included in the cladogram); B) box plot of protein concentration for venoms extracted for each species; C) box plot of pH, where each data point represents the average of two individual measurements. Triangles represent African *Naja* species, diamonds represent Asian *Naja* species. Venom-spitting species are in blue, non-spitting species in violet. The green circle and the green stars represent, respectively, *Hemachatus haemachatus* and *Bitis arietans*.

Rheological tests demonstrated that, contrary to our starting hypothesis, the venoms of both spitting and non-spitting cobras show a Newtonian behaviour, at least over the range reported here (i.e., 100 to 10,000 s^{-1}) (Fig. 6.2). No significant differences between species or groups were evident.

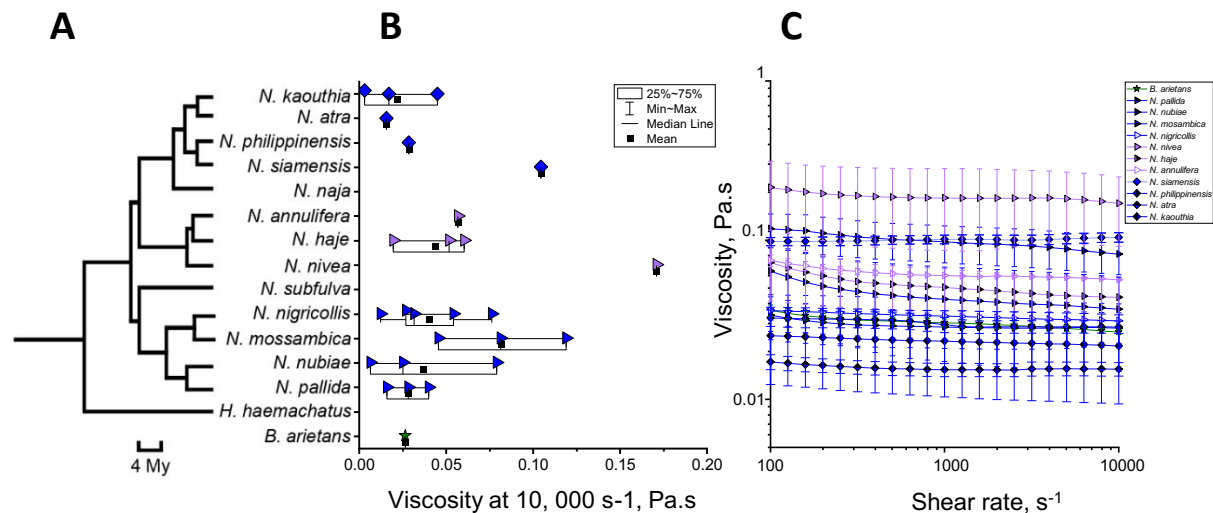


FIGURE 6.2 Rheological properties of the venoms. A) Cladogram of the elapid species analysed, extrapolated from the phylogenetic analyses performed (following [117], viperids separated from elapids about 61 Mya, therefore *B. arietans* has not been included in the cladogram); B) box plot of viscosity at 10,000 s^{-1} for venoms extracted for each species; C) Viscosity vs shear rate for each species. Venom-spitting species are in blue, non-spitting species in violet. The green star represents the viper *B. arietans*. Error bars correspond to standard error from at least two experiments per specimen.

Combining rheological and morphological data to determine the pressure required for venom to flow down the venom channel, Fig. 6.3 shows the results for the African non-spitting cobra *N. nivea*, the African spitting cobra *N. nigricollis* and the viper *B. arietans*. MicroCT scans obtained from [129] indicate two different types of fangs, closed fused (*B. arietans*) and non-fused (*N. nigricollis* and *N. nivea*, Fig. 6.3A), and subsequent measurements provide information as to the fang length/diameter ratio (Fig. 6.3B). The results of fang pressure calculations shown in Fig. 6.3C report that the highest value corresponds to *N. nivea* (2.8×10^6 Pa), while *B. arietans* shows the lowest pressure differential (0.10×10^6 Pa).

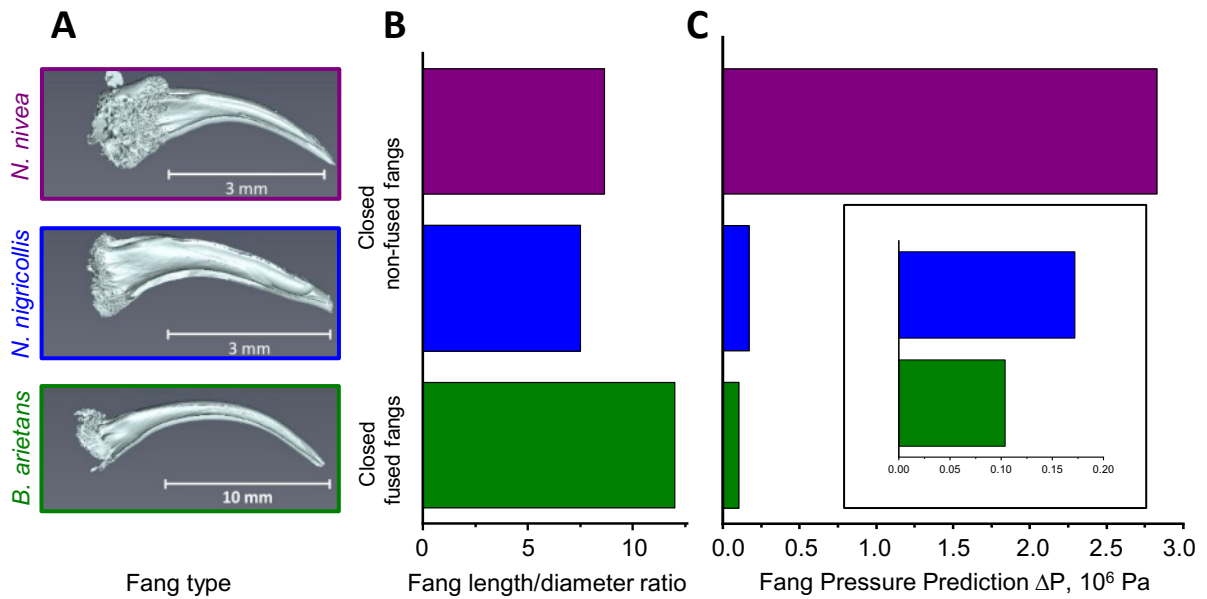


FIGURE 6.3 Fang Pressure Prediction for *N. nivea* (violet), *N. nigricollis* (blue) and *B. Arietans* (green). A) MicroCT images showing fang types (data analysed from [129], available at GigaScience Database, <http://dx.doi.org/10.5524/100389>); B) fang length/diameter ratio; C) ΔP in the fang venom channel using representative rheological data for each species.

6.3.2 PHYLOGENETIC COMPARATIVE METHODS

The results of both MANOVAs showed no significant relationships between spitting behaviour and the multivariate combination of the measured physical properties of the venom (protein concentration, viscosity at $10,000 \text{ s}^{-1}$). An additional MANOVA including pH among the variables was also performed, but then discarded because of the non-significance of the added variable and to simplify the model. The results of the ANCOVAs also showed no significant effect of spitting behaviour, protein concentration or pH on viscosity, or of spitting behaviour on protein concentration. Results of the statistical analyses performed considering the three spitting mode categories are reported in Table 6.2.

TABLE 6.2. Results of statistical testing. The symbol “y” indicates the multivariate variable consisting of protein concentration, power law index and viscosity at 10,000 s⁻¹. Degrees of freedom (Df), F ratios (F) and p-values (P) are reported.

Type of analysis	Model	Variable	Df	F	P
Phylogenetic MANOVA	y ~ spit	spit	3	0.569	0.669
Phylogenetic ANCOVA	visc10000 ~ spit+ProtConc+pH	spit	3	0.976	0.448
		ProtConc	1	3.380	0.094
		pH	1	0.079	0.775
Phylogenetic ANCOVA	ProtConc ~ spit	Spit	3	0.140	0.911

Protein concentration, pH and viscosity at 10,000 s⁻¹ show both Blomberg’s K and, particularly, Pagel’s λ close to 0 (See table 6.3), indicating phylogenetic independence. The same can be said for the multivariate analysis, which considers both protein concentration and viscosity, and for which only Blomberg’s K has been calculated. None of these results was significant, with P-values always higher than 0.05 (between 0.276 and 0.707 for K and equal to 1 for λ).

TABLE 6.3. Results of phylogenetic signal testing.

Tested variable	Blomberg’s K	P	Pagel’s λ	P
Protein concentration	0.333	0.707	7.69 x 10 ⁻⁵	1
pH	0.455	0.375	6.41x 10 ⁻⁵	1
Viscosity at 10,000 s ⁻¹	0.505	0.276	7.69 x 10 ⁻⁵	1
Protein concentration and viscosity at 10,000 s ⁻¹	0.477	0.323		

6.4 DISCUSSION

Young’s study on venom gland pressure in spitting cobras suggested that the force required by the m. adductor mandibulae externus superficialis to expel venom would be reduced if a highly shear thinning venom was present [121]. The sudden increase in shear rate upon entering the venom channel would cause a decrease in the viscosity of the venom, which could therefore be pushed through the fang more easily and thus at the higher velocities that are required to increase the reach of the venom jet [196]. However, upon exiting the fang, the effective shear rate in the airborne venom jet ejected by a spitting cobra would be dramatically reduced, and as such, a higher viscosity in the jet would reduce internal flow, thus slowing down the breaking up of the jet into separate droplets. This provides the

advantage of a more coherent jet of venom, resulting in less drag and thus a longer reach. Given that non-spitting cobras do not eject their venom, they presumably have less need for a higher venom ejection speed, and hence less need for a highly shear-thinning venom.

In light of these biomechanical considerations, a more pronounced shear-thinning behaviour in spitting cobras than in non-spitting cobras was expected, in order to reduce pressure loss inside the venom duct and to increase jet cohesion. Thus, when considering the above and the specific morphological adaptations to spitting in spitting cobras, such as the ridges present along the channel inside their fangs [196], [329], the more circular and anteriorly oriented discharge orifice of their fangs [383], [390], [121], and the apparently higher algescic activity of venoms of the three spitting lineages [401], the rheological properties of the venom between spitting and non-spitting cobras were expected to also be different.

Hence, in light of our findings, it is surprising to find no systematic differences in venom viscosity between spitting and non-spitting species. However, it is worth noting that this result might be influenced by the small number of rheological tests performed for most of the analysed snakes, owing to the relatively small amount of venom a single cobra specimen produces. Nevertheless, differences in viscosity between and within species were found, suggesting that there is enough variability for natural selection to potentially act on. Between species, the average venom viscosities at $10,000\text{ s}^{-1}$ went from a minimum of 0.0103 Pa s (*N. naja*) to a maximum of 0.1709 Pa s (*Naja nivea*) (Figure 6.2).

Similarly, it was found that viscosity could vary greatly even among specimens of the same species. For instance, the average venom viscosities measured for the three *N. nubiae* specimens (NajNubCB001, NajNubCB003 and NajNubCB004) were, respectively, 0.0064 , 0.0252 and 0.0790 Pa s (Figure 6.2B). These results suggest that the venom of all the elapid species analysed may vary in viscosity owing to functional or other non-flow related requirements. Within the range of rheological variability indicated here for spitting cobras, other selective pressures may dictate the observed rheological properties. Although protein concentration and pH have been previously shown to vary and be of influence in snake venoms [406] and in other secreted protein systems (e.g. silk, [21], [407]), these two parameters did not vary significantly in our study.

Snake venom is known to vary in composition depending on different factors, such as diet [408], [409], ontogeny [410]–[412] and, potentially, local adaptation driven by relatively small changes in the physical environment [413]. Compositional alterations in snake venom likely influence its rheology. Environmental changes determined by captivity (e.g., food supply restricted to a single type of prey) can also result in modifications of venom composition. However, most of the evidence produced so far suggests that the effect of captivity on snake venom composition is minimal [414].

In light of this and considering that all venom samples analysed here were sourced from adult snakes fed on the same diet and kept under the same enclosure conditions, age, diet and ecology-related sources of variability have been minimised as much as possible, and thus seem unlikely to play a major role in the findings of this study. Thus, inherited differences in molecular venom composition [141], [415], [416] can be the primary influence for any rheological differences. However, considering that in two studies [157], [401], both found the venoms of African spitting cobras (*N. katiensis*, *N. mossambica*, *N. nigricollis*, *N. nubiae*, *N. pallida*) to show similar compositional patterns in terms of proteins, long chain (high molecular weight) non-protein molecules present in snake venom, such as carbohydrates [417]–[420], could be responsible for the detected variation in rheological properties.

Surprisingly, our rheological testing showed Newtonian behaviour for all analysed snake venoms across the shear rates presented. This appears to be in direct contrast to previous studies where snake venoms have been classified as non-Newtonian [128], [196], [421]. For example, Triep *et al.* [196] suggested that *N. pallida* venom had non-Newtonian behaviour in the range of 1 to 37 s⁻¹. However, upon closer inspection of the data within this range, it is concluded that the apparent shear-thinning behaviour of *N. pallida* venom could be attributed to surface tension effects [422]. As a result, through comparison of our findings to previous studies, and accounting for the potential confounding influence of surface tension artefacts, it is proposed that any venom rheological data obtained below 100 s⁻¹ presented to date should not be considered when determining if a venom is Newtonian or non-Newtonian (see Appendix A7, figure A7). Previous studies have interpreted the rheological behaviour of snake venom based on experimental shear rate values ranging from 1 to 100 s⁻¹

[196], and from 0.01 to 200 s⁻¹ [128]. In these cases, because of the surface tension artefacts, only data from 100 to 200 s⁻¹ (indicating a Newtonian flow behaviour) should be considered.

To explore the delivery mechanism and pressure requirements of venom ejection, rheology data were combined with microCT scans of snake fangs reported by du Plessis *et al.* [129]. For the corresponding calculations, since fang venom channels are typically slightly curved and may have additional pressure-increasing features such as internal ridges [196], [329] and pressure losses due to viscosity, an extended generalised Bernoulli equation (Eqn 6.3) was used. The pressure required for venom to flow through the fang for three of the species was modelled, and three species were considered: *N. nivea* (African non-spitting cobra), *N. nigricollis* (African spitting cobra) and *B. arietans* (viper). Despite the limited number of species investigated, there are clear differences in the pressure required to move venom down the fang. The spitter *N. nigricollis* has a smaller fang length/diameter ratio and a lower pressure requirement, whereas the non-spitter *N. nivea* has a larger fang length/diameter ratio and a higher-pressure requirement. Interestingly, the viper *B. arietans* displayed both the largest fang length/diameter ratio and the lowest pressure requirement overall (Fig. 6.3), likely related to the relatively larger absolute diameter and/or curvature of the fang channel in this species.

It was found that the effect of viscosity and friction of the fluid in the venom channel (which is included in the Reynolds number; see Appendix A6 for details) represents 5% of the pressure loss in *B. arietans*; 17% in *N. nigricollis* (spitter); and 9% in *N. nivea* (non-spitter). It appears that with this approach neither density nor viscosity contributes significantly to pressure losses, and that the major influence is the cross-section area variations along the venom channel ($A_1 > A_2$), which represent between 83 and 95% of the total pressure loss. In light of this, it is concluded that for all the viscosities observed, and for all the snake species analysed in this study, venom viscosity does not strongly influence the pressure requirements of venom ejection, and that what most defines such requirements are the morphological adaptations of the venom delivery systems (i.e., tapering of the fang venom channel). Considering the ‘life–dinner principle’ [372], which suggests that selection for defensive strategies should take precedence over selection for predatory efficiency, the lack of

significant signs of adaptation of venom rheological properties to spitting behaviour is unexpected.

In fact, if the principle is true, considering the lack of consistent differences in venom rheology between spitting and non-spitting cobras, and that venom spitting is an unambiguously defensive behaviour, it is interesting to question why selective pressures have not favoured the emergence of venom spitting in all cobras. A recent study investigating patterns of venom-induced pain across snake species and time has suggested that the common ancestor of all elapids might have possessed early-pain-inducing venom [423]. With the rapid infliction of pain being a requirement of defensive venoms [423], [424], this could indicate that the use of venom for defensive purposes appeared early in elapid evolution, before the evolution of spitting behaviour.

While a trend towards loss of rapidly painful venom is common in snakes [423], venom spitting, coupled with enhanced analgesic activity [401] could be an extension of this basic defensive strategy (i.e. injection of early-pain-inducing venom), which allows contactless defence at a distance, and of shorter duration and higher accuracy than striking/biting [380], [389], [425]. In this scenario, spitting behaviour is probably the evolutionary response to specific selective pressures. Exposure to agile vertebrates (including visually acute primates), as suggested by [401], likely attacking from an elevated position, and for which a defensive strategy involving striking/biting could be hazardous and/or ineffective, could have been one of the drivers of spitting behaviour evolution. It is therefore possible that spitting behaviour would not emerge in the absence of this kind of selective pressures, thus offering a conjecture for why not all cobra species are able to spit venom. Alternatively, the existence of yet unidentified constraints preventing the evolution of spitting in non-spitting species is not to be excluded a priori.

Spitting behaviour has been recently documented for two species of Asian cobras that are generally considered non-spitters and that display very limited modification of their fangs, namely *N. kaouthia* and *N. atra* [390], [402], [403]. These reports suggest that venom spitting can evolve in the presence of very limited adaptation of the dentition, without the greater level of morphological adaptation and precision documented for specialised spitters [196],

[121]. The reason why these species have not evolved the more specialised venom spitting apparatus that other species possess (e.g. *N. mossambica*, *N. nigricollis*, *N. pallida*), may be due to differences in selective pressures, as outlined above, or perhaps the more recent origin of spitting in Asian cobras [401]. In light of these findings, spitting behaviour in cobras should probably not be seen as a binary trait, but may vary continuously in prevalence among the species of the genus *Naja*.

Understanding the evolution, or lack of evolution, of specialised spitting behaviour and associated physical adaptations would likely require studying the efficacy and prevalence of spitting behaviour as a defence against natural predators, an under documented aspect in the literature on this adaptation. Although, perhaps surprisingly, our results did not show any clear adaptation of the rheological properties of venom to spitting behaviour, it was demonstrated that both spitting and non-spitting cobra venoms are Newtonian fluids over a biologically relevant shear rate range, in contrast to previous literature reports. In order to gain a more comprehensive understanding of the mechanics behind venom spitting in cobras, we suggest considering the continuous nature of the prevalence of spitting behaviour and spitting modes, fang morphology and parts of the cobra venom delivery system at play in venom spitting but not included in this study (e.g., m. adductor mandibulae externus superficialis). Furthermore, future studies should increase the sample size in terms of both venom samples, specimens and species, in order to more comprehensively address the remarkably high variability in viscosity detected in the present work. The results in this chapter will stimulate further comparative study of the rheology of venom spitting across the genus *Naja*.

CHAPTER 7: DIFFERENTIAL SCANNING CALORIMETRY OF ECTO-SECRETIONS

“A grain in the balance will determine which individual shall live and which shall die - which variety or species shall increase in number, and which shall decrease, or finally become extinct.” **Charles Darwin**



This chapter corresponds to the paper “Differential Scanning Calorimetry of Ecto-secretions”, to be submitted for publication to the journal *Soft Matter*.

ABSTRACT

Protein structure and function are important to understand ecto-secretions, materials produced by some animals to be used outside their bodies. These materials offer a great system to explore, as they span all ranges of functionality (from chemical to mechanical) and hydration state (wet to dry). However, to date there are no studies comparing thermal properties of different ecto-secretions. This presents a gap in our understanding surrounding how protein stability and the thermal events involved in denaturation are affected by glycosylation, hydration state and phenotype. To address this, this chapter presents the first study using Differential Scanning Calorimetry (DSC), to analyse three exemplar ecto-secretions: venom, mucus and silk. Gastropod locomotive mucus of six terrestrial gastropods was analysed; snake venom extracted from six species (one viper and five *Naja* species); and data previously reported on silkworm silk. The hypothesis is that protein thermostability is affected by the type of protein, presence of highly glycosylated proteins and main function (chemical or mechanical). Our results show that proteins in silk have the lowest thermal stability, while snake venom has the highest. The well documented presence of carbohydrate-binding proteins contributes substantially to the stability of proteins. Our study represents a novel route to provide new details into the relationship of protein type, presence of carbohydrates, hydration degree and primary function, with protein thermal stability. This information will provide more practical details to be considered in the use of ecto-secretions for biotechnological applications.

KEYWORDS: Ecto-secretion, globular protein, fibrous protein, enthalpy of denaturation, glass transition, carbohydrate-binding protein.

7.1 INTRODUCTION

Ecto secretions are produced by specialised glands in the animal, to be used outside their bodies for a wide variety of purposes, from mechanical (silk or gastropod locomotive mucus) to chemical (venoms) [1]–[4], [6], [7], [16], [8]–[15]. Due to their diversity, proteins in ecto-secretions have been under selection to perform in the wet (venom and mucus) and dry (silk) environments and have been subjected to a wide range of environmental stresses, such as mechanical or thermal. Thermal stress is known to denature proteins by removing the water shell, and this will affect protein's function. Ecto-secretions have specific optimisations to keep their properties unaltered over a certain range of temperature, maintaining their main function. For example, the high toxicity of snake venom and enzymatic activity [107], [108], [113], [150], [401], [426]–[428]; mucus' lubricant properties [34], [58]; or silk's high strength [429].

In this group of materials, silk is the most well-known and extensively characterised, studying the solidification mechanisms involved, comparing its denaturation enthalpy to albumin, finding that it is almost ten times lower [430]–[438]. However, the thermal characterisation of snake venom remains almost unexplored and a better knowledge of the thermal properties of snake venoms could offer information related to the presence of carbohydrate-binding proteins and their role in venom stability [152], [171]. In terms of gastropod mucus, to our knowledge, there is only one study analysing its thermal properties, where the main finding was the presence of calcium carbonate in locomotive mucus contributing to the formation of gels and fibres, which are important to maintain mucus' function as a lubricant [87].

Although, these studies propose answers to some questions regarding ecto-secretions' thermal properties, to date there are no reports comparing all of them, considering their protein type (globular or fibrous), hydration state and main function. These ecto-secretions present an immense variety of opportunities for technological applications, from super adhesives to drugs for chronic diseases in humans [95], [100], [102], [103], [193]–[195], [200]. To make this possible, a wider characterisation is necessary, because these ecto-secretions are a unique but still underexploited resource. The study of thermal properties of proteins in ecto-secretions is crucial to understand how these biomolecules interact with the

surrounding water, as well as the role of hydrogen bonding interactions to stabilise molecules [225], [227], [240], [243], [266], [359], [439]. Thus, during industrial processing of synthetic proteins, this information offers an enormous advantage to determine the region at which each component will be thermally stable, maintaining its function unaltered [215], [244], [312], [440] and the relationships between ecto-secretion's protein structure, stability and function.

To fill this gap in our knowledge, I propose that the mechanisms developed by nature to control protein stability in response to a thermal stress are related to the type of proteins, carbohydrate-binding proteins and phenotype. Here I hypothesize that an ecto-secretion that must perform in hydrated environments will be better at holding onto water and have a higher denaturation temperature. To test this, here I present the Differential Scanning Calorimetry (DSC) characterisation of three ecto-secretions as model systems: silkworm silk (data reported before on *B. mori*, *A. pernyi* and *N. edulis* [430]), snake venom (species *B. arietans*, and five *Naja* species, including spitters and non-spitters: *N. mossambica*, *N. annulifera*, *N. naja*, *N. philippinensis*, and *N. kaouthia*), and gastropod locomotive mucus (from species *A. fulica*, *C. aspersum*, *C. nemoralis*, *A. ater*, *A. hortensis* and *L. flavus*). I included egg white proteins [441] and trehalose for comparison purposes.

This analysis allowed us to identify that proteins selected for a chemical function and in a hydrated state, show a different response to thermal stress compared to those in the dry state, whose main function is mechanical. I could identify the main thermal events occurring in all samples (glass transition, aggregation and/or denaturation), establishing the minimum and maximum temperature limits. Enthalpies of denaturation were calculated and used as a parameter to determine the hydration state of the ecto-secretion. In addition, I compare denaturation enthalpy of globular proteins (gastropod mucus, conalbumin, ovalbumin and lysozyme), to that of fibrous proteins in silkworm silk. The integrated analysis described here, represents the first reported on ecto-secretions.

7.2 MATERIALS AND METHODS

7.2.1 MATERIALS

7.2.1.1 GASTROPOD MUCUS

Six terrestrial gastropods were included in this study: the three snails (*A. fulica*, *C. aspersum* and *C. nemoralis*), and three slugs (*A. ater*, *A. hortensis* and *L. flavus*). The five terrestrial gastropods native to the UK, were collected in Hillsborough Park, Hillsborough, Sheffield. The African snails, *A. fulica*, were purchased as juveniles and captive bred. All species were maintained in plastic containers (39 cm x 48 cm x 20 cm) with vermiculite as a substrate, with a thickness of approximately 6 cm. The temperature was controlled, at $22\text{ }^{\circ}\text{C} \pm 1\text{ }^{\circ}\text{C}$, and all containers were kept at high humidity. Animals were fed twice weekly with cucumber, lettuce and sweet potatoes.

Three specimens per species were removed from their containers and cleaned using type II water and placed into a clean and empty plastic container. Afterwards, gastropods were transferred and allowed to move freely across a clean sheet of glass for five minutes, to be sure that only locomotive mucus was deposited. This was then collected from the surface using two sterile razor blades and kept in a 2.0 ml polypropylene graduated centrifuge tube with cap, labelled, stored at room temperature and subjected to tests on the day of collection.

7.2.1.2 SNAKE VENOM

Venom samples were collected from six species: one viper, *B. arietans*; and five *Naja* species including spitters and non-spitters (*N. mossambica*, *N. annulifera*, *N. naja*, *N. philippinensis*, and *N. kaouthia*). All snakes were maintained in individual containers within controlled temperature, humidity and light at the Centre for Snakebite Research and Interventions, Liverpool School of Tropical Medicine (LSTM). Regarding to the protocols referring to the expert husbandry of the snakes, they are regularly inspected and approved by the UK Home Office and the LSTM Animal Welfare and Ethical Review Board. All native venoms were extracted by milking snakes and venoms were transferred from the Petri dish into 2 ml low-protein binding cryotubes (Simport Scientific, Beloeil, Canada) using a pipette. Samples were

kept on ice, and DSC tests were carried out in the Department of Materials Science and Engineering, University of Sheffield.

7.2.1.3 TREHALOSE SOLUTIONS

To compare the effect of carbohydrates and carbohydrate-binding proteins in ecto-secretions and how the presence of sugars can influence their thermal stability, a trehalose solution was prepared at room temperature.

This solution comprises 30 % trehalose dihydrate (Sigma-Aldrich, St. Louis, Missouri, USA), 60 % egg white and 10 vol % type II water. The solution and its percentages were selected based on: a) trehalose is a protein stabiliser [442], [443] b) egg-white and its proteins represent a standard and well-studied and accessible group of globular proteins, suitable for comparison [271], [441]; and c) percentages were selected based on snake venom solids concentration ranging between 25 to 30 %, and the rest water [444].

A free-range egg was dissected, the egg white was separated from the yolk and sample was taken from the centre of the bulk using a 1 ml plastic pipette and added into a 2 ml polypropylene microcentrifuge tube. Trehalose and type II water were weighed and added to the tube. Finally, the tube was then homogenised for 2 minutes using a Sprout mini centrifuge (Heathrow Scientific, Illinois, US) before performing the DSC tests.

7.2.2 Methods

7.2.2.1 DSC

DSC characterisation was carried out on a Diamond DSC instrument (Perkin-Elmer, USA). Heat-cool-heat DSC tests were performed from 25 to 80 °C at a heating/cooling rate of 1.5 °C/min., using Aluminum hermetically sealed pans (Perkin-Elmer, No. B016-9321) for both sample and reference. Due to the low protein concentration in gastropod mucus [49], the reference pan contained the same mass of type II water as the sample. For venoms and trehalose solutions, sample reference was an empty Aluminum hermetically sealed pan. Post-test, pinholes were made on pan lids and samples placed in a vacuum oven overnight at a

temperature of 60 °C. Mass was then measured and used for dry weights determinations. Using Pyris software v11 to identify peaks, denaturation enthalpies were determined considering the dry mass for each sample and peak area calculations corresponding to the endothermic heat flow were obtained using Origin software v2020.

Glass transition temperature, T_g , is characterised by a step in the baseline of the thermogram (a change of slope in the thermogram). Three important values can be identified in the thermogram: an onset, midpoint and endset temperature. In snake venoms and trehalose T_g 's were determined using Pyris software v11. This assumes that the crossover point between two tangents corresponds to T_g : one tangent is determined at the initial straight line representing the baseline; and the second tangent intersecting the slope.

7.3 RESULTS AND DISCUSSION

Tests were undertaken to identify the thermal events of proteins in gastropod locomotive mucus and snake venoms, such as denaturation or glass transition. Trehalose solutions were included in our tests, because it has been reported before that this sugar plays an important role in protein stabilisation, also protein-carbohydrate interactions contributes to increase thermal stability of proteins [445]. Egg white was included too, because it contains globular proteins, homologous to those found in snake venom. Egg white is a source of proteins that can also be obtained in a native state with minimal preparation [446].

7.3.1 PROTEIN DENATURATION IN GASTROPOD MUCUS AND SILK

Protein denaturation is an irreversible and endothermic process, where the peak maximum represents the temperature of the highest heat absorption and the integral of the endotherm gives us the denaturation enthalpy, important for the understanding of the process where proteins exhibit a change in their structure as a result of changes in its hydration sphere [430], [447]. The denaturation enthalpy is also related to the rupture of hydrogen bonds between proteins and water [225]. This process was observed in gastropod locomotive mucus and silk [430], as shown in Figure 7.1, indicating the peak maximum and denaturation enthalpies, including egg white proteins (conalbumin, lysozyme and ovalbumin) [441].

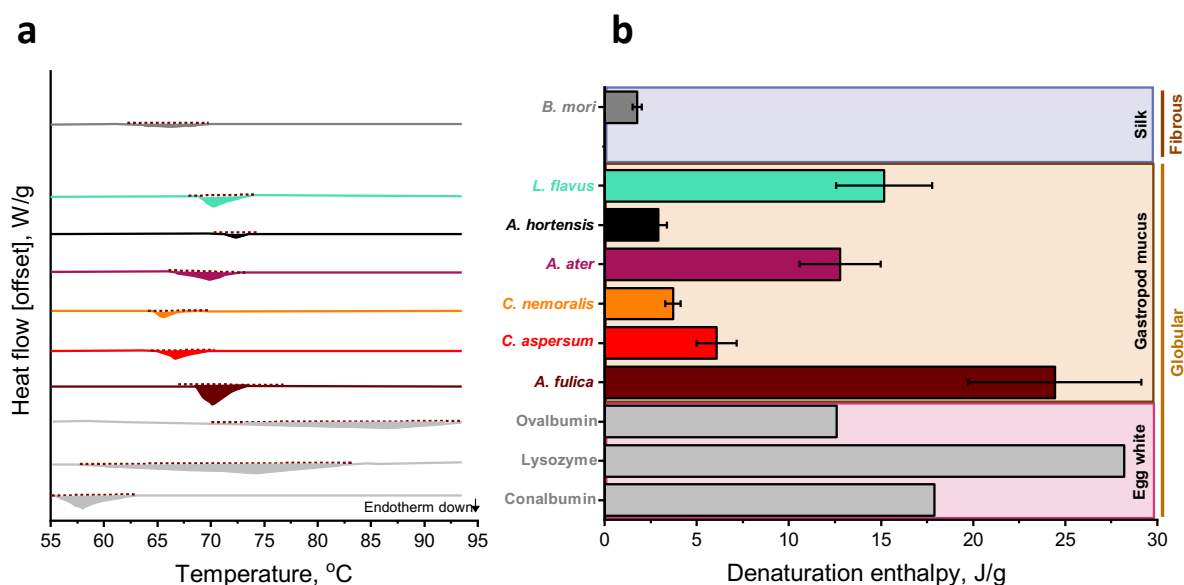


FIGURE 7.1 a) Peak maximum, and b) Denaturation enthalpies corresponding to mucus from *A. fulica*, *A. hortensis*, *A. ater*, *C. nemoralis*, *C. aspersum* and *L. flavus*. ^aValues corresponding to egg white proteins are included for comparison purposes [441]; and ^bnative silk feedstock [430]. Proteins are grouped as globular or fibrous. Standard deviation error bars for snails and slugs correspond to a series of three experiments per species. Areas under peaks are coloured to facilitate identification and comparison between species/components.

Our results indicate that *A. fulica* snail’s mucus has the highest denaturation enthalpy, 24.4 ± 4.7 J/g, compared to the other species tested, suggesting that mucus produced by this snail requires more energy to denature proteins than in the other species. This result can be associated to snail’s natural environment, with an annual average temperature between 23-30 °C, which is approximately 15°C higher than the annual temperature in the UK, of 14 °C [204]. It is also evident that denaturation enthalpy values of gastropod mucus are similar to those reported previously on egg white proteins [441], such as conalbumin (12.6 J/g), lysozyme (28.2 J/g) or ovalbumin (17.9 J/g), but higher compared to silk with a denaturation enthalpy of 1.7 J/g [430]. These thermal events in gastropod mucus, could be related to the high water content (> 98%) and to the hydrogen bonds connecting sugars to proteins [240], suggesting that the stabilisation of proteins in mucins occurs as a result of the interaction with sugar molecules.

Another crucial aspect in the analysis of these thermal variations is the type of proteins. Gastropod mucus’ proteins are globular while in silk they are fibrous. This difference plays a major role in the response of proteins to thermal stress and denaturation. During

denaturation process, protein secondary or tertiary structures are affected, modifying their conformation, in globular proteins the hydrophobic interactions stabilise their tertiary structure. When globular proteins are heated up, for entropy reasons, the hydrophobic side chains contribute to an expansion and partial unfolding of protein structures. Contrary to this, fibrous proteins, which are characterised by a single repetitive structural motif playing the main role of mechanical support [440], [448], are broken on heating. As a result, proteins will form unordered structures, such as random coils, losing their function [449].

This higher thermal stability of proteins in gastropod mucus, compared to silk, can also be linked to the highly glycosylated proteins in mucins. This indicates the presence of carbohydrates-binding proteins, as reported before, carbohydrate moieties prevent the aggregation of unfolded protein structures and contributes to increase the stabilisation of the glycoprotein [450]. For example, sugars have been used extensively as additives by scientists to protect the native structure of proteins as well as the enzymatic activity affected by thermal denaturation. Their findings suggest that carbohydrate binding proteins are possible due to a series of attractive forces, including hydrophilic and hydrophobic interactions [440], [448], [451]–[454].

There is another model proposed by Allison *et al.* [455], explaining why carbohydrates are important in maintaining protein thermal stability, which can be linked to the higher thermal resistance in gastropod mucus compared to silk. That model implies that water molecules eliminated during the drying phase of proteins, are replaced by carbohydrates contributing with hydrogen bonding due to the numerous hydroxyl groups (-OH) in saccharides and therefore, to the stability of proteins. This will prevent changes in protein secondary structures, more specifically, α -helices [451], [455], [456]. According to this model, the opposite interaction is also possible, i.e., proteins can substitute the eliminated water in dehydrated sugars. Actually, it has been studied that hydrogen bonds between proteins and saccharides have the same role as water in the hydrated sugar. This assumption suggests a two-way interaction between these molecules and how important it is on conferring carbohydrate-binding proteins their particular response to a thermal stress [456], [457].

Apart from these processes observed in globular and fibrous proteins, such as gastropod mucus and silk, there is another phenomenon identified in macromolecules and polymers, this is known as the glass transition.

7.3.2 GLASS TRANSITION IN SNAKE VENOMS AND TREHALOSE

Glass transition has been described before in proteins, carbohydrates, and mixtures. This characteristic process is only evident in snake venoms. Compared with trehalose solutions, it indicates that the identified glass transition, T_g , in all samples is in the same range as that observed in the trehalose solution. This representative comparison is evident in figure 7.2.

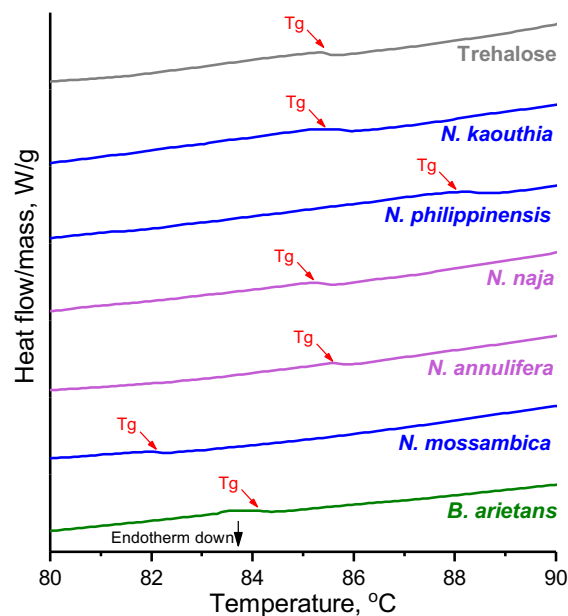


FIGURE 7.2 Representative thermograms of snake venom from the viper *B. arietans*, and cobras *N. mossambica*, *N. annulifera*, *N. naja*, *N. philippinensis* and *N. kaouthia*. Trehalose is included for comparison purposes. Glass transition temperature, T_g , is indicated.

Figure 7.2 shows the thermograms for each snake species and trehalose solution, with T_g highlighted. Note complete thermograms can be seen for all snakes and trehalose in Appendix A8, table A8.2. Contrary to gastropod mucus and silk, snake venoms and trehalose show a clear glass transition, a thermal transition where the material changes from a glassy to a rubbery state on heating [458], [459]. What is interesting here, is the fact that snake venoms

show similar Tg compared to trehalose, suggesting the same thermal response and the presence of a similar component in venoms. This result can be linked to snake venoms composition, because it consists of a mixture of several enzymes, each one of them with a specific function to preserve venom stability and toxicity [107], [108], [113], [150], [401], [426]–[428]. In this group of components, some of the main families identified correspond to C-type lectins, consisting of carbohydrate-binding proteins playing various physiological functions, such as blood coagulation [115], [167], [330], [334], [361]. In venoms analysed here, all of them contain these carbohydrate-binding proteins. According to [460], Tg of trehalose is 85 °C, which ties well with our results [461]. In another study, a protein/polysaccharide mixture, consisting of whey protein concentrate (WPC) and hydroxypropyl methylcellulose (HPMC), Tg was between 80 and 85 °C, for mixtures of 12% WPC and 2% HPMC [462]. This range of temperatures, again, agrees with our results.

Our findings suggest that there is a similar pattern in venoms and trehalose, as a result of heating, which indicates that sugars in snake venom are retarding and preventing denaturation [461]. For example, in one study, analysing the glass transition temperature of hydrolysed fish protein and the collapse in structure, results showed that sugars in the protein/sugar mixtures, reduced Tg, retarding the glass transition point [463].

It has been studied before that some of the effects conferred by trehalose include its ability to stabilize proteins and cell membranes, as well as reduction in protein aggregation. Also, trehalose is a unique molecule which reduces crystallisation of proteins and it is found in nature to protect biological systems in dry or extremely cold environments [445]. There is another study where trehalose solutions were tested in the stability of β -cell exosome-like vesicles (β -ELV), to evaluate functionality and stability of proteins. Their results demonstrated that trehalose reduces aggregation and maintains the integrity of ELV [445]. This is not the only mechanism of action, in fact, trehalose has a stronger interaction with proteins in the absence of water, where the hydrogen bonds are highly stable, based on the steric configuration and proteins' hydration state. This sugar also contributes with its relatively high Tg to the overall stability of the protein/sugar system [456], [464], [465].

In protein/sugar aqueous systems, the understanding of T_g is important in the design of biomaterials to be functional at certain conditions and parameters [462], [466]. Also, this knowledge is crucial in stability studies to establish the best storage condition for a dried protein product in the food industry [463], [467] and in proteomic characterisation of snake venoms, where the vast majority of studies include the use of lyophilized venom [133], [135], [141], [142], [156], [162], [169], [344], [358], [361], [468]–[472].

Snake venom is well-known for its high toxicity and complexity, but these properties are related to its main functions and uses by snakes in their natural environments, which are possible due to the stability of its proteins.

7.3.3 THERMAL TRANSITIONS

In order to compare the thermal transitions described above and identified in snake venom, gastropod mucus and silk, figure 7.3 shows the main thermal events (denaturation, crystallisation or glass transition) in proteins, including silk data reported before [430], egg white proteins for comparison purposes [441], and trehalose solution. See Appendix A8, figures A8.1 to A8.2 where thirteen thermograms are included: six gastropod species and six snakes; as well as trehalose solution.

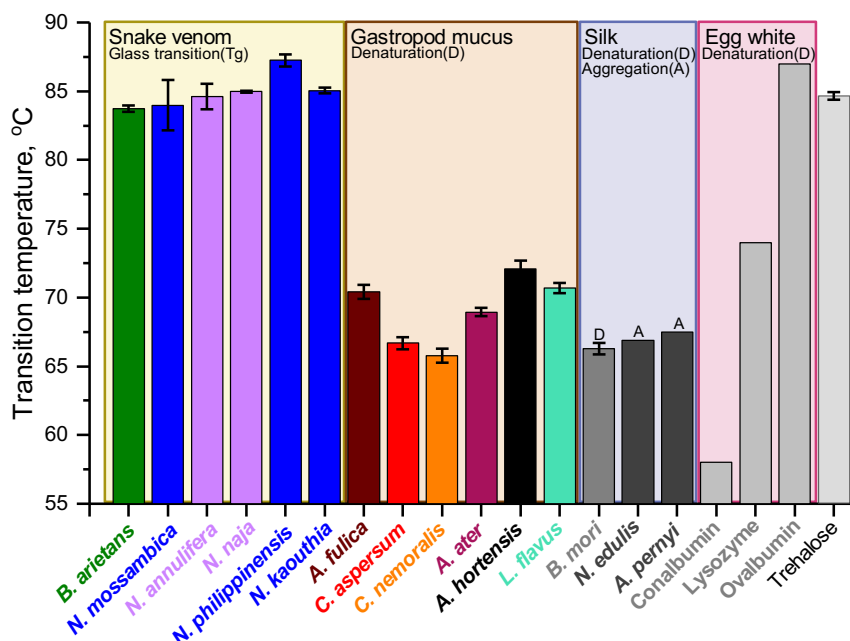


FIGURE 7.3 Transition temperatures associated to thermal events identified in snake venom (*B. arietans*, *N. mossambica*, *N. annulifera*, *N. naja*, *N. philippinensis* and *N. kaouthia*), gastropod mucus (*A. fulica*, *C. Aspersum*, *C. Nemoralis*, *A. ater*, *A. Hortensis* and *L. flavus*), silk (*B. mori*, *N. edulis* and *A. pernyi*) [430], egg white proteins (conalbumin, lysozyme and ovalbumin) [441], and trehalose. The main thermal events are indicated: denaturation (D), glass transition (Tg) and aggregation (A). Standard deviation error bars for gastropod mucus and snake venom correspond to a series of three experiments per species.

From figure 7.3, It is clear that the range at which these thermal processes occur is between 55 and 87 °C. Interestingly, proteins in gastropod mucus and silk exhibit denaturation. Snake venoms and trehalose display glass transition, in the range of temperatures tested and at which the vast majority of proteins are denatured, including egg white [473]–[475]. The highest and lowest values for denaturation temperatures correspond to ovalbumin and conalbumin, two proteins in egg white, with 86 and 55 °C, respectively. In the group of gastropods, the highest and lowest temperatures correspond to the slug *A. hortensis* (72.11 ± 0.43 °C) and land snail *C. nemoralis* (65.64 ± 0.45 °C), respectively. Appendix A8, tables A8.1 and A8.2, shows a summary of thermodynamic properties of gastropods locomotive mucus, snake venom and trehalose. Even when these species and proteins in their natural environments never experience temperatures above 40 °C, the understanding of protein stability as a response to a thermal stress is the basis for the comprehension of how the different components in these ecto-secretions interact with each other to keep the material

stable. Also, to know at which point these chemical structures lose their ability to maintain their function, resisting dehydration more than others [240], [265].

Protein structures and composition play important roles in conferring ecto-secretions their particular characteristics. It is important to know the thermal stability of them, since from a more focused view on the processing, development and application of ecto-secretions, it is crucial to establish the range of temperatures at which these materials maintain their properties and functions. With this information, proteins can be processed before they suffer an irreversible modification [430].




7.3.4 STABILITY OF ECTO-SECRETION' PROTEINS

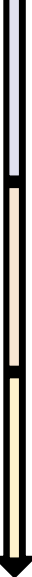
The three model ecto-secretions tested here (snake venom, gastropod mucus and silk) share common characteristics, for example, being produced by specialised glands in the animal for specific purposes, such as predation or protection. The mechanisms developed by nature to control protein hydration in response to thermal stress are related to the type of proteins, globular or fibrous. However, the composition varies between them, and more important, the specific function of each one is also unique. With this in mind, it is not a surprise to discover that their thermal stability is different, even when they contain globular or fibrous proteins and similar protein secondary structures (α -helices, β -sheets, β -turns, random coil or aggregated strands) [29], [36], [162], [243], [282], [292], [352], [476], [477]. Protein stability has different meanings, but in general, it can be described as the ability of a protein to maintain its structure and function in a particular environment [478].

For example, proteins isolated from hyperthermophilic organisms, species living in extreme environments, have a considerably less activity if tests are carried out at lower temperatures. At room temperature protein activity is almost zero, because these biomolecules have been adapted to temperatures close to the boiling point of water. Researchers have been investigating if this group of proteins exhibit a glass transition at higher temperatures compared to other proteins, to identify the main role of proteins at temperatures above 100 °C, and their thermal stability [479].

Thus, regarding to the three types of ecto-secretions studied here, thermal stability is a function of different parameters, such as type of protein, degree of hydration and presence of carbohydrate-binding proteins. Silkworm silk as a mechanical support material consisting mainly of fibrous proteins, is produced as a gel by the silkworm species, but the main function of this material is evident when it is dried. Contrary to gastropod locomotive mucus and snake venom, both containing globular proteins and produced and used as liquids/gels (wet) by the animal and functional at a hydrated state. Also, as it has been demonstrated before, gastropod mucus and snake venom contains carbohydrate-binding proteins [52], [90], [182], [272], [281], [452], [480], [481], which increase the thermal stability of proteins and as a result, ecto-secretion's functionality. For example, in one study on native and non-glycosylated proteins, results indicated that glycosylation increases protein conformational stability when samples are heated up [450]. In another study [482], researchers analysed the effect of glycosylation on the thermal stability of proteins. Their results showed that glycosylated enzymes in *S. cerevisiae*, a species of yeast, exhibit higher thermal stability compared to non-glycosylated enzymes in *E. coli*. Even more interesting, is the fact that their results also showed that glycosylated enzymes were thermally destabilized by carbohydrate elimination.

Although gastropod mucus and its mucins, and C-type lectins present in snake venom, both containing carbohydrate-binding proteins in their components, snake venom has another particular characteristic. This ecto-secretion is also a mixture of several enzymes, such as phospholipases A₂ (PLA₂) or metalloproteinases [108], [130], [168], [169], [361], [362], [470], [480], [483], [484]. This aspect makes another enormous difference comparing these two ecto-secretions as observed in figure 7.4, indicating that thermostability is not only affected by carbohydrates [479]. Even in a more complex protein system, such as snake venom, it may be advantageous to have sugars present that can stabilize any of the hundreds of proteins present, as a result of natural selection, to drive a strategy that can be applied to the entire material easily and allow for changes in the composition, maintaining venom's enzymatic activity, toxicity and stability [115], [131], [156], [168], [189], [485]–[487].

			Protein type	Glycosylation	External hydration state	Primary function
ECTO-SECRETIONS	SILK		Fibrous	Low	Dehydrated	Mechanical
	GASTROPOD MUCUS		Globular	High Mucins	Hydrated	Mechanical
	SNAKE VENOM		Globular	High C-type lectins	Hydrated	Chemical



 Protein thermal stability

 Max

FIGURE 7.4 Protein stability as a function of four different parameters: protein type, glycosylation, external hydration state and primary function.

As described in figure 7.4, the combination of these unique properties gives us the ecto-secretions' thermal stability: type of protein, presence of carbohydrates or glycosylation (carbohydrate-binding proteins), external hydration state (hydrated or dehydrated when the ecto-secretion is used by the animal), and primary function (mechanical or chemical). All of this makes sense by looking at the main function of each ecto-secretion. For example, gastropod locomotive mucus is used for lubrication [13], [34], [93], [488]; snake venom has been designed by nature for defence and predation [14], [331], [116]; and silk cocoon is used during the metamorphosis, to allow the larvae to be an adult moth [8], [24], [32]. The functional requirements for each one of these materials are specific and thermal stability is an indicator of how well proteins retain water. In line with this, the less thermally stable ecto-secretion is silk, because this ecto-secretions requires denaturation, so would have a lower thermal stability by association. This does not affect silk's functionality, because this material does not require high thermal stability, it requires a high mechanical strength. Contrary to this, snake venom, the highest thermal stable ecto-secretion in our group, do require a high stability and toxicity in order to be effective and active. Venom enzymatic activity has been

tested in samples at different pH and temperatures, showing that it has a wide range of activity before disappearing [139], [152], [164], [169], [335], [471], [489].

The understanding of the thermal properties and stability of these ecto-secretions help us to understand the range of temperatures at which they maintain their protein structures still active and playing their role as biomolecules, contributing to the design of novel biomaterials.

7.4 CONCLUSIONS

Ecto-secretions exhibit several adaptations in order to maintain their functions and this includes protein type and thermal stability. Functionality does not mean that thermal stability needs to be high, i.e., ecto-secretions main function. This can be observed in silk, a natural material with excellent mechanical properties, but with a denaturation enthalpy 14 times lower than the proteins in locomotive mucus of the African snail *A. fulica*. This indicates that the amount of water bonded in silk proteins is lower than in gastropod mucus. Each species uses its ecto-secretions for chemical or mechanical purposes and this could explain such differences in enthalpies and denaturation temperatures.

Opposite to these species, there are snakes with their complex and highly toxic venom, showing a high glass transition temperature, similar to trehalose. This suggests a retarding denaturation process in proteins, which can be linked to the presence of enzymes, high variety of proteins and a retarding carbohydrate agent present in their structure similar to the behaviour of trehalose, as a stabiliser when it is combined with proteins.

All these differences and observations may dictate major changes in protein structures (primary, secondary, tertiary or quaternary), which can be linked to their stability, and this study shows the first comparative study of thermal properties of three model ecto-secretions. The correlation of the different properties, such as compositional, mechanical and thermal, can offer a better understanding of natural materials, for biotechnological applications.

CHAPTER 8: Summary and Future Outlook

How many things have been denied one day,
only to become realities the next!”
Jules Verne



In this thesis, for the first time, ecto-secretions have been studied from a broad approach, characterising their compositional, thermal and mechanical properties to understand how these materials have adapted to maintain their chemical or mechanical function. As a Final Chapter, here I present five sections: Thesis Summary; Ecto-secretions' Structure-Hydration-Function relationships and Performance Map; Proposed Model Systems for each Ecto-secretion; Thesis Main Scientific Contributions; and Future Outlook.

8.1 THESIS SUMMARY

Each one of the results chapters (3 to 7) described the main contributions considering compositional, thermal and/or mechanical properties of the different ecto-secretions included in this study. In order to highlight the main results related to each system, Table 8.1 presents a summary of the main contributions.

TABLE 8.1. Summary of the main chapter’s contributions. See Appendix A9, Table A9, for a detailed list of collection and storage methods, properties measured, and characterisation techniques.

Chapter	3	4	5	6	7
Questions	Does mucus show molecular diversification and specialisation?	How do mucins influence mucus functionality?	Does venom show molecular diversification and specialisation?	Does snake venom viscosity influence the spitting behaviour of cobras?	What is the relationship between hydration and thermostability in ecto-secretions?
Ecto-secretion type	Native locomotive mucus	Native locomotive mucus	Native venom	Native venom	Native locomotive mucus/Native venom
System	<p><i>A. fulica</i> <i>C. aspersum</i> <i>C. nemoralis</i> <i>A. ater</i> <i>A. hortensis</i> <i>L. flavus</i> <i>L. maximus</i> <i>L. haroldi</i> <i>V. sloanei</i> <i>L. stagnalis</i> <i>M. cornuaretis</i> <i>P. diffusa</i></p>	<p><i>A. fulica</i> <i>C. aspersum</i> <i>C. nemoralis</i> <i>A. ater</i> <i>A. hortensis</i> <i>L. flavus</i></p>	<p><i>B. arietans</i> <i>H. haemachatus</i> <i>N. pallida</i> <i>N. nubiae</i> <i>N. mossambica</i> <i>N. nigricollis</i> <i>N. subfulva</i> <i>N. nivea</i> <i>N. haje</i> <i>N. annulifera</i> <i>N. naja</i> <i>N. siamensis</i> <i>N. philippinensis</i> <i>N. atra</i> <i>N. kaouthia</i></p>	<p><i>B. arietans</i> <i>H. haemachatus</i> <i>N. pallida</i> <i>N. nubiae</i> <i>N. mossambica</i> <i>N. nigricollis</i> <i>N. subfulva</i> <i>N. nivea</i> <i>N. haje</i> <i>N. annulifera</i> <i>N. naja</i> <i>N. siamensis</i> <i>N. philippinensis</i> <i>N. atra</i> <i>N. kaouthia</i></p>	<p><i>A. fulica</i> <i>C. aspersum</i> <i>C. nemoralis</i> <i>A. ater</i> <i>A. hortensis</i> <i>L. flavus</i> <i>B. arietans</i> <i>H. haemachatus</i> <i>N. pallida</i> <i>N. nubiae</i> <i>N. mossambica</i> <i>N. nigricollis</i> <i>N. subfulva</i> <i>N. nivea</i> <i>N. haje</i> <i>N. annulifera</i> <i>N. naja</i> <i>N. siamensis</i> <i>N. philippinensis</i> <i>N. atra</i> <i>N. kaouthia</i> <i>B. mori</i></p>
Properties measured	Compositional and thermal	Compositional, thermal and functional	Compositional and thermal	Compositional and functional	Thermal
Contributions	<p>- Locomotive mucus of terrestrial and freshwater species shows the presence of β structures linked to mucus’ properties. - Species can be accurately classified based on their FTIR spectra.</p>	<p>-Proteins in mucins have a major effect on the rheological properties of mucus. - Mucus’ functions as a lubricant, respond to their natural environment.</p>	<p>-Proteins in snake venom and their interaction with carbohydrates, contribute to the thermal stability, maintaining protein structures under thermal stress. - FTIR spectra provides enough information to classify species.</p>	<p>-Spitting and non-spitting cobra venoms are Newtonian fluids - Morphological adaptations of the venom delivery systems are the main factor on the spitting behaviour.</p>	<p>-Gastropod mucus and snake venom have higher thermostability, compared to silk. - Ecto-secretions’ thermostability is influenced by globular proteins and carbohydrate-binding proteins.</p>

8.2 ECTO-SECRETIONS' STRUCTURE-HYDRATION-FUNCTION RELATIONSHIPS, AND PERFORMANCE MAP

My results show that ecto-secretions' properties allow them to maintain their function under natural conditions. Table 8.2 shows the three groups of properties characterised in this thesis, including the main parameters associated with each one.

TABLE 8.2. Ecto-secretions' main parameters. Numbers indicate average values measured at room temperature. Snake venom values correspond to six snake species (*B. arietans*, *N. mossambica*, *N. annulifera*, *N. philippinensis*, *N. naja* and *N. kaouthia*); gastropod mucus refers to six species (*A. fulica*, *C. aspersum*, *C. nemoralis*, *A. ater*, *A. hortensis* and *L. flavus*); and silk feedstock correspond to one species (*B. mori*). Standard deviation values in snake venom and gastropod mucus represent three repeats per species. Protein secondary structures in silk were determined by Gaussian fitting (following the procedure described in Chapters 3 and 5) performed on FTIR data provided by Dr Pete R. Laity, Natural Materials Group, The University of Sheffield. He prepared the dry silk films and collected FTIR data.

Property	Parameter		Ecto-secretion		
			Snake venom	Gastropod mucus	Silk
Compositional	*Protein secondary structures, %	Aggregated strands	8.35 ± 2.82	8.23 ± 2.35	3.77 ± 0.44
		Random coil	18.62 ± 6.08	45.14 ± 11.49	56.59 ± 9.74
		α-helices	10.15 ± 2.19	9.11 ± 3.81	2.94 ± 0.41
		β-turns	2.60 ± 0.69	10.83 ± 2.60	24.73 ± 6.51
		β-sheet	60.26 ± 8.83	26.66 ± 5.51	11.82 ± 4.24
	Molecular weight, kDa	Min	10	41	24 [490]
		Max	240	377	440 [490]
Protein concentration, mg/ml		128.45 ± 18.30	0.49 ± 0.15	240 ± 25 [490]	
Thermal	Protein type		Globular	Globular	Fibrous
	Thermodynamics of proteins	Transition temperature, °C	85.18 ± 3.12	68.96 ± 2.50	66.26 ± 0.41 [430]
		Denaturation enthalpy, J/g	--	10.84 ± 3	1.77 ± 0.24 [430]
	Presence of highly glycosylated components		Yes, CLEC	Yes, mucins	Low
External hydration state		Wet	Wet	Dry	
Mechanical	Viscosity, Pa.s		**0.047 ± 0.026	21.05 ± 10.23	1757-2242 [491]

*Calculated from the amide I peak. **At 10, 000 s⁻¹, a relevant biological shear rate.

Interestingly, in chapters 3 to 7, it is evident that gastropod mucus and snake venom share a common molecular organisation and type of proteins, with variations in the percentages of protein secondary structures. For example, the presence of β -sheets was identified in gastropod mucus and snake venom. In mucus from the twelve species analysed here, β -sheets were observed in all species. These β -sheets in snake venoms are an important part of toxins' structure. The same structures have been reported before in silk, contributing to its remarkable mechanical properties [429]. Also, the presence of α -helices and random coil, contribute to proteins' thermostability, because the interactions between these two structures concentrate more energy in thermostable proteins [492]. As observed in gastropod mucus and snake venom, these structures are present in all species.

Protein concentration and molecular weight are other parameters contributing to the thermal and/or mechanical properties of ecto-secretions, because the apparent viscosity increases at higher concentrations and molecular weights [493].

As discussed in Chapter 7, the presence of carbohydrate-binding proteins and type of proteins in ecto-secretions are linked to a higher thermal stability. This was demonstrated in Chapters 3 and 5 that both, gastropod mucus and snake venom, show a higher content of glycosylated proteins compared to silk. However, some researchers are focusing their attention on modifying the silk gland protein, to glycoengineer the silkworm and produce a more stable N-glycan [494], to increase silk's thermostability [495].

Therefore, it was not a surprise to conclude that in terms of thermostability, silk is the less stable ecto-secretion. However, this property is again, correlated to ecto-secretion's main function: chemical or mechanical; and to its external hydration state: wet or dry.

Each one of these parameters represent a special piece conforming a map, where all of them are interconnected and have evolved to make these materials unique and functional, suitable to each environment. Figure 8.1 shows the Performance Map, indicating the relationship between most of the parameters included in table 8.2. Viscosity is plotted as a function of protein concentration. These two variables were selected from table 8.2, because a clear numerical variation is observed.

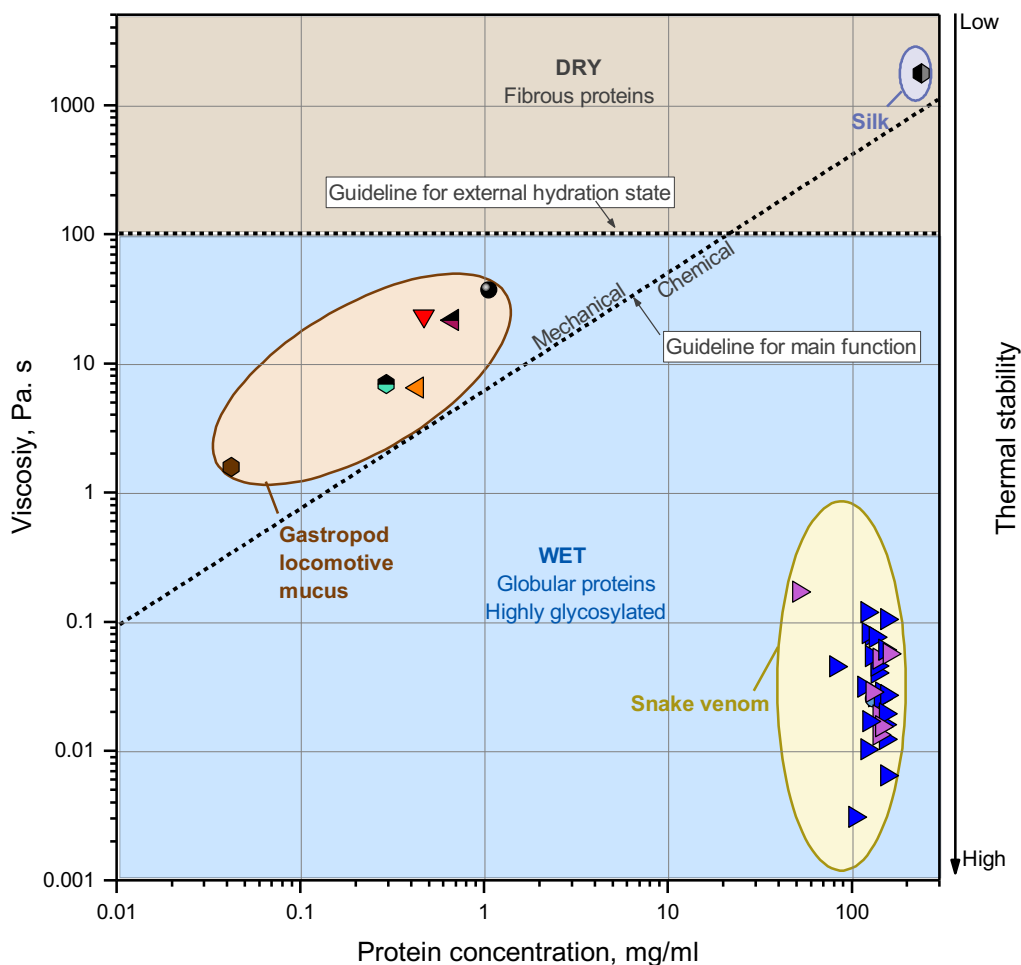


FIGURE 8.1 Ecto-secretions' Performance Map. Symbols represent each one of the species analysed in this thesis, grouped in three clusters: snake venom, gastropod locomotive mucus and silk. All clusters are representative of the species tested in this thesis. Two guidelines are included as a reference to identify the external hydration state and main function.

Snake venom and gastropod mucus are two ecto-secretions developed by nature to be functional as wet materials, contrary to silk. The only one ecto-secretion with a chemical function, due to their toxins, is snake venom. Figure 8.1 highlights these differences, including all species analysed here. It is proposed that this can be used as an Ecto-secretions' Property Chart, where depending on the type of protein, main function and hydration state, the user could identify the range for protein concentration, and the corresponding expected viscosity and thermal stability. This will be useful also in the short and long terms for the study and design of protein-based materials.

8.3. MODEL SYSTEMS

A Model System has been widely used in different scientific fields, to design specific and appropriate studies to understand more about biological systems. This Model System need to have specific characteristics, such as availability, cost, maintenance, etc. In order to select the most representative species for each one of the ecto-secretions described in this thesis, the following characteristics were considered:

- Availability: is the species easy to find? is the species widely distributed (found in different countries)?
- Ecto-secretion's production: yield from the animal (For example, in gastropods, time to produce mucus).
- Compositional, thermal and mechanical properties: based on my results, the median for each parameter was calculated, i.e., the middle values. The parameters considered were protein concentration, solids concentration, β -strands, random coil, denaturation enthalpies or glass transition temperature, and viscosity at 25 and 80 °C (for gastropod mucus), and viscosity at 10, 000 s^{-1} (for snake venoms at a biological relevant shear rate).

Figure 8.2, shows a list of species per both groups, highlighting the Model Systems.

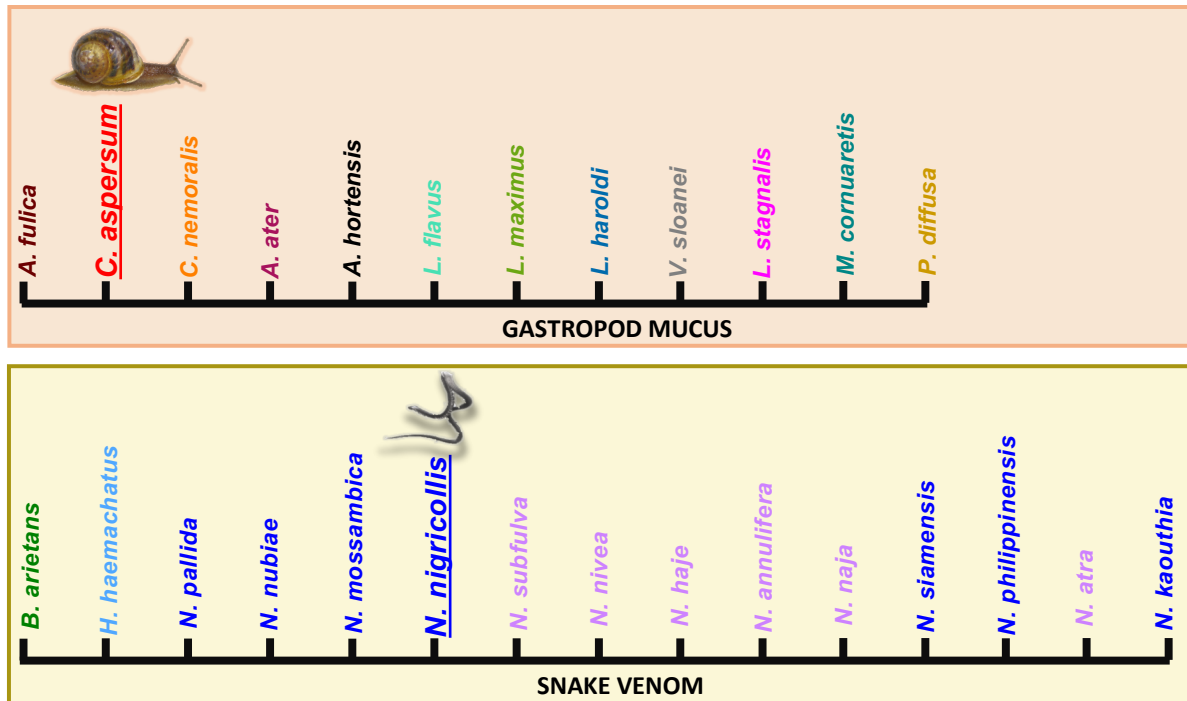


FIGURE 8.2 Model systems indicating the most representative species.

Based on the characteristics considered for Model’s selection, the most representative species are *C. aspersum* and *N. nigricollis*, corresponding to gastropods and snakes, respectively. It is important to mention that the African snail *A. fulica*, is widespread in different habitats with tropical and subtropical climates (including Italy, France, Spain and Portugal, in Europe) [496]. However, in terms of compositional, thermal and functional properties, this species is non representative.

Regarding to silkworm silk, the best well-known and understood species is *B. mori* and several studies included the mechanical and compositional characterisation of silk, while some others the thermal analysis of this ecto-secretion. This is not a native species, it is a domesticated one and it has been called a transgenic silkworm, ease to handle, low-cost, and high-yield [495]. For these reasons this species is included as a Model System.

8.4. THESIS IMPACT

The main conclusions of this thesis on how ecto-secretions are specialised animal adaptations, will hopefully make a significant contribution to the field and help establish this group of materials as one cohesive unit. Additionally, the integrated approach described here could have an important impact on the processing of biomaterials inspired by these ecto-secretions.

8.4.1 PLATFORM TO TEST ECTO-SECRETIONS

In this thesis, I developed the ability to test and compare ecto-secretions from a Materials Science perspective, to understand how these materials behave considering the structure-hydration-function relationship. This Platform (a set of properties, parameters and techniques) contributed to explain the most remarkable characteristics of these materials, such as their adaptability to cope with changes in temperature and hydration.

The correlation between the main observed parameters in the three categories of properties measured (compositional, thermal and mechanical/functional), represents the first comparative study between ecto-secretions. Through this analysis, I have elucidated the main role of proteins and how they are capable of giving ecto-secretions a vast diversity of thermal and mechanical properties.

8.4.2 ECTO-SECRETIONS' FTIR SPECTRA PROVIDE PHYLOGENETICAL INFORMATION

Gastropods and snakes are found in a wide variety of ecosystems, and species have morphological and structural adaptations, including variations in the compositional properties of their ecto-secretions.

FTIR spectra collected from native ecto-secretions, provided an enormous amount of information to be considered for detailed analyses. This information allowed me to determine the main protein secondary structures of proteins and for the first time, to classify gastropods and snakes using spectral features. The results provided data relevant to the phylogeny of

these species, representing a novel and important opportunity to study the variety of gastropods or snakes. Contrary to the highly cost and time-consuming methods considering proteomics, FTIR could be included as a reliable technique to help researchers to fill knowledge gaps on the understanding of species classification. Gastropod mucus responds to animal's natural environment, and it is not a surprise to discover that spectral features also vary based on these parameters. Snake venom also showed similar spectral characteristics in species sharing the same geographical location, behaviour or taxonomic family.

8.4.3 MUCINS IN GASTROPOD MUCUS SHOW AN ADAPTIVE RESPONSE TO THEIR NATURAL ENVIRONMENT

Mucins as the major components in gastropod mucus, show variations based on animal's natural environment. This group of highly glycosylated proteins confers locomotive mucus its unique properties as a lubricant, responding to a mechanical or thermal stress.

Species native from the UK showed a similar pattern when comparing their rheological properties at different temperatures, but not the African snail, *A. fulica*, because this species is native from tropical and subtropical climates with an annual temperature around 25.7 °C [496], [497]. Our findings showed that mucins in its mucus, have a different response when temperature is increased, i.e., contribute to a substantial reduction in mucus' dehydration and maintains its function unaltered almost 20 °C after the other species have undergone denaturation. By looking at the natural environment of both groups of species, it is clear that natural conditions have contributed to mucins response, trying to keep their properties unaffected when an increase in temperature is clear.

8.4.4 SNAKE VENOMS ARE NEWTONIAN FLUIDS

Previous studies analysing snake venoms in spitting and non-spitting species, concluded that this ecto-secretion was non-Newtonian, based on the observed shear-thinning behaviour [128], [126]. This assumption was valid based on the rheological data and also on theories assuming that in order to facilitate the spitting of venom, a higher viscosity would aid jet cohesion after venom ejection, maintaining the jet of venom from breaking up into droplets

for more time, improving spitting distance and accuracy by reducing physical forces [389], [421], [498], [499].

However, when calculating the torque effects of the rheometer, to determine the limits where a valid experimental window was acceptable, it was demonstrated that previous assumptions were based on artifacts. Even more interesting was the fact to compare our rheological data with a standard Newtonian fluid, water, and to identify surface tension effects at specific shear rates.

With these findings, then it was possible to define the valid experimental window corresponding to reliable data. We demonstrated that both spitting and non-spitting cobra venoms are Newtonian fluids over a biologically relevant shear rate range, in contrast to those previous reports. The spitting behaviour as it was wrongly assumed in previous studies, is not controlled by venom viscosity, but due to other physical or morphological factors.

8.4.5 SNAKE FANG'S MORPHOLOGICAL ADAPTATIONS CONTROL THE SPITTING BEHAVIOUR

If rheological properties of snake venom were not the main factor controlling spitting behaviour in cobra species, then there were other factors to be considered. In previous studies it has been stated that the venom delivery system of spitting cobras has specific morphological adaptations that enable them to eject their venom over several meters, and which is one of the main differences with non-spitting species. For example, the venom channel orifice in spitting species, has a more circular shape [129], [421], [498] and has internal ridges reducing the pressure loss [421].

All these adaptations were considered in our pressure differential calculations, using models in fluid mechanics, to derive our own equation to determine pressure loss in spitting and non-spitting species. Our findings demonstrated that fang morphology properties contribute substantially to pressure variation in the venom channel, making possible to eject venom, and the pressure loss is mainly due to the converging radius in the venom channel.

8.4.6 GLYCOSYLATION CONTRIBUTES TO THERMAL STABILITY OF PROTEINS

Glycosylation in gastropod mucus not only contributes to its mechanical properties, but also to its thermal stability. Also, the same protein modification in snake venom makes it highly thermally stable. (Chapters 3, 5 and 7).

The glycosylated proteins in these two ecto-secretions, higher compared to silk, are one of the factors influencing their higher thermal stability, compared to silk. This suggests that the external hydration state needed to maintain the ecto-secretion active is a crucial parameter to keep the hydration sphere or to substitute the reduction in water. When water molecules are eliminated from the molecule, carbohydrates can contribute to replace these molecules and then to increase the thermal stability of proteins.

Our findings corroborate this phenomenon and it was clear with the identified sugar residues in all gastropod mucus and snake venoms. The average values of denaturation enthalpies in gastropod mucus compared to silk were 10.84 J/g and 1.7 J/g, respectively, showing that mucus requires more energy for protein denaturation than proteins in silk.

8.5. FUTURE OUTLOOK

This thesis brings a novel study of ecto-secretions, considering the different properties that affect their function. However, this new approach also raises additional questions, which from my perspective, could be answer in future studies. Compositional, thermal and mechanical properties of gastropods were analysed. Marine species were not considered in this study due to external factors, such as availability, collection process, maintenance, etc. As a new direction, it would therefore be interesting to include species in the Littorinoidea family, because they have a particular behaviour: they can be found in the water or in rocks and cracks above the water surface [106], [500]. This would provide additional information to the performance of locomotive mucus in these snails and how it is affected by minerals and extreme environments. Additionally, FTIR characterisation on mucus from these species could be incorporated into the hierarchical discriminant analysis, to identify how close marine species in this family are to freshwater and terrestrial gastropods, based on spectral features.

The study of locomotive mucus as a lubricant offers enormous and valuable details to the comprehension of gastropods and this unique type of animal locomotion. Although, this thesis offers the first study incorporating different techniques to characterise this ecto-secretion, there is a second type of mucus which has promising applications in medicine: the adhesive. In previous reports it has been demonstrated that it has higher protein concentration and viscosity than locomotive mucus [49]. Thus, the characterisation of this type of mucus from some of the twelve gastropod species included in this thesis, to compare their compositional, thermal and rheological properties, would corroborate the assumption that protein structures, concentration and their interaction with sugar molecules have a direct impact on the thermal and mechanical properties of mucus. Additionally, extensional rheology tests on this particular mucus could be done to determine the tensile strength of mucus, to establish which species has the highest values, making it suitable as a good candidate for medical applications in super-adhesives [501], [95].

Another fascinating ecto-secretion is snake venom and in Chapter 6, we demonstrated that these ecto-secretions are Newtonian fluids, contrary to previous assumptions reported in the literature. This discovery has contributed substantially to this field, but there are no reports describing how the properties of venom change when it has been spat, i.e., when the material is outside of the fangs. Therefore, the incorporation of studies combining computational fluid dynamics (CFD) with surface tension and contact angle measurements in spitting and non-spitting cobra venom, could contribute with additional data to the understanding of the physical forces acting on the airborne jet.

Finally, the three types of ecto-secretions studied in this thesis, from my perspective are the most representative examples, but do not include all of them. Although, the promising applications in soft-robotics and medicine of these materials are enormous, the study of other ecto-secretions could expand our understanding of how different parameters, such as protein structures, glycosylation and hydration state, are correlated to the main function of the material (mechanical or chemical). Other ecto-secretions to be considered for future studies include saliva from molluscs, such as the octopus *O. vulgaris* [20], [18]; venom from the Gila monster *H. suspectum*, a venomous lizard native from Mexico and the United States [502],

[503]; mucus produced by the hagfish *E. goliath*, an eel-shaped marine fish [504]; or adhesive mucus produced by the Velvet worm *E. rowelli* [505].

REFERENCES

- [1] R. C. Lewontin, “The Units of Selection,” *Annu. Rev. Ecol. Syst.*, vol. 1, no. 1, pp. 1–18, 1970.
- [2] R. Dawkins, “Replicator Selection and the Extended Phenotype,” *Z. Tierpsychol.*, vol. 47, no. 1, pp. 61–76, 1978.
- [3] J. P. Bhanu, “Secretion machinery at the cell plasma membrane,” *Curr Opin Struct Biol.*, vol. 17, no. 4, pp. 437–443, 2007.
- [4] J. L. Ross, Y. M. Ali, and D. M. Warshaw, “Cargo Transport: Molecular Motors Navigate a Complex Cytoskeleton,” *Curr Opin Cell Biol.* 2008, vol. 20, no. 1, pp. 41–47, 2008.
- [5] G. Ponte and M. V. Modica, “Salivary glands in predatory mollusks: Evolutionary considerations,” *Front. Physiol.*, vol. 8, no. AUG, 2017.
- [6] J. A. González, F. Amich, S. Postigo-Mota, and J. R. Vallejo, “The use of wild vertebrates in contemporary Spanish ethnoveterinary medicine,” *J. Ethnopharmacol.*, vol. 191, pp. 135–151, 2016.
- [7] C. Holland, F. Vollrath, A. J. Ryan, and O. O. Mykhaylyk, “Silk and synthetic polymers: Reconciling 100 degrees of separation,” *Adv. Mater.*, vol. 24, no. 1, pp. 105–109, 2012.
- [8] A. A. Walker, C. Holland, and T. D. Sutherland, “More than one way to spin a crystallite: multiple trajectories through liquid crystallinity to solid silk,” *Proc. R. Soc. B Biol. Sci.*, vol. 282, pp. 1–9, 2015.
- [9] K. M. Jörger, I. Stöger, Y. Kano, H. Fukuda, T. Knebelsberger, and M. Schrödl, “On the origin of Acochlidia and other enigmatic euthyneuran gastropods, with implications for the systematics of Heterobranchia,” *BMC Evol. Biol.*, vol. 10, no. 1, pp. 1–20, 2010.
- [10] M. Iwamoto, D. Ueyama, and R. Kobayashi, “The advantage of mucus for adhesive locomotion in gastropods,” *J. Theor. Biol.*, vol. 353, pp. 133–141, 2014.
- [11] A. M. Smith, “The structure and function of adhesive gels from invertebrates,” *Integr. Comp. Biol.*, vol. 42, no. 6, pp. 1164–1171, 2002.
- [12] C. M. Wade, P. B. Mordan, and F. Naggs, “Evolutionary relationships among pulmonate land snails and slugs (Pulmonata. Stylommatophora),” *Biol. J. Linn. Soc.*, vol. 87, no. May, pp. 593–610, 2006.
- [13] G. M. Barker, *Gastropods on land: phylogeny, diversity and adaptive morphology.* 2009.
- [14] V. Suranse, A. Srikanthan, and K. Sunagar, “Animal Venoms: Origin, Diversity and Evolution,” *eLS. John Wiley Sons, Ltd Chichester*, pp. 1–20, 2018.
- [15] D. V. Tambourgi and C. W. van den Berg, “Animal venoms/toxins and the complement system,” *Mol. Immunol.*, vol. 61, pp. 153–162, 2014.
- [16] Y. N. Utkin, “Animal venom studies: Current benefits and future developments,” *World J. Biol. Chem.*, vol. 6, no. 2, pp. 28–33, 2015.
- [17] I. D. Mandel, “The Functions of Saliva,” *J. Dent. Res.*, vol. 66, pp. 623–627, Feb. 1987.
- [18] M. Nande, P. Presa, Á. Roura, P. L. R. Andrews, and M. Pérez, “Prey capture, ingestion, and digestion dynamics of *Octopus vulgaris* paralarvae fed live zooplankton,” *Front. Physiol.*, vol. 8, no. AUG, pp. 1–16, 2017.
- [19] F. Ghiretti, “Toxicity of Octopus Saliva Against Crustacea,” *Ann. N. Y. Acad. Sci.*, vol. 90, no. 3, pp. 726–741, 1960.
- [20] L. Cariello and L. Zanetti, “ α - and β -cephalotoxin: Two paralyzing proteins from posterior salivary glands of *Octopus vulgaris*,” *Comp. Biochem. Physiol. Part C*,

- Comp.*, vol. 57, no. 2, pp. 169–173, 1977.
- [21] C. Holland, A. E. Terry, D. Porter, and F. Vollrath, “Natural and unnatural silks,” *Polymer (Guildf.)*, vol. 48, no. 12, pp. 3388–3392, 2007.
- [22] C. Holland, D. Porter, and F. Vollrath, “Comparing the rheology of mulberry and ‘wild’ silkworm spinning dopes,” *Biopolymers*, 2012.
- [23] B. Kundu and S. C. Kundu, “Bio-inspired fabrication of fibroin cryogels from the muga silkworm *Antheraea assamensis* for liver tissue engineering,” *Biomed. Mater.*, vol. 8, no. 5, 2013.
- [24] Z. Dong *et al.*, “Analysis of proteome dynamics inside the silk gland lumen of *Bombyx mori*,” *Sci. Rep.*, vol. 6, no. April, pp. 1–10, 2016.
- [25] C. R. So *et al.*, “Sequence basis of Barnacle Cement Nanostructure is Defined by Proteins with Silk Homology,” *Sci. Rep.*, 2016.
- [26] X.-X. Xia, Z.-G. Qian, C. S. Ki, Y. H. Park, D. L. Kaplan, and S. Y. Lee, “Native-sized recombinant spider silk protein produced in metabolically engineered *Escherichia coli* results in a strong fiber,” *Proc. Natl. Acad. Sci.*, vol. 107, no. 32, pp. 14059–14063, 2010.
- [27] X.-X. Xia, Z.-G. Qian, C. S. Ki, Y. H. Park, D. L. Kaplan, and S. Y. Lee, “Native-sized recombinant spider silk protein produced in metabolically engineered *Escherichia coli* results in a strong fiber,” *Proc. Natl. Acad. Sci.*, 2010.
- [28] S. H. Lim, Y. T. Kim, S. P. Lee, I. J. Rhee, J. S. Lim, and B. H. Lim, *Sericulture training manual*. Food and Agriculture Organization of the United Nations, 1990.
- [29] W. Huang, S. Ling, C. Li, F. G. Omenetto, and D. L. Kaplan, “Silkworm silk-based materials and devices generated using bio-nanotechnology,” *Chem. Soc. Rev.*, vol. 47, no. 17, pp. 6486–6504, 2018.
- [30] C. J. Zhou, Y. Li, S. W. Yao, and J. H. He, “Silkworm-based silk fibers by electrospinning,” *Results Phys.*, vol. 15, no. September, pp. 1–5, 2019.
- [31] D. T. Pham and W. Tiyaboonchai, “Fibroin nanoparticles: a promising drug delivery system,” *Drug Deliv.*, vol. 27, no. 1, pp. 431–448, 2020.
- [32] R. I. Kunz, R. M. C. Brancalhão, L. D. F. C. Ribeiro, and M. R. M. Natali, “Silkworm Sericin: Properties and Biomedical Applications,” *Biomed Res. Int.*, vol. 2016, pp. 1–19, 2016.
- [33] J. Newar and A. Ghatak, “Studies on the Adhesive Property of Snail Adhesive Mucus,” *Langmuir*, vol. 31, no. 44, pp. 12155–12160, 2015.
- [34] R. H. Ewoldt, C. Clasen, A. E. Hosoi, and G. H. McKinley, “Rheological fingerprinting of gastropod pedal mucus and synthetic complex fluids for biomimicking adhesive locomotion,” *Soft Matter*, vol. 3, no. 5, pp. 634–643, 2007.
- [35] M. Struthers, G. Rosair, J. Buckman, and C. Viney, “The physical and chemical microstructure of the *Achatina fulica* epiphragm,” *J. Molluscan Stud.*, vol. 68, no. 2, pp. 165–171, 2002.
- [36] B. J. Lincoln, T. R. E. Simpson, and J. L. Keddie, “Water vapour sorption by the pedal mucus trail of a land snail,” *Colloids Surfaces B Biointerfaces*, vol. 33, no. 3–4, pp. 251–258, 2004.
- [37] S. Becker and H. Terlau, “Toxins from cone snails: Properties, applications and biotechnological production,” *Appl. Microbiol. Biotechnol.*, vol. 79, no. 1, pp. 1–9, 2008.
- [38] A. Ansart, P. A. Aulne, L. Madec, and P. Vernon, “Influence of temperature acclimation and gut content on the supercooling ability of the land snail *Cornu aspersum*,” *Comp. Biochem. Physiol. - A Mol. Integr. Physiol.*, vol. 150, no. 1, pp. 14–20, 2008.
- [39] A. Pereira, A. Rey, N. Uribe, and J. Castro, “Caracterización Físico-Química,” vol. 48,

- no. 2, 2016.
- [40] Y. S. Kim *et al.*, “A New Glycosaminoglycan from the Giant African Snail *Achatina fulica*,” *J. Biol. Chem.*, vol. 271, no. 20, pp. 11750–11755, 1996.
- [41] J. Liu, F. Shang, Z. Yang, M. Wu, and J. Zhao, “Structural analysis of a homogeneous polysaccharide from *Achatina fulica*,” *Int. J. Biol. Macromol.*, vol. 98, pp. 786–792, 2017.
- [42] S. G. Cabbiness *et al.*, “Polyamines in some tarantula venoms,” *Toxicon*, vol. 18, no. 5–6, pp. 681–683, 1980.
- [43] S. M. Mello, A. Linardi, A. L. Rennó, C. A. B. Tarsitano, E. M. Pereira, and S. Hyslop, “Renal kinetics of *Bothrops alternatus* (Urutu) snake venom in rats,” *Toxicon*, vol. 55, no. 2–3, pp. 470–480, 2010.
- [44] B. Joseph and J. George, “Scorpion toxins and its applications,” *Int. J. Toxicol. Pharmacol. Res.*, vol. 4, no. 3, pp. 57–61, 2012.
- [45] W. Danpaiboon *et al.*, *Ophiophagus hannah* venom: Proteome, components bound by *Naja kaouthia* antivenin and neutralization by n. *kaouthia* neurotoxin-specific human ScFv, vol. 6, no. 5. 2014.
- [46] I. R. Cohen and A. Marron, “The evolution of universal adaptations of life is driven by universal properties of matter: energy, entropy, and interaction,” *F1000Research*, vol. 9, no. 626, pp. 1–28, 2020.
- [47] A. Wanninger and T. Wollesen, “The evolution of molluscs,” *Biol. Rev.*, vol. 94, no. 1, pp. 102–115, 2019.
- [48] J. Moore, “Mollusca: general and Gastropoda,” in *Mollusca: General and Gastropoda. In An Introduction to the Invertebrates*, 2006, pp. 120–134.
- [49] A. M. Smith and M. C. Morin, “Biochemical differences between trail mucus and adhesive mucus from marsh periwinkle snails,” *Biol. Bull.*, vol. 203, no. 3, pp. 338–346, 2002.
- [50] S. K. . Lai and Y.-Y. W. D. W. J. Hanes, “Micro- and macrorheology of mucus Samuel,” *Adv Drug Deliv Rev*, vol. 61, no. 2, pp. 86–100, 2010.
- [51] G. Cilia and F. Fratini, “Antimicrobial properties of terrestrial snail and slug mucus,” *J. Complement. Integr. Med.*, vol. 0, no. 0, pp. 1–10, 2018.
- [52] J. M. Cottrell, I. F. Henderson, and D. J. Wright, “Studies on the glycosaminoglycan component of trail mucus from the terrestrial slug, *Arion ater* L.,” *Comp. Biochem. Physiol. -- Part B Biochem.*, vol. 107, no. 2, pp. 285–296, 1994.
- [53] W. J. Crozier and G. F. Pilz, “The locomotion of *Limax*. I. Temperature coefficient of pedal activity,” *J. Gen. Physiol.*, vol. 6, no. 6, pp. 711–721, Jul. 1924.
- [54] M. W. Denny and J. M. Gosline, “The physical-properties of the pedal mucus of the terrestrial slug, *Ariolimax-columbianus*,” *J. Exp. Biol.*, vol. 88, no. OCT, pp. 375–393, 1980.
- [55] I. Deyrup-Olsen, D. L. Luchtel, and a W. Martin, “Components of mucus of terrestrial slugs (Gastropoda).,” *Am. J. Physiol.*, vol. 245, no. 3, pp. R448–R452, 1983.
- [56] Denny, Mark W. and J. M. Gosline, “The Physical Properties of the Pedal Mucus of the Terrestrial Slug, *Ariolimax Columbianus*,” *J. Exp. Biol.*, vol. 88, no. 1, pp. 375–394, 1980.
- [57] M. W. Denny, “The role of gastropod pedal mucus in locomotion,” *Nature*, vol. 285, pp. 160–161, 1980.
- [58] M. W. Denny, “Mechanical properties of pedal mucus and their consequences for gastropod structure and performance,” *Integr. Comp. Biol.*, vol. 24, no. 1, pp. 23–36, 1984.
- [59] D. R. Skingsley, A. J. White, and A. Weston, “Analysis of Pulmonate Mucus By Infrared Spectroscopy,” *J. Molluscan Stud.*, vol. 66, no. 3, pp. 363–372, 2000.

- [60] S. W. Werneke, C. Swann, K. S. Hamilton, A. M. Smith, and L. A. Farquharson, “The role of metals in molluscan adhesive gels,” *J. Exp. Biol.*, vol. 210, no. 12, pp. 2137–2145, 2007.
- [61] A. M. Smith, T. M. Robinson, M. D. Salt, K. S. Hamilton, B. E. Silvia, and R. Blasiak., “Robust cross-links in molluscan adhesive gels: Testing for contributions from hydrophobic and electrostatic interactions,” *Comp Biochem Physiol B Biochem Mol Biol.*, vol. 152, no. 2, pp. 110–117, 2009.
- [62] J. M. Pawlicki, L. B. Pease, C. M. Pierce, T. P. Startz, Y. Zhang, and A. M. Smith, “The effect of molluscan glue proteins on gel mechanics,” *J. Exp. Biol.*, vol. 207, no. 7, pp. 1127–1135, 2004.
- [63] A. M. Wilks, S. R. Rabice, H. S. Garbacz, C. C. Harro, and A. M. Smith, “Double-network gels and the toughness of terrestrial slug glue,” *J. Exp. Biol.*, vol. 218, no. 19, pp. 3128–3137, 2015.
- [64] M. Braun, M. Menges, F. Opoku, and A. M. Smith, “The relative contribution of calcium, zinc and oxidation-based cross-links to the stiffness of *Arion subfuscus* glue,” *J. Exp. Biol.*, vol. 216, no. 8, pp. 1475–1483, 2013.
- [65] T. M. Fung, C. Gallego Lazo, and A. M. Smith, “Elasticity and energy dissipation in the double network hydrogel adhesive of the slug *Arion subfuscus*,” *Philosophical Transactions of the Royal Society B: Biological Sciences*, vol. 374, no. 1784, pp. 1–8, 2019.
- [66] W. F. Ponder, D. J. Colgan, J. M. Healy, N. Alexander, L. R. L. Simone, and E. E. Mielke, “Caenogastropoda,” in *Phylogeny and Evolution of the Mollusca*, no. June 2015, 2008, pp. 331–383.
- [67] N. M. Hallinan and D. R. Lindberg, “Comparative analysis of chromosome counts infers three paleopolyploidies in the mollusca,” *Genome Biol. Evol.*, vol. 3, no. 1, pp. 1150–1163, 2011.
- [68] C. M. Wade, P. B. Mordan, and B. Clarke, “A phylogeny of the land snails (Gastropoda: Pulmonata),” *Proc. R. Soc. B Biol. Sci.*, vol. 268, no. 1465, pp. 413–422, 2001.
- [69] D. R. Uit de Weerd and E. Gittenberger, “Phylogeny of the land snail family Clausiliidae (Gastropoda: Pulmonata),” *Mol. Phylogenet. Evol.*, vol. 67, no. 1, pp. 201–216, 2013.
- [70] V. S. Ayyagari and K. Sreerama, “Molecular phylogeny and evolution of Pulmonata (Mollusca: Gastropoda) on the basis of mitochondrial (16S, COI) and nuclear markers (18S, 28S): an overview,” *J. Genet.*, vol. 99, no. 1, 2020.
- [71] H. Wägele and A. Klussmann-Kolb, “Opisthobranchia (Mollusca, Gastropoda) - More than just slimy slugs. Shell reduction and its implications on defence and foraging,” *Front. Zool.*, vol. 2, pp. 1–18, 2005.
- [72] A. J. Saadi and C. M. Wade, “Resolving the basal divisions in the stylommatophoran land snails and slugs with special emphasis on the position of the Scolodontidae,” *Mol. Phylogenet. Evol.*, vol. 139, no. April, pp. 1–9, 2019.
- [73] Ö. Doğan, M. Schrödl, and Z. Chen, “The complete mitogenome of *Arion vulgaris* Moquin-Tandon, 1855 (Gastropoda: Stylommatophora): mitochondrial genome architecture, evolution and phylogenetic considerations within Stylommatophora,” *PeerJ*, vol. 8, pp. 1–30, 2020.
- [74] K. S. Zając *et al.*, “A comprehensive phylogeographic study of *Arion vulgaris* Moquin-Tandon, 1855 (Gastropoda: Pulmonata: Arionidae) in Europe,” *Org. Divers. Evol.*, vol. 20, no. 1, pp. 37–50, 2020.
- [75] G. L. Xie *et al.*, “A novel gene arrangement among the Stylommatophora by the complete mitochondrial genome of the terrestrial slug *Meghimatium bilineatum*

- (Gastropoda, Arionoidea),” *Mol. Phylogenet. Evol.*, vol. 135, no. March, pp. 177–184, 2019.
- [76] A. M. Smith, T. J. Quick, R. L. S. Peter, A. M. Smith, T. J. Quick, and R. L. S. T. Peter, “Differences in the Composition of Adhesive and Non-Adhesive Mucus From the Limpet *Lottia limatula*,” *Biol. Bull.*, vol. 196, no. 1, pp. 34–44, 1999.
- [77] M. S. Davies and A. M. Hatcher, “Limpet mucus as a depuration route and potential biomonitor,” *Ecotoxicology*, vol. 8, no. 3, pp. 177–187, Jun. 1999.
- [78] S. J. Hawkins, “Physical factors affecting the fate of pedal mucus produced by the common limpet *patella vulgata*,” *J. Mar. Biol. Assoc. United Kingdom*, vol. 72, no. 3, pp. 633–643, 1992.
- [79] F. Guo, Z. bin Huang, M. qin Huang, J. Zhao, and C. huan Ke, “Effects of small abalone, *Haliotis diversicolor*, pedal mucus on bacterial growth, attachment, biofilm formation and community structure,” *Aquaculture*, vol. 293, no. 1–2, pp. 35–41, 2009.
- [80] A. Klöppel, F. Brümmer, D. Schwabe, and G. Morlock, “Detection of Bioactive Compounds in the Mucus Nets of *Dendropoma maxima*, Sowerby 1825 (Prosobranch Gastropod Vermetidae, Mollusca),” *J. Mar. Biol.*, vol. 2013, pp. 1–9, 2013.
- [81] J. M. Pawlicki, L. B. Pease, C. M. Pierce, T. P. Startz, Y. Zhang, and A. M. Smith, “The effect of molluscan glue proteins on gel mechanics,” *J. Exp. Biol.*, vol. 207, no. 7, pp. 1127–1135, Mar. 2004.
- [82] M. S. Davies and S. J. Hutchinson, “Crystalline calcium in littorinid mucus trails,” *Hydrobiologia*, vol. 309, no. 1–3, pp. 117–121, 1995.
- [83] D. D. Bretz and R. V. Dimock, “Behaviorally important characteristics of the mucous trail of the marine gastropod *Ilyanassa Obsoleta*,” *J. Exp. Mar. Bio. Ecol.*, vol. 71, no. 2, pp. 181–191, 1983.
- [84] R. H. Ewoldt, A. E. Hosoi, and G. H. McKinley, “Nonlinear viscoelastic biomaterials: Meaningful characterization and engineering inspiration,” *Integr. Comp. Biol.*, vol. 49, no. 1, pp. 40–50, 2009.
- [85] A. O’Hanlon, C. D. Williams, and M. J. Gormally, “Terrestrial slugs (Mollusca: Gastropoda) share common anti-predator defence mechanisms but their expression differs among species,” *J. Zool.*, vol. 307, no. 3, pp. 203–214, 2019.
- [86] A. Sallam and N. El-Wakeil, “Biological and Ecological Studies on Land Snails and Their Control,” *Integr. Pest Manag. Pest Control - Curr. Futur. Tactics*, no. 1, 2012.
- [87] T. Zhong, L. Min, Z. Wang, F. Zhang, and B. Zuo, “Controlled self-assembly of glycoprotein complex in snail mucus from lubricating liquid to elastic fiber,” *RSC Adv.*, vol. 8, no. 25, pp. 13806–13812, 2018.
- [88] A. R. Toledo-Piza, E. Nakano, R. E. G. Rici, and D. A. Maria, “Proliferation of fibroblasts and endothelial cells is enhanced by treatment with *Phyllocaulis boraceiensis* mucus,” *Cell Prolif.*, vol. 46, no. 1, pp. 97–108, 2013.
- [89] J. Jaspe and S. J. Hagen, “Do protein molecules unfold in a simple shear flow?,” *Biophys. J.*, vol. 91, no. 9, pp. 3415–3424, 2006.
- [90] G. Petrou and T. Crouzier, “Mucins as multifunctional building blocks of biomaterials,” *Biomater. Sci.*, vol. 6, no. 9, pp. 2282–2297, 2018.
- [91] K. A. Dill, D. O. V. Alonso, and K. Hutchinson, “Thermal stabilities of globular proteins,” *Biochemistry*, no. 28, pp. 5439–5449, 1989.
- [92] J. Cabral-Oliveira, J. Pratas, S. Mendes, and M. A. Pardal, “Trace Elements in Edible Rocky Shore Species: Effect of Sewage Discharges and Human Health Risk Implications,” *Hum. Ecol. Risk Assess.*, vol. 21, no. 1, pp. 135–145, 2015.
- [93] S. Lee, J. W. M. Bush, A. E. Hosoi, and E. Lauga, “Crawling beneath the free surface: Water snail locomotion,” *Phys. Fluids*, vol. 20, no. 8, pp. 1–14, 2008.
- [94] D. Trivedi, C. D. Rahn, W. M. Kier, and I. D. Walker, “Soft robotics: Biological

- inspiration, state of the art, and future research,” *Appl. Bionics Biomech.*, vol. 5, no. 3, pp. 99–117, 2008.
- [95] A. D. Celiz *et al.*, “Tough adhesives for diverse wet surfaces,” *Science (80-.)*, vol. 357, pp. 378–381, 2017.
- [96] V. Gentili *et al.*, “HelixComplex snail mucus as a potential technology against O3 induced skin damage,” *PLoS One*, vol. 15, no. 2, pp. 1–13, 2020.
- [97] D. Tsoutsos, D. Kakagia, and K. Tamparopoulos, “The efficacy of Helix aspersa Müller extract in the healing of partial thickness burns: A novel treatment for open burn management protocols,” *J. Dermatolog. Treat.*, vol. 20, no. 4, pp. 219–222, 2009.
- [98] M. Watanabe and H. Tsukagoshi, “Soft sheet actuator generating traveling waves inspired by gastropod’s locomotion,” *Proc. - IEEE Int. Conf. Robot. Autom.*, pp. 602–607, 2017.
- [99] M. S. Davies and S. J. Hawkins, “Mucus from marine molluscs,” *Adv. Mar. Biol.*, vol. 34, no. 34, pp. 1–71, 1998.
- [100] J. Kim, D. W. Kim, S. Baik, G. W. Hwang, T. il Kim, and C. Pang, “Snail-Inspired Dry Adhesive with Embedded Microstructures for Enhancement of Energy Dissipation,” *Adv. Mater. Technol.*, vol. 4, no. 11, pp. 1–9, 2019.
- [101] A. Rey, N. Uribe, P. Ae, C. Jp, and U. N. Caracterizaci, “Actividad antimicrobiana de la lactoferrina:,” vol. 48, no. 2, 2016.
- [102] P. A. Vergara Gómez, “Universidad Austral de Chile Universidad Austral de Chile,” pp. 1–23, 2015.
- [103] J. K. Nguyen, N. Masub, and J. Jagdeo, “Bioactive ingredients in Korean cosmeceuticals: Trends and research evidence,” *J. Cosmet. Dermatol.*, vol. 19, no. 7, pp. 1555–1569, 2020.
- [104] J. Chan, F. T. Pan, and Z. Li, “Design and Motion Control of Biomimetic Soft Crawling Robot for GI Tract Inspection,” *Proc. World Congr. Intell. Control Autom.*, vol. 2018-July, pp. 1366–1369, 2019.
- [105] M. Rogóż, K. Dradrach, C. Xuan, and P. Wasylczyk, “A Millimeter-Scale Snail Robot Based on a Light-Powered Liquid Crystal Elastomer Continuous Actuator,” *Macromol. Rapid Commun.*, vol. 40, no. 16, pp. 1–5, 2019.
- [106] F. Baroudi, J. Al Alam, Z. Fajloun, and M. Millet, “Snail as sentinel organism for monitoring the environmental pollution; a review,” *Ecol. Indic.*, vol. 113, no. October 2019, p. 106240, 2020.
- [107] D. V. Tambourgi and C. W. van den Berg, “Animal venoms/toxins and the complement system,” *Mol. Immunol.*, vol. 61, no. 2, pp. 153–162, Oct. 2014.
- [108] N. R. Casewell, W. Wüster, F. J. Vonk, R. A. Harrison, and B. G. Fry, “Complex cocktails: The evolutionary novelty of venoms,” *Trends Ecol. Evol.*, vol. 28, no. 4, pp. 219–229, 2013.
- [109] B. Fry, “From genome to ‘venome’: molecular origin and evolution of the snake venom proteome inferred from phylogenetic analysis of toxin sequences and related body proteins,” *Genome research*, vol. 15, no. 3. pp. 403–420, 2005.
- [110] B. L. Dhananjaya, A. Nataraju, C. D. Raghavendra Gowda, B. K. Sharath, and C. J. M. D’Souza, “Vanillic acid as a novel specific inhibitor of snake venom 5'-nucleotidase: A pharmacological tool in evaluating the role of the enzyme in snake envenomation,” *Biochem.*, vol. 74, no. 12, pp. 1315–1319, 2009.
- [111] N. R. Casewell, T. N. W. Jackson, A. H. Laustsen, and K. Sunagar, “Causes and Consequences of Snake Venom Variation,” *Trends Pharmacol. Sci.*, vol. 41, no. 8, pp. 570–581, 2020.
- [112] S. Li *et al.*, “Proteomic characterization of two snake venoms: Naja naja atra and Agkistrodon halys,” *Biochem. J.*, vol. 384, no. 1, pp. 119–127, 2004.

- [113] C. M. Modahl, A. Roointan, J. Rogers, K. Currier, and S. P. Mackessy, “Interspecific and intraspecific venom enzymatic variation among cobras (*Naja* sp. and *Ophiophagus hannah*),” *Comp. Biochem. Physiol. Part - C Toxicol. Pharmacol.*, vol. 232, pp. 1–10, 2020.
- [114] J. P. Chippaux, V. Williams, and J. White, “Snake venom variability: methods of study, results and interpretation,” *Toxicon*, vol. 29, no. 11, pp. 1279–1303, 1991.
- [115] J. J. Calvete, L. Sanz, Y. Angulo, B. Lomonte, and J. M. Gutiérrez, “Venoms, venomomics, antivenomics,” *FEBS Lett.*, vol. 583, no. 11, pp. 1736–1743, 2009.
- [116] T. D. Kazandjian *et al.*, “Convergent Evolution of Pain-Inducing Defensive Venom Components in Spitting Cobras,” *Science (80-.)*, vol. 371, no. 6527, pp. 386–390, 2021.
- [117] Y. Zheng and J. J. Wiens, “Combining phylogenomic and supermatrix approaches, and a time-calibrated phylogeny for squamate reptiles (lizards and snakes) based on 52 genes and 4162 species,” *Mol. Phylogenet. Evol.*, vol. 94, pp. 537–547, 2016.
- [118] D. R. Goldman and A. W. Seefeld, “Ocular Toxicity Associated with Indirect Exposure to African Spitting Cobra Venom,” *WEM*, vol. 21, no. 2, pp. 134–136, 2010.
- [119] L. Chanhom, M. J. Cox, T. Vasaruchapong, N. Chaiyabutr, and V. Sitprija, “Characterization of venomous snakes of Thailand,” *Asian Biomed.*, vol. 5, no. 3, pp. 311–328, 2011.
- [120] G. Westhoff, M. Boetig, H. Bleckmann, and B. A. Young, “Target tracking during venom ‘spitting’ by cobras,” *J. Exp. Biol.*, vol. 213, pp. 1797–1802, 2010.
- [121] B. A. Young, K. Dunlap, K. Koenig, and M. Singer, “The buccal buckle : the functional morphology of venom spitting in cobras,” *J. Exp. Biol.*, vol. 207, pp. 3483–3494, 2004.
- [122] W. K. Hayes *et al.*, “Spitting versus Biting : Differential Venom Gland Contraction Regulates Venom Expenditure in the Black-Necked Spitting Cobra : *Naja nigricollis nigricollis*,” *J. Herpetol.*, vol. 42, no. 3, pp. 453–460, 2019.
- [123] B. A. Young and M. O’Shea, “Analyses of venom spitting in African cobras (Elapidae: Serpentes),” *African Zool.*, vol. 40, no. 1, pp. 71–76, 2005.
- [124] B. A. Young, M. Boetig, and G. Westhoff, “Functional bases of the spatial dispersal of venom during cobra ‘spitting’ .,” *Physiol. Biochem. Zool.*, vol. 82, no. 1, pp. 80–9, 2009.
- [125] S. Rasmussen, B. Young, and H. Krimm, “On the ‘spitting’ behaviour in cobras (Serpentes: Elapidae),” *J. Zool.*, vol. 237, no. 1, pp. 27–35, 1995.
- [126] M. Triep *et al.*, “3D Flow in the Venom Channel of a Spitting Cobra: Do the Ridges in the Fangs Act as Fluid Guide Vanes?,” *PLoS One*, vol. 8, no. 5, pp. 1–11, 2013.
- [127] A. Balmert, D. Hess, C. Brücker, H. Bleckmann, and G. Westhoff, “Spitting cobras: fluid jets in nature as models for technical applications,” *SPIE Smart Struct. Mater. + Nondestruct. Eval. Heal. Monit.*, vol. 7975, pp. 797514–797514–7, 2011.
- [128] B. A. Young, F. Herzog, P. Friedel, S. Rammensee, A. Bausch, and J. L. Van Hemmen, “Tears of venom: Hydrodynamics of reptilian envenomation,” *Phys. Rev. Lett.*, vol. 106, no. 19, pp. 1–4, 2011.
- [129] A. du Plessis, C. Broeckhoven, and S. G. le Roux, “Snake fangs: 3D morphological and mechanical analysis by microCT, simulation, and physical compression testing,” *Gigascience*, vol. 7, no. 1, pp. 1–8, 2018.
- [130] D. Das, N. Urs, V. Hiremath, B. S. Vishwanath, and R. Doley, “Biochemical and biological characterization of *Naja kaouthia* venom from North-East India and its neutralization by polyvalent antivenom,” *J. Venom Res.*, vol. 4, pp. 31–8, 2013.
- [131] R. J. Harris, C. N. Zdenek, D. Harrich, N. Frank, and B. G. Fry, “An appetite for destruction: Detecting prey-selective binding of α -neurotoxins in the venom of Afro-

- Asian elapids,” *Toxins (Basel)*, vol. 12, no. 3, pp. 1–12, 2020.
- [132] V. V. Ryabinin, R. H. Ziganshin, V. G. Starkov, V. I. Tsetlin, and Y. N. Utkin, “Intraspecific Variability in the Composition of the Venom from Monocled Cobra (*Naja kaouthia*),” *Russ. J. Bioorganic Chem.*, vol. 45, no. 2, pp. 107–121, 2019.
- [133] A. Deka, A. Gogoi, D. Das, J. Purkayastha, and R. Doley, “Proteomics of *Naja kaouthia* venom from North East India and assessment of Indian polyvalent antivenom by third generation antivenomics,” *J. Proteomics*, vol. 207, no. May, p. 103463, 2019.
- [134] R. S. Kornhauser, “A Pharmacological Characterisation of Cobra and Black Snake Venoms,” Monash University, 2015.
- [135] J. Cascardi, B. A. Young, H. D. Husic, and J. Sherma, “Protein variation in the venom spat by the red spitting cobra, *Naja pallida* (Reptilia : Serpentes),” *Toxicon*, vol. 37, pp. 1271–1279, 1999.
- [136] C. W. Vogel and H. J. Müller-Eberhard, “Cobra venom factor: Improved method for purification and biochemical characterization,” *J. Immunol. Methods*, vol. 73, no. 1, pp. 203–220, 1984.
- [137] H. Takahashi and K. Hayashi, “Purification and Characterization of Anticomplement Factor (Cobra Venom Factor) from the *Naja Naja Atra* Venom,” *Biochem. Biophys. Acta*, vol. 701, pp. 102–110, 1982.
- [138] Y. N. Utkin *et al.*, “First tryptophan-containing weak neurotoxin from cobra venom,” *Toxicon*, vol. 39, no. 7, pp. 921–927, 2001.
- [139] N. H. Tan and S. Swaminathan, “Purification and properties of the l-amino acid oxidase from monocellate cobra (*Naja naja kaouthia*) venom,” *Int. J. Biochem.*, vol. 24, no. 6, pp. 967–973, 1992.
- [140] A. Debnath *et al.*, “A lethal cardiotoxic-cytotoxic protein from the Indian monocellate cobra (*Naja kaouthia*) venom,” *Toxicon*, vol. 56, no. 4, pp. 569–579, 2010.
- [141] A. K. Mukherjee and C. R. Maity, “Biochemical composition, lethality and pathophysiology of venom from two cobras - *Naja naja* and *N. kaouthia*,” *Comp. Biochem. Physiol. - B Biochem. Mol. Biol.*, vol. 131, no. 2, pp. 125–132, 2002.
- [142] K. Kulkeaw, W. Chaicumpa, Y. Sakolvaree, P. Tongtawe, and P. Tapchaisri, “Proteome and immunome of the venom of the Thai cobra, *Naja kaouthia*,” *Toxicon*, vol. 49, no. 7, pp. 1026–1041, 2007.
- [143] C. C. Yang and L. S. Chang, “Role of the N-terminal region in phospholipases A2 from *Naja naja atra* (Taiwan cobra) and *Naja nigricollis* (spitting cobra) venoms,” *Toxicon*, vol. 26, no. 8, pp. 721–731, 1988.
- [144] Inn-Ho Tsai, Shih-Hsiung Wu, and Tung-Bin Lo, “Complete amino acid sequence of a phospholipase A2 from the venom of *Naja naja atra* (Taiwan cobra),” *Toxicon*, vol. 19, no. 1, pp. 141–152, 1981.
- [145] C. C. Yang, K. King, and T. . Sun, “Chemical Modification of Lysine and Histidine Residues in Phospholipase A2 from the Venom of *Naja Naja Atra* (Taiwan Cobra),” *Toxicon*, vol. 19, no. 5, pp. 645–659, 1981.
- [146] C. M. Teng, Y. P. Kuo, L. G. Lee, and C. Ouyang, “Characterization of the anticoagulants from taiwan cobra (*Naja naja atra*) snake venom,” *Toxicon*, vol. 25, no. 2, pp. 201–210, 1987.
- [147] A. H. Wang and C. . Yang, “Crystallographic Studies of Snake Venom Proteins from Taiwan Cobra (*Naja naja atra*),” *J. Biol. Chem.*, vol. 256, no. 17, pp. 9279–9282, 1981.
- [148] H. W. Huang *et al.*, “Cobra venom proteome and glycome determined from individual snakes of *Naja atra* reveal medically important dynamic range and systematic geographic variation,” *J. Proteomics*, vol. 128, pp. 92–104, 2015.
- [149] M. J. Klowden, A. J. Vitale, M. J. Trumble, C. R. Wesson, and W. R. Trumble, “A

- bioassay for cobra cardiotoxin activity using semi-isolated cockroach heart,” *Toxicon*, vol. 30, no. 3, pp. 295–301, 1992.
- [150] K. A. Vyas, H. V. Patel, A. A. Vyas, and W. G. Wu, “Glycosaminoglycans bind to homologous cardiotoxins with different specificity,” *Biochemistry*, vol. 37, no. 13, pp. 4527–4534, 1998.
- [151] R. J. Harris, C. N. Zdenek, A. Nouwens, C. Sweeney, N. Dunstan, and B. G. Fry, “A symmetry or asymmetry: Functional and compositional comparison of venom from the left and right glands of the Indochinese spitting cobra (*Naja siamensis*),” *Toxicon X*, vol. 7, p. 100050, 2020.
- [152] D. V. Binh, T. T. Thanh, and P. V. Chi, “Proteomic characterization of the thermostable toxins from *naja naja* venom,” *J. Venom. Anim. Toxins Incl. Trop. Dis.*, vol. 16, no. 4, pp. 631–638, 2010.
- [153] M. Ismail, M. H. M. Aly, M. A. Abd-Elsalam, and A. M. Morad, “A three-compartment open pharmacokinetic model can explain variable toxicities of cobra venoms and their alpha toxins,” *Toxicon*, vol. 34, no. 9, pp. 1011–1026, 1996.
- [154] M. Ismail, A. M. Al-Bekairi, A. M. El-Bedaiwy, and M. A. Abd-El Salam, “The ocular effects of spitting cobras: II. Evidence that cardiotoxins are responsible for the corneal opacification syndrome,” *Clin. Toxicol.*, vol. 31, no. 1, pp. 45–62, 1993.
- [155] D. Iddon, R. D. G. Theakston, and C. L. Ownby, “A study of the pathogenesis of local skin necrosis induced by *Naja nigricollis* (spitting cobra) venom using simple histological staining techniques,” *Toxicon*, vol. 25, no. 6, pp. 665–672, 1987.
- [156] C. C. Yang, K. King, and T. P. Sun, “Carbamylation with cyanate of basic phospholipase A2 from the venom of *Naja nigricollis* (Spitting cobra),” *Toxicon*, vol. 19, no. 6, pp. 783–795, 1981.
- [157] D. Petras *et al.*, “Snake venomics of African spitting cobras: Toxin composition and assessment of congeneric cross-reactivity of the Pan-African EchiTAb-Plus-ICP antivenom by antivenomics and neutralization approaches,” *J. Proteome Res.*, vol. 10, no. 3, pp. 1266–1280, 2011.
- [158] O. Katali *et al.*, “Protein Identification of Venoms of the African Spitting Cobras, *Naja mossambica* and *Naja nigricincta nigricincta*,” *Toxins (Basel)*, vol. 12, no. 8, pp. 1–11, 2020.
- [159] J. Grüntzig, W. Lenz, B. Berkemeier, and D. Mebs, “Experimental studies on the spitting cobra ophthalmia (*Naja nigricollis*),” *Graefes Arch Clin Exp Ophthalmol*, vol. 223, pp. 196–201, 1985.
- [160] R. M. Kini and H. J. Evans, “Mechanism of platelet effects of cardiotoxins from *Naja nigricollis* *crawshawii* (spitting cobra) snake venom,” *Thromb. Res.*, vol. 52, no. 3, pp. 185–195, 1988.
- [161] H. J. Evans, R. Franson, G. D. Qureshi, and W. F. Moo-penn, “Isolation of Anticoagulant Proteins from Cobra Venom,” *J. Biol. Chem.*, vol. 255, no. 8, pp. 3793–3797, 1980.
- [162] A. M. Torres, H. Y. Wong, M. Desai, S. Mochhala, P. W. Kuchel, and R. M. Kini, “Identification of a novel family of proteins in snake venoms. Purification and structural characterization of nawaprin from *Naja nigricollis* snake venom,” *J. Biol. Chem.*, vol. 278, no. 41, pp. 40097–40104, 2003.
- [163] C. M. Ward, D. V. Vinogradov, R. K. Andrews, and M. C. Berndt, “Characterization of mocarhagin, a cobra. Venom metalloproteinase from *Naja mocambique* *mocambique*, and related proteins from other elapidae venoms,” *Toxicon*, vol. 34, no. 10, pp. 1203–1206, 1996.
- [164] A. Sánchez *et al.*, “Proteomic and toxinological characterization of the venom of the South African Ringhals cobra *Hemachatus haemachatus*,” *J. Proteomics*, vol. 181, pp.

- 104–117, 2018.
- [165] R. L. J. Graham, S. McClean, E. J. O’Kane, D. Theakston, and C. Shaw, “Adenosine in the venoms from viperinae snakes of the genus *Bitis*: Identification and quantitation using LC/MS and CE/MS,” *Biochem. Biophys. Res. Commun.*, vol. 333, no. 1, pp. 88–94, 2005.
- [166] D. Paixão-Cavalcante, A. K. Kuniyoshi, F. C. V. Portaro, W. D. da Silva, and D. V. Tambourgi, “African Adders: Partial Characterization of Snake Venoms from Three *Bitis* Species of Medical Importance and Their Neutralization by Experimental Equine Antivenoms,” *PLoS Negl. Trop. Dis.*, vol. 9, no. 2, pp. 1–18, 2015.
- [167] C. R. Wang, E. R. Bubner, B. Jovcevski, P. Mittal, and T. L. Pukala, “Interrogating the higher order structures of snake venom proteins using an integrated mass spectrometric approach,” *J. Proteomics*, vol. 216, pp. 1–9, 2020.
- [168] J. J. Calvete, J. Escolano, and L. Sanz, “Snake venomomics of *Bitis* species reveals large intragenus venom toxin composition variation: Application to taxonomy of congeneric taxa,” *J. Proteome Res.*, vol. 6, no. 7, pp. 2732–2745, 2007.
- [169] S. N. C. Gimenes *et al.*, “Isolation and biochemical characterization of a γ -type phospholipase A2 inhibitor from *Crotalus durissus collilineatus* snake serum,” *Toxicon*, vol. 81, pp. 58–66, 2014.
- [170] S. N. C. Gimenes *et al.*, “Biochemical and functional characterization of a new recombinant phospholipase A2 inhibitor from *Crotalus durissus collilineatus* snake serum,” *Int. J. Biol. Macromol.*, vol. 164, pp. 1545–1553, 2020.
- [171] K. C. Oliveira, P. J. Spencer, R. S. Ferreira, and N. Nascimento, “New insights into the structural characteristics of irradiated crotamine,” *J. Venom. Anim. Toxins Incl. Trop. Dis.*, vol. 21, no. 1, pp. 1–10, 2015.
- [172] J. M. Gutiérrez, J. J. Calvete, A. G. Habib, R. A. Harrison, D. J. Williams, and D. A. Warrell, “Snakebite envenoming,” *Nat. Rev. Dis. Prim.*, vol. 3, p. 17063, 2017.
- [173] B. R. Blais, T. A. Sprague, and K. Uchida, “Commonly uncommon: *Gila* Monster (*Heloderma suspectum*) nocturnal activity at Sabino Canyon Recreation Area,” *Son. Herpetol.*, vol. 30, no. 4, pp. 70–71, 2017.
- [174] K. W. Sanggaard *et al.*, “Characterization of the gila monster (*Heloderma suspectum suspectum*) venom proteome,” *Data Br.*, vol. 3, pp. 137–142, 2015.
- [175] M. Hoshino *et al.*, “Primary structure of helodermin, a VIP-secretin-like peptide isolated from *Gila* monster venom,” *FEBS Lett.*, vol. 178, no. 2, pp. 233–239, 1984.
- [176] P. L. Alves, F. M. F. Abdalla, R. F. Alponi, and P. F. Silveira, “Anti-obesogenic and hypolipidemic effects of a glucagon-like peptide-1 receptor agonist derived from the saliva of the *Gila* monster,” *Toxicon*, vol. 135, pp. 1–11, 2017.
- [177] F. Pérez-Miles *et al.*, “*Ami*, a new Theraphosid genus from Central and South America, with the description of six new species (Araneae: Mygalomorphae),” *Zootaxa*, vol. 68, no. 1915, pp. 54–68, 2008.
- [178] G. G. Chicchi, G. Gimenez-Callego, E. Ber, M. L. Garcia, R. Winquist, and M. A. Cascieri, “Purification and characterization of a unique, potent inhibitor of apamin binding from *Leiurus quinquestriatus hebraeus* venom,” *J. Biol. Chem.*, vol. 263, no. 21, pp. 10192–10197, 1988.
- [179] P. T. Shah *et al.*, “Scorpion venom: A poison or a medicine-mini review,” *Indian J. Geo-Marine Sci.*, vol. 47, no. 4, pp. 773–778, 2018.
- [180] T. J. Hauke and V. Herzig, “Dangerous arachnids—Fake news or reality?,” *Toxicon*, vol. 138, pp. 173–183, 2017.
- [181] N. N. Kvitko and D. B. Vasil, “Effect of Native Venom of Red Cobra (*Najapallida*) on Morphological and Rheological Properties of Erythrocytes,” *Bull. Exp. Biol. Med.*, vol. 120, no. 10, pp. 1055–1057, 1995.

- [182] P. Bhattacharjee and D. Bhattacharyya, "Therapeutic use of snake venom components: A voyage from ancient to modern India," *Mini. Rev. Org. Chem.*, vol. 11, no. 1, pp. 45–54, 2014.
- [183] R. S. Cherki, E. Kolb, Y. Langut, L. Tsveyer, N. Bajayo, and A. Meir, "Two tarantula venom peptides as potent and differential NaV channels blockers," *Toxicon*, vol. 77, pp. 58–67, 2014.
- [184] A. L. Copley, S. Banerjee, and A. Devi, "Studies of snake venoms on blood coagulation I. The thromboserpentin (thrombin-like) enzyme in the venoms," *Thromb. Res.*, vol. 2, no. 6, pp. 487–508, 1973.
- [185] K. C. Cardoso *et al.*, "A transcriptomic analysis of gene expression in the venom gland of the snake *Bothrops alternatus* (urutu)," *BMC Genomics*, vol. 11, no. 1, pp. 9–12, 2010.
- [186] S. Hart, "Cone snail toxins take off," *Bio Sci.*, vol. 47, no. 3, pp. 131–134, 1997.
- [187] B. M. Olivera *et al.*, "Peptide neurotoxins from fish-hunting cone snails," *Science (New York, N.Y.)*, vol. 230, no. 4732, pp. 1338–43, 1985.
- [188] B. Pajovic, M. Radosavljevic, M. Radunovic, N. Radojevic, and B. Bjelogric, "Arthropods and their products as aphrodisiacs--review of literature.," *Eur. Rev. Med. Pharmacol. Sci.*, vol. 16, no. 4, pp. 539–47, 2012.
- [189] J. White, "Snake venoms and coagulopathy," *Toxicon*, vol. 45, no. 8, pp. 951–967, 2005.
- [190] J. Pai-dhungat, "Gila Monster Lizard & Incretin-mimetics," vol. 65, no. April, p. 2017, 2017.
- [191] E. R. Chu, S. A. Weinstein, J. White, and D. A. Warrell, "Venom ophthalmia caused by venoms of spitting elapid and other snakes: Report of ten cases with review of epidemiology, clinical features, pathophysiology and management," *Toxicon*, vol. 56, no. 3, pp. 259–272, 2010.
- [192] S. Malbranque *et al.*, "Case report: Fatal diffuse thrombotic microangiopathy after a bite by the 'Fer-de-Lance' pit viper (*Bothrops lanceolatus*) of Martinique," *Am. J. Trop. Med. Hyg.*, vol. 78, no. 6, pp. 856–861, 2008.
- [193] P. Bhattacharjee and D. Bhattacharyya, "Factor V activator from *Daboia russelli russelli* venom destabilizes β -amyloid aggregate, the hallmark of Alzheimer disease," *J. Biol. Chem.*, vol. 288, no. 42, pp. 30559–30570, 2013.
- [194] C. Pérez-Peinado, S. Defaus, and D. Andreu, "Hitchhiking with nature: Snake venom peptides to fight cancer and superbugs," *Toxins (Basel)*, vol. 12, no. 4, pp. 1–23, 2020.
- [195] R. M. Kini and C. Y. Koh, "Snake venom three-finger toxins and their potential in drug development targeting cardiovascular diseases," *Biochem. Pharmacol.*, pp. 1–10, 2020.
- [196] M. Triep *et al.*, "3D Flow in the Venom Channel of a Spitting Cobra: Do the Ridges in the Fangs Act as Fluid Guide Vanes?," *PLoS One*, vol. 8, no. 5, 2013.
- [197] H. A. Pearson and C. Peers, "Physiological roles for amyloid β peptides," *J. Physiol.*, vol. 575, no. 1, pp. 5–10, 2006.
- [198] WHO, "Cancer Fact Sheets," 2018. [Online]. Available: <https://www.who.int/news-room/fact-sheets/detail/cancer>. [Accessed: 09-Sep-2020].
- [199] M. S. Nobile *et al.*, "Fuzzy modeling and global optimization to predict novel therapeutic targets in cancer cells," *Bioinformatics*, vol. 36, no. 7, pp. 2181–2188, 2020.
- [200] C. B. Falcao and G. Radis-Baptista, "Crotamine and crotalicidin, membrane active peptides from *Crotalus durissus terrificus* rattlesnake venom, and their structurally-minimized fragments for applications in medicine and biotechnology," *Peptides*, vol. 126, no. October 2019, p. 170234, 2020.

- [201] WHO, “Cardiovascular diseases (CVDs),” 2017. [Online]. Available: [https://www.who.int/news-room/fact-sheets/detail/cardiovascular-diseases-\(cvds\)](https://www.who.int/news-room/fact-sheets/detail/cardiovascular-diseases-(cvds)). [Accessed: 09-Sep-2020].
- [202] R. Gamboa, “Physiopathology of essential arterial hypertension,” *Acta Médica Peru.*, vol. 23, no. 2, pp. 76–82, 2006.
- [203] S. B. Wachter and E. M. Gilbert, “Beta-adrenergic receptors, from their discovery and characterization through their manipulation to beneficial clinical application,” *Cardiol.*, vol. 122, no. 2, pp. 104–112, 2012.
- [204] V. Sridhar, L. S. Vinesh, and M. Jayashankar, “Mapping the potential distribution of *Achatina fulica* (Bowdich) (Stylommatophora : Achatinidae) in India using CLIMEX , a bioclimatic software,” *Pest Manag. Ecosyst.*, vol. 20, no. 1, pp. 14–21, 2014.
- [205] W. Suwannapan, S. Ngankoh, T. E-kobon, and P. Chumnanpuen, “Mucous cell distribution and mucus production during early growth periods of the giant African snail (*Achatina fulica*),” *Agric. Nat. Resour.*, vol. 53, pp. 423–428, 2019.
- [206] Y. Song *et al.*, “Biodegradation and disintegration of expanded polystyrene by land snails *Achatina fulica*,” *Sci. Total Environ.*, vol. 746, pp. 1–9, 2020.
- [207] J. A. White-McLean, “Terrestrial Mollusc Tool,” *USDA/APHIS/PPQ Center for Plant Health Science and Technology and the University of Florida*, 2011. [Online]. Available: <http://idtools.org/id/mollusc>. [Accessed: 14-Sep-2020].
- [208] P. Uetz, P. Freed, and J. Hosek, “The reptile database,” 2019. [Online]. Available: <http://www.reptile-database.org/>. [Accessed: 16-Sep-2020].
- [209] O. Posth *et al.*, “Classification of analysis methods for characterization of magnetic nanoparticle properties,” *XXI IMEKO World Congr. "Measurement Res. Ind.*, 2015.
- [210] F. S. Rocha, A. J. Gomes, C. N. Lunardi, S. Kaliaguine, and G. S. Patience, “Experimental methods in chemical engineering: Ultraviolet visible spectroscopy—UV-Vis,” *Can. J. Chem. Eng.*, vol. 96, no. 12, pp. 2512–2517, 2018.
- [211] A. Barth, “Infrared spectroscopy of proteins,” *Biochim. Biophys. Acta - Bioenerg.*, vol. 1767, no. 9, pp. 1073–1101, 2007.
- [212] J. L. Brunelle and R. Green, *One-dimensional SDS-polyacrylamide gel electrophoresis (1D SDS-PAGE)*, 1st ed., vol. 541. Elsevier Inc., 2014.
- [213] G. Widmann, “Interpreting TGA curves,” *UserCom*, pp. 1–20, 2001.
- [214] P. Relkin, “Differential scanning calorimetry: A useful tool for studying protein denaturation,” *Thermochim. Acta*, vol. 246, no. 2, pp. 371–386, 1994.
- [215] M. Félix, C. Carrera, A. Romero, C. Bengoechea, and A. Guerrero, “Rheological approaches as a tool for the development and stability behaviour of protein-stabilized emulsions,” *Food Hydrocoll.*, vol. 104, pp. 1–11, 2020.
- [216] M. Sauer, J. Hofkens, and J. Enderlein, *Basic Principles of Fluorescence Spectroscopy in Handbook of Fluorescence Spectroscopy and Imaging: From Single Molecules to Ensembles*, 1st ed. Weinheim: Wiley VCH Verlag GmbH, 2011.
- [217] E. M. Nickless, S. E. Holroyd, G. Hamilton, K. C. Gordon, and J. J. Wargent, “Analytical method development using FTIR-ATR and FT-Raman spectroscopy to assay fructose, sucrose, glucose and dihydroxyacetone, in *Leptospermum scoparium* nectar,” *Vib. Spectrosc.*, vol. 84, pp. 38–43, 2016.
- [218] S. D. Sawant, “FT-IR spectroscopy: principle, technique and mathematics,” *Int. J. Pharma Bio Sci.*, vol. 2, no. 1, pp. 513–519, 2011.
- [219] M. Boulet-Audet, T. Lefèvre, T. Buffeteau, and M. Pézolet, “Attenuated total reflection infrared spectroscopy: An efficient technique to quantitatively determine the orientation and conformation of proteins in single silk fibers,” *Appl. Spectrosc.*, vol. 62, no. 9, pp. 956–962, 2008.

- [220] Specac Ltd, “The Specac Quest™: How the ATR accessory works,” 2016. [Online]. Available: <https://www.specac.com/en/documents/application-notes/how-atr-works>. [Accessed: 06-Aug-2020].
- [221] ThermoFisher, “User Guide: Spectra Multicolor High Range Protein Ladder,” 2019. [Online]. Available: <https://www.thermofisher.com/order/catalog/product/26625#/26625>. [Accessed: 21-Sep-2020].
- [222] MBL, “The principle and method of SDS-polyacrylamide gel electrophoresis (SDS-PAGE),” 2016. [Online]. Available: <https://www.mblintl.com/products/sds-polyacrylamide-gel-electrophoresis-mbli/>. [Accessed: 28-Sep-2020].
- [223] Bio-Rad, “Electrophoresis: Molecular Weight Determination by SDS-PAGE,” 2004. [Online]. Available: <http://www.discover.bio-rad.com>. [Accessed: 28-Sep-2020].
- [224] A&D, “AnD MX-50 Moisture Analyzer,” 2020. [Online]. Available: https://www.and-store.com/products/moisture_analyzers/details/?productid=3774. [Accessed: 28-Sep-2020].
- [225] I. V. Sochava, T. V. Belopolskaya, and O. I. Smirnova, “DSC study of reversible and irreversible thermal denaturation of concentrated globular protein solutions,” *Biophys. Chem.*, vol. 22, no. 4, pp. 323–336, 1985.
- [226] PerkinElmer, “Differential Scanning Calorimetry: DSC 8000 Equilibration,” 2010. [Online]. Available: https://www.perkinelmer.com/uk/lab-solutions/resources/docs/TCH_DSC8000Equilibration.pdf. [Accessed: 28-Sep-2020].
- [227] C. M. Johnson, “Differential scanning calorimetry as a tool for protein folding and stability,” *Arch. Biochem. Biophys.*, vol. 531, no. 1–2, pp. 100–109, 2013.
- [228] Malvern, “A Basic Introduction to Rheology,” 2016. [Online]. Available: <https://cdn.technologynetworks.com/TN/Resources/PDF/WP160620BasicIntroRheology.pdf>. [Accessed: 27-Sep-2020].
- [229] H. A. Barnes, J. F. Hutton, and K. Walters, *An Introduction to Rheology (Rheology Series)*, 6th ed. Amsterdam: Elsevier Science, 1989.
- [230] M. Leonowicz *et al.*, “Rheological fluids as a potential component of textile products,” *Fibres Text. East. Eur.*, vol. 103, no. 1, pp. 28–33, 2014.
- [231] J. Parameswaranpillai, N. Hameed, J. Pionteck, and E. M. Woo, “Handbook of epoxy blends,” *Handb. Epoxy Blends*, no. June 2017, pp. 1–1121, 2017.
- [232] AntonPaar, “Basics of rheology,” 2020. [Online]. Available: <https://wiki.anton-paar.com/uk-en/basics-of-rheology/>. [Accessed: 27-Sep-2020].
- [233] M. Kansiz, P. Heraud, B. Wood, F. Burden, J. Beardall, and D. McNaughton, “Fourier transform infrared microspectroscopy and chemometrics as a tool for the discrimination of cyanobacterial strains,” *Phytochemistry*, vol. 52, no. 3, pp. 407–417, 1999.
- [234] R. Briandet, E. K. Kemsley, and R. H. Wilson, “Discrimination of Arabica and Robusta in Instant Coffee by Fourier Transform Infrared Spectroscopy and Chemometrics,” *J. Agric. Food Chem.*, vol. 44, no. 1, pp. 170–174, 1996.
- [235] H. Panayiotou and S. Kokot, “Matching and discrimination of single human-scalp hairs by FT-IR micro-spectroscopy and chemometrics,” *Anal. Chim. Acta*, vol. 392, no. 2–3, pp. 223–235, 1999.
- [236] H. H. Nieuwoudt, B. A. Prior, I. S. Pretorius, M. Manley, and F. F. Bauer, “Principal component analysis applied to Fourier transform infrared spectroscopy for the design of calibration sets for glycerol prediction models in wine and for the detection and classification of outlier samples,” *J. Agric. Food Chem.*, vol. 52, no. 12, pp. 3726–3735, 2004.
- [237] M. Boulet-Audet, F. Vollrath, and C. Holland, “Identification and classification of

- silks using infrared spectroscopy,” *J. Exp. Biol.*, vol. 218, no. 19, pp. 3138–3149, 2015.
- [238] E. Goormaghtigh, J. M. Ruyschaert, and V. Raussens, “Evaluation of the information content in infrared spectra for protein secondary structure determination,” *Biophys. J.*, vol. 90, no. 8, pp. 2946–2957, 2006.
- [239] J. B. Madsen, K. I. Pakkanen, and S. Lee, “Thermostability of bovine submaxillary mucin (BSM) in bulk solution and at a sliding interface,” *J. Colloid Interface Sci.*, vol. 424, pp. 113–119, 2014.
- [240] S. Lousinian, A. R. Mackie, N. M. Rigby, C. Panayiotou, and C. Ritzoulis, “Microcalorimetry of the intestinal mucus: Hydrogen bonding and self-assembly of mucin,” *Int. J. Biol. Macromol.*, vol. 112, pp. 555–560, 2018.
- [241] Specac Ltd, “The Specac Quest: How the ATR accessory works.” 2016.
- [242] H. W. Kwak, J. E. Ju, M. Shin, C. Holland, and K. H. Lee, “Sericin Promotes Fibroin Silk I Stabilization Across a Phase- Separation,” pp. 2–8, 2017.
- [243] X. Hu, D. Kaplan, and P. Cebe, “Determining beta-sheet crystallinity in fibrous proteins by thermal analysis and infrared spectroscopy,” *Macromolecules*, vol. 39, no. 18, pp. 6161–6170, 2006.
- [244] H. Yun, M. K. Kim, H. W. Kwak, J. Y. Lee, M. H. Kim, and K. H. Lee, “The role of glycerol and water in flexible silk sericin film,” *Int. J. Biol. Macromol.*, vol. 82, pp. 945–951, 2016.
- [245] H. Zhang, L. Deng, M. Yang, S. Min, L. Yang, and L. Zhu, “Enhancing effect of glycerol on the tensile properties of bombyx mori cocoon sericin films,” *Int. J. Mol. Sci.*, vol. 12, no. 5, pp. 3170–3181, 2011.
- [246] J. Kong and S. Yu, “Fourier Transform Infrared Spectroscopic Analysis of Protein Secondary Structures Protein FTIR Data Analysis and Band Assignment,” *Acta Biochim. Biophys. Sin. (Shanghai)*, vol. 39, no. 8, pp. 549–559, 2007.
- [247] B. R. Singh, D. B. DeOliveira, F.-N. Fu, and M. P. Fuller, “Fourier transform infrared analysis of amide III bands of proteins for the secondary structure estimation,” *Biomol. Spectrosc. III*, vol. 1890, no. May 1993, pp. 47–55, 1993.
- [248] D. Simonova and Iliana, “Application of Fourier Transform Infrared Spectroscopy for Tumor Diagnosis,” *Rev. Med. Biothechnology*, vol. 276, no. 276, pp. 4200–4207, 2013.
- [249] G. F. Mohsin, F. J. Schmitt, C. Kanzler, A. Hoehl, and A. Hornemann, “PCA-based identification and differentiation of FTIR data from model melanoidins with specific molecular compositions,” *Food Chem.*, vol. 281, no. July 2018, pp. 106–113, 2019.
- [250] R. Chophi, S. Sharma, and R. Singh, “Discrimination of vermilion (sindoor) using attenuated total reflectance fourier transform infrared spectroscopy in combination with PCA and PCA-LDA,” *J. Forensic Sci.*, pp. 1–14, 2020.
- [251] R. A. Fischer, “The use of mutiple measurements in taxonomic problems,” *Ann. Eugen.*, vol. 7, pp. 179–188, 1936.
- [252] L. Mariey, J. P. Signolle, C. Amiel, and J. Travert, “Discrimination, classification, identification of microorganisms using FTIR spectroscopy and chemometrics,” *Vib. Spectrosc.*, vol. 26, no. 2, pp. 151–159, 2001.
- [253] J. H. Ward, “Hierarchical Grouping to Optimize an Objective Function,” *Am. Stat. Assoc. J.*, vol. 58, no. 301, pp. 236–244, 1963.
- [254] J. Coates, “Interpretation of Infrared Spectra, A Practical Approach,” *Encycl. Anal. Chem.*, pp. 1–23, 2006.
- [255] W. Zhang, B. N. Markiewicz, R. S. Doerksen, and A. B. S. Iii, “C≡N Stretching Vibration of 5-Cyanotryptophan as an Infrared Probe of Protein Local Environment: What Determines Its Frequency?,” vol. 18, no. 10, pp. 7027–7034, 2017.
- [256] L. J. Smith, K. M. Fiebig, H. Schwalbe, and C. M. Dobson, “The concept of a random

- coil Residual structure in peptides and denatured proteins,” *Fold. Des.*, vol. 1, no. 5, pp. 95–106, 1996.
- [257] J. Coates, “Interpretation of infrared spectra, a practical approach,” *Encycl. Anal. Chem.*, pp. 10815–10837, 2000.
- [258] M. W. Denny, “The role of mucus in the locomotion and adhesion of the pulmonate slug, *ariolimax columbianus*,” Duke University, 1973.
- [259] B. Hausdorf, “Macroevolution in progress: Competition between semislugs and slugs resulting in ecological displacement and ecological release,” *Biol. J. Linn. Soc.*, vol. 74, no. 3, pp. 387–395, 2001.
- [260] A. M. Smith, “The Structure and Function of Adhesive Gels from Invertebrates,” *Integr. Comp. Biol.*, vol. 42, no. 6, pp. 1164–1171, 2002.
- [261] W. Nuansing *et al.*, “Structural analysis and mapping of individual protein complexes by infrared nanospectroscopy,” *Nat. Commun.*, vol. 4, no. 1, pp. 1–9, 2013.
- [262] M. Denny, “Locomotion: The Cost of Gastropod Crawling,” *Science (80-.)*, vol. 208, pp. 1288–1290, Jun. 1980.
- [263] J. Grdadolnik, “Saturation effects in FTIR spectroscopy: intensity of amide I and amide II bands in protein spectra,” *Acta Chim. Slov*, vol. 50, pp. 23–25, 2003.
- [264] M. Khajehpour, J. L. Dashnau, and J. M. Vanderkooi, “Infrared spectroscopy used to evaluate glycosylation of proteins,” *Anal. Biochem.*, vol. 348, no. 1, pp. 40–48, 2006.
- [265] Y. Matsuura *et al.*, “Thermodynamics of protein denaturation at temperatures over 100°C: CutA1 mutant proteins substituted with hydrophobic and charged residues,” *Sci. Rep.*, vol. 5, pp. 1–9, 2015.
- [266] N. Errington, T. Iqbalsyah, and A. J. Doig, “Structure and stability of the alpha-helix: lessons for design,” *Methods Mol. Biol.*, vol. 340, pp. 3–26, 2006.
- [267] J. S. Nowick, “Exploring β -Sheet Structure and Interactions with Chemical Model Systems,” *Acc Chem Res*, vol. 41, no. 10, pp. 1319–1330, 2008.
- [268] A. M. C. Marcelino and L. M. Gierasch, “Roles of β -turns in protein folding: From peptide models to protein engineering,” *Biopolymers*, vol. 89, no. 5, pp. 380–391, 2008.
- [269] C. A. Luis Cuevas-Velázquez Alejandra Covarrubias-Robles, “Las proteínas desordenadas y su función,” *Rev. Espec. en Ciencias Químico-Biológicas*, vol. 14, no. 2, p. 9, 2011.
- [270] J. Carmicheal *et al.*, “Presence and structure-activity relationship of intrinsically disordered regions across mucins,” *FASEB J.*, vol. 34, no. 2, pp. 1939–1957, 2020.
- [271] M. Offengenden and J. Wu, “Egg white ovomucin gels: Structured fluids with weak polyelectrolyte properties,” *RSC Adv.*, vol. 3, no. 3, pp. 910–917, 2013.
- [272] K. A. Hayes *et al.*, “Insights from an integrated view of the biology of apple snails (caenogastropoda: Ampullariidae),” *Malacologia*, vol. 58, no. 1–2, pp. 245–302, 2015.
- [273] S. Joo, S. Jung, S. Lee, R. H. Cowie, and D. Takagi, “Freshwater snail feeding: Lubrication-based particle collection on the water surface,” *J. R. Soc. Interface*, vol. 17, no. 165, 2020.
- [274] L. Navarini, A. Cesàro, and S. B. Ross-Murphy, “Viscoelastic properties of aqueous solutions of an exocellular polysaccharide from cyanobacteria,” *Carbohydr. Polym.*, vol. 18, no. 4, pp. 265–272, 1992.
- [275] A. R. Toledo-Piza, I. Lebrun, M. R. Franzolin, and E. Nakano, “The mucus of the mollusk *Phyllocaulis boraceiensis*: biochemical profile and the search for microbiological activity,” *The Veliger*, vol. 51, no. 3, pp. 137–144, 2012.
- [276] S. Ballance, M. Howard, K. N. White, C. R. McCrohan, D. J. Thornton, and J. K. Sheehan, “Partial characterisation of high-molecular weight glycoconjugates in the trail mucus of the freshwater pond snail *Lymnaea stagnalis*,” *Comp. Biochem. Physiol.*

- *Biochem. Mol. Biol.*, vol. 137, no. 4, pp. 475–486, 2004.
- [277] R. Jugdaohsingh, M. M. Campbell, R. P. H. Thompson, C. R. McCrohan, K. N. White, and J. J. Powell, “Mucus Secretion by the Freshwater Snail *Lymnaea stagnalis* Limits Aluminum Concentrations of the Aqueous Environment,” *Environ. Sci. Technol.*, vol. 32, no. 17, pp. 2591–2595, 1998.
- [278] M. Gutternigg, S. Bürgmayr, G. Pörtl, J. Rudolf, and E. Staudacher, “Neutral N-glycan patterns of the gastropods *Limax maximus*, *Cepaea hortensis*, *Planorbarius corneus*, *Arianta arbustorum* and *Achatina fulica*,” *Glycoconj. J.*, vol. 24, no. 8, pp. 475–489, 2007.
- [279] A. Barth and C. Zscherp, “What vibrations tell us about proteins,” *Q. Rev. Biophys.*, vol. 35, no. 4, pp. 369–430, 2002.
- [280] U. Lindahl, J. Couchman, and K. Kimata, “Proteoglycans and Sulfated Glycosaminoglycans,” in *Essentials of Glycobiology*, 3rd ed., A. Varki, R. D. Cummings, and J. D. Esko, Eds. New York: Cold Spring Harbor Laboratory Press, 2017.
- [281] H. J. Gabius, “Glycans: Bioactive signals decoded by lectins,” *Biochem. Soc. Trans.*, vol. 36, no. 6, pp. 1491–1496, 2008.
- [282] V. P. Gupta and T. A. Keiderking, “Vibrational CD of the amide II band in some model polypeptides and proteins,” *Biopolymers*, vol. 32, pp. 239–248, 1992.
- [283] J. Quinteiro, J. Rodríguez-Castro, J. Castillejo, J. Iglesias-Piñeiro, and M. Rey-Méndez, “Phylogeny of slug species of the genus *Arion*: Evidence of monophyly of Iberian endemics and of the existence of relict species in Pyrenean refuges,” *J. Zool. Syst. Evol. Res.*, vol. 43, no. 2, pp. 139–148, 2005.
- [284] L. V. Flórez, P. H. W. Biedermann, T. Engl, and M. Kaltenpoth, “Defensive symbioses of animals with prokaryotic and eukaryotic microorganisms,” *Nat. Prod. Rep.*, vol. 32, no. 7, pp. 904–936, 2015.
- [285] R. Chase, R. P. Croll, and L. L. Zeichner, “Aggregation in snails, *Achatina fulica*,” *Behav. Neural Biol.*, vol. 30, no. 2, pp. 218–230, 1980.
- [286] Z. P. He *et al.*, “Complete mitochondrial genome of the giant african snail, *achatina fulica* (Mollusca: Achatinidae): A novel location of putative control regions (CR) in the mitogenome within Pulmonate species,” *Mitochondrial DNA*, vol. 27, no. 2, pp. 1084–1085, 2016.
- [287] P. Artacho and R. F. Nespolo, “Natural Selection Reduces Energy Metabolism in the garden snail, *Helix Aspersa* (*Cornu Aspersum*),” *Evolution*, vol. 63, no. 4. pp. 1044–1050, 2009.
- [288] S. K. Lai, Y. Y. Wang, R. Cone, D. Wirtz, and J. Hanes, “Altering mucus rheology to ‘solidify’ human mucus at the nanoscale,” *PLoS One*, vol. 4, no. 1, pp. 1–6, 2009.
- [289] D. L. Luchtel, I. Deyrup-Olsen, and A. W. Martin, “Ultrastructure and lysis of mucin-containing granules in epidermal secretions of the terrestrial slug *Ariolimax columbianus* (Mollusca: Gastropoda:Pulmonata),” *Cell Tissue Res.*, vol. 266, no. 2, pp. 375–383, 1991.
- [290] S. S. Dhanisha, C. Guruvayoorappan, S. Drishya, and P. Abeesh, “Mucins: Structural diversity, biosynthesis, its role in pathogenesis and as possible therapeutic targets,” *Crit. Rev. Oncol. Hematol.*, vol. 122, no. October 2017, pp. 98–122, 2018.
- [291] D. J. Thornton, “From Mucins to Mucus: Toward a More Coherent Understanding of This Essential Barrier,” *Proc. Am. Thorac. Soc.*, vol. 1, no. 1, pp. 54–61, 2004.
- [292] J. Perez-vilar and R. L. Hill, “The Structure and Assembly of Secreted Mucins,” *J. Biol. Chem.*, vol. 274, no. 45, pp. 31751–31754, 1999.
- [293] L. S. Peck, E. Prothero-Thomas, and N. Hough, “Pedal mucus production by the Antarctic limpet *Nacella concinna* (Strebel, 1908),” *J. Exp. Mar. Bio. Ecol.*, vol. 174,

- no. 2, pp. 177–192, 1993.
- [294] S. S. Dhanisha, C. Guruvayoorappan, S. Drishya, and P. Abeesh, “Mucins: Structural diversity, biosynthesis, its role in pathogenesis and as possible therapeutic targets,” *Crit. Rev. Oncol. Hematol.*, vol. 122, no. June 2017, pp. 98–122, 2018.
- [295] W. J. Waddell, “A simple ultraviolet spectrophotometric method for the determination of protein,” *J. Lab. Clin. Med.*, 1956.
- [296] N. J. Kruger and J. M. Walker, *Protein Protocols The Handbook*, Second Edi. Hatfield, UK, 2002.
- [297] M. P. Ireland, “Distribution of essential and toxic metals in the terrestrial gastropod *Arion ater*,” *Environ. Pollut.*, vol. 20, no. 4, pp. 271–278, 1979.
- [298] M. Salt, N. Litra, A. Bradshaw, M. Zeitler, A. M. Smith, and A. Bell, “Cross-linking by protein oxidation in the rapidly setting gel-based glues of slugs,” *J. Exp. Biol.*, vol. 214, no. 10, pp. 1699–1706, 2011.
- [299] L. Stabili, R. Schirosi, M. G. Parisi, S. Piraino, and M. Cammarata, “The mucus of *Actinia equina* (Anthozoa, Cnidaria): An unexplored resource for potential applicative purposes,” *Mar. Drugs*, vol. 13, no. 8, pp. 5276–5296, 2015.
- [300] L. Velkova and W. Voelter, “Structure and antibacterial activity of isolated peptides from the mucus of garden snail *Cornu aspersum* , Bulgarian Chemical Communications C , 50,” vol. 50, no. December, pp. 195–200, 2018.
- [301] W. G. Lesniak *et al.*, “Concurrent quantification of tryptophan and its major metabolites,” *Anal. Biochem.*, vol. 443, no. 2, pp. 222–231, 2013.
- [302] J. M. Antosiewicz and D. Shugar, “UV–Vis spectroscopy of tyrosine side-groups in studies of protein structure. Part 2: selected applications,” *Biophys. Rev.*, vol. 8, no. 2, pp. 163–177, 2016.
- [303] G. Petrou and T. Crouzier, “Mucins as multifunctional building blocks of biomaterials,” *Biomater. Sci.*, vol. 6, no. 9, pp. 2282–2297, 2018.
- [304] R. Bansil and B. S. Turner, “The biology of mucus: Composition, synthesis and organization,” *Adv. Drug Deliv. Rev.*, vol. 124, pp. 3–15, 2018.
- [305] F.-X. Schmid, “Biological Macromolecules: UV-visible Spectrophotometry,” *Encycl. Life Sci.*, pp. 1–4, 2001.
- [306] G. Radicioni *et al.*, “The innate immune properties of airway mucosal surfaces are regulated by dynamic interactions between mucins and interacting proteins: the mucin interactome,” *Mucosal Immunol.*, vol. 9, no. 6, pp. 1442–1454, 2016.
- [307] C. Butnarusu, N. Barbero, D. Pacheco, P. Petrini, and S. Visentin, “Mucin binding to therapeutic molecules: The case of antimicrobial agents used in cystic fibrosis,” *Int. J. Pharm.*, vol. 564, no. April, pp. 136–144, 2019.
- [308] J. L. Crammer and A. Neuberger, “The state of tyrosine in egg albumin and in insulin as determined by spectrophotometric titration,” *Biochem. J.*, vol. 37, no. 2, pp. 302–310, 1943.
- [309] M. Ogawa, S. Nakamura, T. Atsuchi, T. Tamiya, T. Tsuchiya, and S. Nakai, “Macromolecular antimicrobial glycoprotein, achacin, expressed in a methylotrophic yeast *Pichia pastoris*,” *FEBS Lett.*, vol. 448, no. 1, pp. 41–44, 1999.
- [310] S. Ulagesan and H. Kim, “Antibacterial and Antifungal Activities of Proteins Extracted from Seven Different Snails,” *Appl. Sci.*, vol. 8, no. 8, p. 1362, 2018.
- [311] S. Ito *et al.*, “High molecular weight lectin isolated from the mucus of the giant african snail *Achatina fulica*,” *Biosci. Biotechnol. Biochem.*, vol. 75, no. 1, pp. 20–25, 2011.
- [312] V. M. Hernandez-Izquierdo and J. M. Krochta, “Thermoplastic processing of proteins for film formation - A review,” *J. Food Sci.*, vol. 73, no. 2, pp. 30–39, 2008.
- [313] G. Peters *et al.*, “Human laryngeal mucus from the vocal folds: Rheological characterization by particle tracking microrheology and oscillatory shear rheology,”

- Appl. Sci.*, vol. 11, no. 7, pp. 1–15, 2021.
- [314] B. S. Schuster, J. S. Suk, G. F. Woodworth, and J. Hanes, “Nanoparticle diffusion in respiratory mucus from humans without lung disease,” *Biomaterials*, vol. 34, no. 13, pp. 3439–3446, 2013.
- [315] A. L. Innes *et al.*, “Ex vivo sputum analysis reveals impairment of protease-dependent mucus degradation by plasma proteins in acute asthma,” *Am. J. Respir. Crit. Care Med.*, vol. 180, no. 3, pp. 203–210, 2009.
- [316] B. C. Huck *et al.*, “Macro- And Microrheological Properties of Mucus Surrogates in Comparison to Native Intestinal and Pulmonary Mucus,” *Biomacromolecules*, vol. 20, no. 9, pp. 3504–3512, 2019.
- [317] X. Murgia, P. Pawelzyk, U. F. Schaefer, C. Wagner, N. Willenbacher, and C. M. Lehr, “Size-Limited Penetration of Nanoparticles into Porcine Respiratory Mucus after Aerosol Deposition,” *Biomacromolecules*, vol. 17, no. 4, pp. 1536–1542, 2016.
- [318] R. Bansil and B. S. Turner, “Mucin structure, aggregation, physiological functions and biomedical applications,” *Curr. Opin. Colloid Interface Sci.*, vol. 11, no. 2–3, pp. 164–170, 2006.
- [319] D. B. Hill *et al.*, “A biophysical basis for mucus solids concentration as a candidate biomarker for airways disease,” *PLoS One*, vol. 9, no. 2, pp. 1–11, 2014.
- [320] J. K. Towns, “Moisture content in proteins: its effects and measurement,” *J. Chromatogr. A*, vol. 705, no. 1, pp. 115–127, 1995.
- [321] C. M. Wade, P. B. Mordan, and F. Naggs, “Evolutionary relationships among the Pulmonate land snails and slugs (Pulmonata, Stylommatophora),” *Biol. J. Linn. Soc.*, vol. 87, no. 4, pp. 593–610, 2006.
- [322] E. L. Davies and K. Arbuckle, “Coevolution of snake venom toxic activities and diet: Evidence that ecological generalism favours toxicological diversity,” *Toxins (Basel)*, vol. 11, no. 12, pp. 1–14, 2019.
- [323] E. Kochva, “The origin of snakes and evolution of the venom apparatus,” *Toxicon*, vol. 25, no. 1, pp. 65–106, 1987.
- [324] N. R. Casewell, W. Wüster, F. J. Vonk, R. A. Harrison, and B. G. Fry, “Complex cocktails: The evolutionary novelty of venoms,” *Trends Ecol. Evol.*, vol. 28, no. 4, pp. 219–229, 2013.
- [325] A. L. Allcock *et al.*, *Evolution of venomous animals and their toxins*. Toxinology, 2017.
- [326] P. Gopalakrishnakone, H. Inagaki, C. Vogel, A. K. Mukherjee, and T. R. Rahmy, *Snake Venoms*, First. Springer Netherlands, 2017.
- [327] S. L. Thornton, “Snakes,” *Encycl. Toxicol.*, pp. 310–312, 2014.
- [328] O. H. Del Brutto and V. J. Del Brutto, “Neurological complications of venomous snake bites: A review,” *Acta Neurol. Scand.*, vol. 125, no. 6, pp. 363–372, 2012.
- [329] R. A. Berthé, “Spitting behaviour and fang morphology of spitting cobras,” Universität Bonn, 2011.
- [330] R. A. Hutton and D. A. Warrell, “Action of snake venom components on the haemostatic system,” *Blood Rev.*, vol. 7, no. 3, pp. 176–189, 1993.
- [331] T. M. A. El-Aziz, A. G. Soares, and J. D. Stockand, “Snake venoms in drug discovery: Valuable therapeutic tools for life saving,” *Toxins (Basel)*, vol. 11, no. 10, pp. 1–25, 2019.
- [332] B. Kalita, A. J. Saviola, and A. K. Mukherjee, “From venom to drugs : a review and critical analysis of Indian snake venom toxins envisaged as anticancer drug prototypes,” *Drug Discov. Today*, pp. 1–13, 2021.
- [333] B. Lomonte and J. J. Calvete, “Strategies in ‘snake venomics’ aiming at an integrative view of compositional, functional, and immunological characteristics of venoms,” *J.*

- Venom. Anim. Toxins Incl. Trop. Dis.*, vol. 23, no. 1, pp. 1–12, 2017.
- [334] C. R. Ferraz *et al.*, “Multifunctional toxins in snake venoms and therapeutic implications: From pain to hemorrhage and necrosis,” *Front. Ecol. Evol.*, vol. 7, no. JUN, pp. 1–19, 2019.
- [335] S. M. Munekiyo and S. P. Mackessy, “Effects of temperature and storage conditions on the electrophoretic, toxic and enzymatic stability of venom components,” *Comp. Biochem. Physiol. - B Biochem. Mol. Biol.*, vol. 119, no. 1, pp. 119–127, 1998.
- [336] N. B. Egen and F. E. Russell, “Effects of preparatory procedures on the venom from a rattlesnake (*Crotalus molossus molossus*), as determined by isoelectric focusing,” *Toxicon*, vol. 22, pp. 654–656, 1984.
- [337] J. A. Gené, B. Lomonte, J. M. Gutiérrez, and L. Cerdas, “Changes in the electrophoretic pattern of the venom of the bushmaster (*Lachesis muta stenophrys*) stored under various conditions,” *Rev. Biol. Trop.*, vol. 33, pp. 63–65, 1985.
- [338] V. M. Gregory-Dwyer, N. B. Egen, A. Bianchi Bosisio, P. G. Righetti, and F. E. Russell, “An isoelectric focusing study of seasonal variation in rattlesnake venom proteins,” *Toxicon*, vol. 24, pp. 995–1000, 1986.
- [339] WHO, “Blood products and related biologicals,” *WHO Guidelines for the Production, Control and Regulation of Snake Antivenom Immunoglobulins*, 2018. .
- [340] C. L. Ownby, T. R. Colberg, and Q. Li, “Presence of heat-stable hemorrhagic toxins in snake venoms,” *Toxicon*, vol. 32, no. 8, pp. 945–954, 1994.
- [341] P. Becker Pertuzatti, M. Teixeira Barcia, S. Gómez-Alonso, H. Teixeira Godoy, and I. Hermosin-Gutierrez, “Phenolics profiling by HPLC-DAD-ESI-MSn aided by principal component analysis to classify Rabbiteye and Highbush blueberries,” *Food Chem.*, vol. 340, no. August 2020, p. 127958, 2021.
- [342] W. Cheng *et al.*, “Sensible Functional Linear Discriminant Analysis Effectively Discriminates Enhanced Raman Spectra of Mycobacterium Species,” *Analytical Chem.*, pp. 1–8, 2021.
- [343] I. M. B. Francischetti, V. My-Pham, J. Harrison, M. K. Garfield, and J. M. C. Ribeiro, “*Bitis gabonica* (Gaboon viper) snake venom gland: Toward a catalog for the full-length transcripts (cDNA) and proteins,” *Gene*, vol. 337, no. SUPPL., pp. 55–69, 2004.
- [344] R. T. Cristina *et al.*, “Protein structure of the venom in nine species of snake: From bio-compounds to possible healing agents,” *Brazilian J. Med. Biol. Res.*, vol. 53, no. 1, pp. 1–7, 2020.
- [345] C. Sakuma *et al.*, “Analysis of protein denaturation, aggregation and post-translational modification by agarose native gel electrophoresis,” *Int. J. Biol. Macromol.*, vol. 172, pp. 589–596, 2021.
- [346] R. M. Kini, V. S. Rao, and J. S. Joseph, “Procoagulant proteins from snake venoms,” *Haemostasis*, vol. 31, no. 3–6, pp. 218–224, 2001.
- [347] N. J. Youngman *et al.*, “Utilising venom activity to infer dietary composition of the Kenyan horned viper (*Bitis worthingtoni*),” *Comp. Biochem. Physiol. Part - C Toxicol. Pharmacol.*, vol. 240, pp. 1–6, 2021.
- [348] B. L. Dhananjaya and C. J. M. D’Souza, “An overview on nucleases (DNase, RNase, and phosphodiesterase) in snake venoms,” *Biochem.*, vol. 75, no. 1, pp. 1–6, 2010.
- [349] S. D. Aird, “Ophidian envenomation strategies and the role of purines,” *Toxicon*, vol. 40, no. 4, pp. 335–393, 2002.
- [350] X. Y. Du and K. J. Clemetson, “Snake venom L-amino acid oxidases,” *Toxicon*, vol. 40, no. 6, pp. 659–665, 2002.
- [351] L. F. M. Izidoro *et al.*, “Snake venom L-amino acid oxidases: Trends in pharmacology and biochemistry,” *Biomed Res. Int.*, vol. 2014, pp. 1–19, 2014.
- [352] A. Ullah, “Structure–Function Studies and Mechanism of Action of Snake Venom L-

- Amino Acid Oxidases,” *Front. Pharmacol.*, vol. 11, pp. 1–17, 2020.
- [353] C. W. Vogel and D. C. Fritzing, “Cobra venom factor: Structure, function, and humanization for therapeutic complement depletion,” *Toxicon*, vol. 56, no. 7, pp. 1198–1222, 2010.
- [354] Y. Yamazaki and T. Morita, “Structure and function of snake venom cysteine-rich secretory proteins,” *Toxicon*, vol. 44, no. 3, pp. 227–231, 2004.
- [355] T. Tadokoro, C. Modahl, K. Maenaka, and N. Aoki-Shioi, “Cysteine-Rich Secretory Proteins (CRISPs) from Venomous Snakes: An Overview of the Functional Diversity in a Large and Underappreciated Superfamily,” *Toxins (Basel)*, vol. 12, no. 175, pp. 1–20, 2020.
- [356] A. Bocian *et al.*, “Comparison of methods for measuring protein concentration in venom samples,” *Animals*, vol. 10, no. 3, pp. 1–9, 2020.
- [357] J. A. Eble, “Structurally robust and functionally highly versatile—C-type lectin (-related) proteins in snake venoms,” *Toxins (Basel)*, vol. 11, no. 3, 2019.
- [358] Z. Latinović *et al.*, “The procoagulant snake venom serine protease potentially having a dual, blood coagulation factor v and X-activating activity,” *Toxins (Basel)*, vol. 12, no. 6, pp. 1–15, 2020.
- [359] A. D. Robertson and K. P. Murphy, “Protein structure and the energetics of protein stability,” *Chem. Rev.*, vol. 97, no. 5, pp. 1251–1267, 1997.
- [360] S. Vonhoff, J. Condliffe, and H. Schiffter, “Implementation of an FTIR calibration curve for fast and objective determination of changes in protein secondary structure during formulation development,” *J. Pharm. Biomed. Anal.*, vol. 51, no. 1, pp. 39–45, 2010.
- [361] A. Munawar, S. A. Ali, A. Akrem, and C. Betzel, “Snake venom peptides: Tools of biodiscovery,” *Toxins (Basel)*, vol. 10, no. 11, pp. 1–29, 2018.
- [362] A. Ullah, K. Ullah, H. Ali, C. Betzel, and S. U. Rehman, “The sequence and a three-dimensional structural analysis reveal substrate specificity among snake venom phosphodiesterases,” *Toxins (Basel)*, vol. 11, no. 11, pp. 1–24, 2019.
- [363] J. D. Bloom, S. T. Labthavikul, C. R. Otey, and F. H. Arnold, “Protein stability promotes evolvability,” *Proc. Natl. Acad. Sci. U. S. A.*, vol. 103, no. 15, pp. 5869–5874, 2006.
- [364] C. H. Wang and W. G. Wu, “Amphiphilic β -sheet cobra cardiotoxin targets mitochondria and disrupts its network,” *FEBS Lett.*, vol. 579, no. 14, pp. 3169–3174, 2005.
- [365] M. Polláková, V. Petrilla, Z. Andrejčáková, M. Petrillová, D. Sopková, and E. Petrovová, “Spitting cobras: Experimental assay employing the model of chicken embryo and the chick chorioallantoic membrane for imaging and evaluation of effects of venom from African and Asian species (*Naja ashei*, *Naja nigricollis*, *Naja siamensis*, *Naja sumatrana*),” *Toxicon*, vol. 189, pp. 79–90, 2021.
- [366] D. G. Broadley and W. Wüster, “A review of the southern African ‘non-spitting’ cobras (serpentes: Elapidae: *Naja*),” *J. Herpetol. Assoc. Africa*, vol. 53, no. 2, pp. 101–122, 2004.
- [367] R. N. V. Krishna Deepak and R. Sankararamkrishnan, “Unconventional N-H...N Hydrogen Bonds Involving Proline Backbone Nitrogen in Protein Structures,” *Biophys. J.*, vol. 110, no. 9, pp. 1967–1979, 2016.
- [368] S. Fernandez *et al.*, “In vitro toxic effects of puff adder (*Bitis arietans*) venom, and their neutralization by antivenom,” *Toxins (Basel)*, vol. 6, no. 5, pp. 1586–1597, 2014.
- [369] H. Khalid, M. M. Mukhtar, and N. Konstantakopoulos, “Cytotoxicity of *Naja nubiae* (Serpentes: Elapidae) and *Echis ocellatus* (Serpentes: Viperidae) Venoms from Sudan,” *J. Toxins*, vol. 2015, pp. 1–7, 2015.

- [370] W. H. Heyborne, S. P. Mackessy, and I. Introduction, "Cysteine-Rich Secretory Proteins in Reptile Venoms," in *Handbook of Venoms and Toxins of Reptiles*, 2020, pp. 341–352.
- [371] W. Wüster *et al.*, "Integration of nuclear and mitochondrial gene sequences and morphology reveals unexpected diversity in the forest cobra (*Naja melanoleuca*) species complex in Central and West Africa (Serpentes: Elapidae)," *Zootaxa*, vol. 4455, no. 1, pp. 68–98, 2018.
- [372] R. Dawkins and J. R. Krebs, "Arms races between and within species," *Proc. R. Soc. L.*, vol. 205, pp. 489–511, 1979.
- [373] D. Eilam, "Die hard: a blend of freezing and fleeing as a dynamic defense - implications for the control of defensive behavior," *Neurosci. Biobehav. Rev.*, vol. 29, pp. 1181–1191, 2005.
- [374] J. O. Schmidt, "Pain and lethality induced by insect stings: an exploratory and correlational study," *Toxins (Basel)*, vol. 11, pp. 427–441, 2019.
- [375] Y. S. Chan, R. C. F. Cheung, L. X. Xia, J. H. Wong, T. B. Ng, and W. Y. Chan, "Snake venom toxins: toxicity and medicinal applications," *Appl. Microbiol. Biotechnol.*, vol. 100, 2016.
- [376] F. J. Vonk *et al.*, "Evolutionary origin and development of snake fangs," *Nature*, vol. 454, no. 7204, pp. 630–633, Jul. 2008.
- [377] C. Broeckhoven and A. du Plessis, "Has snake fang evolution lost its bite? New insights from a structural mechanics viewpoint," *Biol. Lett.*, vol. 13, no. 8, p. 20170293, 2017.
- [378] H. M. I. Kerckamp, N. R. Casewell, and F. J. Vonk, "Evolution of the snake venom delivery system," in *Evolution of Venomous Animals and Their Toxins*, P. Gopalakrishnakone and A. Malhotra, Eds. SPRINGER, 2017, pp. 303–316.
- [379] K. V Kardong, P. Dullemeijer, and J. A. M. Fransen, "Feeding Mechanism in the Rattlesnake *Crotalus durissus*," *Amphib. E. J. Brill*, vol. 7, pp. 271–302, 1986.
- [380] B. A. Young, M. Blair, K. Zahn, and J. Marvin, "Mechanics of venom expulsion in *Crotalus*, with special reference to the role of the fang sheath," *Anat. Rec.*, vol. 264, no. 4, pp. 415–426, Dec. 2001.
- [381] K. Jackson, "The evolution of venom-delivery system in snakes," *Zool Jour. Linn. Soc.*, vol. 137, pp. 337–354, 2003.
- [382] B. Young and K. Kardong, "Mechanisms controlling venom expulsion in the western diamondback rattlesnake, *Crotalus atrox*," *J. Exp. Zool. Part A Ecol. Genet. Physiol.*, vol. 307A, no. 1, pp. 18–27, 2007.
- [383] C. M. Bogert, "Dentitional phenomena in cobras and other elapids with notes on adaptive modifications of fangs," *Bull. Am. Museum Nat. Hist.*, vol. 81, no. 3, pp. 260–285, 1943.
- [384] L. J. Vitt and J. P. Caldwell, *Herpetology: an introductory biology of amphibians and reptiles*. Academic Press, 2013.
- [385] W. Wüster, "Taxonomic changes and toxinology: Systematic revisions of the asiatic cobras (*Naja naja* species complex)," *Toxicon*, vol. 34, no. 4. pp. 399–406, 1996.
- [386] W. Wüster *et al.*, "The phylogeny of cobras inferred from mitochondrial DNA sequences: Evolution of venom spitting and the phylogeography of the African spitting cobras (Serpentes: Elapidae: *Naja nigricollis* complex)," *Mol. Phylogenet. Evol.*, vol. 45, no. 2, pp. 437–453, 2007.
- [387] R. A. Berthé, S. de Pury, H. Bleckmann, and G. Westhoff, "Spitting cobras adjust their venom distribution to target distance," *J. Comp. Physiol. A Neuroethol. Sensory, Neural, Behav. Physiol.*, vol. 195, no. 8, pp. 753–757, 2009.
- [388] N. Panagides *et al.*, "How the cobra got its flesh-eating venom: Cytotoxicity as a

- defensive innovation and its co-evolution with hooding, aposematic marking, and spitting,” *Toxins (Basel)*, vol. 9, no. 3, pp. 1–22, 2017.
- [389] G. A.-W. Westhoff G. A4 - Tzschätzsch, K. A4 - Bleckmann, H., “The spitting behavior of two species of spitting cobras A Neuroethology, sensory, neural, and behavioral physiology,” *J. Comp. Physiol.*, vol. v. 191, no. 10, pp. 873–881–2005 v.191 no.10, 2005.
- [390] W. Wüster and R. Thorpe, “Dentitional phenomena in cobras revisited: spitting and fang structure in the Asiatic species of *Naja* (Serpentes: Elapidae),” *Herpetologica*, vol. 48, no. 4, pp. 424–434, 1992.
- [391] G. Westhoff, K. Tzschätzsch, and H. Bleckmann, “The spitting behavior of two species of spitting cobras,” *J. Comp. Physiol. A Neuroethol. Sensory, Neural, Behav. Physiol.*, vol. 191, no. 10, pp. 873–881, 2005.
- [392] J. B. Slowinski, A. Knight, and A. P. Rooney, “Inferring Species Trees from Gene Trees: A Phylogenetic Analysis of the Elapidae (Serpentes) Based on the Amino Acid Sequences of Venom Proteins,” *Mol. Phylogenet. Evol.*, vol. 8, no. 3, pp. 349–362, 1997.
- [393] W. Wüster *et al.*, “The phylogeny of cobras inferred from mitochondrial DNA sequences: Evolution of venom spitting and the phylogeography of the African spitting cobras (Serpentes: Elapidae: *Naja nigricollis* complex),” *Mol. Phylogenet. Evol.*, vol. 45, no. 2, pp. 437–453, 2007.
- [394] D. R. Nelsen *et al.*, “Poisons, toxins, and venoms: redefining and classifying toxic biological secretions and the organisms that employ them,” *Biol. Rev. Camb. Philos. Soc.*, vol. 89, pp. 450–465, Sep. 2014.
- [395] J. Kurt and H. Aurich, “The effect of pH value and temperature on the stability of L-aminoacidoxidase from the venom of the sand viper,” *Acta Biol. Med. Ger.*, vol. 35, pp. 175–182, 1976.
- [396] C. Bon, “Pharmacokinetics of venom toxins and their modification by antivenom therapy,” *J. Toxicol. Toxin Rev.*, vol. 22, pp. 129–138, 2003.
- [397] P. H. Ribeiro *et al.*, “Mechanism of the cytotoxic effect of L-amino acid oxidase isolated from *Bothrops alternatus* snake venom,” *Int. J. Biol. Macromol.*, vol. 92, 2016.
- [398] S. Sanhajariya, S. Duffull, and G. Isbister, “Pharmacokinetics of snake venom,” *Toxins (Basel)*, vol. 10, p. 73, 2018.
- [399] C. E. Synolakis and H. S. Badeer, “On combining the Bernoulli and Poiseuille equation—A plea to authors of college physics texts,” *Am. J. Phys.*, vol. 57, no. 11, pp. 1013–1019, 1989.
- [400] A. Aitken and M. P. Learmonth, “Protein Determination by UV Absorption,” *Protein Protoc. Handbook*, pp. 3–6, 2009.
- [401] T. D. Kazandjian *et al.*, “Convergent Evolution of Pain-Inducing Defensive Venom Components in Spitting Cobras,” *Science (80-)*, vol. 371, no. 6527, pp. 386–390, Jan. 2021.
- [402] A. Paterna, “Spitting behaviour in the Chinese cobra *Naja atra*,” *Herpetol. Bull.*, vol. 148, pp. 22–25, 209AD.
- [403] V. Santra and W. Wüster, “*Naja kaouthia* (Monocled Cobra). Behavior / spitting,” *Herpetol. Rev.*, vol. 48, pp. 455–456, 2017.
- [404] S. P. Blomberg, T. Garland, and A. R. Ives, “Testing for phylogenetic signal in comparative data: behavioral traits are more labile,” *Evolution (N. Y.)*, vol. 57, pp. 717–745, 2003.
- [405] M. Pagel, “Inferring the historical patterns of biological evolution,” *Nature*, vol. 401, pp. 877–884, 1999.

- [406] T. Takahashi and A. Ohsaka, "Purification and some properties of two hemorrhagic principles (HR2a and HR2b) in the venom of *Trimeresurus flavoviridis*; complete separation of the principles from proteolytic activity," *BBA - Protein Struct.*, vol. 207, no. 1, pp. 65–75, 1970.
- [407] A. E. Terry, D. P. Knight, D. Porter, and F. Vollrath, "pH Induced Changes in the Rheology of Silk Fibroin Solution from the Middle Division of *Bombyx mori* Silkworm," *Biomacromolecules*, vol. 5, no. 3, pp. 768–772, Apr. 2004.
- [408] J. C. Daltry, W. Wüster, and R. S. Thorpe, "Diet and snake venom evolution," *Nature*, vol. 379, pp. 537–540, 1996.
- [409] H. L. Gibbs, L. Sanz, J. E. Chiucchi, T. M. Farrell, and J. J. Calvete, "Proteomic analysis of ontogenetic and diet-related changes in venom composition of juvenile and adult Dusky Pigmy rattlesnakes (*Sistrurus miliarius barbouri*)," vol. 74, pp. 2169–2179, 2011.
- [410] A. Alape-Girón *et al.*, "Snake venomomics of the lancehead pitviper *Bothrops asper*: geographic, individual, and ontogenetic variations," *J. Proteome Res.*, vol. 7, pp. 3556–3571, 2008.
- [411] V. Cipriani *et al.*, "Correlation between ontogenetic dietary shifts and venom variation in Australian brown snakes (*Pseudonaja*)," *Comp. Biochem. Phys. C*, vol. 197, pp. 53–60, 2017.
- [412] S. P. Mackessy, N. M. Sixberry, W. H. Heyborne, and T. Fritts, "Venom of the Brown Treesnake, *Boiga irregularis*: ontogenetic shifts and taxa-specific toxicity," *Toxicon*, vol. 47, pp. 537–548, 2006.
- [413] G. Zancolli *et al.*, "When one phenotype is not enough: divergent evolutionary trajectories govern venom variation in a widespread rattlesnake species," *Proc. R. Soc. Lond. B*, vol. 286, p. 20182735, 2019.
- [414] I. B. de Farias *et al.*, "Functional and proteomic comparison of *Bothrops jararaca* venom from captive specimens and the Brazilian Bothropic Reference Venom," *J. Proteomics*, vol. 174, no. December 2017, pp. 36–46, 2018.
- [415] F. Silva-de-França *et al.*, "Naja annulifera Snake: New insights into the venom components and pathogenesis of envenomation.," *PLOS Negl. Trop. Dis.*, vol. 13, p. e0007017, 2019.
- [416] N. H. Tan and C. S. Tan, "A comparative study of cobra (*Naja*) venom enzymes," *Biochem. Physiol. B Comp. Biochem.*, vol. 90, pp. 745–750, 1988.
- [417] A. L. Bieber, "Metal and nonprotein constituents in snake venoms," in *Snake Venoms*, Heidelberg: Springer-Verlag, 1979, pp. 295–306.
- [418] D. C. Gowda and E. A. Davidson, "Structural features of carbohydrate moieties in snake venom glycoproteins," *Biochem. Biophys. Res. Co.*, vol. 182, pp. 294–301, 1992.
- [419] J. Nawarak, S. Phutrakul, and S. T. Chen, "Analysis of lectin-bound glycoproteins in snake venom from the Elapidae and Viperidae families," *J. Proteome Res.*, vol. 3, no. 3, pp. 383–392, 2004.
- [420] S. G. Soares and L. L. Oliveira, "Venom-Sweet-Venom: N-Linked Glycosylation in Snake Venom Toxins," *Protein Pept. Lett.*, vol. 16, pp. 913–919, 2009.
- [421] A. Balmert, D. Hess, C. Brücker, H. Bleckmann, and G. Westhoff, "Spitting cobras: fluid jets in nature as models for technical applications," *Bioinspiration, Biomimetics, and Bioreplication*, vol. 7975, no. March 2011, p. 797514, 2011.
- [422] R. H. Ewoldt, H. Johnston, T. Michael, and L. M. Caretta, "Experimental Challenges of Shear Rheology: How to Avoid Bad Data," in *Complex Fluids in Biological Systems*, S. Spagnolie, Ed. Springer Biological Engineering Series, 2015, pp. 207–241.
- [423] H. Ward-Smith, K. Arbuckle, A. Naude, and W. Wüster, "Fangs for the Memories? A Survey of Pain in Snakebite Patients Does Not Support a Strong Role for Defense in

- the Evolution of Snake Venom Composition,” *Toxins (Basel)*, vol. 12, p. 201, 2020.
- [424] T. Eisner and S. Camazine, “Spider leg autotomy induced by prey venom injection: An adaptive response to ‘pain’?,” *Proc. Natl. Acad. Sci. USA*, vol. 80, pp. 3382–3385, 1983.
- [425] K. V. Kardong and V. Bels, “Rattlesnake strike behavior: kinematics,” *J. Exp. Biol.*, vol. 201, pp. 837–850, 1998.
- [426] K. Jeyaseelan, A. Armugam, M. Donghui, and N. H. Tan, “Structure and phylogeny of the venom group I phospholipase A2 gene,” *Mol. Biol. Evol.*, vol. 17, no. 7, pp. 1010–1021, 2000.
- [427] W. G. Wu, “Diversity of cobra cardiotoxin,” *J. Toxicol. - Toxin Rev.*, vol. 16, no. 3, pp. 115–134, 1997.
- [428] A. Ménez, “Molecular Immunology of Snake Toxins,” *Pharmac. Ther.*, vol. 30, pp. 91–113, 1985.
- [429] Y. Cheng, L. D. Koh, D. Li, B. Ji, M. Y. Han, and Y. W. Zhang, “On the strength of β -sheet crystallites of Bombyx mori silk fibroin,” *J. R. Soc. Interface*, vol. 11, no. 96, pp. 1–8, 2014.
- [430] C. Holland, N. Hawkins, M. Frydrych, P. Laity, D. Porter, and F. Vollrath, “Differential Scanning Calorimetry of Native Silk Feedstock,” *Macromol. Biosci.*, vol. 19, no. 3, pp. 6–11, 2019.
- [431] G. Freddi, H. Kato, M. Tsukada, G. Allara, and H. Shiozaki, “Physical properties and dyeability of NaOH-treated silk fibers,” *J. Appl. Polym. Sci.*, vol. 55, no. 3, pp. 481–487, 1995.
- [432] G. Freddi, A. Bianchi Svilokos, H. Ishikawa, and M. Tsukada, “Chemical composition and physical properties of Gonometa rufobunnae silk,” *J. Appl. Polym. Sci.*, vol. 48, no. 1, pp. 99–106, 1993.
- [433] P. Cunniff *et al.*, “Mechanical and thermal properties of dragline silk from the spider Nephila clavipes,” *Polym. Adv. Technol.*, vol. 5, no. 8, pp. 401–410, 1994.
- [434] G. Ramgopal, R. Ramani, P. Ramachandra, and C. Ranganathaiah, “Structural modifications in bivoltine silk fiber under thermal treatment,” *J. Appl. Polym. Sci.*, vol. 63, no. 3, pp. 395–400, 1997.
- [435] G. Freddi, G. Pessina, and M. Tsukada, “Swelling and dissolution of silk fibroin (Bombyx mori) in N-methyl morpholine N-oxide,” *Int. J. Biol. Macromol.*, vol. 24, no. 2–3, pp. 251–263, 1999.
- [436] T. Tanaka *et al.*, “Thermal properties of bombyx mori and several wild silkworm silks phase transition of liquid silk,” *J. Therm. Anal. Calorim.*, vol. 70, no. 3, pp. 825–832, 2002.
- [437] M. Tsukada, M. Majibur, T. Tanaka, and H. Morikawa, “Thermal characteristics and physical properties of silk fabrics grafted with phosphorous flame retardant agents,” *Text. Res. J.*, vol. 81, no. 15, pp. 1541–1548, 2011.
- [438] X. Fang, T. Wyatt, J. Wu, and D. Yao, “An effective and simple process for obtaining high strength silkworm (Bombyx mori) silk fiber,” *Fibers Polym.*, vol. 16, no. 12, pp. 2609–2616, 2015.
- [439] R. Ragone, “Hydrogen-bonding classes in proteins and their contribution to the unfolding reaction,” *Protein Sci.*, vol. 10, no. 10, pp. 2075–2082, 2001.
- [440] D. L. Kaplan, “Fibrous proteins -silk as a model system,” *Polym. Degrad. Stab.*, vol. 59, pp. 25–32, 1998.
- [441] M. Ferreira, C. Hofer, and A. Raemy, “A calorimetric study of egg white proteins,” *J. Therm. Anal.*, vol. 48, no. 3, pp. 683–690, 1997.
- [442] C. Olsson, H. Jansson, and J. Swenson, “The Role of Trehalose for the Stabilization of Proteins,” *J. Phys. Chem. B*, vol. 120, no. 20, pp. 4723–4731, 2016.

- [443] J. K. Kaushik and R. Bhat, "Why is trehalose an exceptional protein stabilizer? An analysis of the thermal stability of proteins in the presence of the compatible osmolyte trehalose," *J. Biol. Chem.*, vol. 278, no. 29, pp. 26458–26465, 2003.
- [444] I. Avella *et al.*, "Unexpected lack of specialisation in the flow properties of spitting cobra venom," *J. Exp. Biol.*, vol. 224, pp. 1–11, 2021.
- [445] S. Bosch *et al.*, "Trehalose prevents aggregation of exosomes and cryodamage," *Sci. Rep.*, vol. 6, no. 5, pp. 1–11, 2016.
- [446] M. G. Rossmann and P. Argos, "Exploring structural homology of proteins," *J. Mol. Biol.*, vol. 105, no. 1, pp. 75–95, 1976.
- [447] E. Morintale, A. Harabor, C. Constantinescu, and P. Rotaru, "Use of heat flows from DSC curve for calculation of specific heat of the solid materials," *Ann. Univ. Craiova, Phys.*, vol. 23, pp. 89–94, 2013.
- [448] K. Gekko, S. Koga, and F. Science, "Increased of Sugars Thermal and Stability of Collagen in the Presence Sugars and polyols," *J. Biochem.*, vol. 94, no. 1, pp. 199–205, 1983.
- [449] E. Tornberg, "Effects of heat on meat proteins - Implications on structure and quality of meat products," *Meat Sci.*, vol. 70, pp. 493–508, 2005.
- [450] C. Wang, M. Eufemi, C. Turano, and A. Giartosio, "Influence of the carbohydrate moiety on the stability of glycoproteins," *Biochemistry*, vol. 35, no. 23, pp. 7299–7307, 1996.
- [451] M. del Carmen Fernandez-Alonso, D. Diaz, M. Alvaro Berbis, F. Marcelo, J. Canada, and J. Jimenez-Barbero, "Protein-Carbohydrate Interactions Studied by NMR: From Molecular Recognition to Drug Design," *Curr. Protein Pept. Sci.*, vol. 13, no. 8, pp. 816–830, 2013.
- [452] H. J. Gabius, H. C. Siebert, S. André, J. Jiménez-Barbero, and H. Rüdiger, "Chemical biology of the sugar code," *ChemBioChem*, vol. 5, no. 6, pp. 740–764, 2004.
- [453] J. Jimenez-Barbero, F. Cañada, J. Asensio, N. Aboitiz, and P. Vidal, "Hevein Domains: An Attractive Model to Study Carbohydrate–Protein Interactions at Atomic Resolution," *Adv. Carbohydr. Chem. Biochem.*, vol. 60, pp. 303–354, 2006.
- [454] J. L. Asensio, F. J. Cañada, M. Bruix, A. Rodriguez-Romero, and J. Jimenez-Barbero, "The interaction of hevein with N-acetylglucosamine-containing oligosaccharides. Solution structure of hevein complexed to chitobiose," *Eur J Biochem*, vol. 2, pp. 621–633, 1995.
- [455] S. D. Allison, B. Chang, T. W. Randolph, and J. F. Carpenter, "Hydrogen bonding between sugar and protein is responsible for inhibition of dehydration-induced protein unfolding," *Arch. Biochem. Biophys.*, vol. 365, no. 2, pp. 289–298, 1999.
- [456] N. Soltanizadeh, L. Mirmoghtadaie, F. Nejati, L. I. Najafabadi, M. K. Heshmati, and M. Jafari, "Solid-state protein-carbohydrate interactions and their application in the food industry," *Compr. Rev. Food Sci. Food Saf.*, vol. 13, no. 5, pp. 860–870, 2014.
- [457] T. Arakawa, S. J. Prestrelski, W. C. Kenney, and J. F. Carpenter, "Factors affecting short-term and long-term stabilities of proteins," *Adv. Drug Deliv. Rev.*, vol. 46, pp. 307–326, 2001.
- [458] K. Monkos, "Determination of the glass-transition temperature of proteins from a viscometric approach," *Int. J. Biol. Macromol.*, vol. 74, pp. 1–4, 2015.
- [459] J. Guan *et al.*, "Glass transitions in native silk fibres studied by dynamic mechanical thermal analysis," *Soft Matter*, vol. 12, no. 27, pp. 5926–5936, 2016.
- [460] S. Cardona, C. Schebor, M. P. Buera, M. Karel, and J. Chirife, "Thermal stability of invertase in reduced-moisture amorphous matrices in relation to glassy state and trehalose crystallization," *J. Food Sci.*, vol. 62, no. 1, pp. 105–112, 1997.
- [461] K. D. Roe and T. P. Labuza, "Glass transition and crystallization of amorphous

- trehalose-sucrose mixtures,” *Int. J. Food Prop.*, vol. 8, no. 3, pp. 559–574, 2005.
- [462] F. L. Jara and A. M. R. Pilosof, “Glass transition temperature of protein/polysaccharide co-dried mixtures as affected by the extent and morphology of phase separation,” *Thermochim. Acta*, vol. 487, no. 1–2, pp. 65–73, 2009.
- [463] M. Medina-Vivanco, P. J. A. Sobral, A. M. Sereno, and M. D. Hubinger, “Denaturation and the glass transition temperatures of myofibrillar proteins from osmotically dehydrated tilapia: Effect of sodium chloride and sucrose,” *Int. J. Food Prop.*, vol. 10, no. 4, pp. 791–805, 2007.
- [464] E. C. López-Díez and S. Bone, “The interaction of trypsin with trehalose: an investigation of protein preservation mechanisms,” *Biochim Biophys Acta*, vol. 1673, no. 3, pp. 139–148, 2004.
- [465] J. Buitink, I. J. Van Den Dries, F. A. Hoekstra, M. Alberda, and M. A. Hemminga, “High critical temperature above T_g may contribute to the stability of biological systems,” *Biophys. J.*, vol. 79, no. 2, pp. 1119–1128, 2000.
- [466] L. Slade and H. Levine, “Water relationships in starch transitions,” *Carbohydr. Polym.*, vol. 21, no. 2–3, pp. 105–131, 1993.
- [467] J. M. Aguilera, G. Levi, and M. Karel, “Effect of Water Content on the Glass Transition and Caking of Fish Protein Hydrolyzates,” *Biotechnol. Prog.*, vol. 9, no. 6, pp. 651–654, 1993.
- [468] I. H. Tsai, H. C. Chang, J. M. Chen, A. C. Cheng, and K. H. Khoo, “Glycan structures and intrageneric variations of venom acidic phospholipases A₂ from *Tropidolaemus pitvipers*,” *FEBS J.*, vol. 279, no. 15, pp. 2672–2682, 2012.
- [469] J. S. Yoneda, A. J. Miles, A. P. U. Araujo, and B. A. Wallace, “Differential dehydration effects on globular proteins and intrinsically disordered proteins during film formation,” *Protein Sci.*, vol. 26, no. 4, pp. 718–726, 2017.
- [470] C. C. Liu, C. C. Lin, Y. C. Hsiao, P. J. Wang, and J. S. Yu, “Proteomic characterization of six Taiwanese snake venoms: Identification of species-specific proteins and development of a SISCAPA-MRM assay for cobra venom factors,” *J. Proteomics*, vol. 187, pp. 59–68, 2018.
- [471] F. Costal-Oliveira *et al.*, “L-amino acid oxidase from *Bothrops atrox* snake venom triggers autophagy, apoptosis and necrosis in normal human keratinocytes,” *Sci. Rep.*, vol. 9, no. 1, pp. 1–14, 2019.
- [472] F. Calderón-Celis, L. Cid-Barrio, J. R. Encinar, A. Sanz-Medel, and J. J. Calvete, “Absolute venomomics: Absolute quantification of intact venom proteins through elemental mass spectrometry,” *J. Proteomics*, vol. 164, pp. 33–42, 2017.
- [473] J. Ahmed, H. S. Ramaswamy, I. Alli, and V. G. S. Raghavan, “Protein denaturation, rheology, and gelation characteristics of radio-frequency heated egg white dispersions,” *Int. J. Food Prop.*, vol. 10, no. 1, pp. 145–161, 2007.
- [474] D. Porter and F. Vollrath, “The role of kinetics of water and amide bonding in protein stability,” *Soft Matter*, vol. 4, no. 2, pp. 328–336, 2008.
- [475] P. Relkin, “Differential scanning calorimetry: A useful tool for studying protein denaturation,” *Thermochim. Acta*, vol. 246, no. 2, pp. 371–386, 1994.
- [476] A. A. Walker, C. Holland, and T. D. Sutherland, “More than one way to spin a crystallite: multiple trajectories through liquid crystallinity to solid silk,” *Proc. R. Soc. B Biol. Sci.*, vol. 282, no. 1809, p. 20150259, 2015.
- [477] V. M. Girish, S. Kumar, L. Joseph, C. Jobichen, R. M. Kini, and J. Sivaraman, “Identification and Structural Characterization of a New Three-Finger Toxin Hemachatoxin from *Hemachatus haemachatus* Venom,” *PLoS One*, vol. 7, no. 10, pp. 1–9, 2012.
- [478] M. C. Deller, L. Kong, and B. Rupp, “Protein stability: A crystallographer’s

- perspective,” *Acta Crystallogr. Sect. Struct. Biol. Commun.*, vol. 72, pp. 72–95, 2016.
- [479] D. Ringe and G. A. Petsko, “The ‘glass transition’ in protein dynamics: What it is, why it occurs, and how to exploit it,” *Biophys. Chem.*, vol. 105, no. 2–3, pp. 667–680, 2003.
- [480] T. Morita, “Structures and functions of snake venom CLPs (C-type lectin-like proteins) with anticoagulant-, procoagulant-, and platelet-modulating activities,” *Toxicon*, vol. 45, no. 8, pp. 1099–1114, 2005.
- [481] A. M. Smith and M. C. Morin, “Biochemical differences between trail mucus and adhesive mucus from marsh periwinkle snails,” *Biol. Bull.*, vol. 203, no. 3, pp. 338–346, 2002.
- [482] O. Olsen and K. K. Thomsen, “Improvement of bacterial β -glucanase thermostability by glycosylation,” *J. Gen. Microbiol.*, vol. 137, no. 3, pp. 579–585, 1991.
- [483] R. M. Kini, “Structure-function relationships and mechanism of anticoagulant phospholipase A2 enzymes from snake venoms,” *Toxicon*, vol. 45, no. 8, pp. 1147–1161, 2005.
- [484] P. H. Kao, K. C. Chen, S. R. Lin, and L. Sen Chang, “The structural and functional contribution of N-terminal region and His-47 on Taiwan cobra phospholipase A2,” *J. Pept. Sci.*, vol. 14, no. 3, pp. 342–348, 2008.
- [485] F. Kornalík, “The influence of snake venom enzymes on blood coagulation,” *Pharmacol. Ther.*, vol. 29, no. 3, pp. 353–405, 1985.
- [486] D. B. Kunkel, S. C. Curry, M. V. Vance, and P. J. Ryan, “Reptile envenomations,” *Clin. Toxicol.*, vol. 21, no. 4–5, pp. 503–526, 1983.
- [487] C. W. Radcliffe *et al.*, “Immobilization of mice following envenomation by cobras (*Naja mossambica pallida*),” *Bull. Psychon. Soc.*, vol. 21, no. 3, pp. 3–6, 1983.
- [488] N. J. Shirlcliffe, G. McHale, and M. I. Newton, “Wet adhesion and adhesive locomotion of snails on anti-adhesive non-wetting surfaces,” *PLoS One*, vol. 7, no. 5, pp. 5–9, 2012.
- [489] C. Teng, W. Jy, and C. Ouyang, “Cardiotoxin from *Naja Naja Atra* Snake Venom: A Potentiator of Platelet Aggregation,” *Toxicon*, vol. 22, no. 3, pp. 463–470, 1984.
- [490] P. R. Laity, E. Baldwin, and C. Holland, “Changes in Silk Feedstock Rheology during Cocoon Construction: The Role of Calcium and Potassium Ions,” *Macromol. Biosci.*, vol. 19, no. 3, pp. 1–11, 2018.
- [491] P. R. Laity and C. Holland, “Thermo-rheological behaviour of native silk feedstocks,” *Eur. Polym. J.*, vol. 87, pp. 519–534, 2017.
- [492] M. Miotto *et al.*, “Insights on protein thermal stability: A graph representation of molecular interactions,” *Bioinformatics*, vol. 35, no. 15, pp. 2569–2577, 2019.
- [493] C. M. Beliciu and C. I. Moraru, “The effect of protein concentration and heat treatment temperature on micellar casein-soy protein mixtures,” *Food Hydrocoll.*, vol. 25, no. 6, pp. 1448–1460, 2011.
- [494] P. Fisher, J. Thomas-Oates, A. J. Wood, and D. Ungar, “The N-Glycosylation Processing Potential of the Mammalian Golgi Apparatus,” *Front. Cell Dev. Biol.*, vol. 7, no. August, pp. 1–11, 2019.
- [495] M. Kiyoshi, K. I. Tatematsu, M. Tada, H. Sezutsu, H. Shibata, and A. Ishii-Watabe, “Structural insight and stability of TNFR-Fc fusion protein (Etanercept) produced by using transgenic silkworms,” *J. Biochem.*, vol. 169, no. 1, pp. 25–33, 2021.
- [496] CABI, “Invasive Species Compendium,” *Achatina fulica (giant African land snail)*, 2020. [Online]. Available: <https://www.cabi.org/isc/>. [Accessed: 16-May-2021].
- [497] F. S. Albuquerque *et al.*, “Distribution, feeding behavior and control strategies of the exotic land snail *Achatina fulica* (Gastropoda: Pulmonata) in the northeast of Brazil,” *Brazilian J. Biol.*, vol. 68, no. 4, pp. 837–842, 2008.

- [498] B. A. Young and K. V. Kardong, “The functional morphology of hooding in cobras,” *J. Exp. Biol.*, vol. 213, no. 9, pp. 1521–1528, 2010.
- [499] B. A. Young, M. Boetig, and G. Westhoff, “Functional bases of the spatial dispersal of venom during cobra ‘spitting,’” *Physiol. Biochem. Zool.*, vol. 82, no. 1, pp. 80–89, 2009.
- [500] R. Reboreda and M. S. Davies, “Characterisation by X-ray microanalysis of metal granules in the mucus trails of *Littorina littorea* (Gastropoda) along a putative pollution gradient,” *Ecotoxicology*, vol. 15, no. 5, pp. 403–410, 2006.
- [501] A. M. Wilks, S. R. Rabice, H. S. Garbacz, C. C. Harro, and A. M. Smith, “Double-network gels and the toughness of terrestrial slug glue,” *J. Exp. Biol.*, vol. 218, no. 19, pp. 3128–3137, Oct. 2015.
- [502] A. Coulter-Parkhill, S. McClean, V. A. Gault, and N. Irwin, “Therapeutic Potential of Peptides Derived from Animal Venoms: Current Views and Emerging Drugs for Diabetes,” *Clin. Med. Insights Endocrinol. Diabetes*, vol. 14, pp. 1–13, 2021.
- [503] M. Muttenthaler, G. F. King, D. J. Adams, and P. F. Alewood, “Trends in peptide drug discovery,” *Nat. Rev. Drug Discov.*, vol. 20, no. 4, pp. 309–325, 2021.
- [504] P. A. Rühls, J. Bergfreund, P. Bertsch, S. J. Gstöhl, and P. Fischer, “Complex fluids in animal survival strategies,” *Soft Matter*, vol. 17, no. 11, pp. 3022–3036, 2021.
- [505] A. Baer, S. Schmidt, S. Haensch, M. Eder, G. Mayer, and M. J. Harrington, “Mechanoresponsive lipid-protein nanoglobules facilitate reversible fibre formation in velvet worm slime,” *Nat. Commun.*, vol. 8, no. 1, pp. 1–7, 2017.
- [506] T. Soares and E. Santos, “Preliminary design of fuel filling systems applying the extended bernoulli equation on numerical calculation tools,” *SAE Tech. Pap.*, vol. 13, pp. 1–6, 2013.
- [507] B. R. Munson, D. F. Young, and T. H. Okiishi, *Fundamentals of fluid mechanics*, 6th ed. New Jersey: John Wiley and Sons, Inc., 2006.

APPENDICES

APPENDIX A1. CHAPTER 4: UV-Vis

Fourier self-deconvolution and curve fitting were performed as it is described in **Section 2.2.2**. Four peaks were selected for all species and are highlighted in **figure A1**, in order to include absorbances at four different wavelength ranges, considered in equations 1 and 2. Peak 1, corresponds to 212-215 nm; Peak 2, 222-225 nm; Peak 3, 227-230 nm; and Peak 4, 257-260 nm. Only two or three of the four peaks are obtained for each spectrum.

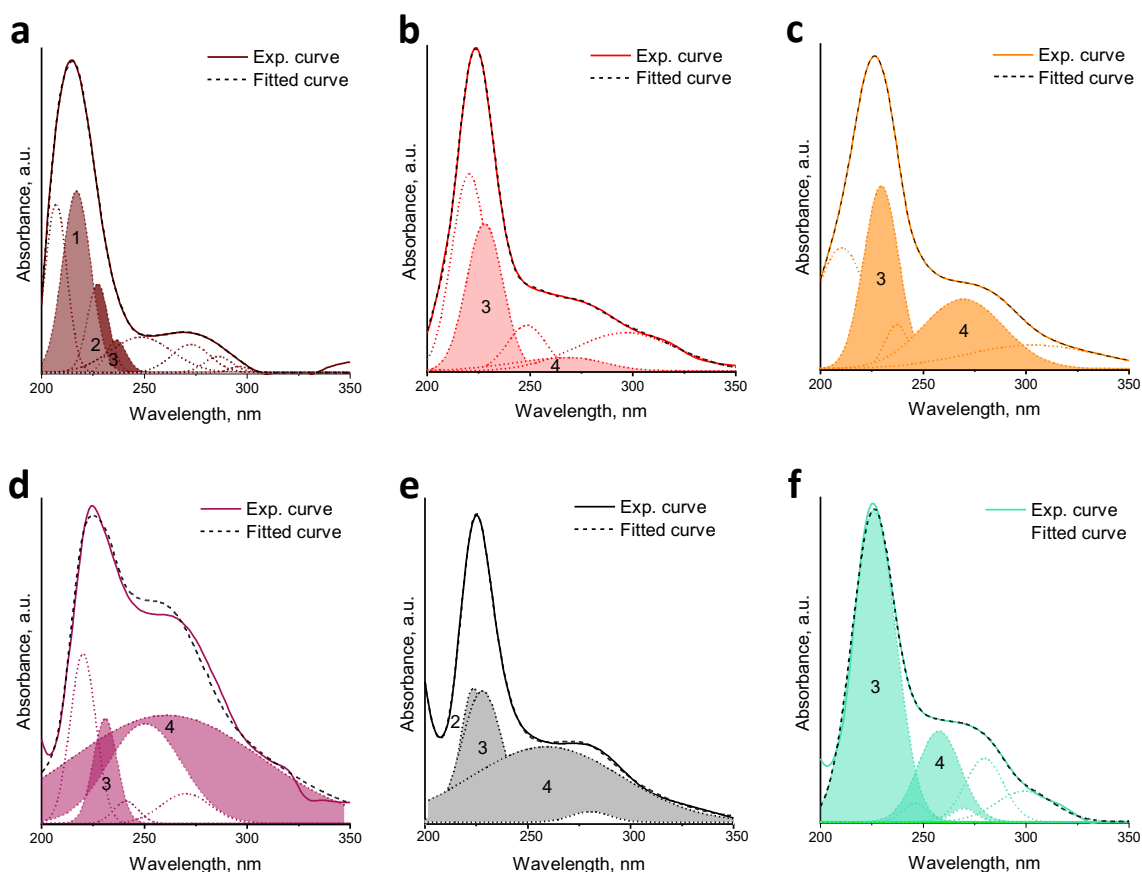


FIGURE A1.1 Gaussian fitting corresponding to a) *A. fulica*, b) *C. aspersum*, c) *C. nemoralis*, d) *A. ater*, e) *A. hortensis* and f) *L. flavus*. Peaks 1, 2, 3 and 4 correspond to coloured areas.

Figure A2 shows the relative percentage of each peak obtained for the six species, considering only Peaks 1, 2, 3 and 4, respectively.

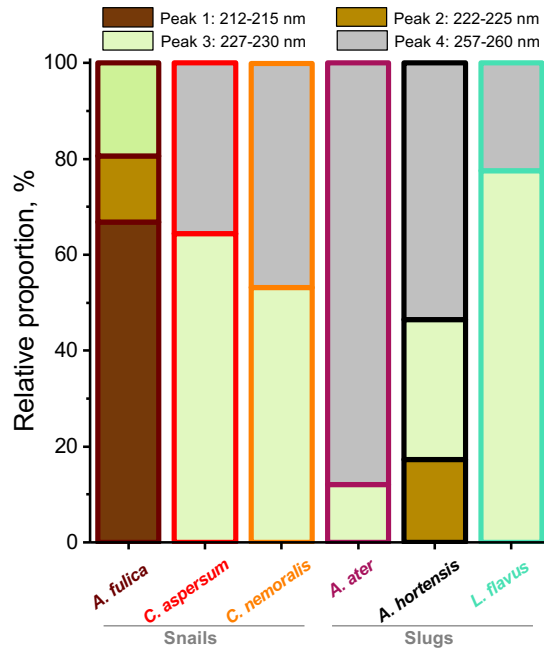


FIGURE A1.2 Relative proportion of peaks 1, 2, 3 and 4 for each species, obtained from UV-vis Gaussian fitting.

Peak 1 is only obtained in *A. fulica* spectrum, while peaks 3 and 4 are observed in the other five spectra.

APPENDIX A2. CHAPTER 4: RHEOLOGY

Figure A2. G' and G'' for the six species, where $G' > G''$.

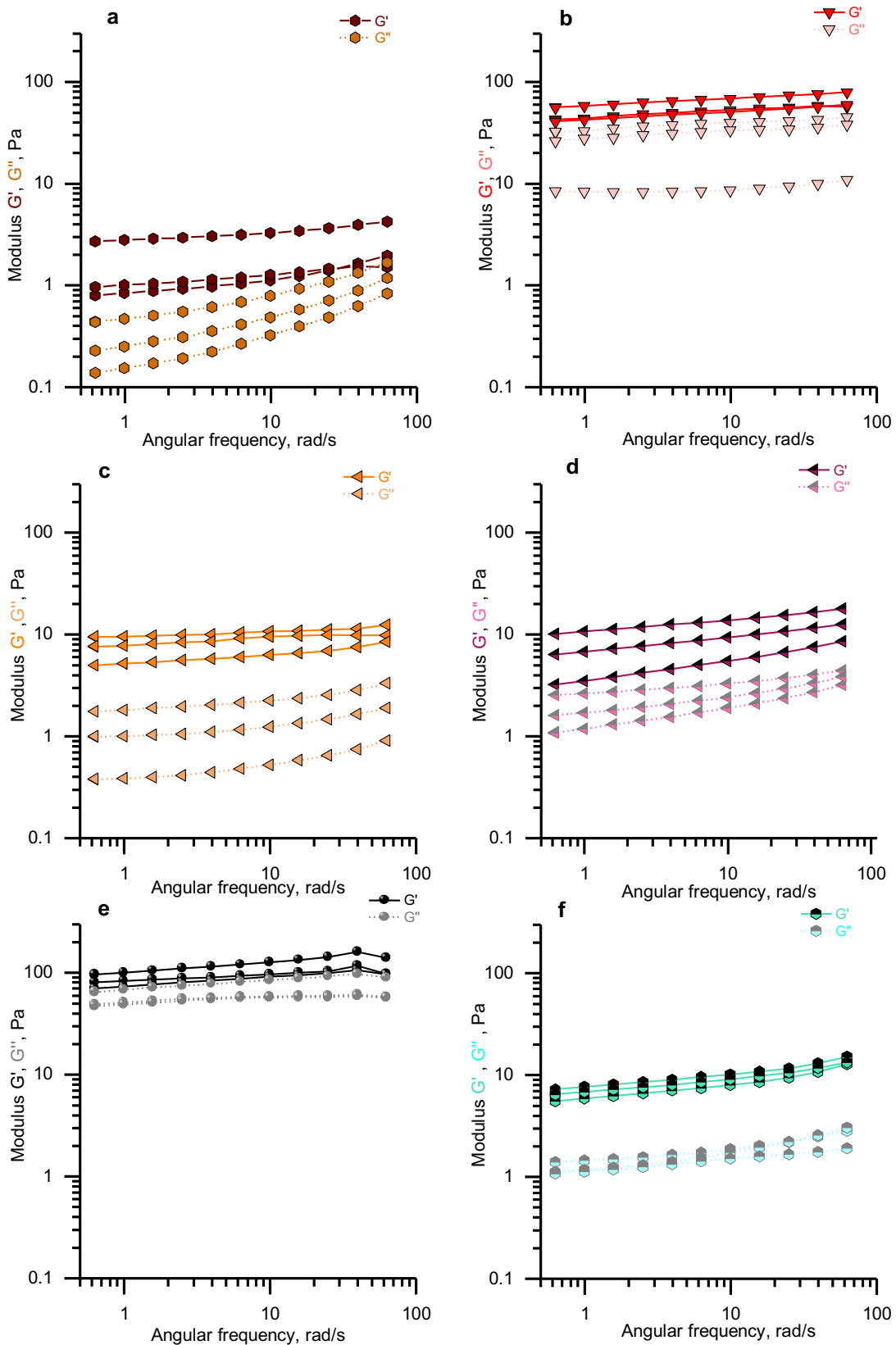


FIGURE A2 Oscillatory measurements of a) *A. fulica*, b) *C. aspersum*, c) *C. nemoralis*, d) *A. ater*, e) *A. hortensis* and f) *L. maximus* native mucus. Each line represents an individual data set.

APPENDIX A3. CHAPTER 5: SNAKES' DETAILS

TABLE A3. Details for each snake included in this study

Family	Species	Specimen code	Behaviour	Continent	Origin
Viperidae	<i>B. arietans</i>	BitAriNGA003	Non-spitter	Africa	Nigeria
Elapidae	<i>H. haemachatus</i>	HemHaeCB001	Primitive spitter		Captive bred
	<i>N. pallida</i>	NajPalKEN001	Spitter		Kenya
		NajPalKEN002			
		NajPalTZA002			
	<i>N. nubiae</i>	NajNubCB001			Captive bred
		NajNubCB003			
		NajNubCB004			
	<i>N. mossambica</i>	NajMosTZA001			Tanzania
		NajMosTZA002			
		NajMosTZA003			
	<i>N. nigricollis</i>	NajNigNGA001			Nigeria
		NajNigNGA002			
		NajNigNGA003			
		NajNigNGA004			
		NajNigTGO001			
	<i>N. subfulva</i>	NajMelCMR001			Cameroon
		NajMelUGA001			
<i>N. nivea</i>	NajNivZAF003	South Africa			
	NajNivZAF004				
<i>N. haje</i>	NajHajUGA001	Uganda			
	NajHajUGA004				
<i>N. annulifera</i>	NajAnnCB002	Captive bred			
<i>N. naja</i>	NajNajCB001				
<i>N. siamensis</i>	NajSiaCB002				
<i>N. philippinensis</i>	NajPhiCB001	Spitter	Asia		
<i>N. atra</i>	NajAtrCBT002	Non-spitter			
<i>N. kaouthia</i>	NajKaoCB001	Spitter			
	NajKaoCB002				
	NajKaoCB003				

APPENDIX A4. CHAPTER 5: SDS-PAGE

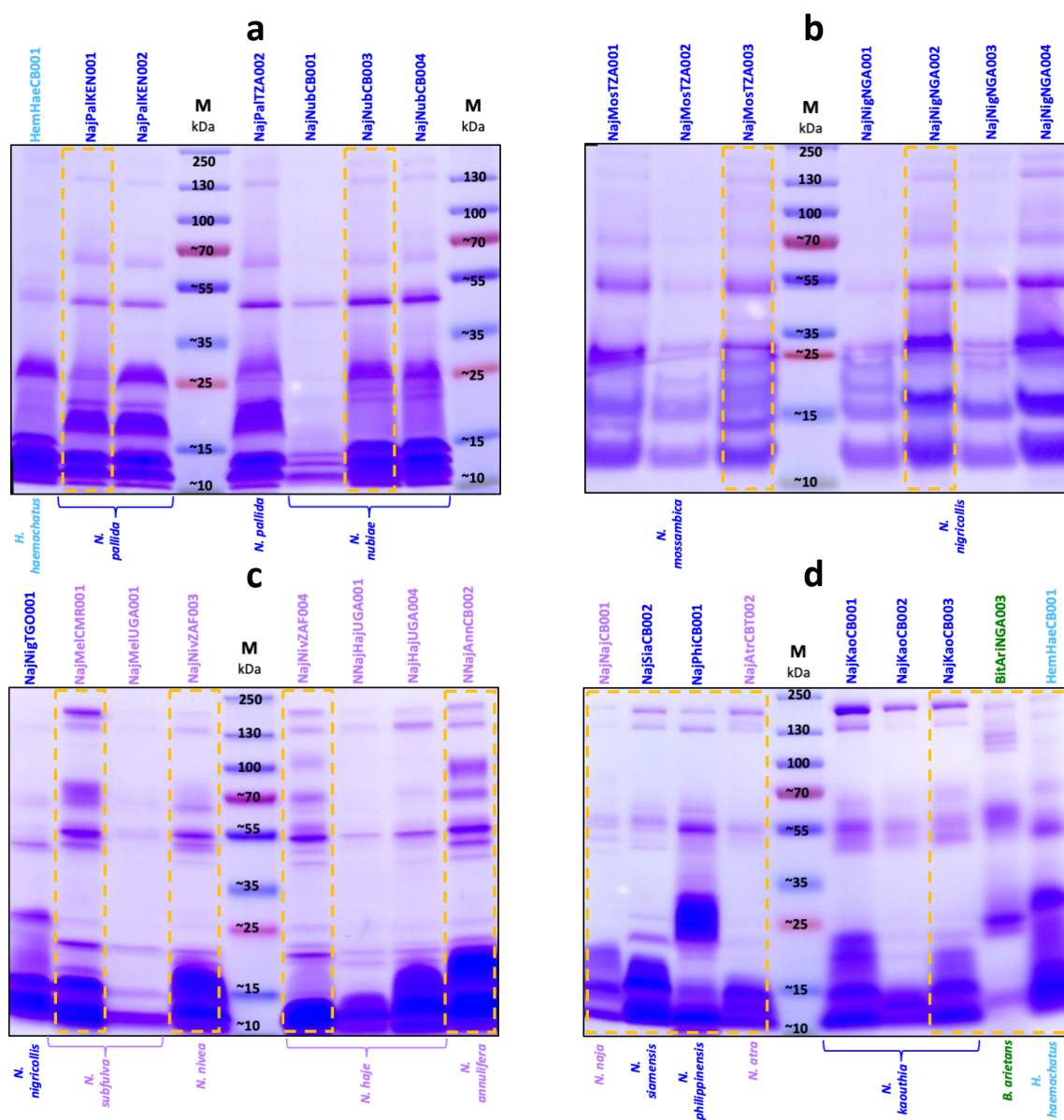


FIGURE A4 Electrophoregrams for all snakes corresponding to species: a) *H. haemachatus*, *N. pallida*, and *N. nubiae*; b) *N. mossambica* and *N. nigricollis*; c) *N. nigricollis*, *N. subfulva*, *N. nivea*, *N. haje* and *N. annulifera*; and d) *N. naja*, *N. siamensis*, *N. philippinensis*, *N. atra*, *N. kaouthia*, *B. arietans* and *H. haemachatus* (this last species corresponds to the same primitive snake shown in figure A4a). Specimen codes correspond to snakes described in table A3. Yellow dotted rectangles highlight selected profiles shown in figure 5.1, for comparison purposes.

APPENDIX A5. CHAPTER 6: PROPERTIES OF VENOMS' SAMPLES

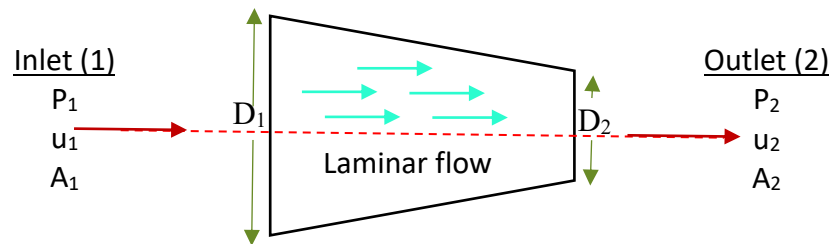
TABLE A5. Properties of the venom samples per specimen

Species	Specimen code	Total solids concentration, w/w	Spitting mode	Continent	Origin	
<i>B. arietans</i>	BitAriNGA003	0.2253	Non-spitter	Africa	Nigeria	
<i>H. haemachatus</i>	HemHaeCB001	0.2540	Mixed		Captive bred	
<i>N. pallida</i>	NajPaKEN001	0.2688	Streams		Kenya	
	NajPaKEN002	0.2688			Tanzania	
	NajPaTZA002	0.2688			Captive bred	
<i>N. nubiae</i>	NajNubCB001	0.3082				
	NajNubCB003	0.3082				
	NajNubCB004	0.3082				
<i>N. mossambica</i>	NajMosTZA001	0.2758			Tanzania	
	NajMosTZA002	0.2758				
	NajMosTZA003	0.2758				
<i>N. nigricollis</i>	NajNigNGA001	0.2723			Mist	Nigeria
	NajNigNGA002	0.2723				
	NajNigNGA003	0.2723				
	NajNigNGA004	0.2723				
	NajNigTGO001	0.2959				Togo
<i>N. subfulva</i>	NajMelCMR001	0.2240		Non-spitter	Cameroon	
	NajMelUGA001	0.2516			Uganda	
<i>N. nivea</i>	NajNivZAF003	0.2985	South Africa			
<i>N. haje</i>	NajNivZAF004	0.2996	Uganda			
	NajHajUGA001	0.2879				
	NajHajUGA004	0.2996				
<i>N. annulifera</i>	NajAnnCB002	0.3150	Asia		Captive bred	
<i>N. naja</i>	NajNajCB001	0.2604				
<i>N. siamensis</i>	NajSiaCB002	0.3094				Mist
<i>N. philippinensis</i>	NajPhiCB001	0.200				Streams
<i>N. atra</i>	NajAtrCBT002	0.2500				Non-spitter
<i>N. kaouthia</i>	NajKaoCB001	0.2871				Streams
	NajKaoCB002	0.2871				
	NajKaoCB003	0.2871				

APPENDIX A6. CHAPTER 6: DELTA PRESSURE EQUATION

There is pressure loss in fangs associated to converging diameter, meaning that $r_{\text{base of the fang}} > r_{\text{end of the fang and close to the exit orifice}}$, which is in line with our fang measurements using microCT data (data analysed from [129]; available at GigaScience Database, <http://dx.doi.org/10.5524/100389>). However, this is not the only effect in pressure loss, because there is also the effect of venom flowing in the venom channel, i.e., viscous pressure loss. Then Poiseuille's law is not correct in this case because there is no constant diameter in the venom channel (and fang's morphology), and Bernoulli's equation is only accepted if there is no viscous pressure loss. Therefore, an extended generalized Bernoulli equation must be used in order to have an approximation of the pressure loss in the venom channel considering radius variations and viscosity [399].

If the venom channel is considered as a converging radius pipe:



Then, the generalized Bernoulli's equation considered for the venom channel can be written as:

$$P_1 + \frac{u_1^2 \cdot \rho}{2} = P_2 + \frac{u_2^2 \cdot \rho}{2} + h_f \cdot \rho \cdot g \quad (\text{equation A6.1})$$

Where:

P_1 and P_2 are the pressures at the inlet (1) and outlet (2) points, in Pa.

u_1 and u_2 are the velocities at the inlet (1) and outlet (2) points, in $\text{m} \cdot \text{s}^{-1}$.

ρ is the density of venom, in $\text{kg} \cdot \text{m}^{-3}$.

h_f corresponds to losses due to viscosity, in m.

g is the acceleration of gravity, $9.81 \text{ m} \cdot \text{s}^{-2}$.

h_f can be expressed as [506]:

$$h_f = \frac{f \cdot l}{D} \cdot \frac{\bar{u}^2}{2g} \quad (\text{equation A6.2})$$

Where:

f is the friction factor, dimensionless.

l is the length of the venom channel, in m.

D is the average diameter of the venom channel, in m.

\bar{u} is the average velocity of the venom in the venom channel, in m, and it can be calculated with the following equation:

$$\bar{u} = \frac{Q}{\bar{A}} \quad (\text{equation A6.3})$$

Where:

Q is the volumetric flow in the venom channel, in $\text{m}^3 \cdot \text{s}^{-1}$.

\bar{A} is the average cross section area of the venom channel, in m^2 .

The friction factor, for laminar flow, can be expressed as:

$$f = \frac{64}{Re} \quad (\text{equation A6.4})$$

Where:

Re is the Reynolds number, dimensionless.

If we combine equations A6.4 and A6.2, we obtain:

$$h_f = \frac{64}{Re} \cdot \frac{l}{D} \cdot \frac{\bar{u}^2}{2g} \quad (\text{equation A6.5})$$

And combining equations A6.5 and A6.1:

$$P_1 + \frac{u_1^2 \cdot \rho}{2} = P_2 + \frac{u_2^2 \cdot \rho}{2} + \frac{64}{Re} \cdot \frac{l}{D} \cdot \frac{\bar{u}^2}{2} \cdot \rho \quad (\text{equation A6.6})$$

From the Continuity Equation [507]:

$$A_1 \cdot u_1 = A_2 \cdot u_2 \quad (\text{equation A6.7})$$

Where:

A_1 and A_2 are the cross-section areas at the inlet and outlet points, in m^2 .

Rearranging equation A6.7:

$$u_2 = \frac{A_1 \cdot u_1}{A_2} \quad (\text{equation A6.8})$$

If we define $P_1 - P_2 = \Delta P$, rearrange equation s6, and combining with equation A6.8:

$$\Delta P = P_1 - P_2 = \frac{\rho}{2} \cdot u_1^2 \left(\left(\frac{A_1}{A_2} \right)^2 - 1 \right) + \frac{64}{Re} \cdot \frac{l}{D} \cdot \frac{\bar{u}^2}{2} \cdot \rho \quad (\text{equation 6.3})$$

Which is the equation used to calculate the pressure loss in the venom channel.

APPENDIX A7. CHAPTER 6: RHEOLOGY- EXPERIMENTAL WINDOW

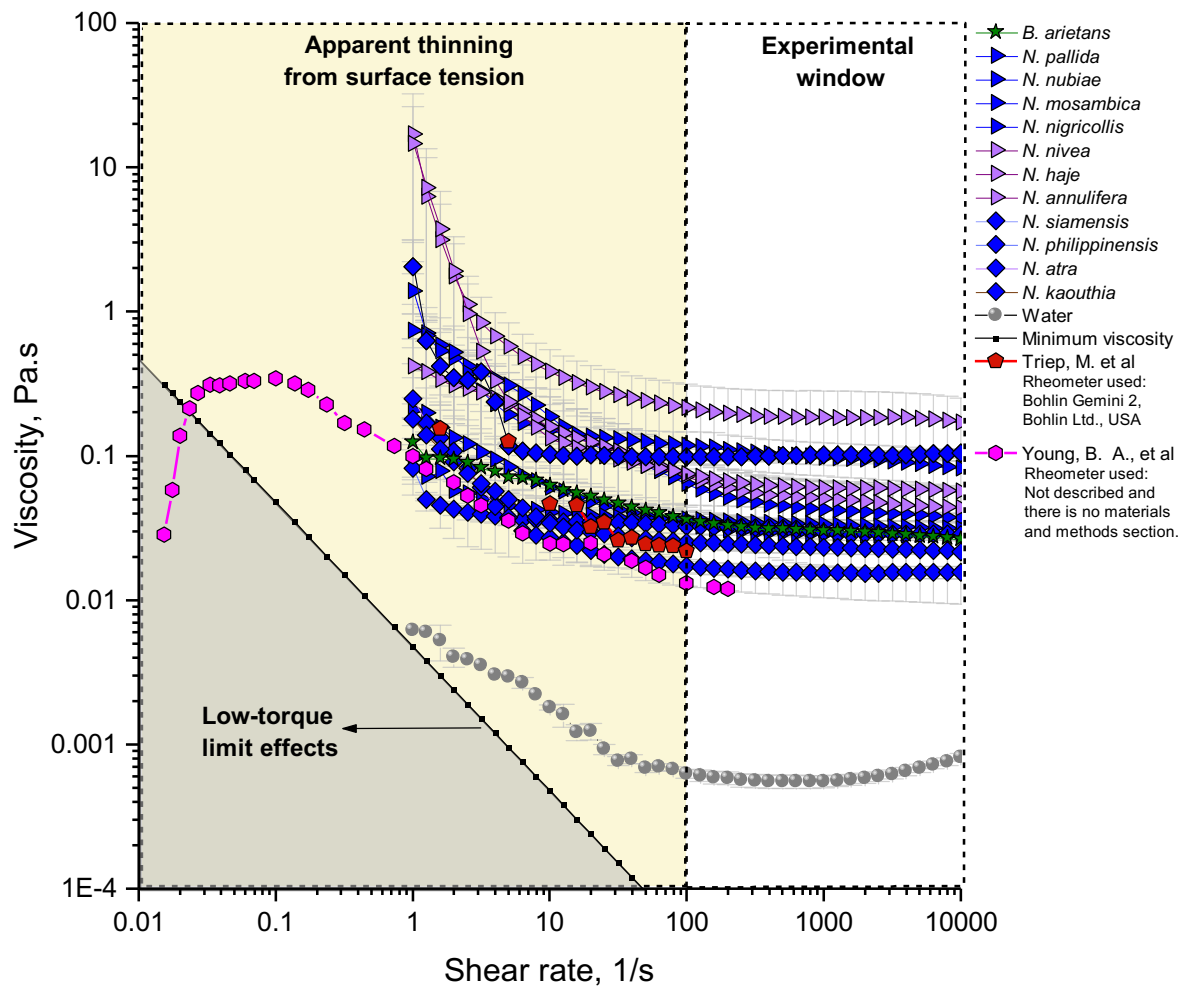


FIGURE A7 Rheological data comparing previous studies and indicating data attributed to artifacts, and reliable data (experimental window).

APPENDIX A8: CHAPTER 7. DSC

Figures A8.1 to A8.8, show thermograms of the six species, indicating the thermal events.

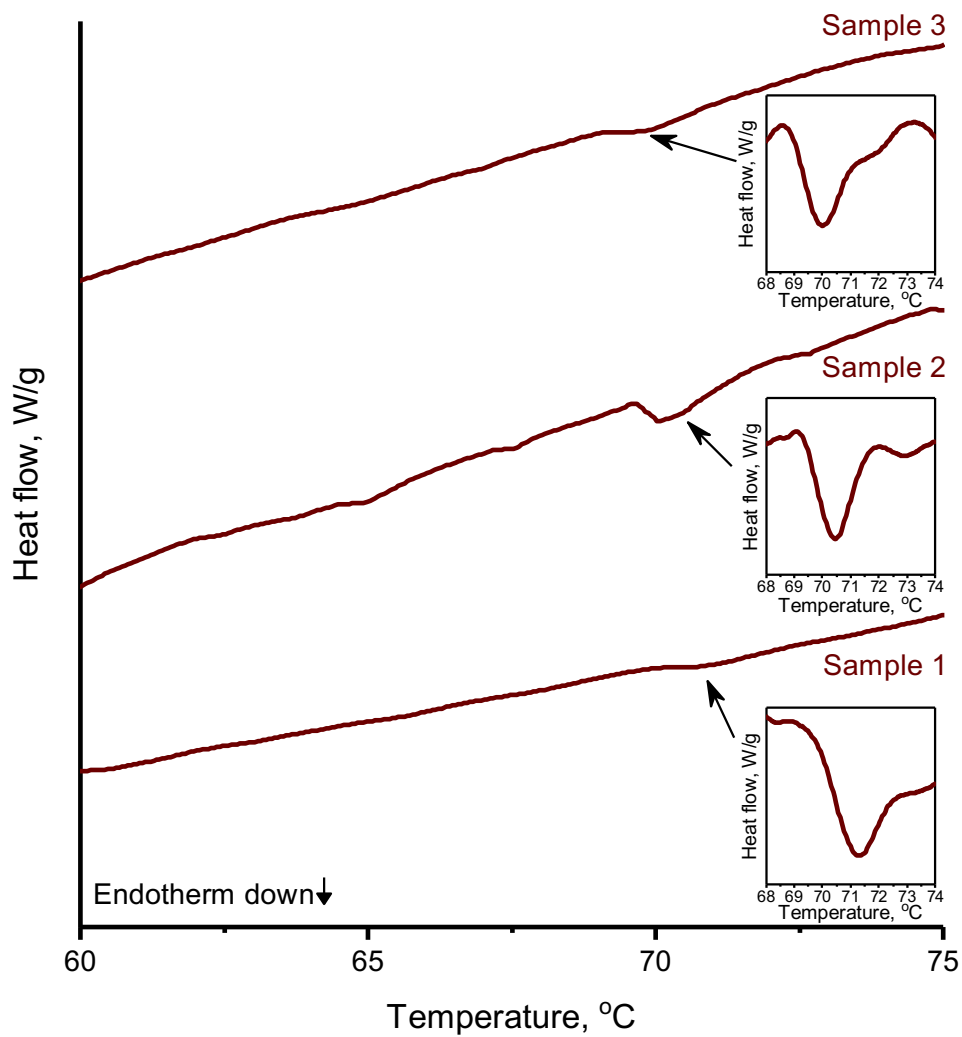


FIGURE A8.1 Thermogram of *A. fulica* mucus corresponding to the three measurements.

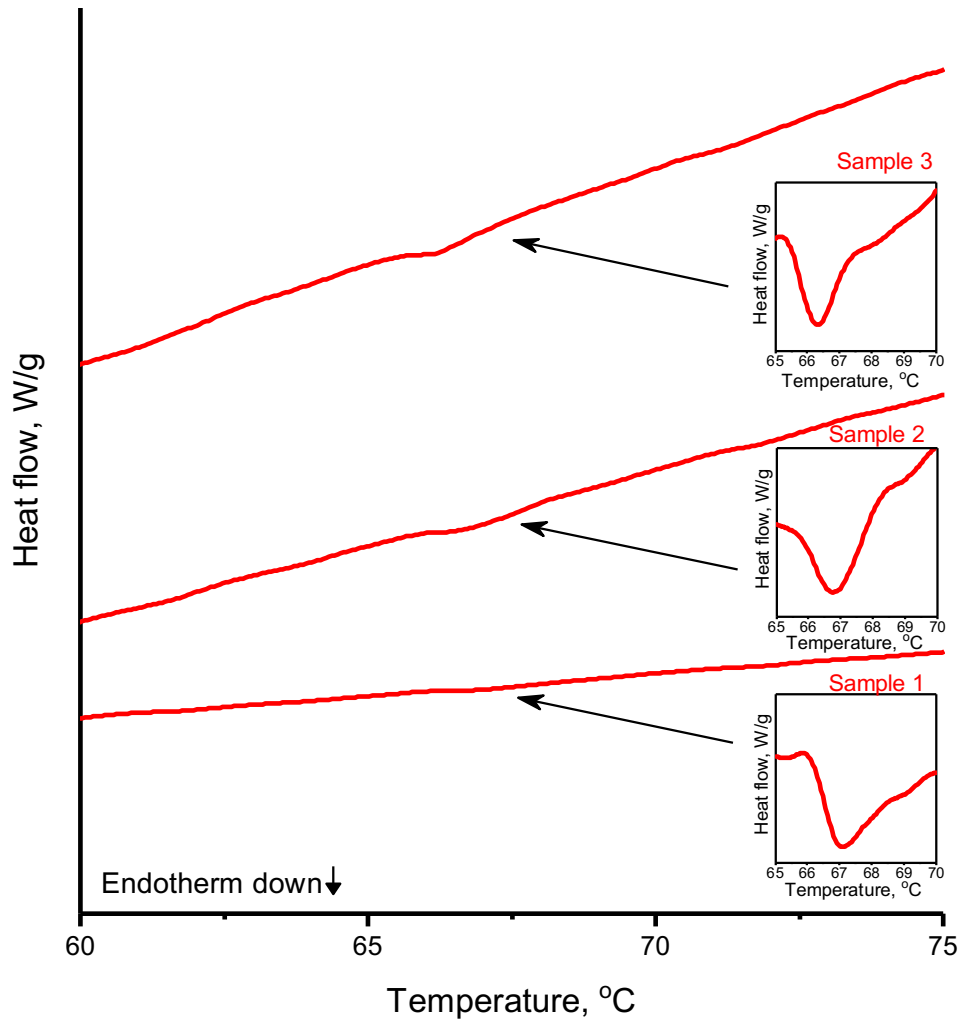


FIGURE A8.2 Thermogram of *C. aspersum* mucus corresponding to the three measurements.

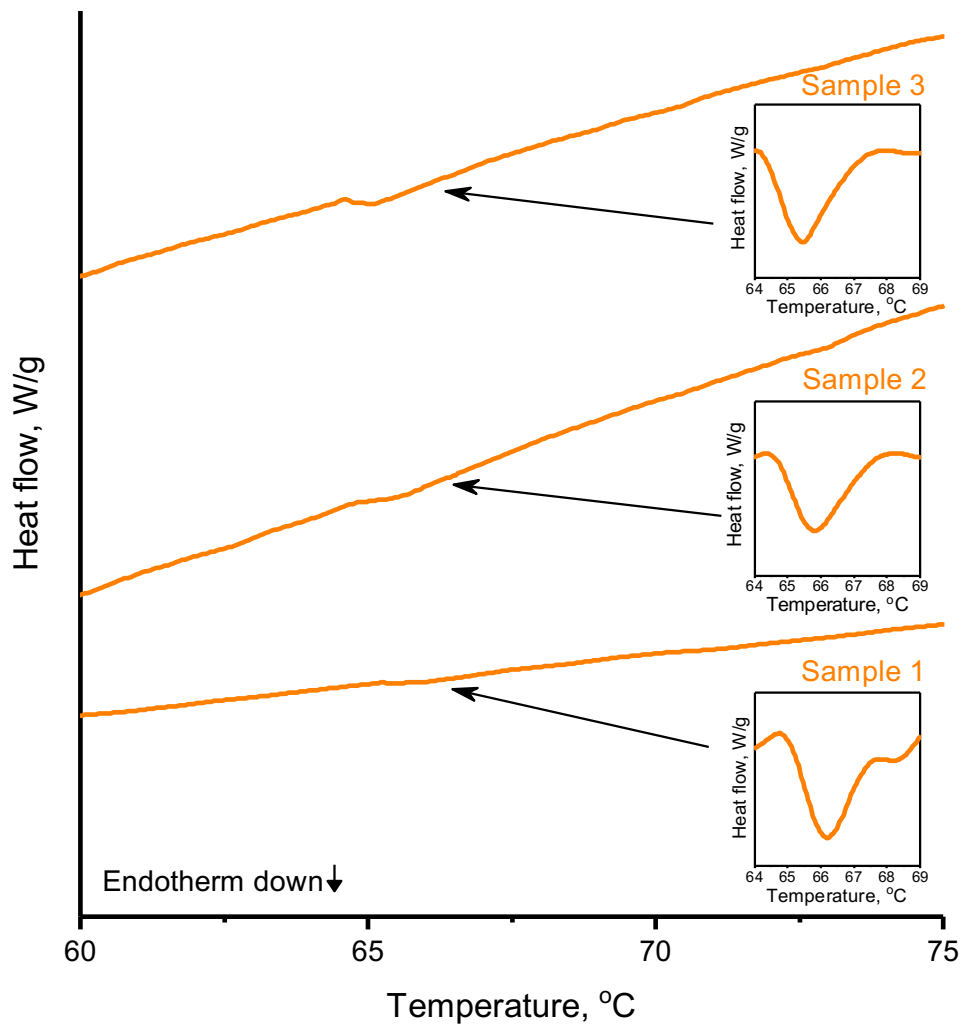


FIGURE A8.3 Thermogram of *C. nemoralis* mucus corresponding to the three measurements.

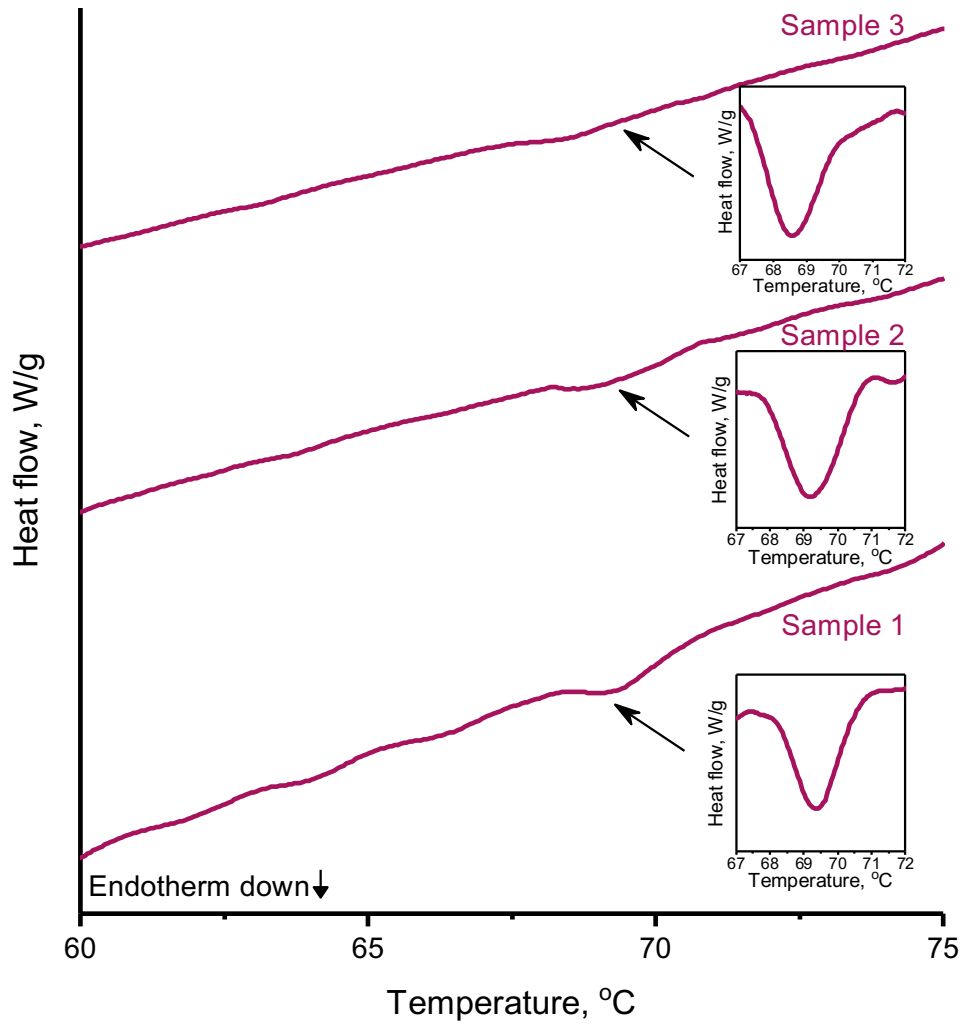


FIGURE A8.4 Thermogram of *A. ater* mucus corresponding to the three measurements.

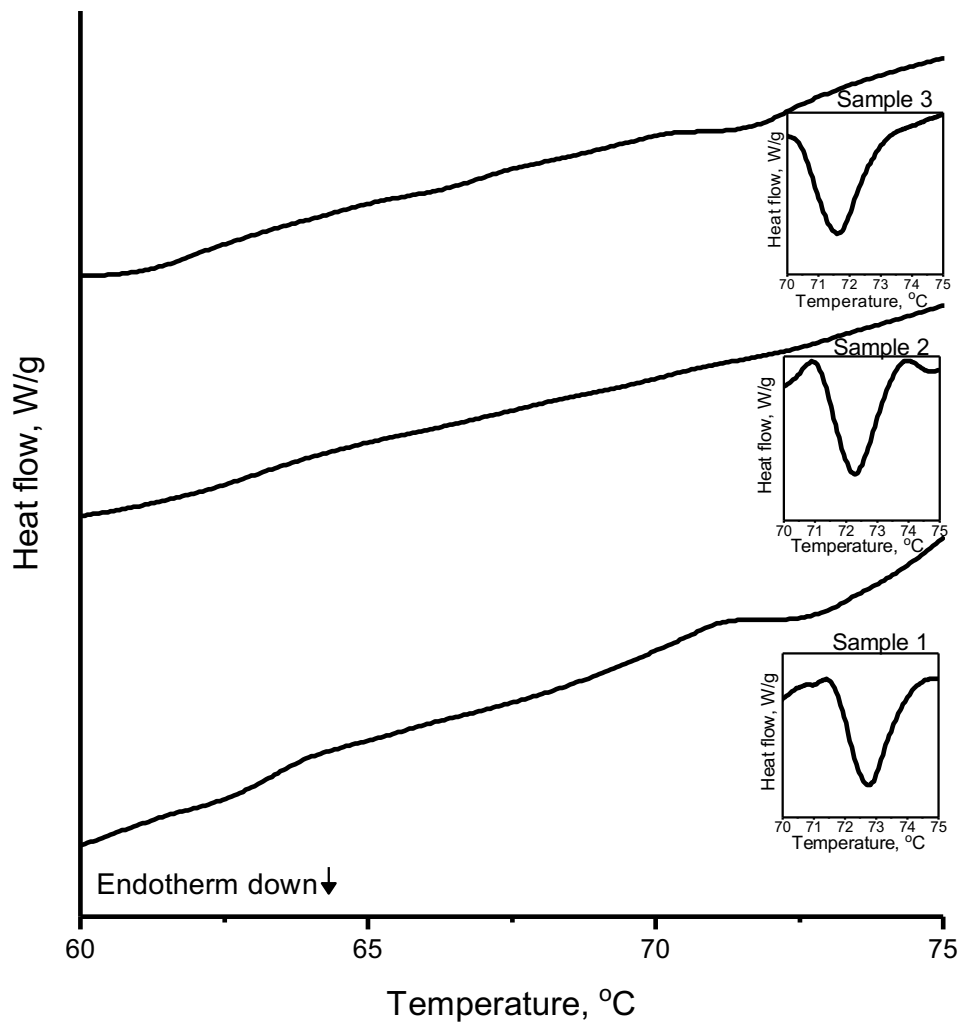


FIGURE A8.5 Thermogram of *A. hortensis* mucus corresponding to the three measurements.

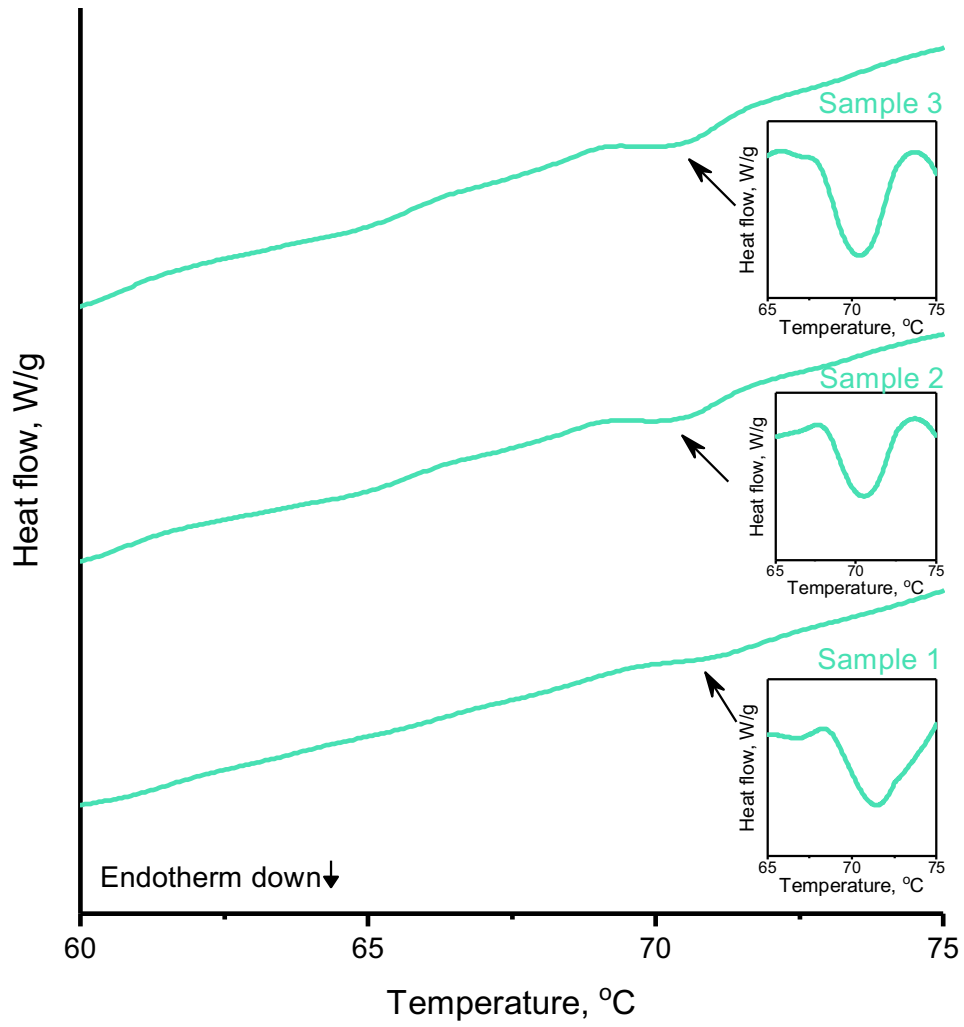


FIGURE A8.6 Thermogram of *L. flavus* mucus corresponding to the three measurements.

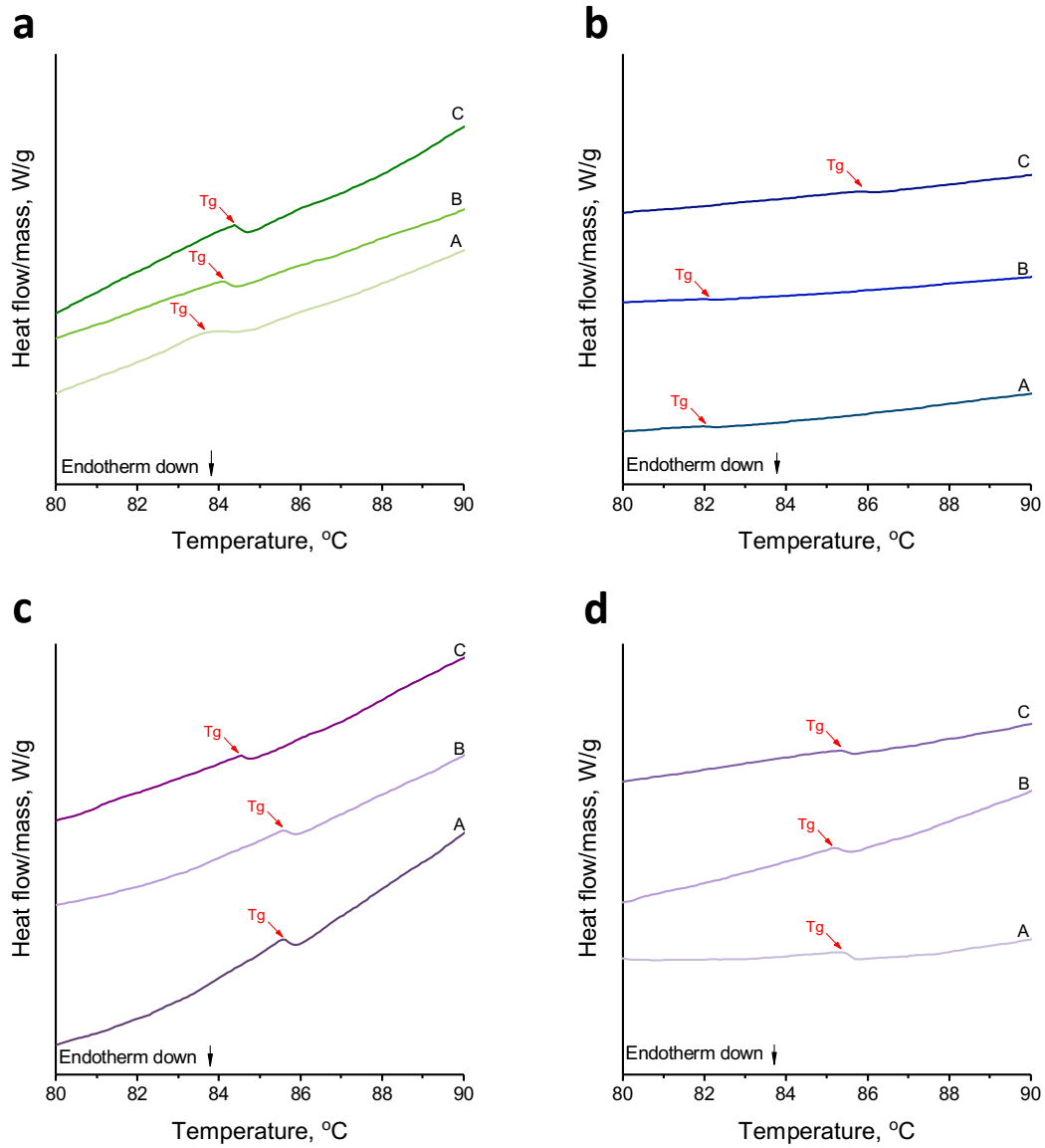


FIGURE A.8.7 Thermograms of a) *B. arietans*, b) *N. mossambica*, c) *N. annulifera*, and d) *N. naja* venom. Each species was tested three times.

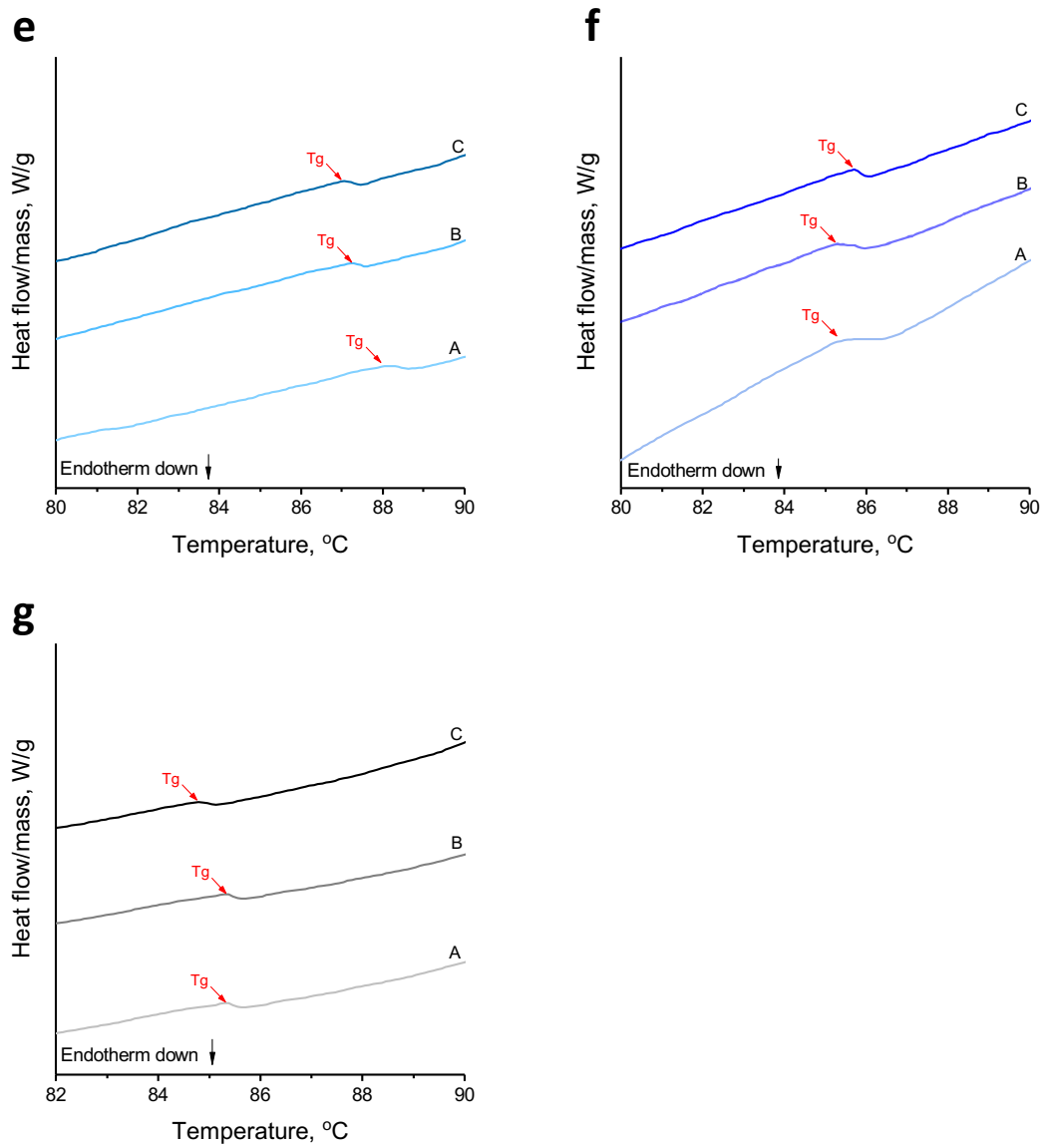


FIGURE A8.8 Thermograms of e) *N. philippinensis*, f) *N. kaouthia* venom, and g) trehalose. Each sample was tested three times.

TABLE A.8.1 DSC calculations of different thermal properties of *A. fulica*, *A. hortensis*, *A. ater*, *C. nemoralis*, *C. aspersum* and *L. flavus*.

Species	Property measured	Mean value (n=3)	Standard deviation (σ)
<i>A. fulica</i>	Enthalpy of denaturation (J/g)	24.44	4.79
	Onset temperature(°C)	69.44	0.40
	Peak maximum (°C)	70.61	0.715
<i>C. aspersum</i>	Enthalpy of denaturation (J/g)	6.08	1.08
	Onset temperature(°C)	65.73	0.41
	Peak maximum (°C)	66.68	0.43
<i>C. nemoralis</i>	Enthalpy of denaturation (J/g)	3.71	0.41
	Onset temperature(°C)	64.72	0.36
	Peak maximum (°C)	65.64	0.45
<i>A. ater</i>	Enthalpy of denaturation (J/g)	12.78	2.21
	Onset temperature(°C)	66.82	0.49
	Peak maximum (°C)	69.02	0.39
<i>A. hortensis</i>	Enthalpy of denaturation (J/g)	2.92	0.45
	Onset temperature(°C)	71.14	0.90
	Peak maximum (°C)	72.11	0.43
<i>L. flavus</i>	Enthalpy of denaturation (J/g)	15.16	2.60
	Onset temperature(°C)	69.42	0.65
	Peak maximum (°C)	70.70	0.38

TABLE A.8.2 DSC calculations of different thermal properties of *B. arietans*, *N. mossambica*, *N. annulifera*, *N. naja*, *N. philippinensis*, *N. kaouthia* venom, and trehalose.

Species	Property measured	Mean value (n=3)	Standard deviation (σ)
<i>B. arietans</i>	ΔC_p (J/g °C)	0.19	0.05
	Tg onset (°C)	83.54	0.29
	Tg midpoint (°C)	83.74	0.22
	Tg endpoint (°C)	84.00	0.14
<i>N. mossambica</i>	ΔC_p (J/g °C)	0.10	0.03
	Tg onset (°C)	83.61	1.76
	Tg midpoint (°C)	83.97	1.83
	Tg endpoint (°C)	84.12	1.69
<i>N. annulifera</i>	ΔC_p (J/g °C)	0.11	0.02
	Tg onset (°C)	84.35	0.82
	Tg midpoint (°C)	84.62	0.92
	Tg endpoint (°C)	84.85	0.98
<i>N. naja</i>	ΔC_p (J/g °C)	0.13	0.02
	Tg onset (°C)	84.82	0.16
	Tg midpoint (°C)	84.97	0.07
	Tg endpoint (°C)	85.25	0.18
<i>N. philippinensis</i>	ΔC_p (J/g °C)	0.10	0.01
	Tg onset (°C)	86.68	0.14
	Tg midpoint (°C)	87.24	0.46
	Tg endpoint (°C)	87.31	0.20
<i>N. kaouthia</i>	ΔC_p (J/g °C)	0.12	0.03
	Tg onset (°C)	85.04	0.20
	Tg midpoint (°C)	85.31	0.09
	Tg endpoint (°C)	85.57	0.05
Trehalose	ΔC_p (J/g °C)	0.077	0.01
	Tg onset (°C)	84.18	0.54
	Tg midpoint (°C)	84.67	0.27
	Tg endpoint (°C)	84.97	0.47

APPENDIX A9: CHAPTER 8. THESIS SUMMARY

TABLE A9. Summary showing the list of species studied, collection and storage methods, properties measured, and techniques for the thesis work. Coloured cells indicate the selection of the corresponding column.

SPECIES	ECTO-SECRETION	COLLECTION METHOD		STORAGE METHOD			PROPERTY AND TECHNIQUE					
		Sterile razor blades	Obtained from the snake, crude venom	Room temperature	Cold (1-10 °C)	Frozen	Compositional			Thermal		Functional
							UV-Vis	FTIR	SDS-PAGE	TGA	DSC	
<i>A. fulica</i>	GASTROPOD MUCUS											
<i>C. aspersum</i>												
<i>C. nemoralis</i>												
<i>A. ater</i>												
<i>A. hortensis</i>												
<i>L. flavus</i>												
<i>L. maximus</i>												
<i>L. haroldi</i>												
<i>V. sloanei</i>												
<i>L. stagnalis</i>												
<i>M. cornuaretis</i>												
<i>P. diffusa</i>												
<i>B. arietans</i>		SNAKE VENOM										
<i>H. haemachatus</i>												
<i>N. pallida</i>												
<i>N. nubiae</i>												
<i>N. mossambica</i>												
<i>N. nigricollis</i>												
<i>N. subfulva</i>												
<i>N. nivea</i>												
<i>N. haje</i>												
<i>N. annulifera</i>												
<i>N. naja</i>												
<i>N. siamensis</i>												
<i>N. philippinensis</i>												
<i>N. atra</i>												
<i>N. kaouthia</i>												

RESEARCH ARTICLE

Unexpected lack of specialisation in the flow properties of spitting cobra venom

Ignazio Avella¹, Edgar Barajas-Ledesma², Nicholas R. Casewell³, Robert A. Harrison³, Paul D. Rowley³, Edouard Crittenden³, Wolfgang Wüster⁴, Riccardo Castiglia⁵, Chris Holland^{2,*} and Arie van der Meijden^{1,*}

ABSTRACT

Venom spitting is a defence mechanism based on airborne venom delivery used by a number of different African and Asian elapid snake species ('spitting cobras'; *Naja* spp. and *Hemachatus* spp.). Adaptations underpinning venom spitting have been studied extensively at both behavioural and morphological level in cobras, but the role of the physical properties of venom itself in its effective projection remains largely unstudied. We hereby provide the first comparative study of the physical properties of venom in spitting and non-spitting cobras. We measured the viscosity, protein concentration and pH of the venom of 13 cobra species of the genus *Naja* from Africa and Asia, alongside the spitting elapid *Hemachatus haemachatus* and the non-spitting viper *Bitis arietans*. By using published microCT scans, we calculated the pressure required to eject venom through the fangs of a spitting and a non-spitting cobra. Despite the differences in the modes of venom delivery, we found no significant differences between spitters and non-spitters in the rheological and physical properties of the studied venoms. Furthermore, all analysed venoms showed a Newtonian flow behaviour, in contrast to previous reports. Although our results imply that the evolution of venom spitting did not significantly affect venom viscosity, our models of fang pressure suggests that the pressure requirements to eject venom are lower in spitting cobras than in non-spitting cobras.

KEY WORDS: Cobra, Venom, Rheology, Viscosity, Concentration, pH

INTRODUCTION

A plethora of defensive behaviours can be found across the animal kingdom. Such variety can be explained by natural selection acting more strongly on defence mechanisms than on offence/predation mechanisms, as suggested by the 'life-dinner principle' (Dawkins and Krebs, 1979). According to this principle, evolutionary selective pressure on the prey is much stronger than on the predator, because in a predator-prey encounter, the prey may lose its

life, while the predator may only lose a meal. Defensive behaviours can be summarised in three main categories: freezing, fleeing and active defence (Eilam, 2005). As part of the latter category, some organisms – for example, hymenoptera, arachnids and venomous snakes – employ venom, defined as an injectable harmful chemical secretion, to mount a more effective defensive attack. The noxious effects of venom increase the dissuading effect of the defence, enabling animals like bees, scorpions and snakes to ward off larger attackers (Schmidt, 2019). Although snake venoms are thought to have mainly evolved for their function in aiding predation (Arbuckle, 2017; Daltry et al., 1996), it is their use in defensive behaviour that makes them relevant to human health (Gutiérrez et al., 2017).

Snake venom consists of a complex mixture of peptides and proteins, small organic molecules and salts in an aqueous medium (Chan et al., 2016). The high peptide and protein content makes venom more viscous than water (Young et al., 2011), and it has been previously identified as a non-Newtonian shear-thinning fluid (Triep et al., 2013; Young et al., 2011). Venomous snakes (superfamily Colubroidea) inject venom into the body of their prey, or defensively into the body of their attackers, through specialised fangs or grooved teeth (Broeckhoven and du Plessis, 2017; Vonk et al., 2008). Members of the families Viperidae, Elapidae and Atractaspididae use an advanced front-fanged venom delivery system (Kerkkamp et al., 2017). In these snakes, the venom originates from the primary venom gland, and is expelled by the pressure of a skeletal muscle (referred to as *m. compressor glandulae* in viperids or *m. adductor mandibulae externus superficialis* in elapids; Haas, 1973) through the primary duct, the secondary (accessory) gland and into the fang, which acts like a hypodermic needle (Fransen et al., 1986; Jackson, 2003; Young and Kardong, 2007; Young et al., 2001). Once injected, venom toxins become systemic via dispersal by the bloodstream and lymphatic system, interacting with the prey/attacker's physiological proteins and receptors, ultimately disrupting the nervous system, the blood coagulation cascade, the cardiovascular and neuromuscular system, and/or homeostasis in general (Kerkkamp et al., 2017).

The Elapidae family of snakes includes taipans, mambas, coral snakes, kraits and cobras. Snakes of this family inject their venom through short, fixed fangs located in the frontal part of the upper jaw, as opposed to the movable front fangs of the Viperidae and Atractaspididae (Bogert, 1943; Vitt and Caldwell, 2013). Cobra species of the genus *Naja* Laurenti 1768 possess venoms with neurotoxic and/or cytotoxic properties, which they use to rapidly immobilise their prey for consumption, or to dissuade predators (Petras et al., 2011; Vitt and Caldwell, 2013). Members of this genus are present in both Africa and Asia (Vitt and Caldwell, 2013; Wüster, 1996; Wüster et al., 2007), and cobras from these two continents form phylogenetically distinct groups, which are thought to have separated about 16 Mya (Wüster et al., 2007).

¹CIBIO/InBIO - Centro de Investigação em Biodiversidade e Recursos Genéticos da Universidade do Porto, 4485-661 Vairão, Portugal. ²Department of Materials Science and Engineering, University of Sheffield, Sheffield S1 3JD, UK. ³Centre for Snakebite Research & Interventions, Liverpool School of Tropical Medicine, Liverpool L3 5QA, UK. ⁴Molecular Ecology and Fisheries Genetics Laboratory, School of Natural Sciences, Bangor University, Bangor LL57 2UW, UK. ⁵Dipartimento di Biologia e Biotechnologie 'Charles Darwin', Università di Roma 'La Sapienza', 00185 Rome, Italy.

*Authors for correspondence (mail@arievandermeijden.nl, christopher.holland@sheffield.ac.uk)

© I.A., 0000-0003-3576-8805; E.B.-L., 0000-0003-2807-2180; N.R.C., 0000-0002-8035-4719; R.A.H., 0000-0001-9842-5573; E.C., 0000-0003-1676-5457; W.W., 0000-0002-4890-4311; R.C., 0000-0002-9011-302X; C.H., 0000-0003-0913-2221; A.v.d.M., 0000-0002-1317-5382

Received 16 May 2020; Accepted 16 February 2021

Several *Naja* species are well known for their peculiar ability to spit venom as an exclusively defensive mechanism, expelling it as pressurised jets or sprays at their attackers (Berthé et al., 2009; Bogert, 1943; Panagides et al., 2017; Rasmussen et al., 1995; Westhoff et al., 2005; Wüster and Thorpe, 1992). These spits are generally aimed at the face and eyes of an aggressor (Westhoff et al., 2005), and once in contact with the eyes, can cause severe pain and inflammatory pathology (Chu et al., 2010; Westhoff et al., 2005). The ability to spit venom likely evolved from non-spitting ancestors on three independent occasions, once in African cobras and once in Asian cobras, and on a third occasion in the closely related rinkhals *Hemachatus haemachatus* (Kazandjian et al., 2021; Panagides et al., 2017; Slowinski et al., 1997; Wüster et al., 2007).

The venom delivery system of spitting cobras possesses several subtle morphological adaptations that enable them to eject their venom over long distances, and which distinguish them from non-spitting cobras. The discharge orifice, for example, has a more circular shape (Bogert, 1943; Wüster and Thorpe, 1992), and is directed more anteriorly, creating a 90 deg bend in the venom channel inside the fang (Balmert et al., 2011; Triep et al., 2013). This channel has internal ridges unique to spitting cobras (Berthé, 2011; Triep et al., 2013) that reduce the pressure loss by about 30% compared with an identical channel without ridges, thus helping to achieve a longer reach of the jet (Triep et al., 2013). Furthermore, spitting cobras actively displace the fang sheath (removing a physical barrier to venom expulsion), unlike other venomous snakes, where displacement of the fang sheath is passive (Young et al., 2004). Additional behavioural adaptations found in African spitting *Naja* species include adjusting head movements to distance from target to optimise the spread of venom (Berthé et al., 2009), and tracking and anticipating target movements to improve accuracy (Westhoff et al., 2010). Spitting cobras also show a certain degree of variation in their spitting modes: as demonstrated by previous studies (Rasmussen et al., 1995; Westhoff et al., 2005), some specialised spitters eject their venom in streams (e.g. *Naja pallida*) while others produce a fine mist (e.g. *Naja nigricollis*). The combination of morphological and behavioural adaptations allows most spitting cobras to eject venom up to at least 1 m, with some species (e.g. *Naja mossambica*) able to spit up to about 3 m (Rasmussen et al., 1995).

To date, considerable research effort has been focused on the anatomical features of the specialised venom delivery apparatus of spitting cobras (Bogert, 1943; Triep et al., 2013; Wüster and Thorpe, 1992; Young et al., 2004; 2009), and on their associated peculiar defensive behaviour (Berthé et al., 2009; Westhoff et al., 2005; 2010). In contrast, the possibility of changes in the composition of the venom itself, as an adaptation for its new role as a venom applied outside of the body, or toxungen (Nelsen et al., 2014), has remained largely neglected. Two recent studies have suggested that the venom of spitting species may have evolved for increased effectiveness when applied externally. Panagides et al. (2017) showed that African spitting cobras have venom that is more potently cytotoxic than that found in African non-spitters. Kazandjian et al. (2021) demonstrated that all three spitting lineages independently evolved venoms with more potent pain-inducing effects. These determine enhanced activation of sensory neurons through synergy between the ancestral cytotoxins widespread among cobras and phospholipases A₂.

However, in addition to new selective pressures relating to its function as a toxungen, venom spitting may also have changed the mechanical demands of the venom, but so far this has not been studied. Since the venom has to pass through the narrow ducts of the

venom apparatus, we expect that a lower venom viscosity (i.e. resistance to flow) would serve to reduce pressure loss during venom expulsion, thereby reducing the energetic requirements of ejection. Furthermore, for a given ejection force, venom projection distance would also be aided by more rapid expulsion, obtainable with a less viscous venom. On the other hand, in spitting cobras, a higher viscosity would aid jet cohesion after venom ejection, keeping the jet of venom from breaking up into droplets for longer, thus improving spitting distance and accuracy by reducing air drag. The reported strong shear-thinning, non-Newtonian behaviour of snake venom (Triep et al., 2013; Young et al., 2011) would result in a reduced viscosity in the high-shear environment of the venom channel, but a high viscosity in the low-shear environment of an airborne jet, and would thus likely aid in meeting these two seemingly conflicting demands.

Here, we measured and compared the rheological properties of the venoms of 12 spitting and non-spitting cobra species of the genus *Naja* from Africa and Asia, the only known 'non-*Naja*' species of spitting elapid, *H. haemachatus*, and the African non-spitting viperid *Bitis arietans* (used as an outgroup). We also compared the protein concentration and pH of the studied venoms, two properties known to play an important role in the stability of some snake venom components (Kurt and Aurich, 1976) and often directly correlated to the severity of the envenomation (Bon, 2003; Ribeiro et al., 2016; Sanhajariya et al., 2018).

Given the morphological differences between the fangs of spitting and non-spitting cobras (Bogert, 1943; Triep et al., 2013; Wüster and Thorpe, 1992; Young et al., 2004, 2009), we hypothesised that the two venom delivery mechanisms (i.e. spitting and biting) might be associated with different pressure requirements for venom ejection. Furthermore, we hypothesised that the venom of spitting cobras has a more pronounced shear-thinning behaviour than the venom of non-spitting cobras, in order to reduce pressure loss inside the venom duct and to increase jet cohesion in the airborne venom. To test this, we calculated and compared the pressure needed for venom to flow through the fang channel of one spitting and one non-spitting cobra species (*Naja nigricollis* and *Naja nivea*, respectively), using previously available microCT scanning data and our rheological data.

MATERIALS AND METHODS

Venom extraction

In total, venom samples of 30 snakes were used in this study. Venom was extracted from 28 cobras belonging to 13 different species of the genus *Naja*, namely: *Naja annulifera* Peters 1854, *Naja atra* Cantor 1842, *Naja haje* (Linnaeus 1758), *Naja kaouthia* Lesson 1831, *Naja mossambica* Peters 1854, *Naja naja* (Linnaeus 1758), *Naja nigricollis* Reinhardt 1843, *Naja nivea* (Linnaeus 1758), *Naja nubiae* Wüster & Broadley 2003, *Naja pallida* Boulenger 1896, *Naja philippinensis* Taylor 1922, *Naja siamensis* Laurenti 1768 and *Naja subfulva* Laurent 1955. Venom was also extracted from one rinkhals, *Hemachatus haemachatus* Bonnaterre 1790, and one puff adder, *Bitis arietans* Merrem 1820, used for comparative analyses, as a 'non-*Naja*' venom spitter and non-spitter, respectively. Twelve of the specimens were captive bred (CB), while the remaining 18 were collected in the wild (see Table 1 for details). All snakes were maintained in individual cages within the temperature, humidity and light-controlled environment of the herpetarium at the Centre for Snakebite Research and Interventions, Liverpool School of Tropical Medicine. This facility and its protocols for the expert husbandry of the snakes are inspected and approved by the UK Home Office and the LSTM Animal Welfare and Ethical Review Board. Before the

Table 1. Properties of the venom samples per specimen

Species	Spitting mode	Specimen ID	Continent	Origin	Wet venom yield (mg)	pH	Protein conc. (mg ml ⁻¹)	Viscosity (Pa s) at 10,000 s ⁻¹
<i>B. arietans</i>	Non-spitter	BitAriNGA003	Africa	Nigeria	1261.0	5.43	132.4	0.02652
<i>H. haemachatus</i>	Mixed	HemHaeCB001	Africa	Captive bred	242.1	5.76	132.5	0.02503
<i>N. annulifera</i>	Non-spitter	NajAnnCB002	Africa	Captive bred	400.3	5.80	159.1	0.05658
<i>N. atra</i>	Streams	NajAtrCBT002	Asia	Captive bred	136.4	5.81	144.5	0.01553
<i>N. haje</i>	Non-spitter	NajNivZAF004	Africa	South Africa	257.9	5.63	152.5	0.01946
		NajHajUGA001	Africa	Uganda	137.1	5.89	140.1	0.05181
<i>N. kaouthia</i>	Streams	NajHajUGA004	Africa	Uganda	337.0	5.90	151.2	0.06024
		NajKaoCB001	Asia	Captive bred	966.4	5.50	124.0	0.01703
		NajKaoCB002	Asia	Captive bred	494.6	5.49	103.3	0.00309
		NajKaoCB003	Asia	Captive bred	681.9	5.69	81.4	0.04501
<i>N. mossambica</i>	Streams	NajMosTZA001	Africa	Tanzania	490.7	5.65	121.0	0.11901
		NajMosTZA002	Africa	Tanzania	183.4	5.75	137.4	0.04564
		NajMosTZA003	Africa	Tanzania	603.1	5.91	122.4	0.08120
<i>N. naja</i>	Non-spitter	NajNajCB001	Asia	Captive bred	169.6	5.66	120.4	0.01029
<i>N. nigricollis</i>	Mist	NajNigNGA001	Africa	Nigeria	140.0	5.60	115.7	0.03149
		NajNigNGA002	Africa	Nigeria	795.7	5.59	133.8	0.07626
		NajNigNGA003	Africa	Nigeria	1116.9	5.60	127.4	0.05422
		NajNigNGA004	Africa	Nigeria	1059.4	5.88	154.9	0.02689
<i>N. nivea</i>	Non-spitter	NajNigTGO001	Africa	Togo	1423.4	5.53	152.7	0.01236
		NajNivZAF003	Africa	South Africa	290.8	5.88	51.1	0.17088
<i>N. nubiae</i>	Streams	NajNubCB001	Africa	Captive bred	293.6	6.01	154.9	0.00643
		NajNubCB003	Africa	Captive bred	1198.8	5.79	127.2	0.07902
		NajNubCB004	Africa	Captive bred	457.3	5.84	142.1	0.02517
<i>N. pallida</i>	Streams	NajPalKEN001	Africa	Kenya	362.4	5.80	150.4	0.01600
		NajPalKEN002	Africa	Kenya	513.8	5.91	145.0	0.02814
		NajPalTZA002	Africa	Tanzania	479.9	6.02	137.5	0.04007
<i>N. philippinensis</i>	Streams	NajPhiCB001	Asia	Captive bred	140.3	5.78	129.0	0.02855
<i>N. siamensis</i>	Mist	NajSiaCB002	Asia	Captive bred	585.1	5.73	154.0	0.10437
<i>N. subfulva</i>	Non-spitter	NajMelCMR001	Africa	Cameroon	126.3	5.98	139.9	0.01878
		NajMelUGA001	Africa	Uganda	155.9	5.89	140.1	0.01340

Mean wet venom yield produced by each snake is shown. The values reported for pH, protein concentration and viscosity were obtained averaging the values of the measurements taken for each individual. Values of single measurements are reported in Tables S1, S2 and S3.

beginning of the experiments, none of the specimens considered for this study had been milked for at least 4 weeks. After milking, the snakes were immediately returned to their enclosures and the venom transferred into 2 ml low-protein binding cryotubes (Simport Scientific, Beloeil, Canada) using a pipette. Table 1 shows the average mass of fresh venom extracted from each specimen. The tubes were then transferred on ice to the laboratory of the Department of Materials Science and Engineering of the University of Sheffield for rheological, pH and concentration measurements on the same day.

Rheological tests

Shear viscosity measurements were performed in the Department of Materials Science and Engineering of the University of Sheffield, using a DHR-2 (TA Instruments, USA) rheometer, equipped with a cone-plate geometry (20 mm diameter, 1 deg angle cone, 27 µm truncation gap, 36 µl to fill), and subjecting samples to a shear rate ramp from 1.0 s⁻¹ to 10,000 s⁻¹ (41 steps, 15 s per step), the maximum shear rate achievable by this instrument and geometry combination. Data below 100 s⁻¹ were not included in later analysis as the apparent shear thinning observed is most likely attributed to surface tension effects and artefacts (see Fig. S1 and Ewoldt et al., 2015). Unless otherwise stated, all samples were tested at a room temperature of 25°C. This temperature was selected as it falls within the range of body temperatures of active snakes (El-Deib, 2005; Lillywhite, 2014) and approximates the temperature at which spitting was elicited from specimens of *N. nigricollis*, *N. pallida*, *N. mossambica* and *H. haemachatus* in previous studies (Westhoff et al., 2005; Young and O'Shea, 2005). Only species where sufficient venom was obtained to perform at least two replicates are shown. We

were able to achieve up to three replicates for 19 of the 30 specimens included in this study. Venom samples that were not sufficient included *H. haemachatus* (African 'non-*Naja*' spitter), *N. subfulva* (African non-spitter) and *N. naja* (Asian non-spitter). In order to control for the potential presence of intraspecific variation in the considered rheological properties, all measurements were carried out on the venoms of single individuals, without pooling them.

Calculating fang venom shear rate

To support the range of shear rates tested and their biological relevance, it is necessary to calculate the natural range of shear rates encountered by venom. If venom is considered to be flowing down a channel, assuming all species spit in the same time and produce the same volume, the maximum shear strain rate at the fang wall is given by:

$$\dot{\gamma}_w = \frac{4Q}{\pi R^3}, \quad (1)$$

where Q is the volumetric flow in m³ s⁻¹, R is the radius of the venom channel in m and $\dot{\gamma}_w$ is the shear rate in s⁻¹. According to data on *N. pallida* obtained by Triep et al. (2013) and du Plessis et al. (2018), the values considered during the venom spitting process are: volume of a single spitting event, $V_{\text{single spit}}=1.0 \times 10^{-8}$ m³; time for a single spitting event, $t_{\text{single spit}}=4 \times 10^{-2}$ s; for *B. arietans*, $R=3.8 \times 10^{-4}$ m (du Plessis et al., 2018); for *N. nigricollis*, $R=2.2 \times 10^{-4}$ m (du Plessis et al., 2018); and for *N. nivea*, $R=2.0 \times 10^{-4}$ m (du Plessis et al., 2018). Therefore $Q=2.5 \times 10^{-7}$ m³ s⁻¹ and using Eqn 1, for *B. arietans*, $\dot{\gamma}_w=5801$ s⁻¹; for *N. nigricollis*, $\dot{\gamma}_w=29,894$ s⁻¹ and for

N. nivea, $\dot{\gamma}_w = 38,051 \text{ s}^{-1}$, which from a rheological perspective is in broad agreement with the $10,000 \text{ s}^{-1}$ shear rate applied in this study.

Calculating the pressure needed to eject venom

If the venom is considered to be flowing down a venom channel of converging radius from R_1 to R_2 , the pressure drop will be the result of the radius reduction from the fang base to the end of the fang where the exit orifice of the venom channel is located, plus the losses due to the viscous material (i.e. venom) flowing in the venom channel (Synolakis and Badeer, 1989). In order to corroborate if the flow is laminar or turbulent for the appropriate use of equations, the Reynolds number for the three species considered needs to be determined. The maximum Reynolds number defined for a Newtonian fluid can be calculated with the following equation:

$$Re_{\max} = \frac{\rho \times u_1 \times D_1}{\mu_{\min}}, \quad (2)$$

where Re_{\max} is the maximum Reynolds number; ρ is the density of the venom = 1084 kg m^{-3} (Triep et al., 2013); u_1 is the venom velocity at the channel inlet = 1.33 m s^{-1} (calculated with information from Triep et al., 2013); D_1 is the diameter at the channel inlet = $7.6 \times 10^{-4} \text{ m}$ for *B. arietans* (du Plessis et al., 2018), $4.4 \times 10^{-4} \text{ m}$ for *N. nigricollis* (du Plessis et al., 2018) and $4.0 \times 10^{-4} \text{ m}$ for *N. nivea* (du Plessis et al., 2018); μ_{\min} is the dynamic viscosity of venom from our own data at $10,000 \text{ s}^{-1} = 0.026 \pm 8.5 \times 10^{-4} \text{ Pa s}$ for *B. arietans*; $0.031 \pm 8.6 \times 10^{-3} \text{ Pa s}$ for *N. nigricollis* and $0.170 \pm 0.079 \text{ Pa s}$ for *N. nivea*.

Assuming that all species have the same velocity at the channel inlet and density, Reynolds numbers are: *B. arietans*, $Re_{\max} = 27.62$; *N. nigricollis*, $Re_{\max} = 23.25$ and *N. nivea*, $Re_{\max} = 4.24$. All these Reynolds numbers are < 100 , corresponding to a laminar flow (in line with the predictions made by Triep et al., 2013), which is below the critical Reynolds number of 2300, above which turbulent flow is observed.

As the flow is in the laminar region, then the following equation, which corresponds to an Extended Generalised Bernoulli Equation, will be used to calculate the total pressure differential in the venom channel (see Appendix for detailed deduction of this equation):

$$\Delta P = P_1 - P_2 = \left(\frac{\rho}{2}\right) \times u_1^2 \left(\left(\frac{A_1}{A_2}\right)^2 - 1 \right) + \left(\left(\frac{64}{Re}\right) \times \left(\frac{l}{D}\right) \times \left(\frac{\bar{u}^2}{2}\right) \times \rho \right), \quad (3)$$

where ΔP is the pressure differential in the venom channel, in Pa; P_1 and P_2 are the pressures at the inlet and outlet points of the venom channel, respectively, in Pa; u_1 and u_2 are the velocities at the inlet and outlet points of the venom channel, respectively, in m s^{-1} ; ρ is the density of the venom, in kg m^{-3} ; A_1 and A_2 are the cross-section areas at the inlet and outlet points, in m^2 ; Re is the Reynolds number; l is the length and D the average diameter of the venom channel,

both in m; \bar{u} is the average velocity of the venom in the venom channel, in m s^{-1} .

To directly relate these calculations to the natural system and the measured rheological data, microCT scans from du Plessis et al. (2018), and available at the GigaScience Database (<http://dx.doi.org/10.5524/100389>), were used to calculate venom channel length and radius. Fang morphology data was available for three species included in this study: *B. arietans* (viper), *N. nigricollis* (African spitting cobra) and *N. nivea* (African non-spitting cobra). MicroCT image stacks were imported into Amira (Thermo Fisher Scientific, v.2019.4) and 10 evenly spaced measurements were taken along the length of the venom channel (l), from the end of the entry orifice into the channel at the base of the fang to the opening point of the exit orifice at the tip of the fang. Of the 10 measurements per species, the average diameter was obtained (D) for input into Eqn 3. The values used for each variable for the three snake species are reported in Table 2.

Protein concentration

Protein concentration was measured for each venom sample using a UV300 Thermo Spectronic spectrometer (Umicam/Thermo, UK). All samples (dilutions consisting of $1.5 \mu\text{l}$ of fresh venom + 1 ml of water) were analysed at room temperature in 1 cm path-length polystyrene cuvettes from 200 to 500 nm wavelength. Double distilled water was used as a blank and for all dilutions. Protein concentration was estimated as follows, using absorbance at 260 and 230 nm (Aitken and Learmonth, 2009):

$$\text{Concentration (mg ml}^{-1}\text{)} = (0.183 \times A_{230 \text{ nm}}) - (0.075 \times A_{260 \text{ nm}}), \quad (4)$$

where $A_{260 \text{ nm}}$ and $A_{230 \text{ nm}}$ correspond to absorbance at 260 nm and 230 nm , respectively.

pH measurements

A Sentron pH meter (Netherlands) equipped with a cupFET pH probe was used to make pH measurements at room temperature. Two $3 \mu\text{l}$ droplets from each undiluted venom sample were measured individually and averaged to generate a pH measurement.

Phylogenetic comparative methods

The aim of the analyses reported here was to test for patterns in the measured parameters between spitting and non-spitting cobra venoms across the sampled species. All the analyses were performed using R 3.6.1 (<https://www.r-project.org/>) implemented using RStudio 1.2.1335, always taking the species phylogeny into account. We used the species tree reported in Kazandjian et al. (2021). This tree contained 46 elapid species belonging to 11 different genera and was generated using a multispecies coalescent model based on DNA sequence alignments of both mitochondrial (partial *cytb* and *ND4* gene sequences) and nuclear genes (*CMOS*, *NT3*, *PRLR*, *UBN1* and *RAG1*). For the analyses in the current study, we pruned the original tree and retained only the species used in the venom rheology tests (i.e. *H. haemachatus* and the various

Table 2. Parameters used to calculate the pressure differential in the venom channel of the fang of *Bitis arietans*, *Naja nigricollis* and *Naja nivea*

	D_1 (m)	D_2 (m)	D (m)	l (m)	u_1 (m s^{-1})	ΔP (Pa)
<i>B. arietans</i>	1.4×10^{-3}	4.4×10^{-4}	7.6×10^{-4}	0.00915	1.33	0.104×10^{-6}
<i>N. nigricollis</i>	8.0×10^{-4}	2.3×10^{-4}	4.4×10^{-4}	0.00333	1.33	0.172×10^{-6}
<i>N. nivea</i>	7.7×10^{-4}	1.0×10^{-4}	4.0×10^{-4}	0.00352	1.33	2.829×10^{-6}

Naja species). The viper *B. arietans* was added manually to the tree as an outgroup, with branch lengths adjusted manually to reflect previous research suggesting that viperids separated from elapids about 61 Mya (Zheng and Wiens, 2016).

Within spitting cobras, a further division can be made in the different ways venom is ejected, which likely require different rheological properties of the venom. Following previous studies (Rasmussen et al., 1995; Westhoff et al., 2005), we divided the modes of venom ejection into three categories: (i) 'streams' where venom is ejected in the form of more or less continuous jets; (ii) 'mist' where venom is ejected in the form of a fine spray; (iii) 'mixed' where venom is ejected in a form in between the other two categories (see Table 1). Information about the venom spitting modes of seven species of spitting elapids considered in this study (*N. atra*, *N. kaouthia*, *N. mossambica*, *N. nigricollis*, *N. pallida*, *N. siamensis* and *H. haemachatus*) was gathered from the literature (Paterna, 2019; Rasmussen et al., 1995; Santra and Wüster, 2017; Westhoff et al., 2005). The spitting mode category for *N. nubiae* and *N. philippinensis* was assigned based on the authors' personal observations. The category 'non-spitter' was assigned to the non-spitting cobras *N. annulifera*, *N. haje*, *N. naja*, *N. nivea* and *N. subfulva*. The spitting mode category assigned to each studied species is reported in Table 1.

To first test if there was a difference between spitting and non-spitting cobras and/or between Asian and African cobras across all the measured physical properties, we performed a MANOVA using spitting behaviour (defined in the analysis as 'spit') as a binary factor (spitter or non-spitter), and the data about protein concentration and viscosity at $10,000\text{ s}^{-1}$ as multivariate dependent variables. We considered spitting behaviour as a binary trait only in this analysis. After this preliminary MANOVA, we performed the same test considering the three different spitting mode categories, in order to look for possible correlation between differences in spitting modes and the measured physical properties of the venoms.

To test if there was a difference in venom viscosity due to spitting behaviour, protein concentration or pH we performed an ANCOVA using viscosity at $10,000\text{ s}^{-1}$ ('visc10000') as dependent variable and 'spit', protein concentration ('ProtConc') and pH as independent variables.

To test if there was a difference in protein concentration due to spitting behaviour, we performed an ANCOVA using protein concentration as dependent variable and 'spit' as independent variable. We looked for possible presence of phylogenetic signal for pH, protein concentration and viscosity at $10,000\text{ s}^{-1}$, calculating both Blomberg's K (Blomberg et al., 2003) and Pagel's λ (Pagel, 1999), using the R packages caper (<https://cran.r-project.org/web/packages/caper/>), geomorph (<https://cran.r-project.org/web/packages/geomorph/>) and phytools (<https://cran.r-project.org/web/packages/phytools/>). Finally, we calculated Blomberg's K for protein concentration and viscosity at $10,000\text{ s}^{-1}$ at the same time.

RESULTS

Physical properties of the venom

For all *Naja* venoms tested, the protein concentrations had an average of 132.6 mg ml^{-1} , ranging from 51.11 mg ml^{-1} (*N. nivea*) to 159.1 mg ml^{-1} (*N. annulifera*). The venoms of *B. arietans* and *H. haemachatus* had similar protein concentrations (132.4 and 132.5 mg ml^{-1} , respectively). No significant differences were found between species or groups (Fig. 1B, see also Table 1 and more details below). The same was also true following quantification of venom pH, where the average pH of the *Naja* venoms was 5.77, ranging from 5.49 (*N. kaouthia*) to 6.02 (*N. pallida*). The pH of *H. haemachatus* venom was 5.76, and finally the pH of *B. arietans* venom was the lowest at 5.43 (Fig. 1C).

Rheological tests demonstrated that, contrary to our starting hypothesis, the venoms of both spitting and non-spitting cobras show a Newtonian behaviour, at least over the range reported here (i.e. 100 to $10,000\text{ s}^{-1}$) (Fig. 2). No significant differences between species or groups were evident (Table 1 and below).

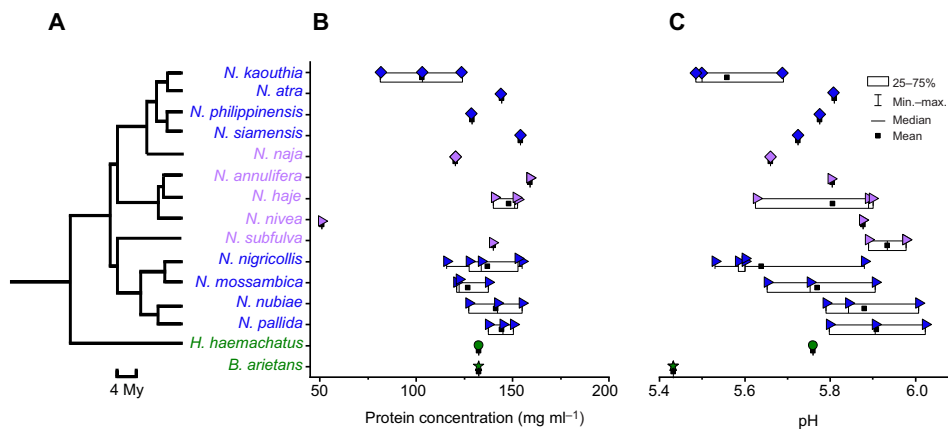


Fig. 1. Physical properties of snake venoms. (A) Cladogram of the elapid species analysed, extrapolated from the phylogenetic analyses performed (following Zheng and Wiens, 2016, viperids separated from elapids ~61 Mya, therefore *Bitis arietans* has not been included in the cladogram). (B) Box plot of protein concentration for venoms extracted for each species. (C) Box plot of venom pH, where each datapoint represents the mean of two individual measurements. Triangles represent African *Naja* spp., diamonds represent Asian *Naja* spp. Venom-spitting species are in blue, non-spitting species in violet. The green circle and the green star represent, respectively, the spitting elapid *Hemachatus haemachatus* and the non-spitting viper outgroup *B. arietans*.

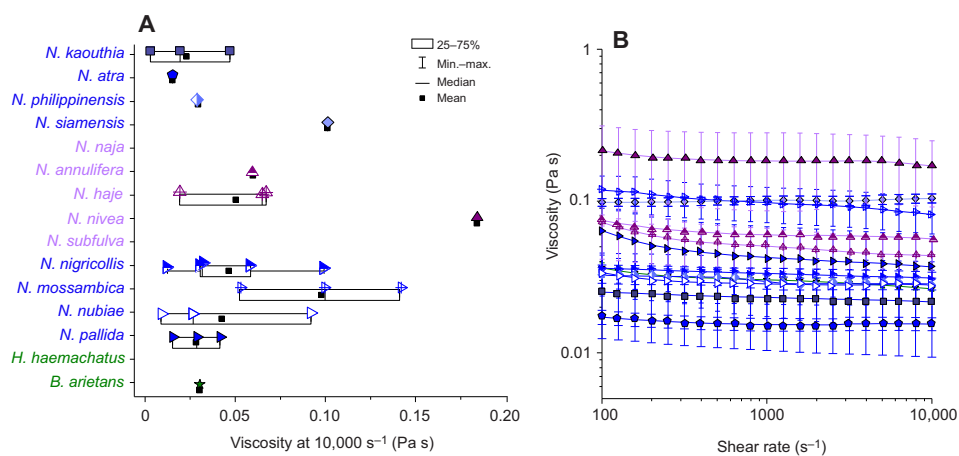


Fig. 2. Rheological properties of snake venoms. (A) Box plot of viscosity at 10,000 s⁻¹ for venoms extracted from each species. (B) Viscosity as a function of shear rate for each species. Note the absence of data for *H. haemachatus*, *N. subfulva* and *N. naja* (venom volume insufficient to run the experiments). The same colour code used in Fig. 1 has been applied. Data are means \pm s.e.m. from at least two experiments per specimen.

Combining rheological and morphological data to determine the pressure required for venom to flow down the venom channel, Fig. 3 shows the results for the African non-spitting cobra *N. nivea*, the African spitting cobra *N. nigricollis* and the viper *B. arietans*. MicroCT scans obtained from du Plessis et al. (2018) indicate two different types of fangs, closed fused (*B. arietans*) and non-fused (*N. nigricollis* and *N. nivea*, Fig. 3A), and subsequent measurements provide information as to the fang length/diameter ratio (Fig. 3B). The results of fang pressure calculations shown in Fig. 3C report that the highest value corresponds to the non-spitter *N. nivea* (2.8×10^6 Pa), while the spitter *N. nigricollis* presents a lower value (0.17×10^6 Pa). The viper *B. arietans* shows the lowest

pressure differential (0.10×10^6 Pa). The pressure differential results for the three snake species are reported in Table 2.

Phylogenetic comparative methods

The results of both MANOVAs showed no significant relationships between spitting behaviour and the multivariate combination of the measured physical properties of the venom (protein concentration, viscosity at 10,000 s⁻¹). An additional MANOVA including pH among the variables was also performed, but then discarded because of the non-significance of the added variable and to simplify the model. The results of the ANCOVAs also showed no significant effect of spitting behaviour, protein concentration or pH on

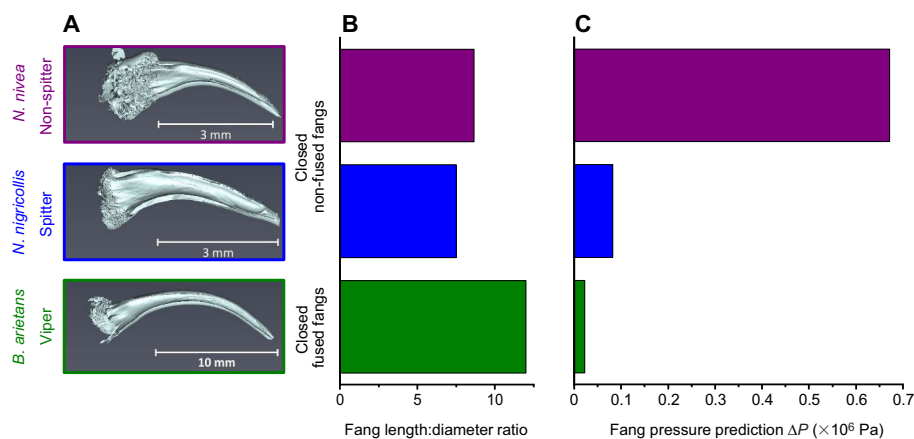


Fig. 3. Fang pressure prediction for *Naja nivea*, *Naja nigricollis* and *Bitis arietans*. (A) MicroCT images showing fang types (data analysed from du Plessis et al., 2018; available at GigaScience Database, <http://dx.doi.org/10.5524/100389>) in the three species. (B) Fang length/diameter ratio. (C) ΔP in the fang venom channel, calculated using representative rheological data for each species.

Table 3. Results of statistical testing

Type of analysis	Model	Variable	d.f.	F	P
Phylogenetic MANOVA	$y \sim \text{Spit}$	Spit	3	0.5692	0.669
Phylogenetic ANCOVA	$\text{visc}10000 \sim \text{Spit} + \text{ProtConc} + \text{pH}$	Spit	3	0.976	0.448
		ProtConc	1	3.38	0.094
		pH	1	0.0794	0.775
Phylogenetic ANCOVA	$\text{ProtConc} \sim \text{Spit}$	Spit	3	0.140	0.911

y indicates the multivariate variable consisting of protein concentration and viscosity at $10,000 \text{ s}^{-1}$.

viscosity, or of spitting behaviour on protein concentration. Results of the statistical analyses performed considering the three spitting mode categories are reported in Table 3.

Protein concentration, pH and viscosity at $10,000 \text{ s}^{-1}$ show both Blomberg's K and, particularly, Pagel's λ close to 0 (Table 4), indicating phylogenetic independence (Karatzas and Shreve, 1998). The same can be said for the multivariate analysis, which takes into account both protein concentration and viscosity, and for which only Blomberg's K has been calculated. None of these results was significant, with P -values always higher than 0.05 (between 0.276 and 0.707 for K and equal to 1 for λ).

DISCUSSION

Young's study on venom gland pressure in spitting cobras suggested that the force required by the *m. adductor mandibulae externus superficialis* to expel venom would be reduced if a highly shear-thinning venom was present (Young et al., 2004). The sudden increase in shear rate upon entering the venom channel would cause a decrease in the viscosity of the venom, which could therefore be pushed through the fang more easily and thus at the higher velocities that are required to increase the reach of the venom jet (Triep et al., 2013). However, upon exiting the fang, the effective shear rate in the airborne venom jet ejected by a spitting cobra would be dramatically reduced, and as such, a higher viscosity in the jet would reduce internal flow, thus slowing down the breaking up of the jet into separate droplets. This provides the advantage of a more coherent jet of venom, resulting in less drag and thus a longer reach. Given that non-spitting cobras do not eject their venom, they presumably have less need for a higher venom ejection speed, and hence less need for a highly shear-thinning venom. In light of these biomechanical considerations, we expected a more pronounced shear-thinning behaviour in spitting cobras than in non-spitting cobras, in order to reduce pressure loss inside the venom duct and to increase jet cohesion.

Thus, when considering the above and the specific morphological adaptations to spitting in spitting cobras, such as the ridges present along the channel inside their fangs (Berthé, 2011; Triep et al., 2013), the more circular and anteriorly oriented discharge orifice of their fangs (Bogert, 1943; Wüster and Thorpe, 1992; Young et al., 2004) and the apparently higher algesic activity of venoms of the three spitting lineages (Kazandjian et al., 2021), we expected the rheological properties of the venom between spitting and non-spitting cobras to also be different. Hence, in light

Table 4. Results of phylogenetic signal testing

Tested variable	Blomberg's K	P	Pagel's λ	P
Protein concentration	0.333852	0.707	7.69e-05	1
pH	0.455545	0.375	6.41e-05	1
Viscosity at $10,000 \text{ s}^{-1}$	0.505132	0.276	7.69e-05	1
Protein concentration and viscosity at $10,000 \text{ s}^{-1}$	0.4774	0.323		

of our findings, it is surprising to find no systematic differences in venom viscosity between spitting and non-spitting species. However, it is worth noting that this result might be influenced by the small number of rheological tests performed for most of the analysed snakes, owing to the relatively small amount of venom a single cobra specimen produces.

Nevertheless, we did find differences in viscosity between and within species, suggesting that there is enough variability for natural selection to potentially act on. Between species, we found that the average venom viscosities at $10,000 \text{ s}^{-1}$ went from a minimum of 0.0103 Pa s (*N. naja*) to a maximum of 0.1709 Pa s (*Naja nivea*) (see Fig. 2A and Table 1). Similarly, we found that viscosity could vary greatly even among specimens of the same species. For instance, the average venom viscosities measured for the three *N. nubiae* specimens (NajNubCB001, NajNubCB003 and NajNubCB004) were, respectively, 0.0064, 0.0252 and 0.0790 Pa s (Table 1 and Table S1). These results suggest that the venom of all the elapid species we analysed may vary in its viscosity owing to functional or other non-flow related requirements. We speculate that, within the range of rheological variability we recovered here for spitting cobras, other selective pressures may dictate the observed rheological properties. Although protein concentration and pH have been previously shown to vary and be of influence in snake venoms (Takahashi and Ohsaka, 1970) and in other secreted protein systems (e.g. silk, Holland et al., 2007; Terry et al., 2004), these two parameters did not vary significantly in our study.

Snake venom is known to vary in composition depending on different factors, such as diet (Daltry et al., 1996; Gibbs et al., 2011), ontogeny (Alape-Girón et al., 2008; Cipriani et al., 2017; Mackessy et al., 2006) and, potentially, local adaptation driven by relatively small changes in the physical environment (Zancolli et al., 2019). Compositional alterations in snake venom likely influence its rheology. Environmental changes determined by captivity (e.g. food supply restricted to a single type of prey) can also result in modifications of venom composition. However, most of the evidence produced so far suggests that the effect of captivity on snake venom composition is minimal (Farias et al., 2018; Freitas-de-Sousa et al., 2015; McCleary et al., 2016). In light of this, and considering that all venom samples analysed here were sourced from adult snakes fed on the same diet and kept under the same enclosure conditions, age, diet and ecology-related sources of variability have been minimised as much as possible, and thus seem unlikely to play a major role in the findings of this study. Thus, we suspect inherited differences in molecular venom composition (Mukherjee and Maity, 2002; Silva-de-França et al., 2019; Tan and Tan, 1988) to be the primary influence for any rheological differences. However, considering that both Petras et al. (2011) and Kazandjian et al. (2021) found the venoms of African spitting cobras (*N. katiensis*, *N. mossambica*, *N. nigricollis*, *N. nubiae*, *N. pallida*) to show similar compositional patterns in terms of proteins, we speculate that long chain (high molecular weight)

non-protein molecules present in snake venom, such as carbohydrates (Bieber, 1979; Gowda and Davidson, 1992; Nawarak et al., 2004; Soares and Oliveira, 2009), could be responsible for the detected variation in rheological properties.

Surprisingly, our rheological testing showed Newtonian behaviour for all analysed snake venoms across the shear rates presented. This appears to be in direct contrast to previous studies where snake venoms have been classified as non-Newtonian (Balmert et al., 2011; Triep et al., 2013; Young et al., 2011). For example, Triep et al. (2013) suggested that *N. pallida* venom had non-Newtonian behaviour in the range of 1 to 37 s⁻¹. However, upon closer inspection of the data within this range, we conclude that the apparent shear-thinning behaviour of *N. pallida* venom could be attributed to surface tension effects (Ewoldt et al., 2015). As a result, through comparison of our findings to previous studies, and accounting for the potential confounding influence of surface tension artefacts, we propose that any venom rheological data obtained below 100 s⁻¹ presented to date should not be considered when determining if a venom is Newtonian or non-Newtonian (see Fig. S1). Previous studies have interpreted the rheological behaviour of snake venom based on experimental shear rate values ranging from 1 to 100 s⁻¹ (Triep et al., 2013), and from 0.01 to 200 s⁻¹ (Young et al., 2011). In these cases, we suggest that, because of the surface tension artefacts, only data from 100 to 200 s⁻¹ (indicating a Newtonian flow behaviour) should be considered.

To explore the delivery mechanism and pressure requirements of venom ejection, we combined our rheology data with microCT scans of snake fangs reported by du Plessis et al. (2018). For the corresponding calculations, since fang venom channels are typically slightly curved and may have additional pressure-increasing features such as internal ridges (Berthé, 2011; Triep et al., 2013) and pressure losses due to viscosity, an extended generalised Bernoulli equation (Eqn 3) was used. We were able to model the pressure required for venom to flow through the fang for three of the species we studied: *N. nivea* (African non-spitting cobra), *N. nigricollis* (African spitting cobra) and *B. arietans* (viper). Despite the limited number of species investigated, there are clear differences in the pressure required to move venom down the fang. The spitter *N. nigricollis* has a smaller fang length/diameter ratio and a lower pressure requirement, whereas the non-spitter *N. nivea* has a larger fang length/diameter ratio and a higher pressure requirement. Interestingly, the viper *B. arietans* displayed both the largest fang length/diameter ratio and the lowest pressure requirement overall (Fig. 3), likely related to the relatively larger absolute diameter and/or curvature of the fang channel in this species. We found that the effect of viscosity and friction of the fluid in the venom channel (which is included in the Reynolds number; see Appendix for details) represents 5% of the pressure loss in *B. arietans*; 17% in *N. nigricollis* (spitter); and 9% in *N. nivea* (non-spitter). It appears that with this approach neither density nor viscosity contributes significantly to pressure losses, and that the major influence is the cross-section area variations along the venom channel ($A_1 > A_2$), which represent between 83 and 95% of the total pressure loss. In light of this, we conclude that for all the viscosities observed, and for all the snake species analysed in this study, venom viscosity does not strongly influence the pressure requirements of venom ejection, and that what most defines such requirements are the morphological adaptations of the venom delivery systems (i.e. tapering of the fang venom channel).

Considering the 'life-dinner principle' (Dawkins and Krebs, 1979), which suggests that selection for defensive strategies should

take precedence over selection for predatory efficiency, the lack of significant signs of adaptation of venom rheological properties to spitting behaviour is unexpected. In fact, if the principle is true, considering the lack of consistent differences in venom rheology between spitting and non-spitting cobras, and that venom spitting is an unambiguously defensive behaviour, it is interesting to question why selective pressures have not favoured the emergence of venom spitting in all cobras.

A recent study investigating patterns of venom-induced pain across snake species and time has suggested that the common ancestor of all elapids might have possessed early-pain-inducing venom (Ward-Smith et al., 2020). With the rapid infliction of pain being a requirement of defensive venoms (Eisner and Camazine, 1983; Ward-Smith et al., 2020), this could indicate that the use of venom for defensive purposes appeared early in elapid evolution, before the evolution of spitting behaviour. While a trend towards loss of rapidly painful venom is common in snakes (Ward-Smith et al., 2020), venom spitting, coupled with enhanced algescic activity (Kazandjian et al., 2021) could be an extension of this basic defensive strategy (i.e. injection of early-pain-inducing venom), which allows contactless defence at a distance, and of shorter duration and higher accuracy than striking/biting (Kardong and Bels, 1998; Westhoff et al., 2010; Young et al., 2001). In this scenario, spitting behaviour is probably the evolutionary response to specific selective pressures. Exposure to agile vertebrates (including visually acute primates, as suggested by Kazandjian et al., 2021), likely attacking from an elevated position, and for which a defensive strategy involving striking/biting could be hazardous and/or ineffective, could have been one of the drivers of spitting behaviour evolution. It is therefore possible that spitting behaviour would not emerge in the absence of this kind of selective pressures, thus offering a conjecture for why not all cobra species are able to spit venom. Alternatively, the existence of yet unidentified constraints preventing the evolution of spitting in non-spitting species is not to be excluded *a priori*.

Spitting behaviour has been recently documented for two species of Asian cobras that are generally considered non-spitters and that display very limited modification of their fangs, namely *N. kaouthia* and *N. atra* (Paterna, 2019; Santra and Wüster, 2017; Wüster and Thorpe, 1992). These reports suggest that venom spitting can evolve in the presence of very limited adaptation of the dentition, without the greater level of morphological adaptation and precision documented for specialised spitters (Triep et al., 2013; Young et al., 2004). The reason why these species have not evolved the more specialised venom spitting apparatus that other species possess (e.g. *N. mossambica*, *N. nigricollis*, *N. pallida*), may be due to differences in selective pressures, as outlined above, or perhaps the more recent origin of spitting in Asian cobras (Kazandjian et al., 2021). In light of these findings, spitting behaviour in cobras should probably not be seen as a binary trait, but may vary continuously in prevalence among the species of the genus *Naja*. Understanding the evolution, or lack of evolution, of specialised spitting behaviour and associated physical adaptations would likely require studying the efficacy and prevalence of spitting behaviour as a defence against natural predators, an under-documented aspect in the literature on this adaptation.

Although, perhaps surprisingly, our results did not show any clear adaptation of the rheological properties of venom to spitting behaviour, we demonstrated that both spitting and non-spitting cobra venoms are Newtonian fluids over a biologically relevant shear rate range, in contrast to previous literature reports. In order to

gain a more comprehensive understanding of the mechanics behind venom spitting in cobras, we suggest considering the continuous nature of the prevalence of spitting behaviour and spitting modes, fang morphology and parts of the cobra venom delivery system at play in venom spitting but not included in this study (e.g. m. adductor mandibulae externus superficialis). Furthermore, future studies should increase the sample size in terms of both venom samples, specimens and species, in order to more comprehensively address the remarkably high variability in viscosity we detected in the present work. We hope our findings will stimulate further comparative study of the rheology of venom spitting across the genus *Naja*.

APPENDIX

Delta pressure equation

There is pressure loss in fangs associated to converging diameter, which means $r_{\text{base of the fang}} > r_{\text{end of the fang}}$ and close to the exit orifice, which is in line with our fang measurements using microCT data (data analysed from du Plessis et al., 2018; available at GigaScience Database, <http://dx.doi.org/10.5524/100389>). However, that is not the only effect in pressure loss, because there is the effect of venom flowing in the venom channel, i.e. viscous pressure loss. Therefore, Poiseuille's law is not correct in this case because the diameter of the venom channel is not constant, and Bernoulli's equation is only accepted if there is no viscous pressure loss. Therefore, an extended generalised Bernoulli equation must be used in order to have an approximation of the pressure loss in the venom channel considering radius variations and viscosity (Synolakis and Badeer, 1989).

If the venom channel is considered as a converging radius pipe (see Fig. S2), then the generalised Bernoulli's equation considered for the venom channel can be written as:

$$P_1 + \left(\frac{u_1^2 \times \rho}{2} \right) = P_2 + \left(\frac{u_2^2 \times \rho}{2} \right) + (h_f \times \rho \times g), \quad (\text{A1})$$

where P_1 and P_2 are the pressures at the inlet and outlet points, in Pa; u_1 and u_2 are the velocities at the inlet and outlet points, in m s^{-1} ; ρ is the density of venom, in kg m^{-3} ; h_f corresponds to losses due to viscosity, in m; g is the acceleration of gravity, 9.81 m s^{-2} .

h_f can be expressed as defined by Soares and Santos (2013), as follows:

$$h_f = \left(\frac{f \times l}{D} \right) \times \left(\frac{\bar{u}^2}{2g} \right), \quad (\text{A2})$$

where f is the friction factor; l is the length of the venom channel, in m; D is the mean diameter of the venom channel, in m; \bar{u} is the mean velocity of the venom in the venom channel, in m s^{-1} , and can be calculated with the following equation:

$$\bar{u} = \frac{Q}{A}, \quad (\text{A3})$$

where Q is the volumetric flow in the venom channel, in $\text{m}^3 \text{ s}^{-1}$; A is the mean cross section area of the venom channel, in m^2 . The friction factor, for laminar flow, can be expressed as:

$$f = \frac{64}{Re}. \quad (\text{A4})$$

If we combine Eqns A2 and A4, we obtain:

$$h_f = \left(\frac{64}{Re} \right) \times \left(\frac{l}{D} \right) \times \left(\frac{\bar{u}^2}{2g} \right). \quad (\text{A5})$$

And combining Eqns A1 and A5:

$$P_1 + \left(\frac{u_1^2 \times \rho}{2} \right) = P_2 + \left(\frac{u_2^2 \times \rho}{2} \right) + \left(\left(\frac{64}{Re} \right) \times \left(\frac{l}{D} \right) \times \left(\frac{\bar{u}^2}{2} \right) \times \rho \right). \quad (\text{A6})$$

From the continuity equation (Munson et al., 2006):

$$A_1 u_1 = A_2 u_2, \quad (\text{A7})$$

where A_1 and A_2 are the cross-section areas at the inlet and outlet points, in m^2 .

Rearranging Eqn A7:

$$u_2 = \frac{A_1 u_1}{A_2}. \quad (\text{A8})$$

If we define $P_1 - P_2 = \Delta P$, rearrange Eqn A6, and combine with Eqn A8, we obtain Eqn 3:

$$\Delta P = P_1 - P_2 = \left(\frac{\rho}{2} \right) \times u_1^2 \left(\left(\frac{A_1}{A_2} \right)^2 - 1 \right) + \left(\left(\frac{64}{Re} \right) \times \left(\frac{l}{D} \right) \times \left(\frac{\bar{u}^2}{2} \right) \times \rho \right), \quad (\text{A9})$$

which is the equation used to calculate the pressure loss in the venom channel.

Acknowledgements

The authors thank Andreas Koeppel (University of Sheffield, Department of Materials Science and Engineering, Sheffield, UK) for his help with some of the rheological measurements, and Professor Anton du Plessis (Research group 3D Innovation, Stellenbosch University, Stellenbosch, South Africa) for providing microCT details of his published paper, which were used to analyse microCT images included in this study. IA thanks Drs Bart Hallmark, Simon Butler and Ian Wilson (Department of Chemical Engineering and Biotechnology, University of Cambridge, UK) for their help during a pilot study on cobra venom rheology, and Pedro Coelho and Yuri Simone (CIBIO/InBIO, Centro de Investigação em Biodiversidade e Recursos Genéticos da Universidade do Porto, Vairão, Portugal) for providing useful comments. The authors thank two anonymous reviewers for their insightful comments which improved the manuscript.

Competing interests

The authors declare no competing or financial interests.

Author contributions

Conceptualization: I.A., C.H., A.v.d.M.; Methodology: I.A., E.B.-L., W.W., C.H., A.v.d.M.; Validation: E.B.-L., C.H., A.v.d.M.; Formal analysis: I.A., E.B.-L., W.W., C.H., A.v.d.M.; Investigation: I.A., E.B.-L., C.H.; Resources: E.B.-L., N.R.C., R.A.H., P.D.R., E.C., W.W., C.H., A.v.d.M.; Data curation: I.A., E.B.-L., P.D.R., E.C.; Writing - original draft: I.A., E.B.-L., N.R.C., R.A.H., W.W., R.C., C.H., A.v.d.M.; Writing - review & editing: I.A., E.B.-L., N.R.C., R.A.H., P.D.R., E.C., W.W., R.C., C.H., A.v.d.M.; Visualization: I.A., E.B.-L., N.R.C., R.A.H., W.W., R.C., C.H., A.v.d.M.; Supervision: C.H., A.v.; Project administration: I.A., C.H., A.v.d.M.; Funding acquisition: I.A., A.v.d.M., C.H.

Funding

I.A. gratefully acknowledges the financial support provided by The Company of Biologists in the form of a Travelling Fellowship (JEBTF 171127). I.A. is supported by a Fundação para a Ciência e a Tecnologia, Portugal (FCT) Doctoral Fellowship (SFRH/BD/137797/2018). A.v.d.M. is financed through FCT under contract number DL57/2016/CP1440/CT0009. E.B.L. acknowledges the CONACYT (Consejo Nacional de Ciencia y Tecnología, Mexico) for its financial support (472130). N.R.C., R.A.H. and W.W. were supported in part by Leverhulme Trust grant RPG-2012-627.

Supplementary information

Supplementary information available online at <https://jeb.biologists.org/lookup/doi/10.1242/jeb.229229.supplemental>

References

- Aitken, A. and Learmonth, M. P. (2009). Protein determination by UV absorption. In *The Protein Protocols Handbook* (ed. J. M. Walker), pp. 3-6. Totowa: Humana Press.
- Alape-Girón, A., Sanz, L., Escolano, J., Flores-Díaz, M., Madrigal, M., Sasa, M. and Calvete, J. J. (2008). Snake venomomics of the lancehead pitviper *Bothrops asper*: geographic, individual, and ontogenetic variations. *J. Proteome Res.* **7**, 3556-3571. doi:10.1021/pr800332p
- Arbuckle, K. (2017). Evolutionary context of venom in animals. In *Evolution of Venomous Animals and Their Toxins* (ed. P. Gopalakrishnakone and A. Malhotra), pp. 3-31. Dordrecht: Springer.
- Balmert, A., Hess, D., Brückner, C., Bleckmann, H. and Westhoff, G. (2011). Spitting cobras: fluid jets in nature as models for technical applications. *Bioinspiration, Biomimetics, and Bioreplication. Proc. SPIE* **7975**, 797514. doi:10.1117/12.880392
- Berthé, R. A. (2011). Spitting behaviour and fang morphology of spitting cobras. *PhD thesis*, Rheinische Friedrich-Wilhelms Universität Bonn, Bonn, Germany.
- Berthé, R. A., de Pury, S., Bleckmann, H. and Westhoff, G. (2009). Spitting cobras adjust their venom distribution to target distance. *J. Comp. Physiol. A* **195**, 753-757. doi:10.1007/s00359-009-0451-6
- Bieber, A. L. (1979). Metal and nonprotein constituents in snake venoms. In *Snake Venoms* (ed. C. Y. Lee), pp. 295-306. Heidelberg: Springer-Verlag.
- Blomberg, S. P., Garland, T. and Ives, A. R. (2003). Testing for phylogenetic signal in comparative data: behavioral traits are more labile. *Evolution* **57**, 717-745. doi:10.1111/j.0014-3820.2003.tb00285.x
- Bogert, C. M. (1943). Dentitional phenomena in cobras and other elapids with notes on adaptive modifications of fangs. *Bull. Am. Museum Nat. Hist.* **81**, 260-285.
- Bon, C. (2003). Pharmacokinetics of venom toxins and their modification by antivenom therapy. *J. Toxicol. Toxin Rev.* **22**, 129-138. doi:10.1081/1TXR-120019025
- Broeckhoven, C. and du Plessis, A. (2017). Has snake fang evolution lost its bite? New insights from a structural mechanics viewpoint. *Biol. Lett.* **13**, 20170293. doi:10.1098/rsbl.2017.0293
- Chan, Y. S., Cheung, R. C. F., Xia, L. X., Wong, J. H., Ng, T. B. and Chan, W. Y. (2016). Snake venom toxins: toxicity and medicinal applications. *Appl. Microbiol. Biotechnol.* **100**, 6165-6181. doi:10.1007/s00253-016-7610-9
- Chu, E. R., Weinstein, S. A., White, J. and Warrell, D. A. (2010). Venom ophthalmia caused by venoms of spitting elapid and other snakes: report of ten cases with review of epidemiology, clinical features, pathophysiology and management. *Toxicol. Vex.* **56**, 259-272. doi:10.1016/j.toxicol.2010.02.023
- Cipriani, V., Debono, J., Goldenberg, J., Jackson, T. N. W., Arbuckle, K., Dobson, J., Kouladrov, I., Li, B., Hay, C., Dunstane, N. et al. (2017). Correlation between ontogenetic dietary shifts and venom variation in Australian brown snakes (*Pseudonaja*). *Comp. Biochem. Phys. C* **197**, 53-60. doi:10.1016/j.cbpc.2017.04.007
- Daltry, J. C., Wüster, W., Thorpe, R. S. (1996). Diet and snake venom evolution. *Nature* **379**, 537-540. doi:10.1038/379537a0
- Dawkins, R. and Krebs, J. R. (1979). Arms races between and within species. *Proc. Royal Soc. Lond. B* **205**, 489-511. doi:10.1098/rspb.1979.0081
- du Plessis, A., Broeckhoven, C. and le Roux, S. G. (2018). Snake fangs: 3D morphological and mechanical analysis by microCT, simulation, and physical compression testing. *GigaScience* **7**, 1-8. doi:10.1093/gigascience/gix126
- Eilam, D. (2005). Die hard: a blend of freezing and fleeing as a dynamic defense - implications for the control of defensive behavior. *Neurosci. Biobehav. Rev.* **29**, 1181-1191. doi:10.1016/j.neubiorev.2005.03.027
- Eisner, T. and Camazine, S. (1983). Spider leg autotomy induced by prey venom injection: an adaptive response to "pain"? *Proc. Natl. Acad. Sci. USA* **80**, 3382-3385. doi:10.1073/pnas.80.11.3382
- El-Deib, S. (2005). Serum catecholamine and hormonal titers in the hibernating snake *Naja haje haje*, with reference to the annual climatic cycle. *J. Therm. Biol.* **30**, 580-587. doi:10.1016/j.jtherbio.2005.08.003
- Ewoldt, R. H., Johnston, M. T. and Caretta, L. M. (2015). Experimental challenges of shear rheology: how to avoid bad data. In *Complex Fluids in Biological Systems. Experiment, Theory, and Computation* (ed. S. Spagnolie), pp. 207-241. New York: Springer.
- Farias, I. B., Morais-Zani, K., Serino-Silva, C., Sant'Anna, S. S., Rocha, M. M. T. D., Grego, K. F., Andrade-Silva, D., Serrano, S. M. T. and Tanaka-Azevedo, A. M. (2018). Functional and proteomic comparison of *Bothrops jararaca* venom from captive specimens and the Brazilian bothropic reference venom. *J. Proteom.* **174**, 36-46. doi:10.1016/j.jprot.2017.12.008
- Fransen, J. A. M., Kardong, K. V. and Dullemeijer, P. (1986). Feeding mechanism in the rattlesnake *Crotalus durissus*. *Amphib-Reptilia* **7**, 271-302. doi:10.1163/156853886X00055
- Freitas-de-Sousa, L. A., Amazonas, D. R., Sousa, L. F., Sant'Anna, S. S., Nishiyama, M. Y., Jr., Serrano, S. M. T., Junqueira-de-Azevedo, I. L. M., Chalkidis, H. M., Moura-da-Silva, A. M. and Mourao, R. H. V. (2015). Comparison of venoms from wild and long-term captive *Bothrops atrox* snakes and characterization of batroxhagin, the predominant class PIII metalloproteinase from the venom of this species. *Biochimie* **118**, 60-70. doi:10.1016/j.biochi.2015.08.006
- Gibbs, H. L., Sanz, L., Chiucci, J. E., Farrell, T. M. and Calvete, J. J. (2011). Proteomic analysis of ontogenetic and diet-related changes in venom composition of juvenile and adult Dusky Pigmy rattlesnakes (*Sistrurus miliarius barbouri*). *J. Proteomics* **74**, 2169-2179. doi:10.1016/j.jprot.2011.06.013
- Gowda, D. C. and Davidson, E. A. (1992). Structural features of carbohydrate moieties in snake venom glycoproteins. *Biochem. Biophys. Res. Co.* **182**, 294-301. doi:10.1016/S0006-291X(05)80144-5
- Gutiérrez, J. M., Calvete, J. J., Habib, A. G., Harrison, R. A., Williams, D. J. and Warrell, D. A. (2017). Snakebite envenoming. *Nat. Rev. Dis. Primers* **3**, 17063. doi:10.1038/nrdp.2017.63
- Haas, G. (1973). Muscles of the jaw and associated structures in the Rhyncocephalia and Squamata. In *Biology of the Reptilia*, Vol. 4 (ed. C. Gans and T. Parsons), pp. 285-490. New York: Academic Press.
- Holland, C., Terry, A. E., Porter, D. and Vollrath, F. (2007). Natural and unnatural silks. *Polymer* **48**, 3388-3392. doi:10.1016/j.polymer.2007.04.019
- Jackson, K. (2003). The evolution of venom-delivery system in snakes. *Zool. J. Linn. Soc.* **137**, 337-354. doi:10.1046/j.1096-3642.2003.00052.x
- Karatzas, I. and Shreve, S. E. (1998). Brownian motion. In *Brownian Motion and Stochastic Calculus*, pp. 47-127. New York: Springer.
- Kardong, K. V. and Bels, V. (1998). Rattlesnake strike behavior: kinematics. *J. Exp. Biol.* **201**, 837-850.
- Kazandjian, T. D., Petras, D., Robinson, S. D., van Thiel, J., Greene, H. W., Arbuckle, K., Barlow, A., Carter, D. A., Wouters, R. M., Whiteley, G. et al. (2021). Convergent evolution of pain-inducing defensive venom components in spitting cobras. *Science* **371**, 386-390. doi:10.1126/science.abb9303
- Kerkkamp, H. M. I., Casewell, N. R. and Vonk, F. J. (2017). Evolution of the snake venom delivery system. In *Evolution of Venomous Animals and Their Toxins* (ed. P. Gopalakrishnakone and A. Malhotra), pp. 303-316. Dordrecht: Springer.
- Kurt, J. and Aurich, H. (1976). The effect of pH value and temperature on the stability of L-aminoacidoxidase from the venom of the sand viper. *Acta Biol. Med. Ger.* **35**, 175-182.
- Lillywhite, H. (2014). Temperature and ectothermy. In *How Snakes Work. Structure, Function and Behavior of the World's Snakes*, pp. 103-116. Oxford: Oxford University Press.
- Mackessy, S. P., Sixberry, N. M., Heyborne, W. H. and Fritts, T. (2006). Venom of the brown treesnake, *Boiga irregularis*: ontogenetic shifts and taxa-specific toxicity. *Toxicol.* **47**, 537-548. doi:10.1016/j.toxicol.2006.01.007
- McCleary, R. J., Sridharan, S., Dunstan, N. L., Mirtschin, P. J. and Kini, R. M. (2016). Proteomic comparisons of venoms of long-term captive and recently wild-caught Eastern brown snakes (*Pseudonaja textilis*) indicate venom does not change due to captivity. *J. Proteom.* **144**, 51-62. doi:10.1016/j.jprot.2016.05.027
- Mukherjee, A. K. and Maity, C. R. (2002). Biochemical composition, lethality and pathophysiology of venom from two cobras *Naja naja* and *N. kaouthia*. *Comp. Biochem. Physiol. B Biochem. Mol. Biol.* **131**, 125-132. doi:10.1016/S1096-4959(01)00473-0
- Munson, B. R., Young, D. F., Okishi, T. H. and Huebsch, W. W. (2006). *Fundamentals of Fluid Mechanics*. New Jersey: John Wiley and Sons, Inc.
- Nawarak, J., Phutrakul, S. and Chen, S. H. (2004). Analysis of lectin-binding glycoproteins in snake venom from the Elapidae and Viperidae families. *J. Proteome Res.* **3**, 383-392. doi:10.1021/pr034052+
- Nelsen, D. R., Nisani, Z., Cooper, A. M., Fox, G. A., Gren, E. C. K., Corbit, A. G. and Hayes, W. K. (2014). Poisons, toxungens, and venoms: redefining and classifying toxic biological secretions and the organisms that employ them. *Biol. Rev.* **89**, 450-465. doi:10.1111/brv.12062
- Page, M. (1999). Inferring the historical patterns of biological evolution. *Nature* **401**, 877-884. doi:10.1038/44766
- Panagides, N., Jackson, T. N. W., Ikonopoulou, M. P., Arbuckle, K., Pretzler, R., Yang, D. C., Ali, S. A., Kouladrov, I., Dobson, J., Sanker, B. et al. (2017). How the cobra got its flesh-eating venom: cytotoxicity as a defensive innovation and its co-evolution with hooding, aposematic marking, and spitting. *Toxins* **9**, 103. doi:10.3390/toxins9030103
- Paterna, A. (2019). Spitting behaviour in the Chinese cobra *Naja atra*. *Herpetol. Bull.* **148**, 22-25. doi:10.33256/hb148.2225
- Petras, D., Sanz, L., Segura, A., Herrera, M., Villalta, M., Solano, D., Vargas, M., Leon, G., Warrell, D. A., Theakston, R. D. G. et al. (2011). Snake venomomics of African spitting cobras: toxin composition and assessment of congeneric cross-reactivity of the pan-African EchiTAB-Plus-ICP antivenom by antivenomics and neutralization approaches. *J. Proteome Res.* **10**, 1266-1280. doi:10.1021/pr101040f
- Rasmussen, S., Young, B. and Krimm, H. (1995). On the 'spitting' behaviour in cobras (Serpentes: Elapidae). *J. Zool., Lond.* **231**, 27-35. doi:10.1111/j.1469-7998.1995.tb02743.x
- Ribeiro, P. H., Zuliani, J. P., Fernandes, C. F., Calderon, L. A., Stábili, R. G., Nomizo, A. and Soares, A. M. (2016). Mechanism of the cytotoxic effect of L-amino acid oxidase isolated from *Bothrops alternatus* snake venom. *Int. J. Biol. Macromol.* **92**, 329-337. doi:10.1016/j.ijbiomac.2016.07.022
- Sanhajariya, S., Duffull, S. and Isbister, G. (2018). Pharmacokinetics of snake venom. *Toxins* **10**, 73. doi:10.3390/toxins10020073
- Santra, V. and Wüster, W. (2017). *Naja kaouthia* (monocled cobra). Behavior/spitting. *Herpetol. Rev.* **48**, 455-456.

- Schmidt, J. O. (2019). Pain and lethality induced by insect stings: an exploratory and correlational study. *Toxins* **11**, 427–441. doi:10.3390/toxins11070427
- Silva-de-França, F., Villas-Boas, I. M., de Toledo Serrano, S. M., Cogliati, B., de Andrade Chudzinski, S. A., Lopes, P. H., Shigueo Kitano, E., Kimori Okamoto, C. and Tambourgi, D. V. (2019). *Naja annulifera* snake: new insights into the venom components and pathogenesis of envenomation. *PLoS Negl. Trop. Dis.* **13**, e0007017. doi:10.1371/journal.pntd.0007017
- Slowinski, J. B., Knight, A. and Rooney, A. P. (1997). Inferring species trees from gene trees: A phylogenetic analysis of the Elapidae (Serpentes) based on the amino acid sequences of venom proteins. *Mol. Phylogenet. Evol.* **8**, 349–362. doi:10.1006/mpev.1997.0434
- Soares, S. G. and Oliveira, L. L. (2009). Venom-sweet-venom: N-Linked glycosylation in snake venom toxins. *Protein Peptide Lett.* **16**, 913–919. doi:10.2174/092986609788923293
- Soares, T. and Santos, E. (2013). Preliminary design of fuel filling systems applying the extended Bernoulli equation on numerical calculation tools. *SAE Tech. Pap.* **13**, 1–6. doi:10.4271/2013-36-0522
- Synolakis, C. E. and Badeer, H. S. (1989). On combining the Bernoulli and Poiseuille equation—A plea to authors of college physics texts. *Am. J. Phys.* **57**, 1013–1019. doi:10.1119/1.15812
- Takahashi, T. and Ohsaka, A. (1970). Purification and some properties of two hemorrhagic principles (HR2a and HR2b) in the venom of *Trimeresurus flavoviridis*: complete separation of the principles from proteolytic activity. *BBA Protein Struct.* **207**, 65–75. doi:10.1016/0005-2795(70)90137-6
- Tan, N. H. and Tan, C. S. (1988). A comparative study of cobra (*Naja*) venom enzymes. *Comp. Biochem. Physiol. B Comp. Biochem.* **90**, 745–750. doi:10.1016/0305-0491(88)90329-X
- Terry, A. E., Knight, D. P., Porter, D. and Vollrath, F. (2004). pH induced changes in the rheology of silk fibroin solution from the middle division of *Bombyx mori* silkworm. *Biomacromolecules* **5**, 768–772. doi:10.1021/bm034381v
- Triep, M., Hess, D., Chaves, H., Brückner, C., Balmert, A., Westhoff, G. and Bleckmann, H. (2013). 3D Flow in the venom channel of a spitting cobra: do the ridges in the fangs act as fluid guide vanes? *PLoS ONE* **8**, 1–11. doi:10.1371/journal.pone.0061548
- Vitt, L. J. and Caldwell, J. P. (2013). *Herpetology: an Introductory Biology of Amphibians and Reptiles*. Academic press.
- Vonk, F. J., Admiraal, J. F., Jackson, K., Reshef, R., De Bakker, M. A. G., Vanderschoot, K., Van Den Berge, I., Van Atten, M., Burgerhout, E., Beck, A. et al. (2008). Evolutionary origin and development of snake fangs. *Nature* **454**, 630–633. doi:10.1038/nature07178
- Ward-Smith, H., Arbuckle, K., Naude, A. and Wüster, W. (2020). Fangs for the memories? A survey of pain in snakebite patients does not support a strong role for defense in the evolution of snake venom composition. *Toxins* **12**, 201. doi:10.3390/toxins12030201
- Westhoff, G., Tzschätzsch, K. and Bleckmann, H. (2005). The spitting behavior of two species of spitting cobras. *J. Comp. Physiol. A Neuroethol. Sensory, Neural, Behav. Physiol.* **191**, 873–881. doi:10.1007/s00359-005-0010-8
- Westhoff, G., Boettig, M., Bleckmann, H. and Young, B. A. (2010). Target tracking during venom 'spitting' by cobras. *J. Exp. Biol.* **213**, 1797–1802. doi:10.1242/jeb.037135
- Wüster, W. (1996). Taxonomic changes and toxinology: systematic revisions of the Asiatic cobras (*Naja naja* species complex). *Toxicon* **34**, 399–406. doi:10.1016/0041-0101(95)00139-5
- Wüster, W. and Thorpe, R. S. (1992). Dentional phenomena in cobras revisited: spitting and fang structure in the Asiatic species of *Naja* (Serpentes: Elapidae). *Herpetologica* **48**, 424–434.
- Wüster, W., Crookes, S., Ineich, I., Mané, Y., Pook, C. E., Trape, J. F. and Broadley, D. G. (2007). The phylogeny of cobras inferred from mitochondrial DNA sequences: evolution of venom spitting and the phylogeography of the African spitting cobras (Serpentes: Elapidae: *Naja nigricollis* complex). *Mol. Phylogenet. Evol.* **45**, 437–453. doi:10.1016/j.ympev.2007.07.021
- Young, B. A. and Kardong, K. V. (2007). Mechanisms controlling venom expulsion in the western diamondback rattlesnake, *Crotalus atrox*. *J. Exp. Zool. Part A Ecol. Genet. Physiol.* **307A**, 18–27. doi:10.1002/jez.a.341
- Young, B. A. and O'Shea, M. (2005). Analyses of venom spitting in African cobras (Elapidae: Serpentes). *Afr. Zool.* **40**, 71–76. doi:10.1080/15627020.2005.11407311
- Young, B. A., Blair, M., Zahn, K. and Marvin, J. (2001). Mechanics of venom expulsion in *Crotalus*, with special reference to the role of the fang sheath. *Anat. Rec.* **264**, 415–426. doi:10.1002/ar.10015
- Young, B. A., Dunlap, K., Koenig, K. and Singer, M. (2004). The buccal buckle: the functional morphology of venom spitting in cobras. *J. Exp. Biol.* **207**, 3483–3494. doi:10.1242/jeb.01170
- Young, B. A., Boettig, M. and Westhoff, G. (2009). Functional bases of the spatial dispersal of venom during cobra "spitting." *Physiol. Biochem. Zool.* **82**, 80–89. doi:10.1086/595589
- Young, B. A., Herzog, F., Friedel, P., Rammensee, S., Bausch, A. and Van Hemmen, J. L. (2011). Tears of venom: hydrodynamics of reptilian envenomation. *Phys. Rev. Lett.* **106**, 198103. doi:10.1103/PhysRevLett.106.198103
- Zancolli, G., Calvete, J. J., Cardwell, M. D., Greene, H. W., Hayes, W. K., Hegarty, M. J., Herrmann, H. W., Holycross, A. T., Lannutti, D. I., Mulley, J. F. et al. (2019). When one phenotype is not enough: divergent evolutionary trajectories govern venom variation in a widespread rattlesnake species. *Proc. Royal Soc. Lond. B* **286**, 20182735. doi:10.1098/rspb.2018.2735
- Zheng, Y. and Wiens, J. J. (2016). Combining phylogenomic and supermatrix approaches, and a time-calibrated phylogeny for squamate reptiles (lizards and snakes) based on 52 genes and 4162 species. *Mol. Phylogenet. Evol.* **94**, 537–547. doi:10.1016/j.ympev.2015.10.009